NASA/TM-20220016292 CD-2021-186

Titan In-Situ Resource Utilization (ISRU) Sample Return (TISR)

Steven Oleson and Geoffrey Landis
Glenn Research Center, Cleveland, Ohio

Ralph Lorenz
Johns Hopkins University, Applied Physics Laboratory, Laurel, Maryland

Elizabeth Turnbull
Glenn Research Center, Cleveland, Ohio

Thomas Packard, Anthony Colozza, and David Smith
HX5, LLC, Brook Park, Ohio

Jeffrey Pekosh, Steven McCarty, Zachary Zoloty, and Laura Burke
Glenn Research Center, Cleveland, Ohio

James Fittje
Science Applications International Corporation, Brook Park, Ohio

John Gyekenyesi
HX5, LLC, Brook Park, Ohio

Paul Schmitz
Power Computing Solutions, Inc., Avon, Ohio

Lucia Tian, Steven Korn, Nick Uguccini, Brent Faller, Christine Schmid,
Christopher Heldman, W. Peter Simon, and Onoufrious Theofylaktos
Glenn Research Center, Cleveland, Ohio

December 2022

NASA STI Program . . . in Profile

Since its founding, NASA has been dedicated to the advancement of aeronautics and space science. The NASA Scientific and Technical Information (STI) Program plays a key part in helping NASA maintain this important role.

The NASA STI Program operates under the auspices of the Agency Chief Information Officer. It collects, organizes, provides for archiving, and disseminates NASA's STI. The NASA STI Program provides access to the NASA Technical Report Server—Registered (NTRS Reg) and NASA Technical Report Server—Public (NTRS) thus providing one of the largest collections of aeronautical and space science STI in the world. Results are published in both non-NASA channels and by NASA in the NASA STI Report Series, which includes the following report types:

- TECHNICAL PUBLICATION. Reports of completed research or a major significant phase of research that present the results of NASA programs and include extensive data or theoretical analysis. Includes compilations of significant scientific and technical data and information deemed to be of continuing reference value. NASA counter-part of peer-reviewed formal professional papers, but has less stringent limitations on manuscript length and extent of graphic presentations.

- TECHNICAL MEMORANDUM. Scientific and technical findings that are preliminary or of specialized interest, e.g., "quick-release" reports, working papers, and bibliographies that contain minimal annotation. Does not contain extensive analysis.

- CONTRACTOR REPORT. Scientific and technical findings by NASA-sponsored contractors and grantees.

- CONFERENCE PUBLICATION. Collected papers from scientific and technical conferences, symposia, seminars, or other meetings sponsored or co-sponsored by NASA.

- SPECIAL PUBLICATION. Scientific, technical, or historical information from NASA programs, projects, and missions, often concerned with subjects having substantial public interest.

- TECHNICAL TRANSLATION. English-language translations of foreign scientific and technical material pertinent to NASA's mission.

For more information about the NASA STI program, see the following:

- Access the NASA STI program home page at http://www.sti.nasa.gov

- E-mail your question to help@sti.nasa.gov

- Fax your question to the NASA STI Information Desk at 757-864-6500

- Telephone the NASA STI Information Desk at 757-864-9658

- Write to:
  NASA STI Program
  Mail Stop 148
  NASA Langley Research Center
  Hampton, VA 23681-2199

NASA/TM-20220016292 CD-2021-186

Titan In-Situ Resource Utilization (ISRU) Sample Return (TISR)

Steven Oleson and Geoffrey Landis
Glenn Research Center, Cleveland, Ohio

Ralph Lorenz
Johns Hopkins University, Applied Physics Laboratory, Laurel, Maryland

Elizabeth Turnbull
Glenn Research Center, Cleveland, Ohio

Thomas Packard, Anthony Colozza, and David Smith
HX5, LLC, Brook Park, Ohio

Jeffrey Pekosh, Steven McCarty, Zachary Zoloty, and Laura Burke
Glenn Research Center, Cleveland, Ohio

James Fittje
Science Applications International Corporation, Brook Park, Ohio

John Gyekenyesi
HX5, LLC, Brook Park, Ohio

Paul Schmitz
Power Computing Solutions, Inc., Avon, Ohio

Lucia Tian, Steven Korn, Nick Uguccini, Brent Faller, Christine Schmid,
Christopher Heldman, W. Peter Simon, and Onoufrious Theofylaktos
Glenn Research Center, Cleveland, Ohio

National Aeronautics and
Space Administration

Glenn Research Center
Cleveland, Ohio 44135

December 2022

Acknowledgments

This work was supported by the NASA Innovative Advanced Concepts Program.

This report is a formal draft or working paper, intended to solicit comments and ideas from a technical peer group.

This report contains preliminary findings, subject to revision as analysis proceeds.

Level of Review: This material has been technically reviewed by technical management.

This report is available in electronic form at http://www.sti.nasa.gov/ and http://ntrs.nasa.gov/

Contents

Titan In-Situ Resource Utilization (ISRU) Sample Return (TISR)

Steven Oleson and Geoffrey Landis
National Aeronautics and Space Administration
Glenn Research Center
Cleveland, Ohio 44135

Ralph Lorenz
Johns Hopkins University
Applied Physics Laboratory
Laurel, Maryland 20723

Elizabeth Turnbull
National Aeronautics and Space Administration
Glenn Research Center
Cleveland, Ohio 44135

Thomas Packard, Anthony Colozza, and David Smith
HX5, LLC
Brook Park, Ohio 44142

Jeffrey Pekosh, Steven McCarty, Zachary Zoloty, and Laura Burke
National Aeronautics and Space Administration
Glenn Research Center
Cleveland, Ohio 44135

James Fittje
Science Applications International Corporation
Brook Park, Ohio 44142

John Gyekenyesi
HX5, LLC
Brook Park, Ohio 44142

Paul Schmitz
Power Computing Solutions, Inc.
Avon, Ohio 44011

Lucia Tian, Steven Korn, Nick Uguccini, Brent Faller, Christine Schmid,
Christopher Heldman, W. Peter Simon, and Onoufrious Theofylaktos
National Aeronautics and Space Administration
Glenn Research Center
Cleveland, Ohio 44135

1.0 Introduction

Titan is unique in the outer solar system in that it is the only moon with a thick atmosphere, and the only body in the solar system outside the Earth with liquid seas on its surface. The Titanian oceans, however, are seas of liquid hydrocarbons, and the rocks on the surface are solid water ice. Like other icy

Moons of the outer solar system, beneath the ice crust, Titan also has a subsurface ocean. Rodriguez et al. refer to it as the “world with two oceans”, an organic-rich body with interior-surface-atmosphere interactions that are comparable in complexity to the Earth (Ref. 1).

Titan is scientifically fascinating in many ways (Refs. 2 to 4). The Compass Team will emphasize just one here: Titan is a high priority target for astrobiology (Refs. 4 to 11). It is a world with a surface and atmosphere rich in the complex organic compounds known as tholins. A detailed understanding of the nature of these complex compounds will require an analysis using a full laboratory on Earth. Because of its value to understanding the organic compounds of the outer solar system which may be the primordial building-blocks of life, return of samples from Titan to laboratories on Earth will be the primary goal of this mission.

While this would give unprecedented science return, returning even a small sample from Titan using conventional technology would be tremendously difficult. Saturn is almost a billion miles from the Earth, about 13 times farther than Mars. A return mission to Saturn requires such a large total-mission ΔV that, with conventional technology, the mass ratios required are prohibitive. Such a sample return would truly be “mission incredible.” But to date, a sample return mission from so distant a target has been assumed to be, not merely incredible, but mission impossible. The Compass Team has proposed (Refs. 2 and 12) that by manufacturing the propellant for the return to Earth using the resources available on Titan, such a mission becomes possible. The task of this report is to show that it is reasonable with credible space technology.

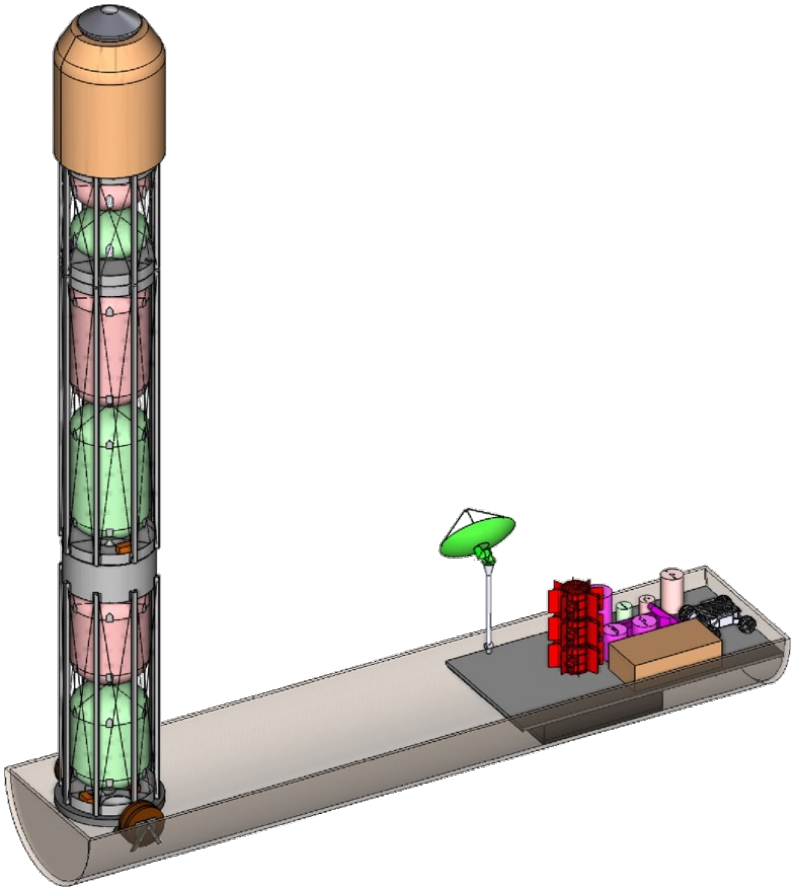

Figure 1.1.—Titan Sample Return Rocket Fueled Using Titan Propellants and Ready for Launch.

2.0 Study Background, Assumptions, and Approach

The following sections describe the Titan environment, propellants and fuels explored, and the overall mission description and concept of operations (CONOPS).

2.1 Titan Environment

Basic information about the Titan surface and atmosphere has been gathered by the Voyager and Cassini missions, along with surface observations by the Huygens Titan lander (Ref. 13). Titan has an average surface temperature of 90.6 K, reaching a maximum temperature of 93.6 K. The atmosphere is primarily N_2 with about 5.6 percent CH_4 (at the surface), with an atmospheric pressure of 147 kPa (1.45 atm). The atmospheric density is 5.43 kg/m^3, about 4.3 times denser than Earth's atmosphere.

Titan has an escape velocity of 2.64 km/s. The surface gravity is 1.35 m/s^2 (0.138 times that of Earth). The lower surface gravity results in lower decrease of atmospheric density with altitude, with a density scale height in the lower atmosphere of about 22 km, more than twice that of the Earth. Due to the greater scale height, the altitude of a low orbit above Titan is notably higher than that of a low Earth orbit. For this study, the Compass Team assumed 1000 km altitude above the surface for the parking orbit, to place the orbit above the drag of residual atmosphere.

Although the lower escape velocity makes launching from the Titan surface slightly easier than launch from Earth, the greater atmospheric pressure and higher scale height combine to make launch more difficult. The high atmospheric pressure also decreases the engine performance. A CH_4/O_2 engine optimized for the surface atmospheric pressure at an expansion ratio of 20:1, produces about 270 s of I_{sp}, while the same engine with an expansion ratio of 150:1 optimized for vacuum operation produces about 350 s of I_{sp}. Compass Team calculations show that roughly 1 km/s of the 3.9 km/s required to launch from the surface into Titan orbit is due to the atmospheric drag (depending on the vehicle area and drag coefficient).

2.2 In-Situ Propellants

Many studies of space development have emphasized the use of the in-situ resources to eliminate the requirement to launch propellants from Earth. Titan has surface lakes of LCH_4 and ethane that amount to more hydrocarbons than the total fossil fuel reserves of the Earth. In addition, surface rocks of water ice are a source of O_2. With water, LCH_4, and ethane easily available, Titan is a rocket scientist's dream for propellants. Unlike Mars, Titan has a thick atmosphere, allowing the use of a non-propulsive, direct aerodescent to reduce the entry velocity and a parachute for soft landing.

In-situ resource utilization (ISRU) for propellant production has been explored for Mars missions but is rarely analyzed for missions farther out in the solar system. As will be demonstrated, propellent production from resources on Titan is significantly different than the concepts proposed for Mars, the Moon, or asteroids. Demonstration of ISRU for sample return from Titan will be a huge step beyond Mars and the first building block in using the resources of the outer solar system.

2.3 Choice of Fuel and Oxidizer

Chemical rocket propellant consists of a fuel and oxidizer combination. The obvious choice for fuel is a native Titan hydrocarbon. CH_4 (and possibly ethane) is abundant, available in liquid form in lakes on the surface, as well as in smaller amounts in the atmosphere. Unlike any other destination in the solar

system, producing rocket fuel on Titan needs no processing: It requires only gathering the available fuel from the environment.

The CH_4/LOx combination is very nearly an ideal rocket propellant. The I_{sp} of 325 s is second only to LH_2/O among hydrocarbon-based rocket fuels, but CH_4's much higher density (0.44 kg/m^3, compared to 0.071 for LH_2), allows for considerably smaller tanks, and eliminates the requirement for cryogenic storage. For these reasons, CH_4/O_2 engines are being developed for the next generation of launch vehicles. Engine development for these vehicles means that this concept will not require new technology but can use designed and tested engines.

The Compass Team considered alternate possibilities as well. Liquid ethane, with a slightly higher density of 0.65 kg/m^3, is also likely to be available on Titan. However, ethane has lower I_{sp}, and is difficult to obtain from the atmosphere. H_2, with higher (>430 s) I_{sp} but lower density, could be produced by electrolysis (and is a byproduct of the production of the O_2 from water ice). However, the team eliminated it as a desirable fuel due to the difficulty of storage.

On Titan, a more difficult choice is the oxidizer. N_2-based oxidizers such as NTO were considered but rejected in favor of refining LOx from Titan's water ice resources. The rocks are gathered, melted using the heat from the radioisotope source, and electrolyzed to produce O_2.

Cryogenic storage is simple because the ambient temperature on Titan is ideally suited for the chosen propellants. The maximum measured surface temperature of 93.6 K is just above CH_4's freezing point at Titan's atmospheric pressure, allowing the mission to store the CH_4 as a liquid fuel with no refrigeration. The temperature is slightly above the 1-bar boiling point of O_2, but the high pressure of Titan's atmosphere means by maintaining a tank pressure of 2.5 bar, (about 1 bar above Titan ambient pressure), the O_2 remains liquid up to 100 K—a comfortable margin above the highest temperature measured on Titan. By a fortunate coincidence, the temperature and pressure at the surface of Titan allows cryogenic propellants to be stored in liquid form without refrigeration. Likewise, although not used in this study, ethane is also liquid at Titan temperatures.

2.4 Propellant Acquisition: CH_4

Landing close to one of the Titan lakes would be a straightforward method of CH_4 acquisition; in essence allowing CH_4 to be acquired using little more than a pipe and a pump. However, this acquisition approach would put significant constraints on the landing site. In addition to other constraints of landing site safety, the site must be at the edge of the lake. This would add a mission requirement that the landing error ellipse be precise, with a risk of a possible mission failure if the landing is out of reach of the CH_4.

Instead, this report proposes to acquire the CH_4 from the atmosphere. On Titan, the CH_4 vapor content of the atmosphere is at or near the saturation point, and hence CH_4 can be condensed out of the atmosphere either by lowering the temperature, or by compressing the atmosphere at constant temperature. The Compass Team chose the second option. The atmosphere is collected, compressed to 8.8 bar, and then allowed to cool to ambient temperature. Methane from the atmosphere is condensed to liquid, and the LCH_4 is transferred to a storage tank to temporarily store it before transferring it to the launch vehicle. The liquification tank is then vented to remove the remaining N_2, and the process is repeated until the required amount of LCH_4 is collected. Pump and compressor power required for this collection process is about 117 W to produce the required CH_4 production rate of about 700 g per day.

2.5 Propellant Acquisition: Oxygen

In the O_2 production system, rocks consisting of water ice are collected by a small rover and transferred to a melting tank, where they are melted using waste heat from the radioisotope power source.

The meltwater is then distilled, again using waste heat, to remove impurities. Heat exchangers are used to scavenge the residual heat from the distilled meltwater. The purified water is then piped to the electrolyzer unit, which separates the water into H_2 and O_2, and the H_2 is vented. The electrolyzer design used is a Proton Exchange Membrane (PEM), a design based on commercial fuel cell technology and similar to electrolyzers considered for other ISRU applications (Ref. 14). The O_2 is dried, to remove any residual water, liquified by exposing it to Titan temperatures, and sent to the storage tank, where it is temporarily stored before transfer to the launch vehicle.

The rate-limiting step in propellant processing is the power required for electrolysis of the water to produce the required O_2, requiring about 3.52 kW-h per kg of O_2 produced. At an electrolyzer energy efficiency of 0.72, power required for this is 484.5 W.

Power is produced by a radioisotope power system (RPS), based on a dynamic radioisotope conversion such as the Dynamic Radioisotope Power System (DRPS). In this case, the efficiency of the power conversion will be increased by the low ambient temperature; the waste heat from the RPS is utilized to melt the water, while electrical power runs the systems and is used to electrolyze the water into H_2 and O_2. Three DRPS are assumed to provide roughly 1 kWe of power for all functions of the outbound and surface mission.

2.6 Overall Mission Concept of Operations

A brief overview of the 17-year mission to return 3 kg of cryogenic samples is shown in the concept of operations, Figure 2.1. A reasonable launch mass of ~ 3.4 t was possible by producing return propellants on Titan. This enabled the use of a Falcon Heavy expendable launcher with a Star 48 upper stage to a C_3 of about 90 km^2/s^2. Additional velocity is added by a Jupiter flyby. After a 7-year trip the vehicle will encounter Titan. Titan's heavy atmosphere allows for a non-propulsive, direct entry like Huygens probe. Since no return stage or spacecraft was needed to be inserted into Titan orbit all that is needed is an entry system. As the propellant ISRU and return system was the focus of this NASA innovative advanced concept (NIAC), the Compass Team chose a representative aerodescent system based on the X37-C concept (Ref. 15). Such a vehicle could allow for entering the Titan atmosphere and then gliding to the desired propellant-rich landing area. The landing could be achieved by skids using a parachute to slow the vehicle. Further work on defining the entry vehicle is needed.

Once on the surface, the rover (or alternative rotor vehicles) will gather both the return cryogenic samples as well as the water ice ore that will be processed into the LOx propellant by the radioisotope powered ISRU system. The CH_4 is simply distilled from the atmosphere. These propellants are then cooled by exposing them to the Titan ~94 K environment and pumped into the three inflatable return launcher stages. About 3 years is needed to produce the roughly 3000 kg of LOx and LCH_4 propellants required. The Titan launcher is elevated and filled slowly with the cryogenic propellants as they are produced. Once filled, the first two stages of the launcher place the in-space stage and return vehicle (RV) into a 1000 km circular orbit above Titan. Such a high orbit is needed due to the thickness of Titan's heavy atmosphere. While the gravity losses from Titan's low gravity (about one seventh that of Earth) make the launch easier than from Earth, the thicker and denser atmosphere causes significant drag. Further studies will look at ways to utilize the atmosphere to assist in the launch, focusing on replacing the chemical first stage with options such as a balloon, rotorcraft, or aircraft launch.

The third (in-space) stage will be used for multiple burns to depart Titan orbit and enter a Saturn orbit that provides Titan and Saturn flybys to minimize the propellant to get on a trajectory to return to Earth. The Titan Samples will be kept cryogenic by continuously exposing them to deep space. Instead of a plutonium power system, an ultralight solar array will be used to power the return vehicle – with power increasing as the vehicle gets closer to Earth and the Sun. A nominal aeroshell/parachute system will

return the sample to Earth's surface. Since a science requirement of the mission was that the sample would not be exposed to temperatures high enough to liquify any of the frozen components of the sample, a small amount of LOx (produced on Titan) will encapsulate the 3 kg of Titan samples, keeping them cold during descent, landing, and the Earth recovery phase.

2.7 Mission Description

This study focused on the elements of the mission which are unique to Titan, and with greatest emphasis on the launch from Titan and the return to Earth. The mission for Titan sample return consists of the following elements:

- Launch from Earth
  - Insertion into the interplanetary trajectory and flight from Earth to the Saturn system (possibly incorporating planetary flyby for gravity assist)
  - Entry descent and landing on Titan
- The RPS-powered mission
  - Operations on Titan (including collection of samples, surface science (if any))
  - Processing of propellant
- The ISRU-fueled launch from the surface of Titan
  - Insertion into the interplanetary trajectory
- The return to Earth portion of the mission
  - Interplanetary flight to Earth
  - Entry descent and landing on Earth
  - Post-mission curation and analysis of samples

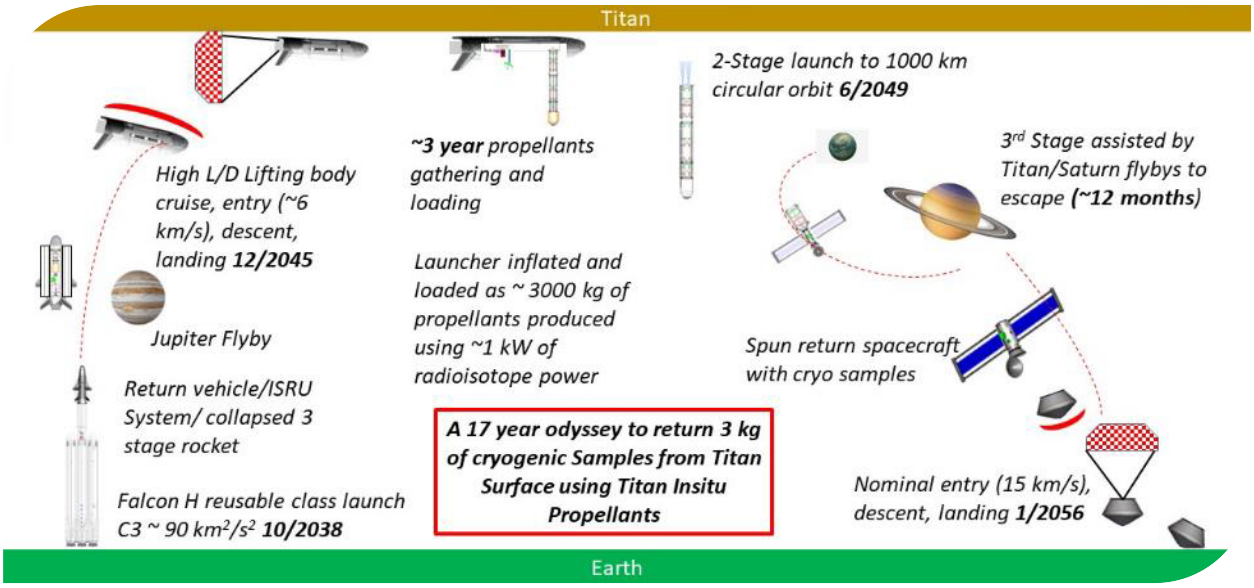

Figure 2.1.—Summary of the Mission CONOPS.

Two approaches to the return phase of the Titan sample return mission were considered: either a direct launch of the Earth return vehicle from the surface of Titan, or an approach where the vehicle carrying the sample is launched from Titan to a rendezvous with a separate Earth return vehicle waiting in Titan or Saturn orbit. The orbital rendezvous approach increases the complexity and requires two vehicles but has the advantage of requiring less mass to be landed on and launched from the surface of Titan. Using only a single return vehicle with no orbital rendezvous simplifies the system at the cost of somewhat more mass landed on Titan. The comparative merits of each approach are very sensitive to the ΔV required for injection into the trans-Earth trajectory. For the current study, a return trajectory utilizing multiply flybys of Titan and a close approach to Saturn was used. This minimized the ΔV for the trans-Earth injection, and hence a direct launch of the Earth return vehicle from Titan was chosen for its reduced complexity and because it maximizes the use of in situ propellants.

In any case, most of the details of the analysis of launch from the Titan surface into the parking orbit around Titan will be the same, and the analysis here can be used for either approach.

2.7.1 Earth to Titan Mission Design for Sample Return

Multiple mission opportunities were looked at for departure trajectories leaving Earth and arriving at Titan. Time constraints hinged on NASA's Dragonfly mission, which will arrive to Titan in 2036 and provide valuable information on landing sites for a sample return mission. As such, the departure date for the sample return mission is to leave no earlier than 2036. To keep the mission on a cohesive timeline, the spacecraft also was not to arrive at Titan any later than 2048 to include 1 to 3 years of ISRU/rocket construction on Titan prior to launching a return trajectory to Earth between 2048 and 2051.

The departure trajectories created in this session were designed to be entirely ballistic and leave Earth with minimal C_3. For all cases, the spacecraft leaves Earth at a radius of 6563 km from the center of Earth and arrives at Titan at a radius of 2675 km from its center. Additionally, arrival at Titan was constrained to 6.5 km/s entry velocity with a flight path angle between –40° and 40° to ensure acceptable conditions for aeroshell capture.

2.7.2 2038 Direct Trajectory Design Reference Mission

The direct trajectory case for the Earth to Titan mission can be seen in Figure 2.2. It departs Earth on December, 24, 2038 and arrives at Titan on October 4, 2048. This trajectory has not yet been completely optimized due to its high C_3 value giving it lower precedence in the study than the other cases, which will be discussed in the subsequent sections. By performing further analysis, the time of flight of this trajectory should be able to be lowered by a couple years, but the C_3 is unlikely to go below 100 km^2/s^2. Table 2.1 provides the details of Titan direct trajectory.

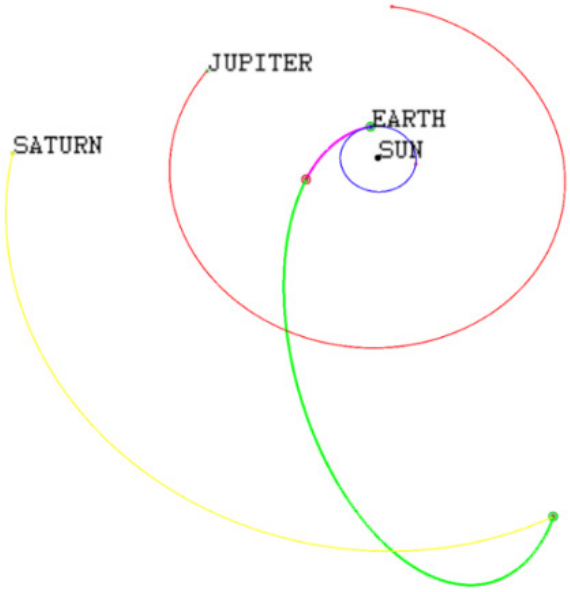

Figure 2.2.—Earth-to-Titan Direct Trajectory.

TABLE 2.1.—DIRECT TRAJECTORY DETAILS

	Earth Departure Conditions (w/r/t Earth's center)	Titan Arrival Conditions (w/r/t Titan's center)
C_3 (km^2/s^2)	109.214	29.689
Velocity (km/s)	15.188	6.033
FPA (degree)	-8.376×10^{-16}	4.944
V_{inf} (km/s)	10.451	5.449
Inclination	9.972	
RAAN	–127.419	
Argument of periapsis	–162.479	
RAAN		123.361
Declination		–28.474
Azimuth Angle		46.163
Departure Date	12/24/38	
Arrival Date	10/4/48	
Time of Flight (year)	9.696	

2.7.3 2038 Jupiter Flyby Design Reference Mission

The trajectory shown in Figure 2.3 is an Earth-to-Titan mission that includes a Jupiter flyby in an attempt to lower the C_3 required when leaving Earth. While the direct case may be altered for changes in the mission timeline, the Jupiter flyby case cannot be moved due to the nature of the synodic period between Earth and Jupiter. This design fits into the decided mission timeline with a departure from Earth on October 27, 2038, a Jupiter flyby on October 21, 2040, and an arrival at Titan on December 9, 2045. Table 2.2 provides the details of a Jupiter flyby trajectory.

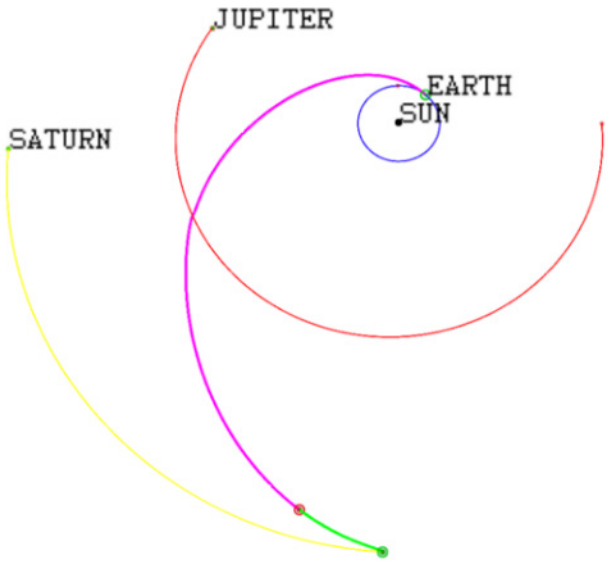

Figure 2.3.—Earth-to-Titan Jupiter-flyby Trajectory.

TABLE 2.2.—JUPITER FLYBY TRAJECTORY DETAILS

	Earth Departure Conditions	Titan Arrival Conditions
C_3 (km^2/s^2)	90.653	35.537
Velocity (km/s)	14.564	6.5
FPA (degree)	-1.747×10^{-15}	–0.332
V_{inf} (km/s)	9.521	5.961
Inclination	–34.956	
RAAN	–148.092	
Argument of Periapsis	–203.089	
Right Ascension		–133.541
Declination		–77.088
Azimuth Angle		13.609
Departure Date	10/27/38	
Arrival Date	12/9/45	
Flyby Dates	10/21/40	
Time of Flight (year)	7.119	

2.7.4 2036 Earth-Venus-Earth-Earth Flyby Design Reference Mission

The Earth-Venus-Earth-Earth flyby trajectory (or EVEE trajectory) utilizes the proximity of Venus to depart Earth with a remarkably low C_3 when compared to the Direct or Jupiter flyby trajectories. This is done by using a flyby of Venus, followed by two consecutive flybys of Earth, to generate enough velocity to reach Titan. These flybys can be seen in Figure 2.4. Table 2.3 provides the details of EVEE trajectory.

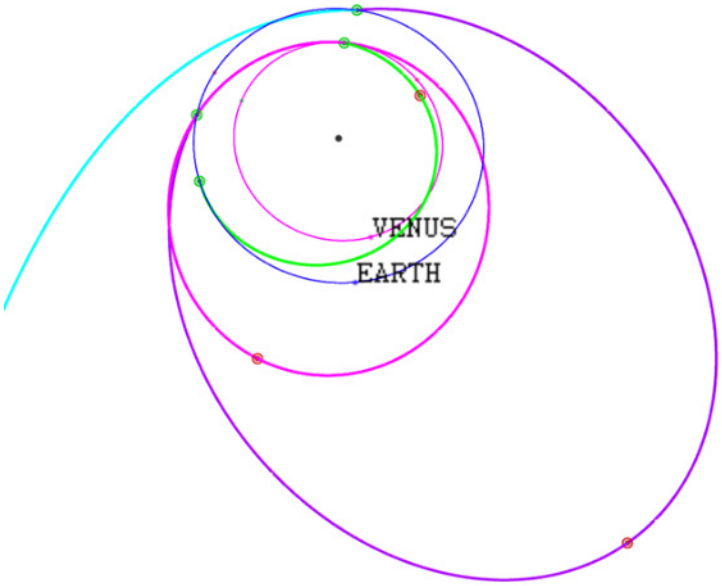

Figure 2.4.—EVEE Trajectory.

TABLE 2.3.—EVEE TRAJECTORY DETAILS

	Earth Departure Conditions	Titan Arrival Conditions
C_3 (km^2/s^2)	10.654	33.667
Velocity (km/s)	11.495	6.355
FPA (degree)	2.269×10^{-14}	–23.571
V_{inf} (km/s)	3.265	5.802
Inclination	–26.627	
RAAN	164.655	
Argument of Periapsis	–204.961	
Right Ascension		–0.278
Declination		45.200
Azimuth Angle		–28.155
Departure Date	3/29/36	
Arrival Date	2/11/47	
Flyby Dates	9/25/36, 3/2/38, 12/4/40	
Time of Flight (year)	10.870	

Table 2.3 shows that with a C_3 of only 10.654 km^2/s^2, the EVEE trajectory can be launched by a number of vehicles, which cannot be said about the Direct or Jupiter flyby cases. Departing Earth on March 29, 2036 and arriving at Titan on February 11, 2047, the EVEE case fits the mission timeline. Due to its long time of flight of 10.870 years, it cannot be altered much in order to ensure it departs no earlier than 2036 and arrives earlier than 2048. The Venus flyby for this mission occurs on September 25, 2036, with the initial Earth flyby on March 2, 2038 and the final Earth flyby on December 4, 2040. This trajectory meets the arrival constraints at Titan with an entry velocity of 6.355 km/s and a flight path angle of –23.571°.

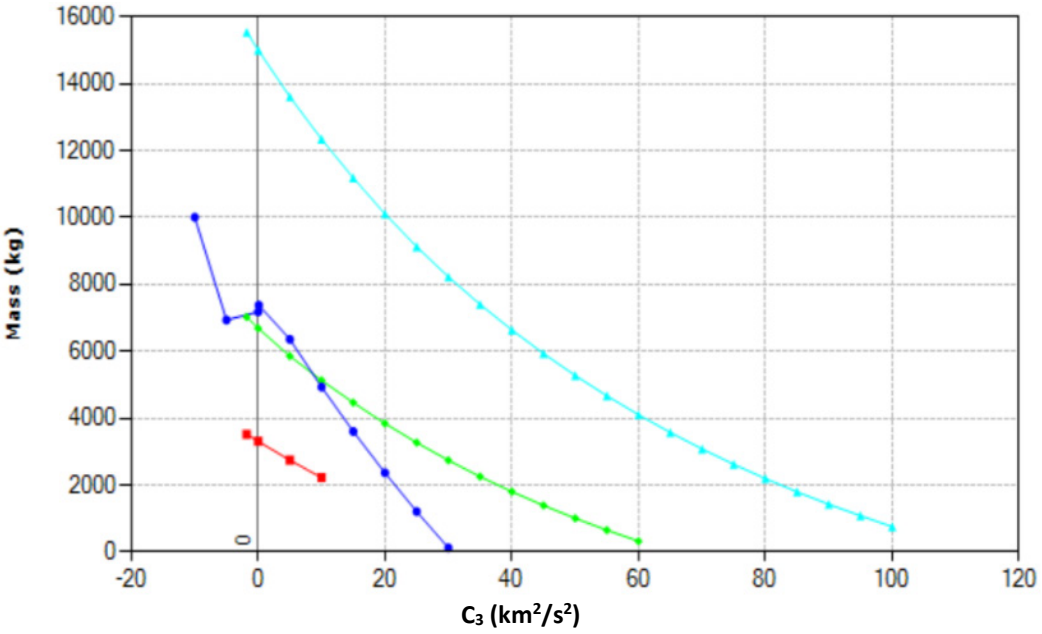

Figure 2.5.—Potential Launch Vehicles for given C_3 and Spacecraft Mass.

2.7.5 Chosen Design and Launch Vehicle Possibilities

More discussion is necessary to determine which trajectory to select. The two competing options are the Jupiter Flyby case and the EVEE case, each with their own benefits and detriments. The primary points of discussion are time of flight to fit the mission timeline and selection of launch vehicles for different required C_3 values. Figure 2.5 shows a plot of potential launch vehicles for a spacecraft's required C_3 and initial mass.

To further point out the restrictions of the Direct case, a $C_3$of almost 110 km^2/s^2 would require a Falcon Heavy (expendable) with some type of upper stage. As such, it would limit the options available for spacecraft design, partly due to the small mass the spacecraft would need to have at launch. While the Jupiter flyby case also requires the Falcon Heavy (Expendable) as a launch vehicle, its C_3 of 90 km^2/s^2 provides more leeway for the spacecraft's mass. It is evident that the EVEE trajectory is particularly attractive in this regard, with a multitude of options available for launch vehicles at 10 km^2/s^2.

While this may seem to point to the EVEE trajectory as the obvious choice for the mission, its downside is its long time of flight with minimal room for changes in launch or arrival date. With departure in 2036 and arrival in 2047, the EVEE case pushes the boundaries of the mission timeline. The Jupiter flyby case becomes the attractive option for changes to the mission timeline, especially if NASA's Dragonfly mission is unable to provide significant data for landing sites at Titan soon after arrival. Departing Earth in 2038 and arriving at Titan at the end of 2045, the Jupiter flyby trajectory provides ample time for Dragonfly's data to be considered as well as for the science performed during the Titan sample return mission.

2.8 Titan Surface to Orbit Trajectory

The vehicle designed here uses two stages to launch from the surface into Titan orbit, and then a third in-space stage capable of multiple restarts was used to take the vehicle from Titan orbit to the Earth return trajectory. This section details the two-stage to orbit (TSTO) model and the resulting trajectory. The ascent was modeled using the Optimal Trajectories by Implicit Simulation (OTIS v4) software (Ref. 16), which is a 3-degrees of freedom (DOF) trajectory optimization program that has been used for a wide

range of mission and spacecraft design problems including the type described in this paper. The optimizer chooses a flight path within the constraints of the problem to minimize drag losses in the lower portion of the atmosphere against gravity losses accumulated through the ascent. Key parameters during the ascent, such as the time history of the vehicle masses, propellant usage, ascent times and mission ΔV were tracked and reported to the Compass Team for design considerations.

The ascent vehicle is modeled as a 3800 kg, gross lift-off mass (GLOM), TSTO vehicle initially at rest on the surface of Titan. The ascent was designed to insert the vehicle into a "low" Titan orbit (LTO) where it would then begin its return leg to Earth. The LTO was defined for this study as a 1000 km, circular orbit which was believed to be sufficiently above Titan's atmosphere to resist the effects of atmospheric drag.

The GLOM for the Titan launch vehicle was set to 3800 kg and includes the landed mass of the ascent vehicle, the Titan sample to be returned and the mass of the propellant required to complete the mission. The numerical objective function for OTIS was the maximum delivered mass to the final LTO.

A key feature of the ascent trajectory designed for this analysis is a burn-coast-burn ascent where a first burn (achieved by the both the first and second stages) is used to ascend above Titan's atmosphere and raise the altitude of apoapsis to nearly 1000 km. The initial burn is followed by a coast to apoapsis, and a final circularization burn by the second stage. Coasting during the ascent reduces propellant requirements and mission ΔV and is possible because of Titan's low gravity (1.352 m/s^2), which is ~13 percent of that of Earth gravity. This coast is only possible once the vehicle is sufficiently above the densest portion of Titan's atmosphere to minimize drag losses during the coast. Alternative ascent profiles are possible but were not considered for this study.

The ascent profile is modeled with pitch-only, in-plane steering. The trajectory considered was designed to minimize drag losses in the lower atmosphere by implementing a long, vertical climb to a high, but optimally determined (bounded > 30 km) altitude. The initial, vertical flight was followed by an optimal pitch over phase to a flight path angle (FPA) = (75° to 89.9°) and a ramp to zero lift angles. The condition of zero-lift was held for flight through maximum dynamic pressure (max Q). Once through max Q, the zero-lift hold on controls was released and the remainder of the ascent used fully time-varying, optimal pitch control. The first stage was jettisoned at an altitude between 33 and 35 km. This altitude was selected as the range where second stage I_{sp} was equal to or higher than the first stage (Figure 2.6). This condition also supported a vehicle design condition that the propellent would be nearly equally split between the first and second stages. Upon first stage jettison, the second stage continued the powered ascent until an apoapsis altitude of ~1000 km was achieved, and the engine was shut off which initiated the coast portion of the burn-coast-burn trajectory design. The trajectory includes a jettison phase for a small payload faring before second stage shut off at an altitude of 150 km. For simplicity, this jettison is modeled as a zero-time phase with no interruption to the burn. Once the vehicle coasts to apoapsis, the second stage was re-ignited to raise periapsis, circularize, and complete the ascent.

2.8.1 Propulsion Model

Propulsion details for the first and second stages of the ascent vehicle are presented in Figure 2.6. The first stage propulsion was modeled as two engines, each with maximum sea level thrust of 6.2 kN and an I_{sp} of 270 s. First stage vacuum thrust was approximately 7kN with an I_{sp} of 317 s. The second stage propulsion was modeled as a single engine with a maximum sea level thrust of 1.2 kN and I_{sp} of 200 s. Second stage vacuum thrust was 7.6 kN with an I_{sp} = 340s.

Both the first and second stage propulsion models included a time-varying, optimal throttle with a range of 25 to 100 percent. Staging was triggered at an altitude where first and second stage I_{sp} were nearly equal (~33 km). The staging condition is indicated on the plot of I_{sp} in Figure 2.6.

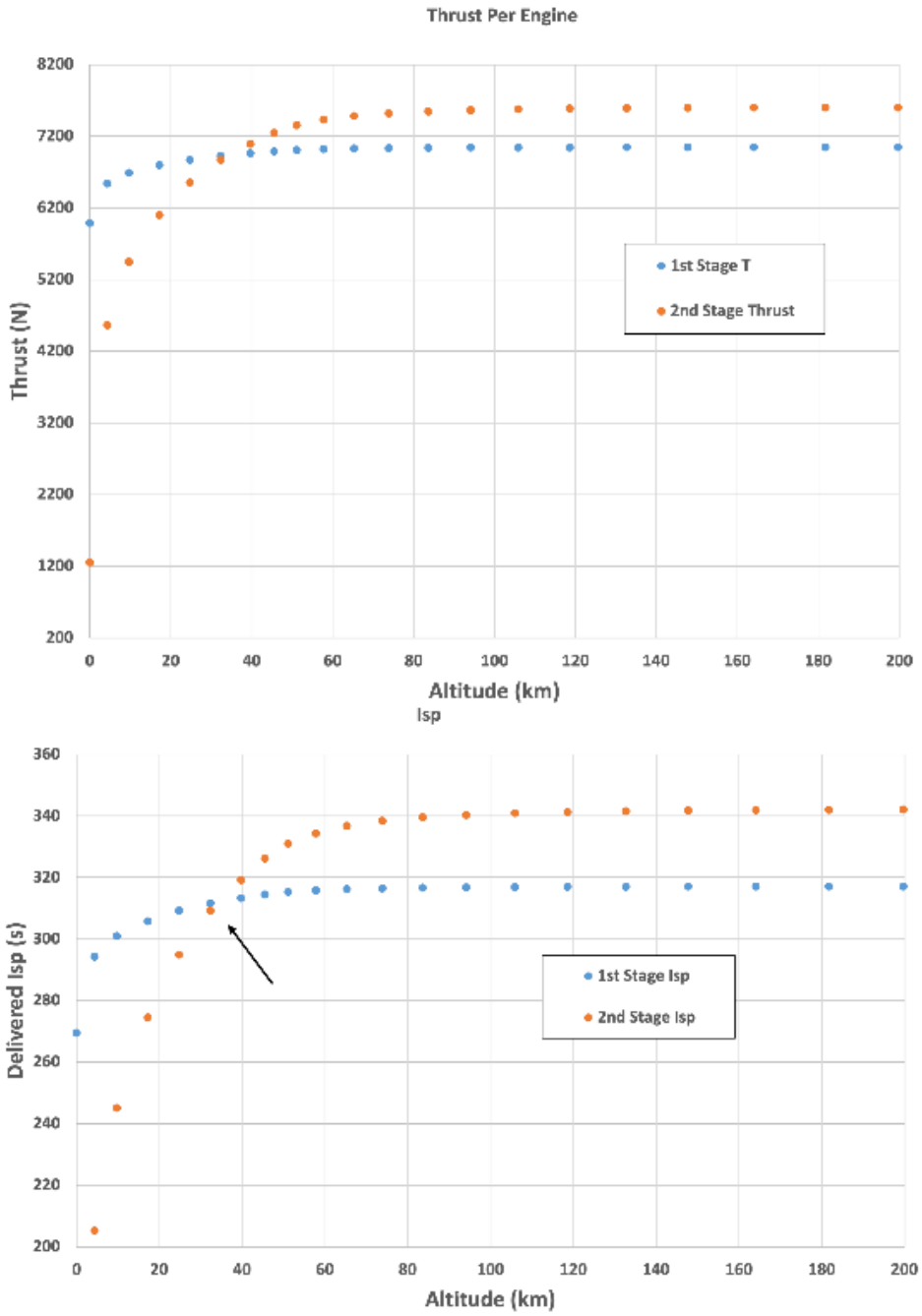

Figure 2.6.—Propulsion for the First and Second Stages with the Approximate Staging Point (alt ~33 km).

2.8.2 Atmosphere and Drag Models

Given the thick and dense atmosphere of Titan, drag losses were anticipated to be a significant aspect of the ascent profile and a critical contributor to the overall ΔV requirements and propellant consumed. Drag was modeled assuming the vehicle was a generic "missile" shape with a drag area of 1.23 m^2 (diameter = 1.25 m). Mach dependent drag coefficient (Cd) were input into OTIS's standard drag model to compute drag forces. Figure 2.7 plots the Mach dependent function of Cd, peaking at a value ~0.55 at Mach 1. For this analysis, coefficients of lift (Cl) and cross-forces (Cc) are assumed to be negligible (Cl = Cc = 0). The effects of winds were not considered for this analysis.

The atmosphere data used in the model were obtained from tables of atmospheric density (ρ), temperature (T) and pressure (P). Plots of these data are included in Figure 2.8 to Figure 2.10 and are described in detail in Wait, et al. (2013) (Ref. 17). Input data are plotted in blue in Figure 2.8 to Figure 2.10, while output from OTIS to an altitude of 1000 km are plotted in yellow and are included as a consistency check on the OTIS atmosphere model.

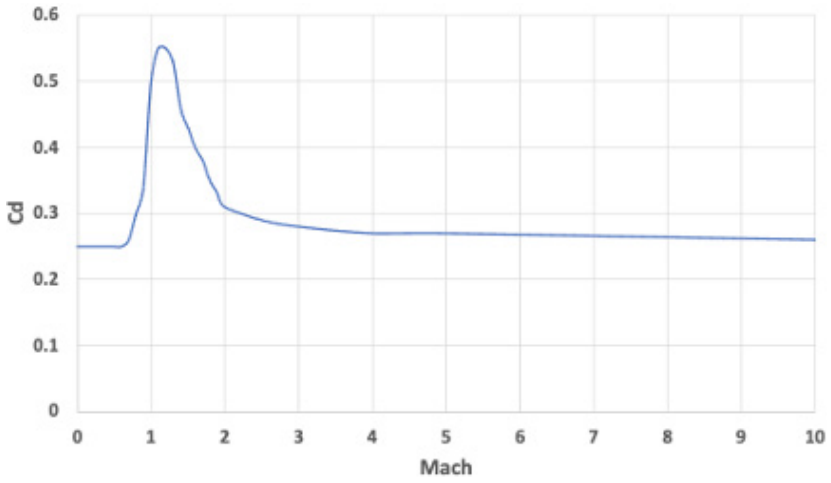

Figure 2.7.—Drag Coefficient (Cd) as a Function of Mach.

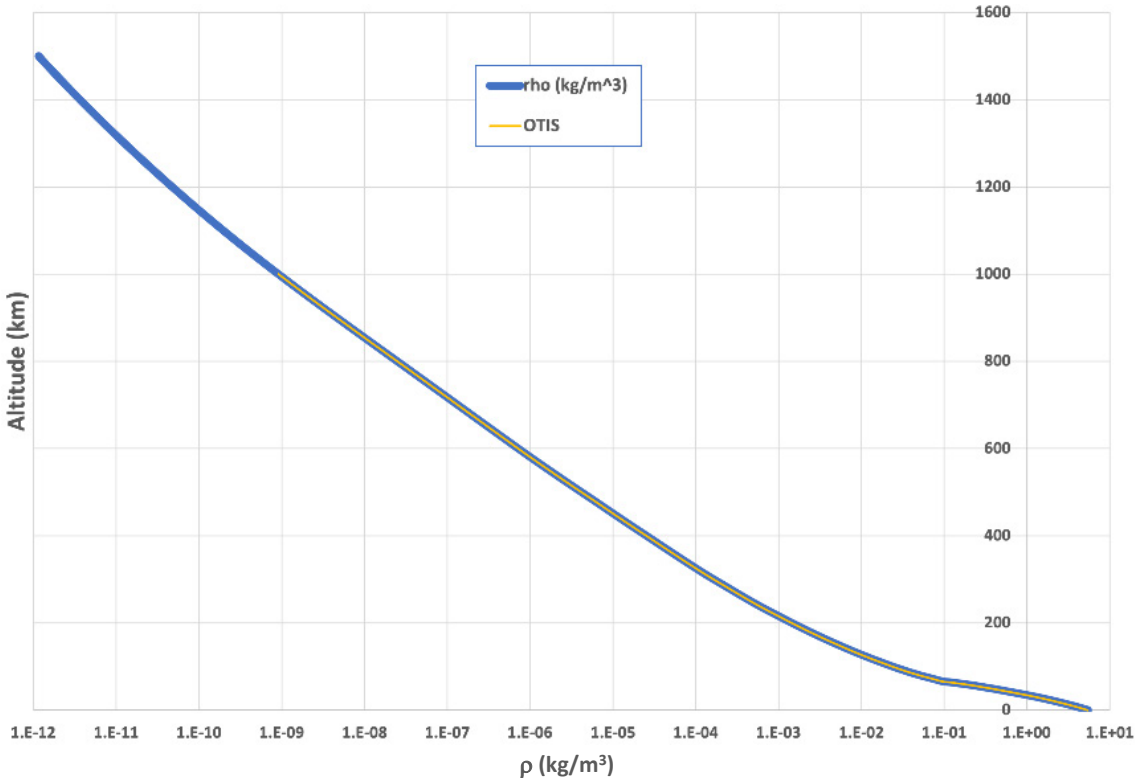

Figure 2.8.—Atmospheric Density Data for Titan. Data Input Data is (blue) and OTIS Output to 1000 km (yellow).

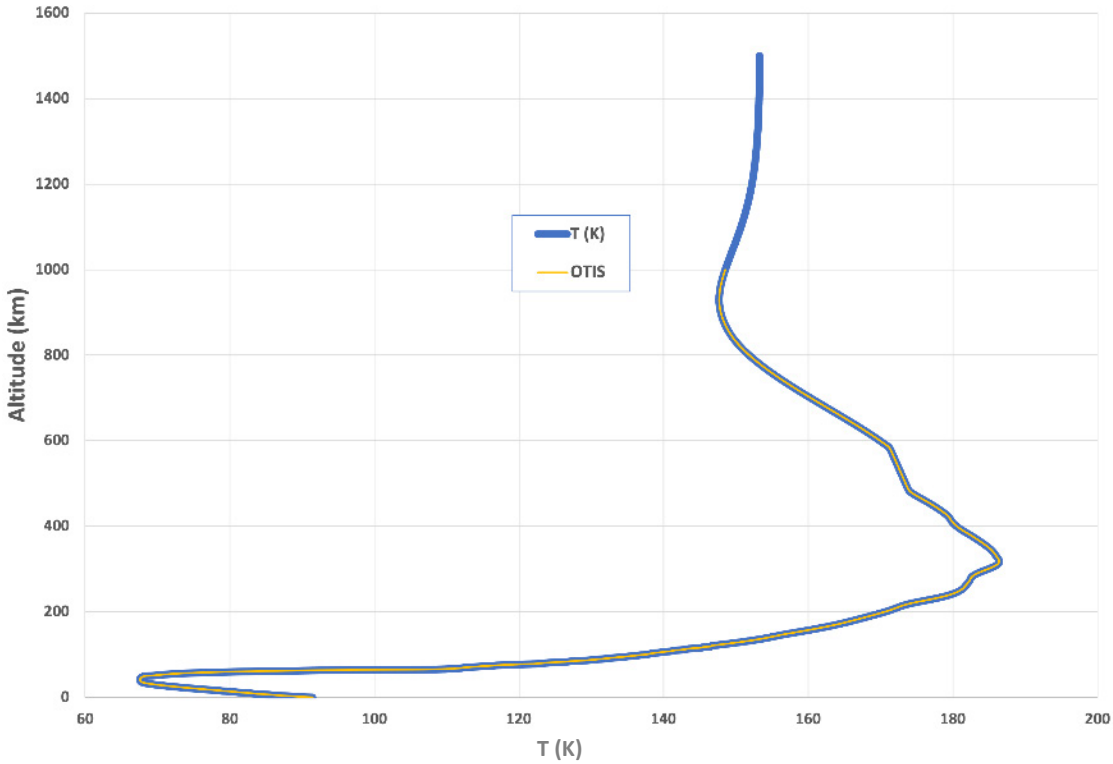

Figure 2.9.—Atmospheric Temperature Data for Titan. Data Input Data is (blue) and OTIS Output to 1000 km (yellow).

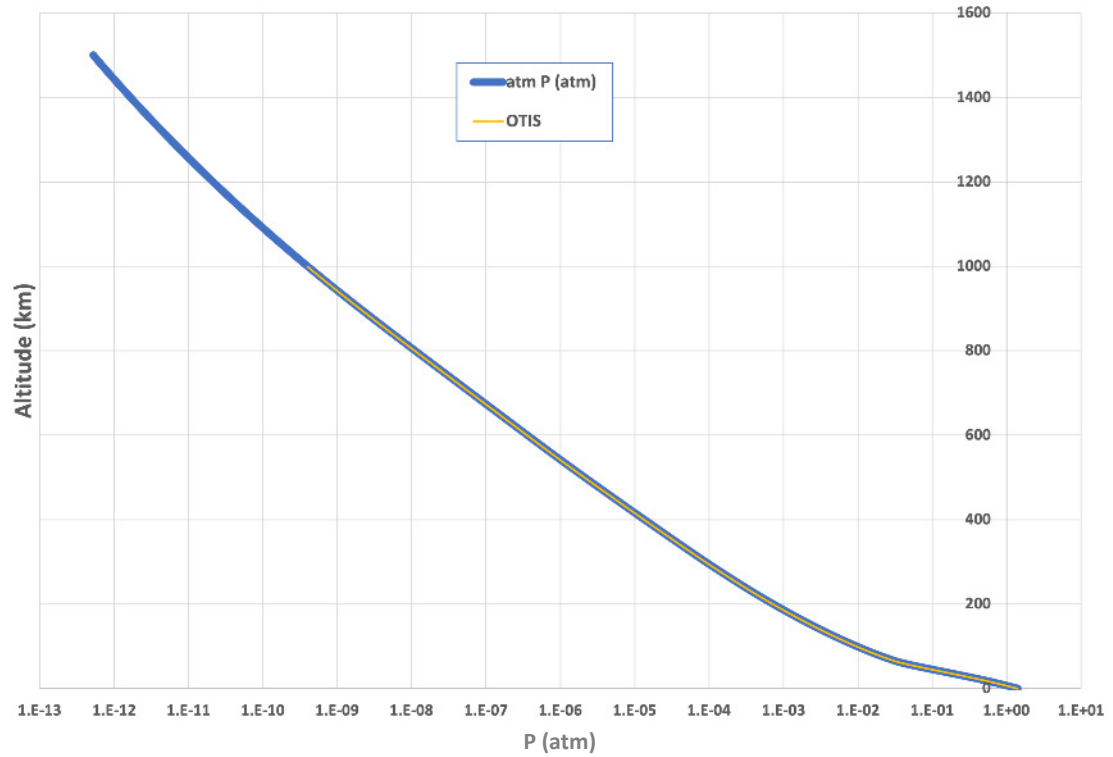

Figure 2.10.—Atmospheric Pressure Data for Titan. Data Input Data is (blue) and OTIS Output to 1000 km (yellow).

2.8.3 Results – Case 1

Results for the launch vehicle ascent optimization are summarized in Table 2.4. As described in the previous paragraphs and as indicated in Table 2.4, the GLOM for the launch vehicle is 3800 kg, which is input as the total wet mass at the time of launch. The launch vehicle delivers a burn out mass of 1009 kg to orbit. The entire trajectory consumes 2577 kg of propellant to achieve a total ΔV of 3.964 km/s. The initial climb to initial engine cut-off (second stage) takes 23 min and consumes 2516 kg of propellant and accounts for nearly 3.7 km/s of the total ΔV. The coast between the initial climb and the final circularization burn is 50 min in duration. The circularization burn consumes approximately 61 kg of propellant and accounts for approximately 0.2 km/s of the total ΔV. The propellant splits between the first and second stages are 1136 and 1441 kg, respectively. The first stage accounts for 1.037 km/s of the total ΔV, while the second stage accounts for the remining 2.927 km/s.

Plots of implicit solution for altitude, velocity and dynamic pressure are shown in Figure 2.11. The trajectory is characterized by a slow, vertical ascent to an altitude > 30 km where it begins a slow pitch over. Much of the pitch over occurs at an altitude closer to 40 km. Initial thrust to weight ratio (T/W) = 2 and is maintained at or near that value through optimal throttling through the majority of the first stage ascent while the vehicle is in Titan's atmosphere. The initial ascent is very slow as OTIS reduces the throttle to minimize drag losses. Velocity for the vehicle during the first stage of the ascent is typically below 100 m/s. It does not increase until the second stage ignites and the vehicle is significantly above the atmosphere.

Total ΔV requirements for this study are higher than those reported in a similar study presented in Donahue (2010) (Ref. 18). These results indicate that the total ΔV of approximately 4 km/s is required to complete the mission (Table 2.4) while Donahue (Ref. 18) reported a total ΔV on the order of 3.3 km/s. However, it should be noted that when looking at the figures in the Donahue paper (Ref. 18), the reported value may only be for the initial climb 300 km. This roughly corresponds to the first powered climb in this study divided between the first and second stages (ΔV ~3.76 km/s). Additional differences between the studies may arise from differences in the underlying drag and atmosphere models and ascent profiles.

TABLE 2.4.—TITAN ASCENT VEHICLE RESULTS

GLOM (kg)	3800		
initial T/W	2.0		
BO mass (kg)	1009		
	Stage 1:	stage 2:	
initial mass (kg)	3800	2472	
BO mass (kg)	2665	1009*	*b.o. alt (km)*
stage 1 drop (kg)	*-193*		*33.0*
final mass (kg)	2472	1009*	
			Total
ΔV (km/s)	1.037	2.927	3.964
prop (kg)	1136	1441	2577
	**includes fairing drop 22.5 kg*		
Flight Phase	Δt (min)	ΔV (km/s)	prop (kg)
Climb	22.6	3.766	2516
Coast to Apoapsis	48.8	0.000	0
Circ Burn	0.7	0.198	61
Total:	72.13	3.964	2577

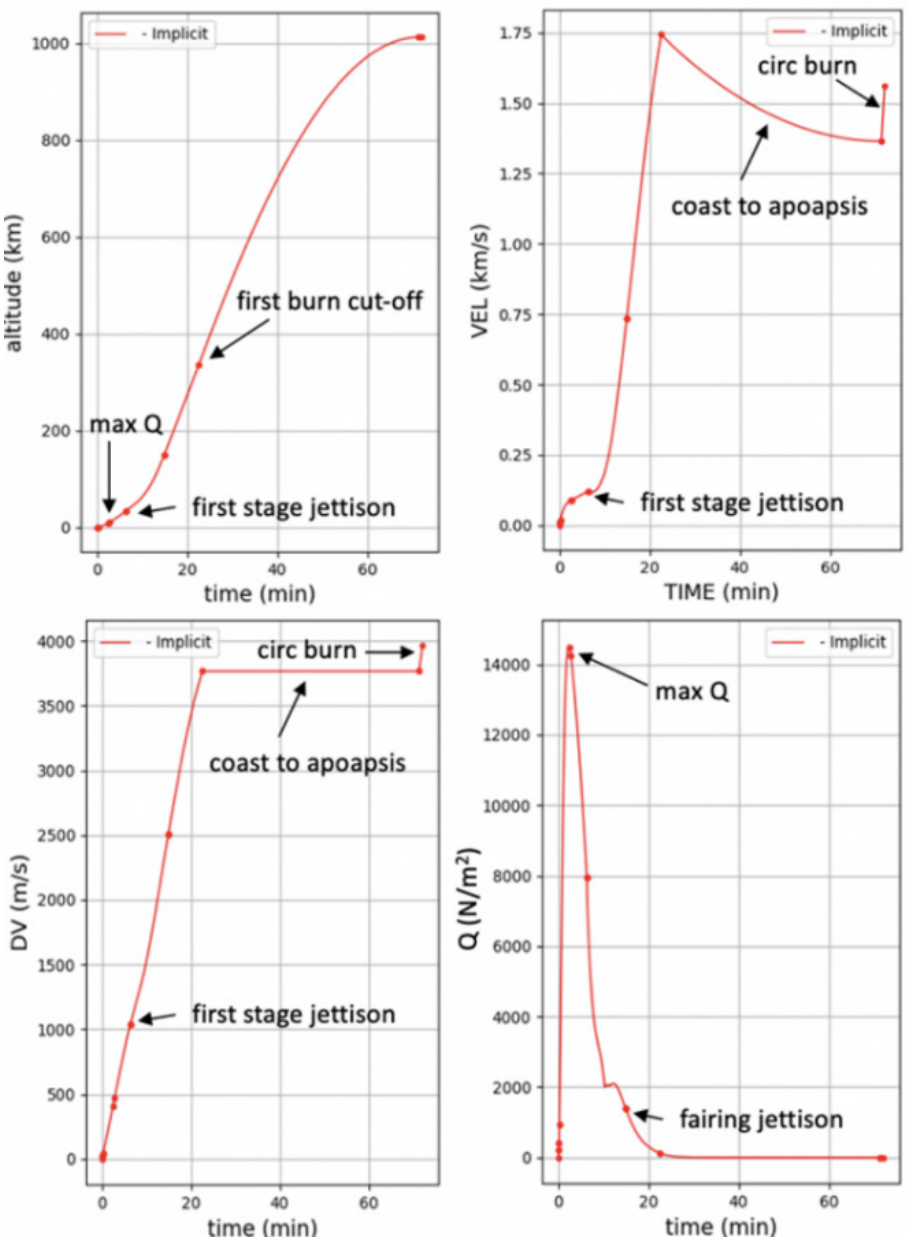

Figure 2.11.—Time History of Altitude, Velocity, ΔV and Dynamic Pressure for the Ascent.

2.8.4 High Altitude Launch

The model detailed in the previous section was modified to a single stage to orbit (SSTO) launch, with multiple versions simulated from various altitudes to assess the ΔV requirements of a high-altitude launch. Launch altitudes ranging from 45 to 50 km above Titan's surface were evaluated and summarized in Figure 2.12. For these simulations, the platform itself was not modeled but is intended to represent a launch from a platform such as balloon or fixed rotor vehicle. The platform is assumed to be at rest with respect to the surface of Titan at the time of launch. Should high altitude launches be considered in the future, a more detailed approach would be necessary.

The vehicle was simulated for a horizontal launch with an assumed GLOM of 1500 kg. The burn-coast-burn character of the ascent trajectory was like the one described for the baseline surface launch with a few notable exceptions. Instead of a vertical launch, as was the case with the surface simulation, the horizontal launch was initiated with a fixed 5 s drop generally resulting in a 20-m separation between the ascent vehicle and the platform and a slightly negative flight path angle before ignition of the engine. The vehicle then began an optimal pitch flight profile through a "pitch-up" and powered climb to an apoapsis altitude of 1000 km and at altitude above 200 km. Once this condition was achieved, the engine shut off and the vehicle coasted to apoapsis where it did a brief circularization burn. The results plotted in Figure 2.12 represent the total ΔV and sum of both burns.

Results from the analysis illustrated in Figure 2.12 indicate a potential ΔV savings of 1 to 1.5 km/s when launching between 45 and 100 km. The potential savings to the ascent vehicle by launching at altitude would need to be compared to the overall mission complexity of requiring a platform to be raised to altitude to achieve the launch. This requires further investigation.

2.8.5 Model Sensitivity to Drag Area

An early version of the TSTO model was used as the baseline case to evaluate the sensitivity of drag on the ascent. The version of the model used for this sensitivity analysis was like the final version but differed in the steering strategy and throttling. This version of the model had a higher overall ΔV equal to 4.2 km/s. The results of this analysis are illustrated in Figure 2.13 with ΔV and the drag loss plotted as a function of the percentage change in the base drag area.

For the range of drag areas considered, the resulting increase to ΔV with increasing drag area was nearly linear with an increase in ΔV of nearly 600 m/s with a 50 percent increase in drag area. It should be noted that a 50 percent increase in drag area results by increasing the vehicle diameter from 1.25 to 1.53 m (+28 cm) and is an indication of the highly sensitive nature of drag and Titan's atmosphere in the ascent profile.

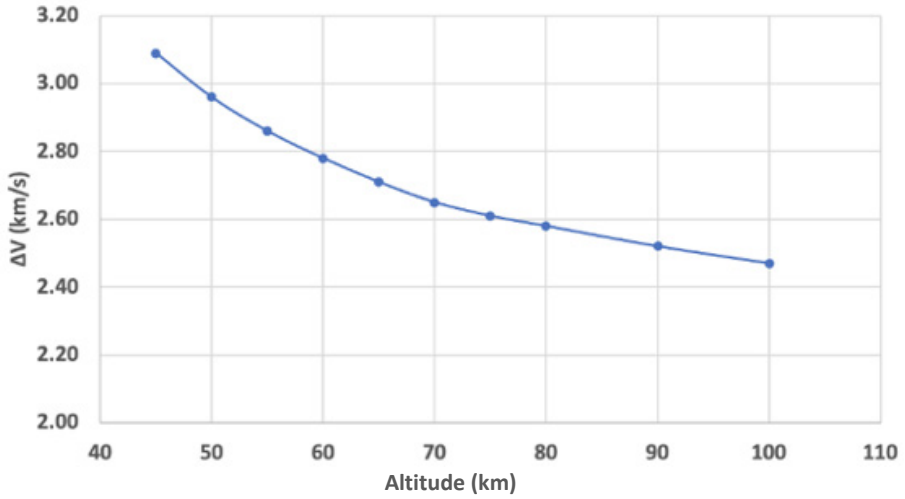

Figure 2.12.—Total ΔV for a SSTO Ascent Vehicle Launched from Various Altitudes Above Titan's Surface.

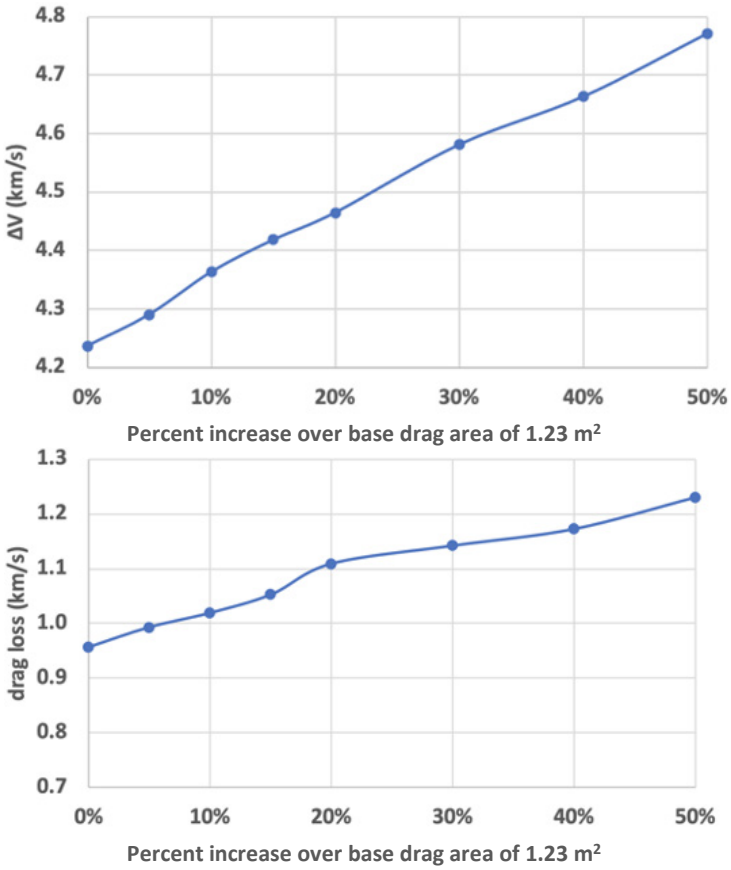

Figure 2.13.—Resulting ΔV and Drag Loss Terms for a Representative TSTO Mission. Results Are Plotted as a Function of Percent Increase in Drag as Compared to the Base Drag Area of 1.23 m^2.

2.9 Return In-Space Trajectory

A direct departure from Titan orbit to Earth requires an impulsive ΔV of 3 km/s, with a flight time of 5.87 years. Use of a Jupiter flyby to decrease the transit ΔV was considered. This can reduce the required ΔV by 0.5 to 0.8 km/s compared to the direct injection, but the required orbital position was not available in the assumed time frame of the mission, and so the Jupiter gravity assist was not considered.

To minimize the ΔV required for leaving the Saturn system into a trajectory toward Earth, a number of different trajectories were analyzed. The approach taken was to escape from Titan orbit into a Saturn-centric orbit followed by a series of flyby passes of Titan to increase the eccentricity and raise the apoapsis. This is then followed by a burn to lower the periapsis to a close pass over the Saturn cloudtops, and at the periapsis pass, a final burn of about 0.5 km/s injects the vehicle into the trans-Earth trajectory. The trajectory is shown in Figure 2.14.

The minimal allowable Saturn periapsis was chosen based on the closest pass by the Cassini orbiter before encountering enough atmosphere for the spacecraft's orientation to be affected by atmospheric torque. This occurred during Cassini orbit 274, during which Cassini passed 2,660 km of Saturn's 1-bar level. Subsequent orbits lowered this periapsis to as low as 2,500 km above Saturn's visible atmosphere but required Cassini's reaction control thrusters to correct the spacecraft's orientation to offset the torque imparted by atmospheric drag (Ref. 19).

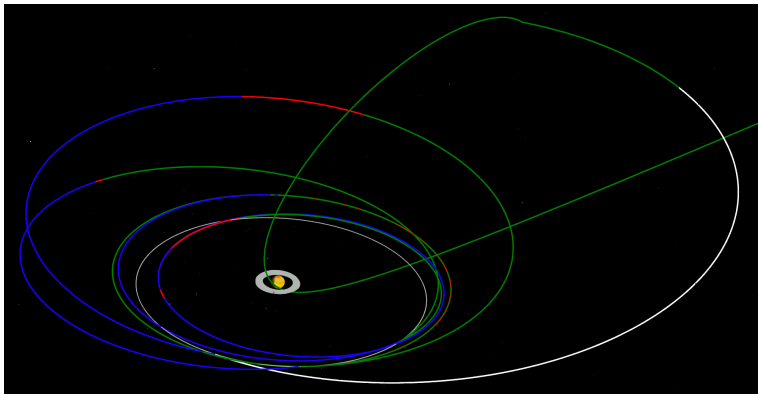

Figure 2.14.—Saturn/Titan Flybys to return sample to Earth.

TABLE 2.5.—SATURN/TITAN FLYBY TOUR TO MINIMIZE RETURN VEHICLE IN-SPACE ΔV

Maneuver	Delta-V (m/s)	Time Elapsed (days)
Titan Departure	693.15	0.00
Tour #1	75.00	54.12
Flyby # 1	-	66.30
Tour #2	24.67	78.03
Flyby #2	-	98.03
Tour #3	68.75	114.70
Flyby #3	-	128.15
Tour #4	36.55	160.97
Flyby #4	-	190.66
Periapsis Lowering	621.95	285.47
Saturn Departure	505.89	365.25
Total	2025.96	2405.37

The lowest ΔV solution found made five Titan flybys before periapsis lowering maneuver and Saturn pass, resulting in a ΔV for the Earth injection of 1.55 km/s. This solution required a duration of 31.5-months for the Saturn system portion of the return. To reduce this time spent in Saturn orbit, a trajectory with four Titan flybys was selected, resulting in a 2 km/s, 12-month sequence. The flyby sequence and ΔVs are summarized in Table 2.5 (Refs. 20 and 21).

2.9.1 Mission Delta-Velocities (ΔV) Details

The results of the mission design and analysis discussed in the previous mission descriptions were incorporated into an iterative process which actively accounts for changes in mass across all subsystems. Additionally, robustness was added to the mission design by including propellant margin, statistical maneuver propellant allotments, and by accounting for propulsive attitude control maneuvers that occur throughout the mission.

Propulsion system parameters were gathered from the mission design and from the propulsion subsystem design when modelling the propulsive maneuvers identified in Table 2.6 and Table 2.7. An iterative process which utilizes the standard rocket equation is used to calculate the propellant used for each propulsive event considered.

2.9.1.1 Mission Stage 1 – Saturnian Operations

Table 2.6 summarizes the sequence of events, which occur from Titan launch through return vehicle deployment.

This segment of the overall mission can be broken into nine phases. The first phase lasts from first stage ignition until just prior to the first stage separation. An additional 1 percent of the deterministic ΔV is assumed to be used to steer the vehicle and correct for atmospheric disturbance torques. This item appears as "First Stage ACS" in Table 2.6. The total ΔV and propellant, broken into Main and reaction control system (RCS) contributions, is highlighted by the first yellow row.

The second phase begins with the separation of the first stage. The change in mass for this event can be seen in the final column. A several second coast is built into the ascent trajectory to allow for adequate separation of the two stages before the second stage ignites and performs its first of two burns. As before, an additional 1 percent of the deterministic ΔV is carried for attitude control. After the first burn completes, the stack coasts up to the second burn point. Once outside of the dense portion of the atmosphere, the fairing is jettisoned, exposing the RV to the tenuous atmosphere and enabling additional control and navigational aids. Additional RCS propellant on-board the RV is carried during this phase to account for any roll about the length of the stack that may have accumulated between first stage separation and the fairing jettison. Finally, the second stage completes the circularization burn placing the stack in a 1000 km circular orbit about Titan.

The next seven phases capture the events between and including second stage separation through RV separation. Phase 3 includes the events leading up to and including the Titan departure burn. Each of the next four phases takes place in between flybys of Titan and include the deterministic flyby targeting burns. Each flyby event increases the energy of the spacecraft orbit about Saturn, ultimately reducing the amount of ΔV required to escape the Saturnian system.

Phase 8 sets up the powered Saturn flyby by lowering the periapsis of the spacecraft orbit and phase 9 is represented by the powered flyby. The propellant required to perform attitude control during coast segments and leading up to planned burns is carried by the RV. Attitude control during the targeting burns and departure burns is accomplished by pulsing the 20 lbf engines on the aft end of the in-space stage.

A 6 percent propellant margin for all main propulsion system burns is carried as a reduction in I_{sp}. This effectively leads to the case where each deterministic burn required the use of all margin devoted to it in order to accomplish the targeted goal. This is true for all nine phases shown in Table 2.6. A 10 percent RCS margin for all RCS burns performed by the RV during phases 2 through 9 is held as inert mass on-board the RV.

TABLE 2.6.—MISSION ΔV SUMMARY FOR SATURNIAN OPERATIONS

Mission DeltaV Summary											
Titan Sample Return: Launch and In-Space Stages											
Phase #	Phase Name	Pre-Event Mass (kg)	Main Chem DV (m/s)	ACS DV (m/s)	Main Isp (s)	ACS Isp (s)	Main Chem Prop (kg)	ACS Prop (kg)	Payload Mass Change (kg)	Post-Event Mass (kg)	Change In Mass (kg)
1	First Stage Launch	3925	1020	0.00	287		1194.12	0.00	0	2730	1194.12
	First Stage ACS	2730	10	0.00	287		9.89	0.00	0	2721	9.89
	First Stage Total		**1030**				**1204**				
2	First Stage Separation	2472	10	0.00	321		7.83	0.00	0	2464	256.21
	Ascent Burn	2464	2530	0.00	321		1359.80	0.00	0	1105	1359.80
	Ascent Burn ACS	1105	26	0.00	321		9.14	0.00	0	1095	9.14
	Fairing Separation	0	0	0.00			0.00	0.00	0	1062	33.16
	Coast ACS-2	1062	0	0.93		231	0.00	0.44	0	1062	0.44
	Orbit Insertion Burn	1062	390	0.00	321		123.58	0.00	0	938	123.58
	Second Stage Total		**2956**	**1**			**1500**	**0.44**			
3	Second Stage Separation	694	0	0.00			0.00	0.00	0	694	243.45
	Null Tip-off Rates	694	0	0.002		231	0.00	0.001	0	694	0.001
	Slew to burn attitude	694	0	0.002		231	0.00	0.001	0	694	0.001
	Titan departure	694	639	0.20	329	329	124.65	0.04	0	569	124.70
	Slew to cruise attitude	569	0	0.003		231	0.00	0.001	0	569	0.001
4	Leg-1 ACS	569	0	0.21		231	0.00	0.05	0	569	0.05
	Slew to burn attitude	569	0	0.003		231	0.00	0.001	0	569	0.001
	Tour 1	569	20	0.20	329	329	3.58	0.04	0	565	3.61
	Slew to cruise attitude	565	0	0.003		231	0.00	0.001	0	565	0.001
5	Leg-2 ACS	565	0	0.21		231	0.00	0.05	0	565	0.05
	Slew to burn attitude	565	0	0.003		231	0.00	0.001	0	565	0.001
	Tour 2	565	45	0.20	329	329	7.83	0.04	0	557	7.87
	Slew to cruise attitude	557	0	0.003		231	0.00	0.001	0	557	0.001
6	Leg-3 ACS	557	0	0.21		231	0.00	0.05	0	557	0.05
	Slew to burn attitude	557	0	0.003		231	0.00	0.001	0	557	0.001
	Tour 3	557	42	0.20	329	329	7.21	0.03	0	550	7.24
	Slew to cruise attitude	550	0	0.003		231	0.00	0.001	0	550	0.001
7	Leg-4 ACS	550	0	0.21		231	0.00	0.05	0	550	0.05
	Slew to burn attitude	550	0	0.003		231	0.00	0.001	0	550	0.001
	Tour 4	550	67	0.20	329	329	11.32	0.03	0	539	11.35
	Slew to cruise attitude	539	0	0.003		231	0.00	0.001	0	539	0.001
8	Leg-5 ACS	539	0	0.22		231	0.00	0.05	0	539	0.05
	Slew to burn attitude	539	0	0.003		231	0.00	0.001	0	539	0.001
	Periapsis Lowering	539	598	0.20	329	329	91.14	0.03	0	448	91.18
	Slew to cruise attitude	448	0	0.004		231	0.00	0.001	0	448	0.001
9	Leg-6 ACS	448	0	0.26		231	0.00	0.05	0	448	0.05
	Slew to burn attitude	448	0	0.004		231	0.00	0.001	0	448	0.001
	Saturn Departure	448	472	0.20	329	329	60.94	0.03	0	387	60.97
	Slew to cruise attitude	387	0	0.004		231	0.00	0.001	0	387	0.001
	In-Space Stage Total		**1884**	**2.8**			**307**	**0.56**			
	Total		**5870**	**3.7**			**3011**	**1.00**			

2.9.1.2 Mission Stage 2 – Earth Return

The sequence of events between and including the RV deployment through sample entry, descent, and landing (EDL) system deployment are summarized in Table 2.7.

The Earth return segment of the mission can be categorized in six phases. Phase 1 reiterates the separation of the RV from the in-space stage and the associated tip-off rate clean-up. Also shown is a recap of the Titan flyby tour and ascent RCS used by the RV. These events are not being double book kept.

Phase 2 begins with the spin-up of the RV about a body axis which is ideally parallel to the fixed parabolic antenna boresight pointing direction. Once a spin rate of 5 rpm is achieved the RV enters a hibernation state where it passively monitors its spin orientation, exiting hibernation to correct excessive error build up in the spin-stabilized pointing direction. Prior to the first Trajectory Correction Maneuver (TCM), the RV will exit hibernation and precess its spin axis such that the parabolic antenna points towards Earth. A burn plan is uploaded and a TCM is performed if necessary. The spin axis is once again precessed towards the Sun and the RV enters a hibernation state again. The next three phases mimic the second.

Phase 6 starts with a spin down from 5 rpm to prepare for the sample EDL system deployment. This occurs hours prior to the sample entry into Earth's atmosphere to keep the sample at a low temperature. The RV orients itself such that the apex of the EDL heat shield points in the nominal deployment direction. The RV spins up to 5 rpm about this axis then deploys the sample. The sample system maintains this spin rate post-deploy, effectively becoming passively spin-stabilized prior to entering Earth's atmosphere. The RV performs a small separation maneuver before entering destructively in Earth's atmosphere.

2.9.2 Redundancy

Due to the projected class of mission, a single fault tolerant approach is used for this design. Exceptions are made for the fuel tanks, structures, DRPS, and rover. Future iterations of this design will continue to refine and update this approach.

2.10 Growth, Contingency, and Margin Policy

The mass growth, contingency, and mass margin policy used by the Compass Team is congruent with the standards described in American Institute for Aeronautics and Astronautics (AIAA) S–120A-2015 (2019) (Ref. 22). This methodology starts with the basic mass of the components and adds the mass growth allowance (MGA). This subtotal is defined as the predicted mass. Mass margin is then added to the predicted mass to calculate the allowable mass. The aerospace community typically refers to the mass margin as system level growth. Figure 2.15 shows this pictorially.

TABLE 2.7.—MISSION ΔV SUMMARY FOR EARTH RETURN

Mission DeltaV Summary											
Titan Sample Return: Return Vehicle											
Phase #	Phase Name	Pre-Event Mass (kg)	Main Chem DV (m/s)	ACS DV (m/s)	Main Isp (s)	ACS Isp (s)	Main Chem Prop (kg)	ACS Prop (kg)	Payload Mass Change (kg)	Post-Event Mass (kg)	Change In Mass (kg)
1	Tour ADC	713	0	4.86		231	0.00	1.53	0	712	1.53
	Null Tip-Off Rates	229	0	0.20		231	0.00	0.02	0	229	0.02
2	Slew to Spin Stabilized Attitude	229	0	0.10		231	0.00	0.01	0	229	0.01
	Spinup	229	0	1.50		231	0.00	0.15	0	229	0.15
	Maintain Spin Stabilized Attitude	229	0	0.03		231	0.00	0.003	0	229	0.003
	Precess to/from COMM Attitude	229	0	0.93		231	0.00	0.09	0	229	0.09
	Precess to TCM Attitude	229	0	0.10		231	0.00	0.01	0	229	0.01
3	TCM-1	229	20	0.10	245	231	1.90	0.01	0	227	1.91
	Precess to Spin Stabilized Attitude	227	0	0.10		231	0.00	0.01	0	227	0.01
	Maintain Spin Stabilized Attitude	227	0	0.03		231	0.00	0.003	0	227	0.003
	Precess to/from COMM Attitude	227	0	0.93		231	0.00	0.09	0	227	0.09
	Precess to TCM Attitude	227	0	0.10		231	0.00	0.01	0	227	0.01
4	TCM-2	227	45	0.10	245	231	4.21	0.01	0	223	4.22
	Precess to Spin Stabilized Attitude	223	0	0.10		231	0.00	0.01	0	223	0.01
	Maintain Spin Stabilized Attitude	223	0	0.03		231	0.00	0.003	0	223	0.003
	Precess to/from COMM Attitude	223	0	0.93		231	0.00	0.09	0	222	0.09
	Precess to TCM Attitude	222	0	0.10		231	0.00	0.01	0	222	0.01
5	TCM-3	222	45	0.10	245	231	4.13	0.01	0	218	4.14
	Precess to Spin Stabilized Attitude	218	0	0.10		231	0.00	0.01	0	218	0.01
	Maintain Spin Stabilized Attitude	218	0	0.03		231	0.00	0.003	0	218	0.003
	Precess to/from COMM Attitude	218	0	0.93		231	0.00	0.09	0	218	0.09
6	Spin Down	218	0	1.50		231	0.00	0.14	0	218	0.14
	Min Time Slew to Deploy Attitude	218	0	2.50		231	0.00	0.24	0	218	0.24
	Spinup To 5 RPM	218	0	3.20		231	0.00	0.31	0	218	0.31
	Deploy Sample	218	0	0.10		231	0.00	0.01	0	218	0.01
	Total		**110**	**19**			**10**	**3**			

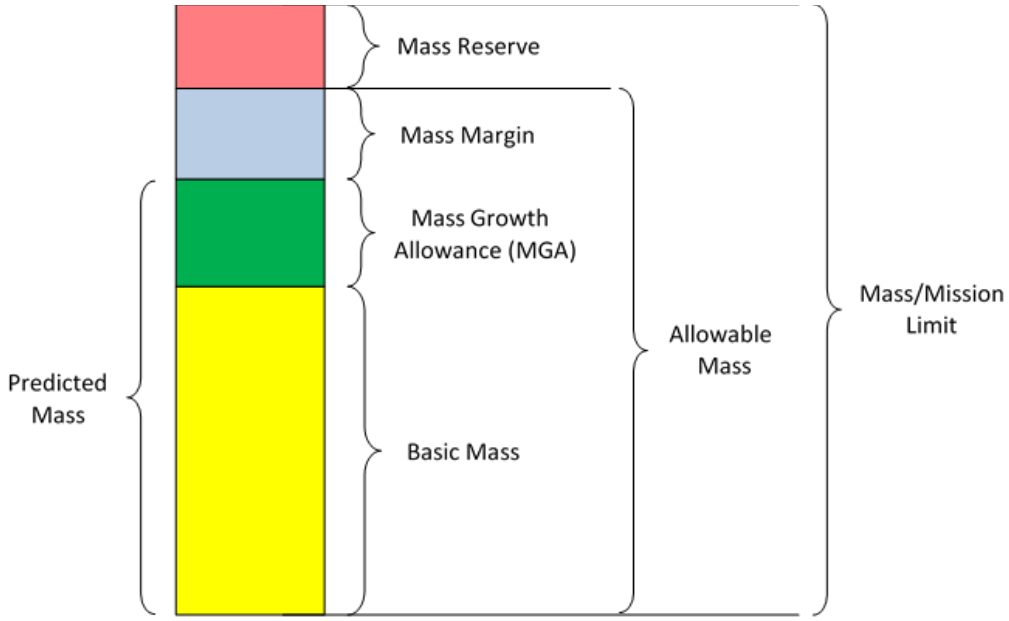

Figure 2.15.—Graphic of General Mass Definitions.

2.10.1 Terms and Definitions Regarding Mass

Mass *The measure of the quantity of matter in a body.*

Basic Mass (aka CBE Mass) *Mass data based on the most recent baseline design. This is the bottoms-up estimate of component mass, as determined by the subsystem leads.*

Note 1: This design assessment includes the estimated, calculated, or measured (actual) mass, and includes an estimate for undefined design details like cables, multi-layer insulation, and adhesives.

Note 2: The MGAs and uncertainties are not included in the basic mass.

Note 3: Compass has referred to this as current best estimate (CBE) in past mission designs.

*Note 4: During the design study, the Compass Team carries the propellant as line items in the propulsion system in the Master Equipment List (MEL). Therefore, propellant is carried in the basic mass listing, but MGA is **not** applied to the propellant. Margins on propellant are handled differently than they are on dry masses.*

CBE Mass *CBE mass. See Basic Mass.*

Dry Mass *The dry mass is the total mass of the system or spacecraft (S/C) when no propellant or pressurants are added.*

Wet Mass *The wet mass is the total mass of the system, including the dry mass and all of the pressurants and propellants (used, predicted boil-off, residuals, reserves, etc.*

Inert Mass *In simplest terms, the inert mass is what the trajectory analyst plugs into the rocket equation to size the amount of propellant necessary to perform the mission delta-Velocities (ΔVs). Inert mass is the sum of the dry mass, along with any non-used, and therefore trapped, wet materials, such as residuals and pressurants. When the propellant being modeled has a time variation along the trajectory, such as is the case with a boil-off rate, the inert mass can be a variable function with respect to time.*

Basic Dry Mass	*This is basic mass (aka CBE mass) minus the propellant, or wet portion of the S/C mass. Mass data is based on the most recent baseline design. This is the bottoms-up estimate of component mass, as determined by the subsystem leads. This does not include the wet mass (e.g., propellant, pressurant, cryo-fluids boil-off, etc.).*
CBE Dry Mass	*CBE dry mass. See Basic Dry Mass.*
Mass Growth Allowance	*MGA is defined as the predicted change to the basic mass of an item based on an assessment of its design maturity, fabrication status, and any in-scope design changes that may still occur.*
Predicted Mass	*This is the basic mass plus the mass growth allowance for to each line item, as defined by the subsystem engineers.* *Note: When creating the MEL, the Compass team uses Predicted Mass as a column header and includes the propellant mass as a line item of this section. Again, propellant is carried in the basic mass listing, but MGA is not applied to the propellant. Margins on propellant are handled differently than they are handled on dry masses. Therefore, the predicted mass as listed in the MEL is a wet mass, with no growth applied on the propellant line items.*
Predicted Dry Mass	*This is the predicted mass minus the propellant or wet portion of the mass. The predicted mass is the basic dry mass plus the mass growth allowance as the subsystem engineers apply it to each line item. This does not include the wet mass (e.g., propellant, pressurant, cryo-fluids boil-off, etc.).*
Mass Reserve (aka Margin)	*This is the difference between the allowable mass for the space system and its total mass. Compass does not set a mass reserve, it is arrived at by subtracting the total mass of the design from the design requirement established at the start of the design study, such as an allowable mass. The goal is to have a mass reserve greater than or equal to zero in order to arrive at a feasible design case. A negative mass reserve would indicate that the design has not yet been closed and cannot be considered feasible. More work would need to be completed.*
Mass Margin	*The extra allowance carried at the system level needed to reach the AIAA recommended "green" mass risk assessment level, which is currently set at >15 percent for the Authorization to Proceed program milestone. This value is defined as the difference between allowable mass and predicted mass, with the percentage being with respect to basic mass:* *percent Mass Margin = (Allowable Mass - Predicted Mass)/Basic Mass*100* *For the current Compass design process, a mass margin of 15 percent is applied with respect to the basic mass and added to the predicted mass. The resulting total mass is compared to the allowable mass as the design progresses. If the total mass is < than the allowable mass, then the mass margin is > 15 percent and the design closes while maintaining a "green" mass risk assessment level.* *If total mass ≥ allowable mass, then the design does not close with the required 15 percent mass margin, and either the total mass needs to be reduced, or the mass risk posture reevaluated, and the mass margin*

	reduced. However, depending on the numerical difference, the design may not close even if the mass margin is set to 0 percent.
System-Level Growth	*See Mass Margin*
Total Mass	*The summation of basic mass, applied MGA, and the mass margin (aka system-level growth).*
Allowable Mass	*The limits against which margins are calculated.*
	Note: Derived from or given as a requirement early in the design, the allowable mass is intended to remain constant for its duration.

Table 2.8 expands definitions for the MEL column titles to provide information on the way masses are tracked through the MEL used in the Compass design sessions. These definitions are consistent with those in Figure 2.15 and in the terms and definitions. This table is an alternate way to present the same information and provide more clarity.

For the conceptual level studies conducted by the Compass Team, a system mass margin of 15 percent based on basic dry mass is used, which is recommended in the AIAA standard (Ref. 22) for a grade of "green" at the authorization to proceed milestone (see Table 2.9). It is worth noting that the Compass Team assumes that a 30 percent MGA + Mass Margin is suitable for a green rating, providing there is more allowable mass that would fit the launch or delivery vehicle to push the percentage slightly above 30 percent. For all elements designed by the Compass Team for this study, a "green" rating was achieved. No margin or growth was carried on the lifting body to deliver the system to Titan. This mass is instead treated as an allocation.

TABLE 2.8.—DEFINITION OF MASSES TRACKED IN MEL

Item	Definition
Basic Mass	Mass data based on the most recent baseline design (includes propellants and pressurants)
	Basic Dry Mass + Propellants + Pressurants + Residuals
MGA (Growth)	Predicted change to the basic dry mass of an item phrased as a percentage of basic dry mass
	MGA percent * Basic Dry Mass = Growth
Predicted Mass	The basic mass plus the MGA
	Basic Dry Mass + Propellant + Growth

TABLE 2.9.—MASS RISK ASSESSMENT

Program Milestone	Recommended MGA (percent)	Recommended Mass Margin (percent)	MGA + Mass Margin (percent)	Grade
Authorization to Proceed	> 15	> 15	> 30	Green
	9 < MGA ≤ 15	10 < Mass Margin ≤ 15	19 < MGA + Mass Margin ≤ 30	Yellow
	≤ 9	≤ 10	≤ 19	Red

2.10.2 Mass Growth

In keeping with the in AIAA standard S–120A-2015(2019) (Ref. 22), Table 2.10 on the following page shows the percent mass growth of a piece of equipment based on both its level of design maturity and its functional subsystem. Note that for designs requiring propellant, propellant margin and residual is either carried in the propellant calculation itself or in the ΔV calculation used to determine the propellant required to fly a mission. Section 2.9.1, Mission Delta-Velocities (ΔV) Details, explicitly details how propellant margins were handled for each leg of the mission and each propellant type.

TABLE 2.10.—AIAA MASS GROWTH ALLOWANCE GUIDELINES FROM AIAA S–120A-2015 (2019) (REF. 22)

Maturity Code		Design Maturity (Basis for Mass Determination)	Percentage Mass Growth Allowance												
			Electrical/Electronic Components			Primary Structure	Secondary Structure	Mechanisms	Propulsion, Fluid Systems Hardware	Batteries	Wire Harnesses	Solar Array	ECLSS*, Crew Systems	Thermal Control	Instrumentation
			0-5 kg	5-15 kg	>15 kg										
E	1	Estimated	20-35	15-25	10-20	18-25	20-35	18-25	15-25	20-25	50-100	20-35	20-30	30-50	25-75
	2	Layout	15-30	10-20	5-15	10-20	10-25	10-20	10-20	10-20	15-45	10-20	10-20	15-30	20-30
C	3	Preliminary Design	5-20	3-15	3-12	4-15	8-15	5-15	5-15	5-15	10-25	5-15	5-15	8-15	10-25
	4	Released Design	5-10	2-10	2-10	2-6	3-8	3-4	2-7	3-7	3-10	3-5	3-8	3-8	3-5
A	5	Existing Hardware	1-5	1-3	1-3	1-3	1-5	1-3	1-3	1-3	1-5	1-3	1-4	1-3	1-3
	6	Actual Mass	Measured mass of specific flight hardware; no MGA; use appropriate measurement uncertainty.												
S	7	CFE or Specification Value	Typically, an NTE value is provided, and no MGA is applied.												
Expanded Definitions of Maturity Categories															
E1		Estimated	a. An approximation based on rough sketches, parametric analysis, or incomplete requirements.												
			b. A guess based on experience.												
			c. A value with unknown basis or pedigree.												
E2		Layout	a. A calculation or approximation based on conceptual designs (layout drawings or models) prior to initial sizing.												
			b. Major modifications to existing hardware.												
C3		Preliminary Design	a. Calculations based on new design after initial sizing but prior to final structural, thermal, or manufacturing analysis.												
			b. Minor modification of existing hardware.												
C4		Released Design	a. Calculations based on a design after final signoff and release for procurement or production.												
			b. Very minor modification of existing hardware.												
A5		Existing Hardware	a. Measured mass from another program, assuming that hardware will satisfy program requirements with no changes.												
			b. Values substituted based on empirical production variation of same or similar hardware or qualification hardware.												
			c. Catalog values.												

Note: The MGA percentage ranges in the above table are applied to the basic mass to arrive at the predicted mass.

* Environmental Control and Life Support System (ECLSS)

3.0 Baseline Design

The Titan In-Situ Resource Utilization (ISRU) Sample Return (TISR) Vehicle consists of multiple elements which were designed iteratively; the return vehicle (including the sample return capsule), the launch vehicle (including the in-space stage, the atmospheric stage (also called the second stage), and the first stage), and the lander/ propellant processing system (consisting of the ISRU system, the ISRU lander support hardware, and the Titan delivery and EDL system). As a note, the Compass Team did not design the Titan delivery and EDL system, instead using an approximated capability of the X-37C as an allocation. This section discusses the design of the mission as a whole, while subsequent sections explore each subsystem design in detail.

3.1 System-Level Summary

Figure 3.1 shows the system block diagram that captures the key elements of the TISR mission concept.

3.2 Top-Level Design Details

The following sections include a top-level look at the masses of each element in the architecture, as well as their summation. The description of each subsystem can be found in each corresponding subsystem subsection.

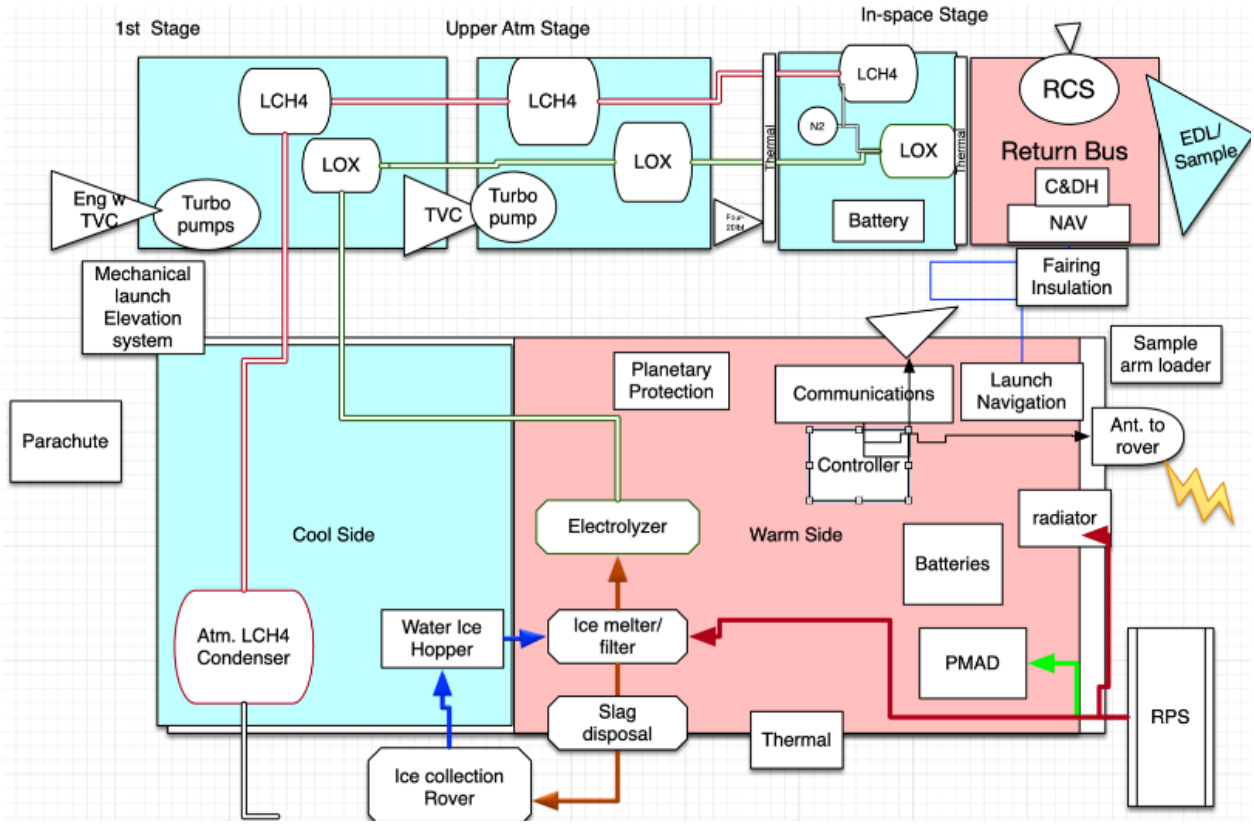

Figure 3.1.—TISR Block Diagram.

3.2.1 Master Equipment List (MEL)

Table 3.1 to Table 3.3 provide the TISR MELs for the return vehicle, launch vehicle, and lander/propellant processing plant, respectively, including their constituent elements. The basic masses reported in the MELs are also captured in Section 4.0 Subsystem Breakdown, where bottoms-up mass estimation is shown at the component level.

TABLE 3.1.—TISR RETURN VEHICLE AND SAMPLE CAPSULE MEL

Description Case 1_Titan_Sample_Return CD-2021-186	Basic Mass	Growth	Growth	Total Mass
	(kg)	(%)	(kg)	(kg)
Titan Sample Return Vehicle	172	20%	35	207
Return Vehicle	123	22%	27	150
Attitude Determination and Control	3.9	16%	0.6	4.5
Command & Data Handling	9.4	47%	4.5	13.9
Communications and Tracking	12.7	10%	1.3	14.0
Electrical Power Subsystem	30.3	43%	13.2	43.5
Thermal Control (Non-Propellant)	17.1	18%	3.1	20.2
Propulsion (Chemical Hardware)	18.4	11%	2.0	20.4
Propellant (Chemical)	14.4	0%	0.0	14.4
Structures and Mechanisms	16.4	15%	2.4	18.8
Sample Capsule	49	17%	8	58
Thermal Control (Non-Propellant)	45.5	18%	8.2	53.7
Science	3.0	0%	0.0	3.0
Structures and Mechanisms	0.9	2%	0.0	0.9

TABLE 3.2.—TISR IN-SPACE STAGE, UPPER ATMOSPHERE STAGE, AND 1ST STAGE MEL

Description Case 1_TSR_Launch_Vehicle CD-2021-186c	Basic Mass	Growth	Growth	Total Mass
	(kg)	(%)	(kg)	(kg)
TSR Launch Vehicle	3522	2%	70	3593
In-Space Stage	430	4%	17	447
Electrical Power Subsystem	7.7	40%	3.1	10.8
Thermal Control (Non-Propellant)	4.7	18%	0.8	5.5
Propulsion (Chemical Hardware)	49.9	14%	6.9	56.8
Propellant (Chemical)	326.4	0%	0.0	326.4
Structures and Mechanisms	41.5	14%	6.0	47.5
Upper Atmosphere Stage	1693	2%	26	1720
Thermal Control (Non-Propellant)	2.5	18%	0.5	3.0
Propulsion (Chemical Hardware)	102.2	15%	15.1	117.3
Propellant (Chemical)	1525.7	0%	0.0	1525.7
Propulsion Power	2.0	50%	1.0	3.0
Structures and Mechanisms	61.0	16%	9.7	70.7
1st Stage	1399	2%	27	1426
Thermal Control (Non-Propellant)	2.5	18%	0.5	3.0
Propulsion (Chemical Hardware)	110.4	15%	16.1	126.5
Propellant (Chemical)	1223.1	0%	0.0	1223.1
Propulsion Power	2.0	50%	1.0	3.0
Structures and Mechanisms	60.9	16%	9.6	70.5

TABLE 3.3.—TISR ISRU SYSTEM, LANDER, AND EDL MEL

Description Case 1_TSR_Propellant_Processing CD-2021-186b	Basic Mass	Growth	Growth	Total Mass
	(kg)	(%)	(kg)	(kg)
TSR Propellant Processing Lander	2288	7%	149	2437
ISRU System	88	21%	18	106
ISRU System	47.3	18%	8.3	55.6
Rover	37.5	25%	9.4	46.9
Structures and Mechanisms	3.0	18%	0.5	3.5
Lander	682	19%	127	810
Radioisotope Power System	395.1	19%	75.6	470.7
Command & Data Handling	16.8	32%	5.3	22.1
Communications and Tracking	24.4	8%	2.0	26.4
Thermal Control (Non-Propellant)	55.0	18%	9.9	64.9
Structures and Mechanisms	191.1	18%	34.4	225.5
Entry, Descent, and Landing	1518	0%	3	1521
Thermal Control (Non-Propellant)	18.0	18%	3.2	21.2
Lifting Body	1500.0	0%	0.0	1500.0

The following MELs are top-level summaries of all subsystem masses. The masses include basic mass and subsystem margin as applied by each subsystem lead at the component level, but do not show the additional 15 percent mass margin added at the spacecraft level. A complete mass list, including system level margin can be found in Table 3.4 to Table 3.7. Due to the complicated nature of this mission, there are also additional elements carried in the systems sheet that are not captured in the MELs due to spreadsheet constraints. Namely, the launch vehicle fairing mass and the mass of the general purpose heat source (GPHS) blocks used within the fairing for thermal control are not included. These are carried and dropped in the appropriate sections of the mission.

3.2.2 Architecture Details – Launch Vehicle Payload Assumptions

Launch vehicle performance for this study is based on a Falcon Heavy Expendable with a Star 63F (Ref. 23) augmentation. The performance to a C_3 of 90 km^2/s^2 is assumed to be approximately 3.5 t. Falcon Heavy performance was taken from the Launch Vehicle Performance Website (Ref. 24) maintained by NASA Launch Service Provider. Additional information on the launch assumptions is contained in the mission description.

3.2.3 Spacecraft Total Mass Summary

Table 3.4 to Table 3.6 capture the bottoms-up CBE and growth percentage of the TISR mission elements that were calculated for each line subsystem by individual subsystem team leads. Section 4.0 subsections provide mass details per subsystem in the master equipment lists.

To meet the AIAA MGA and margin recommendations (Ref. 22), an allocation is necessary for margin on basic dry mass at the system-level, in addition to the growth calculated on each individual subsystem. This additional system-level mass is counted as part of the inert mass to be flown along the required trajectory. Therefore, the additional system-level growth mass impacts the total propellant required for the mission design. Total masses in the following MELs represent the mass of the elements at a particular point in time (namely when loaded with all required propellant). Masses for each element by mission phase are shown in Table 3.7.

TABLE 3.4.—SUMMARY OF RETURN VEHICLE SYSTEM MASS BY DESIGN ELEMENT

MEL Summary: Case 1_Titan_Sample_Return CD-2021-186	Return Vehicle	Sample Capsule	TOTAL
Main Subsystems	Basic Mass (kg)	Basic Mass (kg)	Total Basic Mass(kg)
Attitude Determination and Control	3.9	0.0	3.9
Command & Data Handling	9.4	0.0	9.4
Communications and Tracking	12.7	0.0	12.7
Electrical Power Subsystem	30.3	0.0	30.3
Thermal Control (Non-Propellant)	17.1	45.5	62.6
Propulsion (Chemical Hardware)	18.4	0.0	18.4
Propellant (Chemical)	14.4	0.0	14.4
Science	0.0	3.0	3.0
Structures and Mechanisms	16.4	0.9	17.3
Element Total	***122.5***	***49.4***	***171.9***
Element Dry Mass (no prop,consum)	108.2	49.4	157.6
Element Propellant	14.4	0.0	14.4
Element Mass Growth Allowance (Aggregate)	27.0	8.2	35.2
MGA Percentage	25%	17%	22%
Predicted Mass (Basic + MGA)	135.2	57.6	192.8
System Level Mass Margin	16.2	7.4	23.6
System Level Growth Percentage	15%	15%	15%
Element Dry Mass (Basic+MGA+Margin)	151.4	65.0	216.4
Element Inert Mass (Basic+MGA+Margin)	152.8	65.0	217.8
Total Wet Mass (Allowable Mass)	***165.8***	***65.0***	***230.8***

TABLE 3.5.—SUMMARY OF LAUNCH VEHICLE SYSTEM MASS BY DESIGN ELEMENT

MEL Summary: Case 1_TSR_Launch_Vehicle CD-2021-186c	In-Space Stage	Upper Atmosphere Stage	1st Stage	Fairing and GPHS	TOTAL
Main Subsystems	Basic Mass (kg)	Basic Mass (kg)	Basic Mass (kg)	Basic Mass (kg)	Total Basic Mass(kg)
Electrical Power Subsystem	7.7	0.0	0.0	3.0	10.7
Thermal Control (Non-Propellant)	4.7	2.5	2.5	0.0	9.7
Propulsion (Chemical Hardware)	49.9	102.2	110.4	0.0	262.5
Propellant (Chemical)	326.4	1525.7	1223.1	0.0	3075.2
Propulsion Power	0.0	2.0	2.0	0.0	4.0
Structures and Mechanisms	41.5	61.0	60.9	22.5	185.9
Element Total	***430.2***	***1693.5***	***1398.8***	***25.5***	***3548.0***
Element Dry Mass (no prop,consum)	103.8	167.7	175.8	25.5	472.8
Element Propellant	326.4	1525.7	1223.1	0.0	3075.2
Element Mass Growth Allowance (Aggregate)	16.8	26.2	27.2	3.8	74.0
MGA Percentage	16%	16%	15%	15%	16%
Predicted Mass (Basic + MGA)	120.6	193.9	203.0	29.3	546.8
System Level Mass Margin	15.6	25.2	26.4	3.8	70.9
System Level Growth Percentage	15%	15%	15%	15%	15%
Element Dry Mass (Basic+MGA+Margin)	136.1	219.1	229.3	33.2	617.7
Element Inert Mass (Basic+MGA+Margin)	155.7	243.4	248.4	33.2	680.7
Total Wet Mass (Allowable Mass)	***462.5***	***1744.8***	***1452.4***	***33.2***	***3692.9***

TABLE 3.6.—SUMMARY OF PROPELLANT PROCESSING SYSTEM MASS BY DESIGN ELEMENT

MEL Summary: Case 1_TSR_Propellant_Processing CD-2021-186b	ISRU System	Lander	Entry, Descent, and Landing	TOTAL
Main Subsystems	**Basic Mass (kg)**	**Basic Mass (kg)**	**Basic Mass (kg)**	**Total Basic Mass(kg)**
Radioisotope Power System	0.0	395.1	0.0	395.1
Command & Data Handling	0.0	16.8	0.0	16.8
Communications and Tracking	0.0	24.4	0.0	24.4
ISRU, Thermal Control, Parachute	47.3	55.0	18.0	120.3
Lifting Body	0.0	0.0	1500.0	1500.0
Rover	37.5	0.0	0.0	37.5
Structures and Mechanisms	3.0	191.1	0.0	194.1
Element Total	***87.8***	***682.4***	***1518.0***	***2288.1***
Element Dry Mass (no prop,consum)	87.8	682.4	1518.0	2288.1
Element Propellant	0.0	0.0	0.0	0.0
Element Mass Growth Allowance (Aggregate)	18.2	127.3	3.2	148.8
MGA Percentage	21%	19%	0%	7%
Predicted Mass (Basic + MGA)	106.0	809.7	1521.2	2436.9
System Level Mass Margin	13.2	102.4	0.0	115.5
System Level Growth Percentage	15%	15%	0%	5%
Element Dry Mass (Basic+MGA+Margin)	119.2	912.0	1521.2	2552.4
Element Inert Mass (Basic+MGA+Margin)	119.2	912.0	1521.2	2552.4
Total Wet Mass (Allowable Mass)	***119.2***	***912.0***	***1521.2***	***2552.4***

Not surprisingly, returning a 3 kg cryogenic sample from Titan has huge mass requirements. A previous study (Ref. 18) found that, even with optimistic assumptions, returning a sample from Titan without using in situ propellants required over 10 t of mass and a Space Launch System (SLS) launcher, plus on-orbit rendezvous and an aerocapture system for the return stage. By using in-situ propellants, the launcher requirement is reduced to around 3.4 t and only needs a heavy class launcher (Falcon H expendable as representative). The in-situ approach will need ISRU propellant technologies and unfoldable cryogenic tanks.

The 3.4 t of mass is divided between the delivery lifting body, ISRU plant and rover, the three-stage rocket, the return spacecraft and the return aeroshell. Note that both subsystem growth and system level margins are carried using the ANSI/AIAA mass estimation guidelines (Ref. 22). Per the guidelines, each system has a total growth/margin mass of 30 percent or more, except for the Titan entry/descent/landing system which was allotted a mass of 1500 kg.

As Table 3.7 on the next page shows, the ISRU and support systems tally to approximately a metric ton while the propellants produced are over three times that mass. Indeed, it is interesting to note that the mass of the system sent to Titan (without the return propellants) is less than the fully fueled launcher/return vehicle on Titan.

TABLE 3.7.—SUMMARY OF TISR MASSES BY MISSION PHASE

	Propellant Processing			Launch Vehicle				Return Vehicle		Mission Totals by Phase		
MEL Summary: Case 1_TSR_CD-2021-186	ISRU System	Lander	Entry, Descent, and Landing	In-Space Stage	Upper Atmosphere Stage	1st Stage	Fairing and GPHS	Return Vehicle	Sample Capsule	Total at Earth Departure	Total at Launch from Titan Surface	Total After Circ. Burn during Titan Ascent
Main Subsystems	Basic Mass (kg)	Basic Mass (kg)	Basic Mass (kg)	Basic Mass (kg)	Basic Mass (kg)	Basic Mass (kg)	Basic Mass (kg)	Basic Mass (kg)	Basic Mass (kg)	Basic Mass (kg)	Basic Mass (kg)	Basic Mass (kg)
Radioisotope Power System	0.0	395.1	0.0	0.0	0.0	0.0	0.0	0.0	0.0	395.1	0.0	0.0
Attitude Determination and Control	0.0	0.0	0.0	0.0	0.0	0.0	0.0	3.9	0.0	3.9	3.9	3.9
Command & Data Handling	0.0	16.8	0.0	0.0	0.0	0.0	0.0	9.4	0.0	26.2	9.4	9.4
Communications and Tracking	0.0	24.4	0.0	0.0	0.0	0.0	0.0	12.7	0.0	37.1	12.7	12.7
Electrical Power Subsystem	0.0	0.0	0.0	7.7	0.0	0.0	3.0	30.3	0.0	41.0	41.0	38.0
ISRU, Thermal Control, Parachute	47.3	55.0	18.0	4.7	2.5	2.5	0.0	17.1	45.5	192.5	72.3	67.3
Propulsion (Chemical Hardware)	0.0	0.0	0.0	49.9	102.2	110.4	0.0	18.4	0.0	280.9	280.9	68.3
Propellant (Chemical)	0.0	0.0	0.0	326.4	1525.7	1223.1	0.0	14.4	0.0	0.0	3089.6	340.7
Science/ Rover	37.5	0.0	0.0	0.0	2.0	2.0	0.0	0.0	3.0	44.5	7.0	3.0
Lifting Body	0.0	0.0	1500.0	0.0	0.0	0.0	0.0	0.0	0.0	1500.0	0.0	0.0
Structures and Mechanisms	3.0	191.1	0.0	41.5	61.0	60.9	22.5	16.4	0.9	397.2	203.2	58.8
Element Total	*87.8*	*682.4*	*1518.0*	*430.2*	*1693.5*	*1398.8*	*25.5*	*122.5*	*49.4*	*2918.5*	*3719.9*	*602.1*
Element Dry Mass (no prop,consum)	87.8	682.4	1518.0	103.8	167.7	175.8	25.5	108.2	49.4	2918.5	630.3	261.4
Element Propellant	0.0	0.0	0.0	326.4	1525.7	1223.1	0.0	14.4	0.0	0.0	3089.6	340.7
Element Mass Growth Allowance	18.2	127.3	0.0	16.8	26.2	27.2	3.8	27.0	8.2	254.8	109.2	52.0
MGA Percentage	21%	19%	0%	16%	16%	15%	15%	25%	17%	9%	17%	20%
Predicted Mass (Basic + MGA)	106.0	809.7	1518.0	120.6	193.9	203.0	29.3	135.2	57.6	3173.3	739.6	313.4
System Level Mass Margin	13.2	102.4	0.0	15.6	25.2	26.4	3.8	16.2	7.4	248.3	110.9	47.0
System Level Growth Percentage	15%	15%	0%	15%	15%	15%	15%	15%	15%	9%	15%	15%
Element Dry Mass	119.2	912.0	1518.0	136.1	219.1	229.3	33.2	151.4	65.0	3421.6	850.5	360.4
Total Wet Mass	*119.2*	*912.0*	*1518.0*	*462.5*	*1744.8*	*1452.4*	*33.2*	*165.8*	*65.0*	3421.6	3940.1	701.1

*Note this does not explicitly include any propellant for outbound leg

3.2.4 Power Equipment List (PEL)

Table 3.8, Table 3.9, and Table 3.10 provide the durations assumed to model the power system's power modes.

The power equipment list (PEL) top-level and element level summary from the bottoms-up analysis on the TISR Mission are available in Section 4.3, Electrical Power System (EPS).

TABLE 3.8.—RETURN VEHICLE POWER MODE TITLES AND DESCRIPTION

Mode	Title	Duration
Power mode 1	Prelaunch	6 min
Power mode 2	Launch	90 min
Power mode 3	Cruise/ Sleep	7 years
Power mode 4	Mid-Course Corrections	10 min, 3 times
Power mode 5	Distance Communications	8 h every 3 months
Power mode 6	Prepare EDL Ops	30 min
Power mode 7	Near Earth Communications	8 h every 3 months

TABLE 3.9.—LAUNCH VEHICLE POWER MODE TITLES AND DESCRIPTION

Mode	Title	Duration
Power mode 1	Launch	90 min
Power mode 2	In-Space Stage Coast	12 months
Power mode 3	In-Space Stage Burns	17 min average, 50 min maximum

TABLE 3.10.—PROPELLANT PROCESSING PLANT POWER MODE TITLES AND DESCRIPTION

Mode	Title	Duration
Power mode 1	Propellant Processing	1.5 years
Power mode 2	Communications Only	1 deep space network (DSN) pass, 8 h/day, every 8 days
Power mode 3	Propellant Processing and Rover Recharge	12 h/day

3.3 Concept Drawing and Description

The TISR mission consists of three major elements that will be landed on the Titan surface: the lander element containing the ISRU processing plant; the launch vehicle for ascent off the Titan surface; and the return vehicle located atop the launch vehicle inside a payload fairing and housing the Titan sample to be returned to Earth. All three of these elements are contained in a lifting body entry vehicle used for entry, descent, and landing. The payload bay for the lifting body was scaled up from the X-37 design and is 2-m in diameter and 10-m long to ensure that the length to diameter ratio is kept at 5:1 or less. All of these surface elements can be seen inside the payload bay envelope in Figure 3.2 and Figure 3.3.

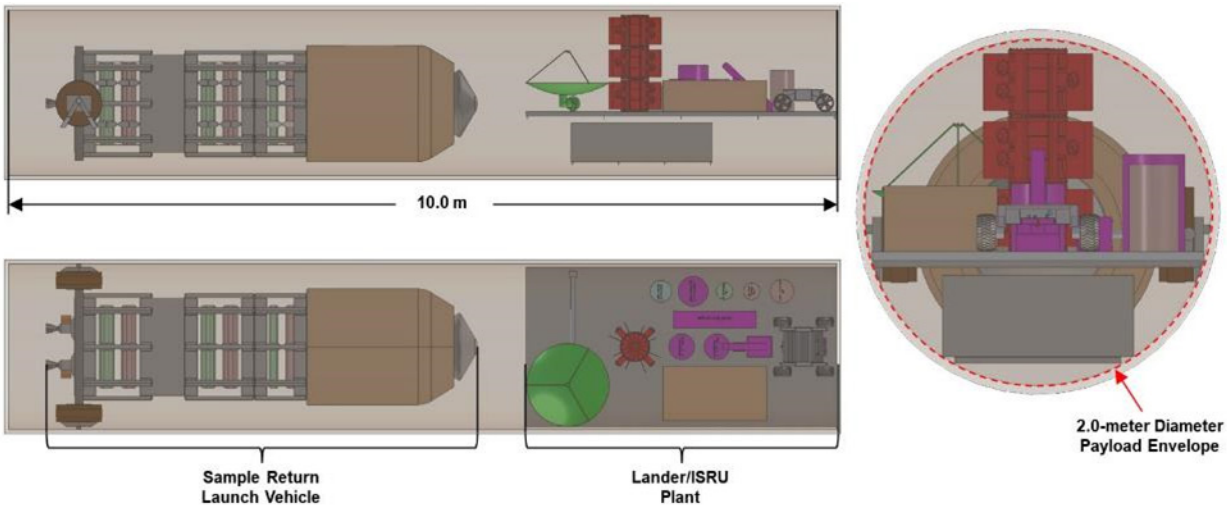

Figure 3.2.—All three major TISR elements inside a representative lifting body payload bay.

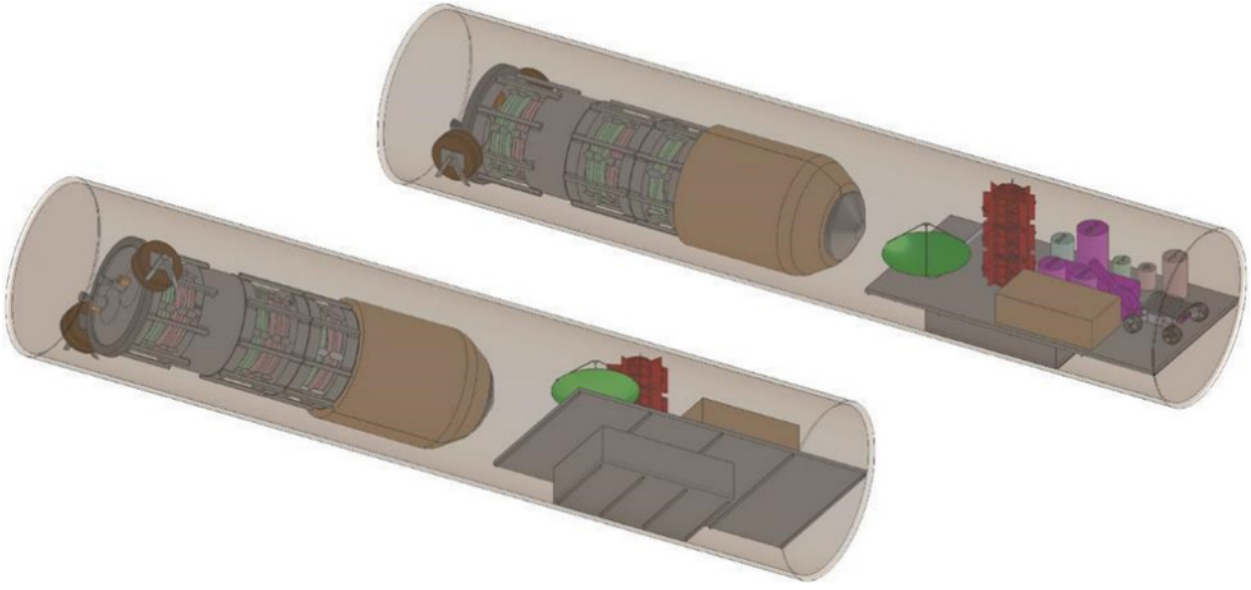

Figure 3.3.—Isometric views of all the major TISR elements inside a representative lifting body payload bay.

During the transit to Titan as well as while on the Titan surface, the payload bay doors will be open to allow many of the components to radiate to keep cool and allow the sample to be deposited into the canister located atop the launch vehicle. It is assumed that the hinges to open the payload bay doors will be located on each side along the length of the payload bay and right at the bay diameter. This location maximizes the exposure to deep space during transit and to the Titan atmosphere while on the surface when the payload door bays are open. While the doors were not modeled for this study as the design of the lifting body was not performed, the doors open in a fashion similar to the space shuttle payload bay doors. Figure 3.4 shows the TISR elements inside the payload bay with the doors in the open position (doors not shown).

The components remaining on the Titan surface after the launch vehicle ascends are considered part of the lander, which includes the mechanisms for elevating the launch vehicle out of the payload bay after the sample is deposited inside the aeroshell contained on the return vehicle. Figure 3.5 shows the mechanisms and their support and interface structures. There are two elevation mechanisms/motors on either side of the base of the launch vehicle. By utilizing two mechanisms, each is required to produce half the torque of one singular mechanism, which would be too large to fit on one side of the launch vehicle. Each mechanism is attached to a plate contained on a support structure that is tied directly into the payload bay wall. The inside face of the elevation motor attaches to another plate that is attached to a 4-in. square ring that wraps around the base of the launch vehicle structure and supports it during elevation and while elevated on the Titan surface. Once the first stage engine ignites, the launch vehicle will separate from this ring to allow for ascent. More details on the elevation motors and associated support structure can be found in the Science section of this document.

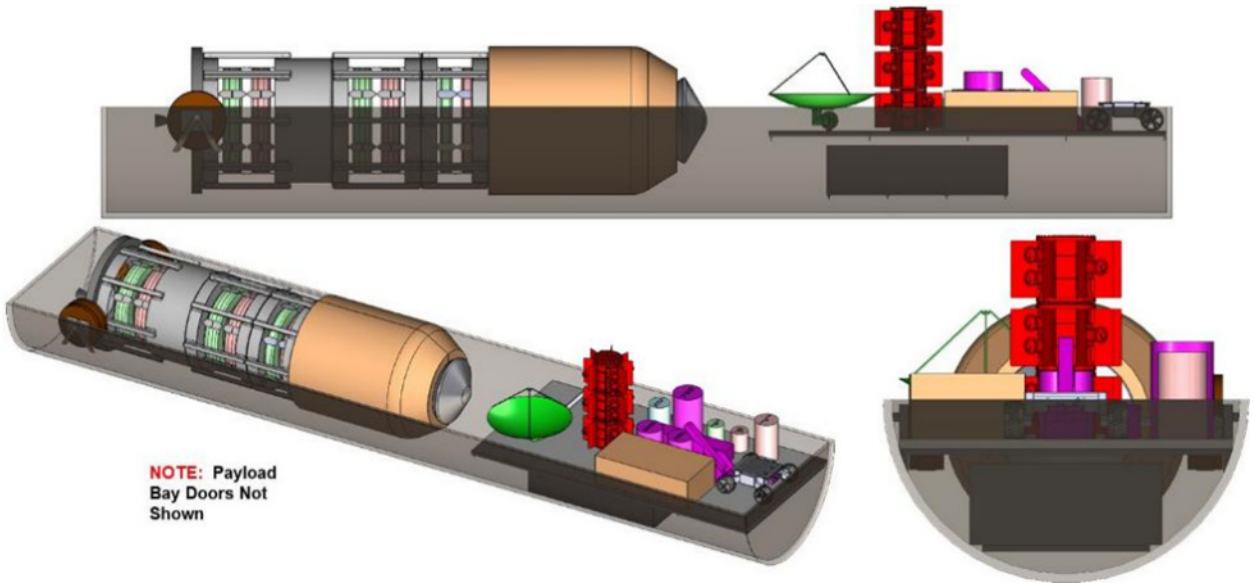

Figure 3.4.—Isometric views of all the major TISR elements inside a representative lifting body payload bay.

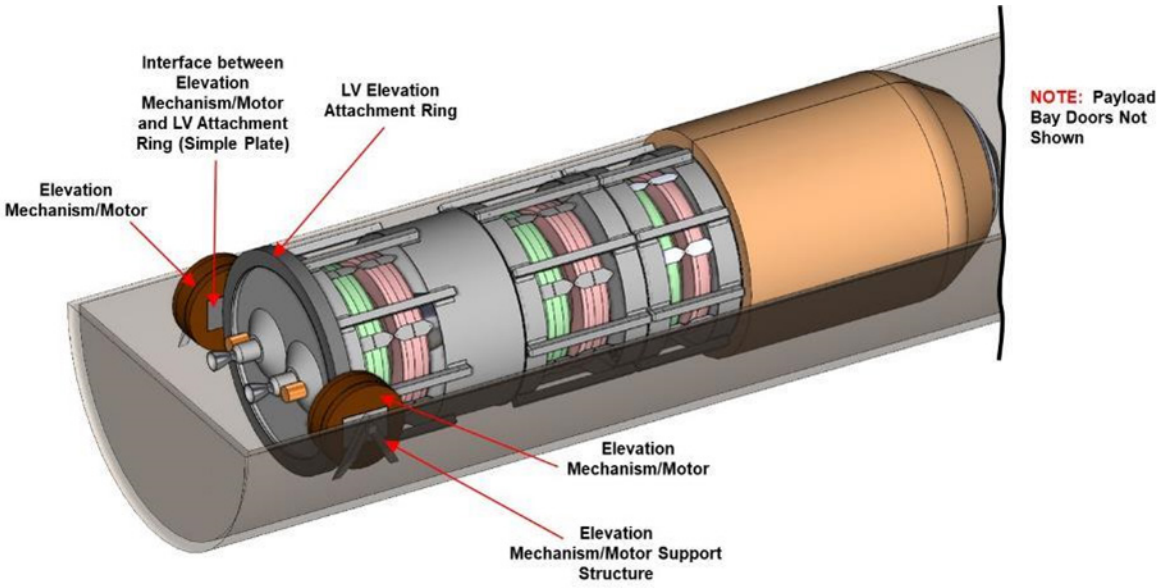

Figure 3.5.—Launch Vehicle elevation motors and support structure

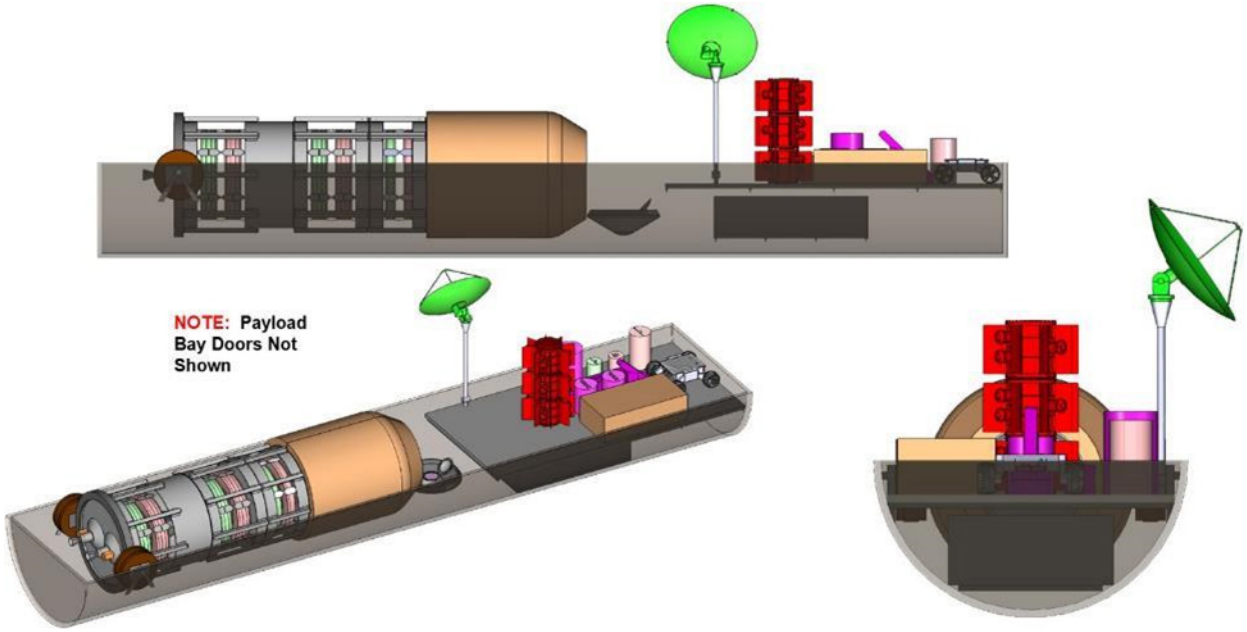

Figure 3.6.—Sample loading configuration on the Titan surface

Prior to elevating the launch vehicle, the Titan sample must be placed inside the sample canister located inside the aeroshell on top of the return vehicle. The Compass Team did not design a concept for physically placing the sample inside the canister during this study. However, the team did develop a design concept for the sample canister and the aeroshell. The aeroshell containing the sample canister will open utilizing a hinge mechanism that will separate the heat shield from the backshell, and rotate the heatshield 90°, exposing the sample canister. The canister itself will also utilize a hinge mechanism to open a portion of the canister to allow the sample to be deposited. A more detailed discussion on the aeroshell and sample canister design can be found later in this section. However, Figure 3.6 shows the open aeroshell and canister as it would be during the sample deposit while on the Titan surface. Note in

this configuration, the 1-m diameter X-band dish antenna is deployed to provide communications while on the Titan surface.

Figure 3.7 shows the stowed launch vehicle elevated inside the payload bay with all of the other lander components. After the initial elevation of the stowed launch vehicle utilizing the elevation motors, the launch vehicle will be deployed and loaded with propellant, and the insulation around the fairing will be dropped just prior to liftoff as shown in Figure 3.8. A more detailed discussion on the launch vehicle components, deployment, and fairing insulation can be found later in this section.

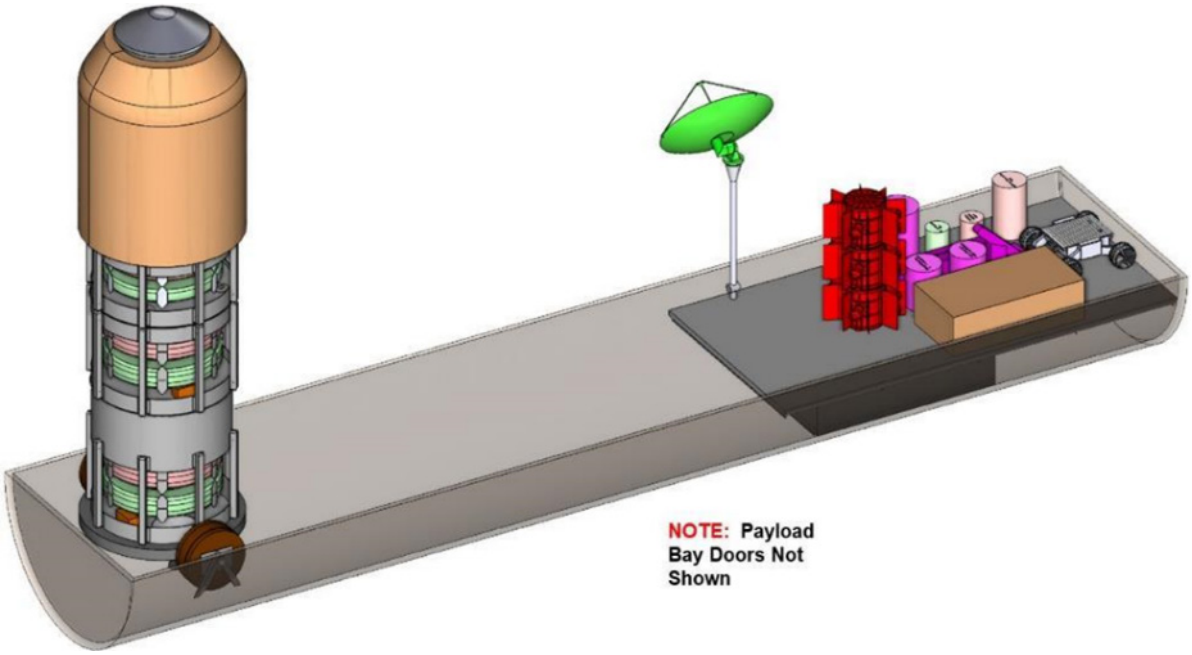

Figure 3.7.—Elevated stowed launch vehicle inside the payload bay.

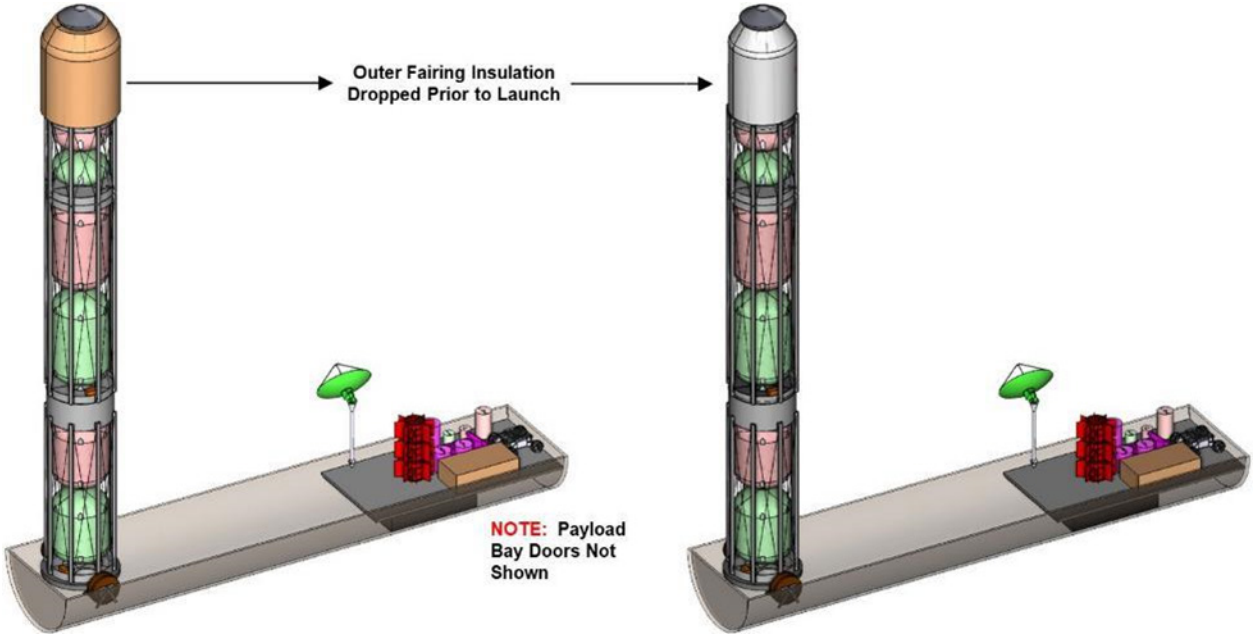

Figure 3.8.—Elevated deployed launch vehicle inside the payload bay.

Figure 3.9 shows the dimensions for the package containing the remainder of the lander components, including the ISRU processing plant, rover/extractor, communications system, and power system. This package is located at the aft end of the payload bay.

The components contained on the top deck of the lander (mounted directly to the inside of the payload bay) include: the three DRPS units of the electrical power system; all the communications system components; the avionics enclosure of the Command and Data Handling (C&DH) system; the rover/excavator; and all the components that make up the ISRU processing plant (Figure 3.10).

The three DRPS units are stacked one on top of the other with the bottom one being integrated to the deck. This configuration allows the top two units and about half of the bottom unit to be above the hinge line of the payload doors, exposing the units to either deep space or the Titan atmosphere, thus providing a better cooling environment for the DRPS units.

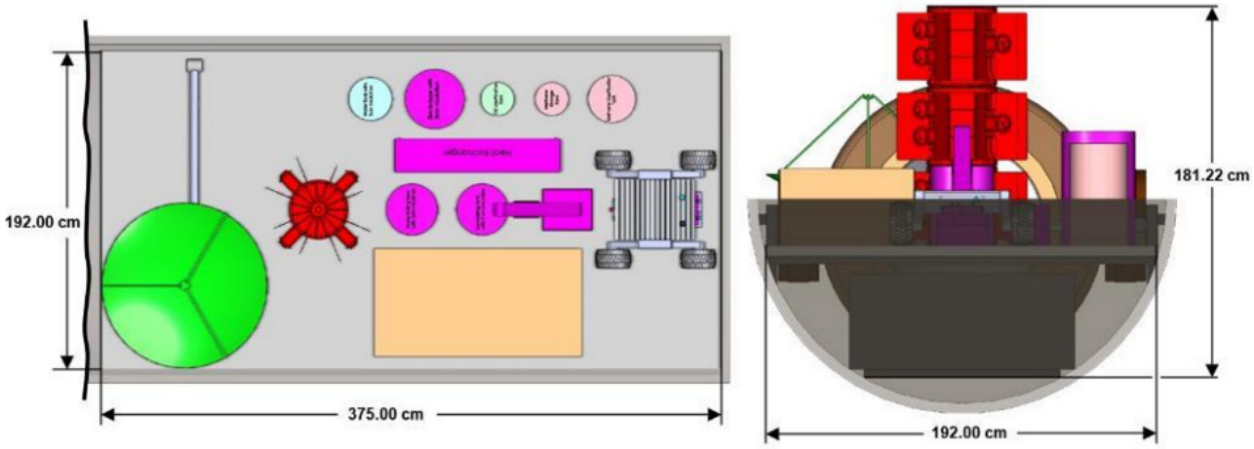

Figure 3.9.—Dimensions of the lander/ISRU processing plant inside the payload bay.

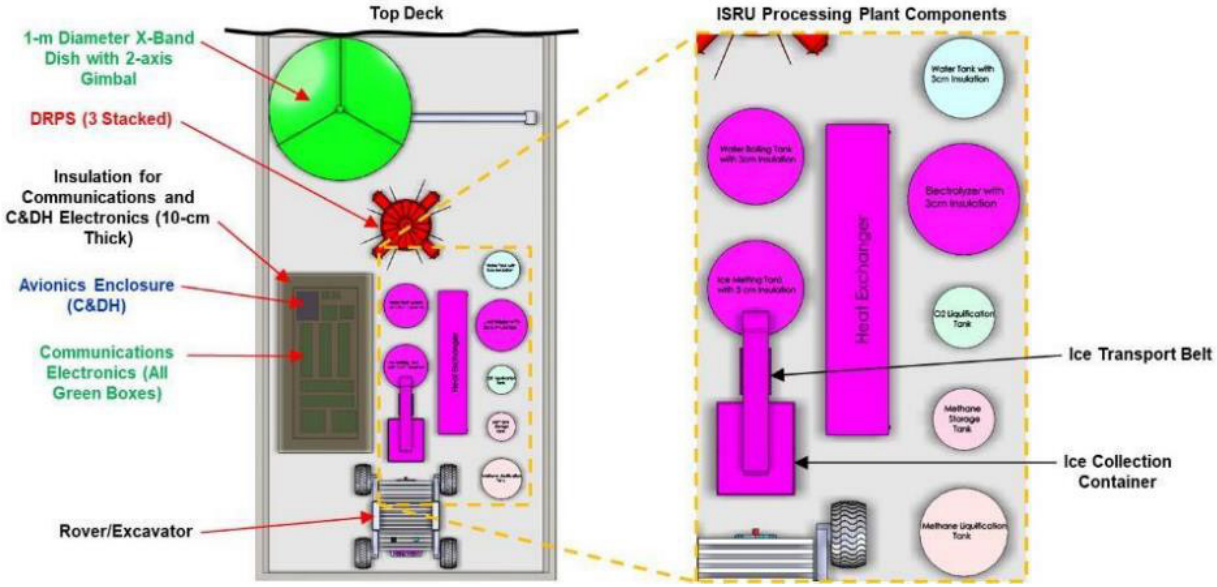

Figure 3.10.—Components located on the top deck of the lander.

The 1-m diameter X-band dish antenna and its 2-axis gimbal lay flat against the deck when stowed. During transit to Titan, the antenna will remain in its stowed position and the entire lifting body will be used to point the antenna in the appropriate direction. After landing on the Titan surface, the antenna will be deployed out on a boom by a mechanism that will rotate it up 90°. From this position, the 2-axis gimbal will provide the necessary pointing for surface communications. All the electronics associated with the communication system, including the electronics for communication with the rover/excavator (antennas patch antennas would be located on the outside of the lifting body), are located inside a box that is covered with 10-cm of insulation to keep the electronics warm while in transit and on the Titan surface. Also located in this insulated box is the avionics enclosure of the C&DH system.

The rover/excavator sits on the deck at the very back of the payload bay. It was not designed during this study, but rather the Team used a representative rover/excavator from a past unpublished Compass design to obtain representative mass, power, and size estimates. The rover/excavator shown in the images is just representative and used to show approximate size and location within the lander system. The rover/excavator is used to excavate the Titan surface and deposit the soil containing ice to the ice collection container of the ISRU processing plant. It may also be used for collecting the sample for Earth return, though that phase of the mission was not designed during this study. Another option for sample collection could be a robotic arm. A ramp would be deployed out of the back of the lifting body to allow the rover to exit to the Titan surface and return to deliver the excavated soil. Design of the ramp system was not performed during this study as it would be part of the lifting body.

Those components that make up the LOx portion of the ISRU processing plant include: the ice collection container; an ice transport belt; an ice melting tank; a water boiling tank; a heat exchanger; a water tank; an electrolyzer; and an O_2 liquification tank. The LCH_4 used as the fuel for the launch vehicle is produced from the CH_4 contained in the Titan atmosphere. This system includes a CH_4 liquification tank and a CH_4 storage tank. It should be noted that all the tanks are covered in 3-cm of foam insulation with the exception of the O_2 liquification tank, CH_4 liquification tank, and the CH_4 storage tank, which utilize the cold Titan environment to keep them at their desired temperatures. Figure 3.10 (right) shows all these components. Section 4.6, Propellant Production provides more details on the propellant processing plant.

Underneath the top deck containing the above-mentioned components is a second, smaller deck. This deck is also integrated directly to the inside of the payload bay wall and serves as the bottom panel of a structural box containing all the electrical power system electronics, DRPS controllers, and battery. The inside walls of this box are covered with 10-cm of foam insulation which encapsulates the electrical power electronics and batteries. The insulation ensures the electronics do not get below their minimum operating temperature when in the cold temperatures during transit and on the Titan surface. A separate deck is required for these components as they are relatively large and would not fit on the top deck without increasing the length of the payload bay. There is sufficient, unused volume below the top deck to fit all of these components in addition to their insulation. Figure 3.11 shows this deck and its insulation and enclosed components.

The TISR launch vehicle is comprised of three stages: the first stage, the upper atmosphere stage (second stage), and the in-space stage (third stage). Atop the in-space stage encapsulated in a payload fairing is the return vehicle, which will be discussed in more detail later in this section.

Inflatable LCH_4 and LOx tanks allow the launch vehicle stages to stow at a much shorter length than when deployed. This is key to allowing the launch vehicle to fit in the 10-m-long payload bay with all the other components that make up the lander and propellant processing plant. Deployment of the stages is done through a set of eight rails evenly distributed around each stage. Each rail is comprised of a set of five square tubes that are nested inside one another when stowed and telescope out upon deployment

using a screw drive. This allows for a 5:1 ratio of deployed to stowed rail length. The overall length of the stowed launch vehicle is 520.59 cm while the deployed length reaches 1173.91 cm. Figure 3.12 shows the stowed launch vehicle along with the overall dimensions and some of the major components for each stage.

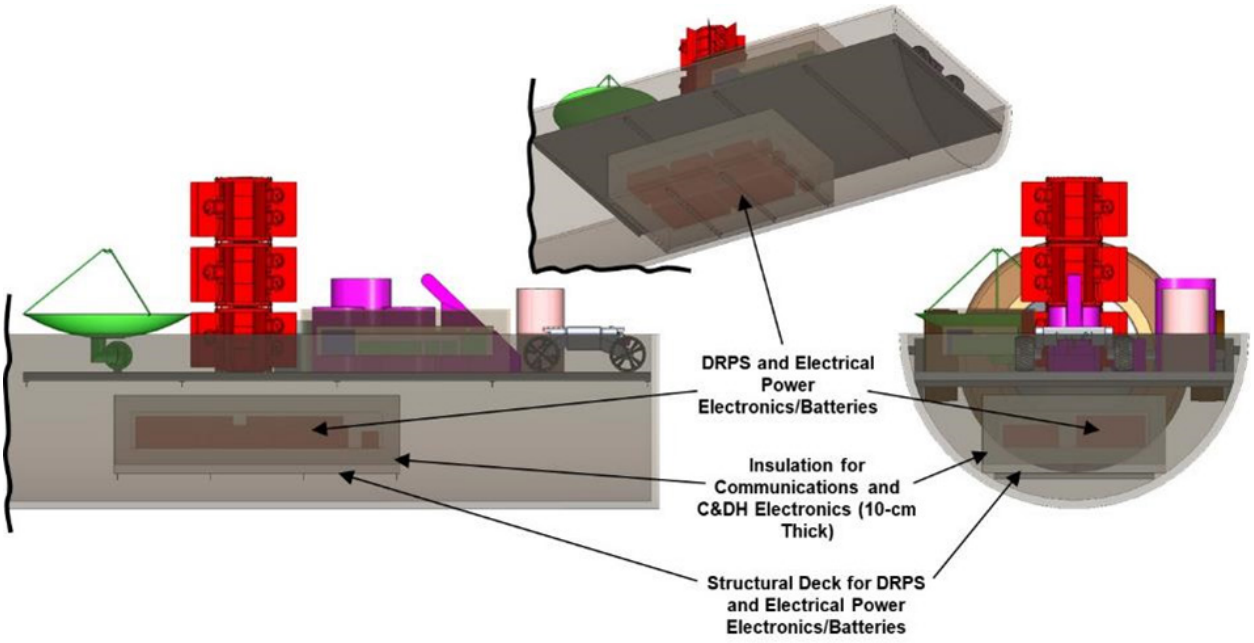

Figure 3.11.—Location of the electrical power electronics and battery.

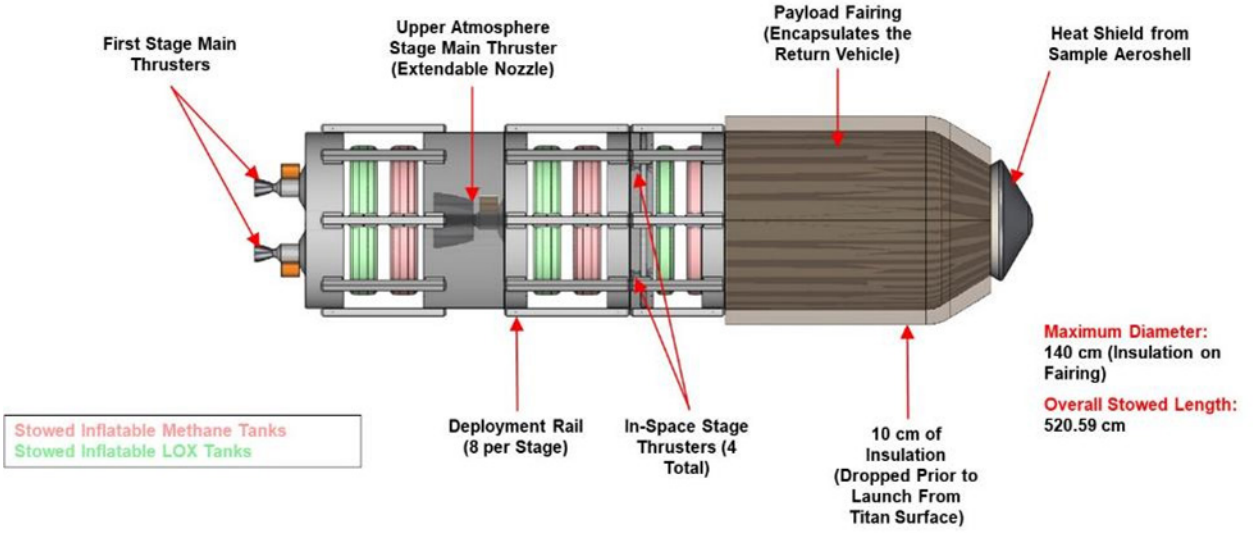

Figure 3.12.—The TISR launch vehicle in its stowed configuration.

A series of cables are used to stiffen the overall deployed structure of the launch vehicle. These cables run between each end of a rail to the opposite end of the adjacent rail producing an “X” pattern between two adjacent rails. Cables are also used to hold the deployed tanks firmly in place once deployed. Each tank has a set of six cables that run from the tabs around the base of one of the tank domes to the cylindrical bus structure of the stage, and another set of six cables that run from tabs around the base of the other tank dome to the other tank in that stage. With this cable layout, the oxidizer and propellant tank for each stage are each attached to the stage bus structure at one end, and to the other tank at the other end. Figure 3.13 shows the fully deployed launch vehicle along with its primary dimensions, components, and provides a good look at the cable layout for each stage. A more detailed discussion on the inflatable tanks and the cable and rails systems can be found in their relative system sections later in this document.

Figure 3.14 shows the first stage in its deployed configuration. This stage contains two main engines, each with its own turbopump and thrust vector control (TVC) unit. The main engines each interface to a circular deck located at the base of the aft end bus cylinder structure. This deck also provides the mounting structure for the two TVC controllers. Identical cylindrical tanks are used for the LCH_4 and LOx tanks with the LOx tank located at the aft end of the stage nearest to the main engines. Another cylindrical bus structure is located at the front of the stage. This cylindrical structure is longer than the aft bus structure as it provides the volume for the large upper atmosphere stage (second stage) main engine when the two stages are attached to one another. As discussed earlier, a set of eight rail structures run between the forward and aft bus cylinders and a series of cables are used to stiffen the overall stage structure and keep the two tanks in place.

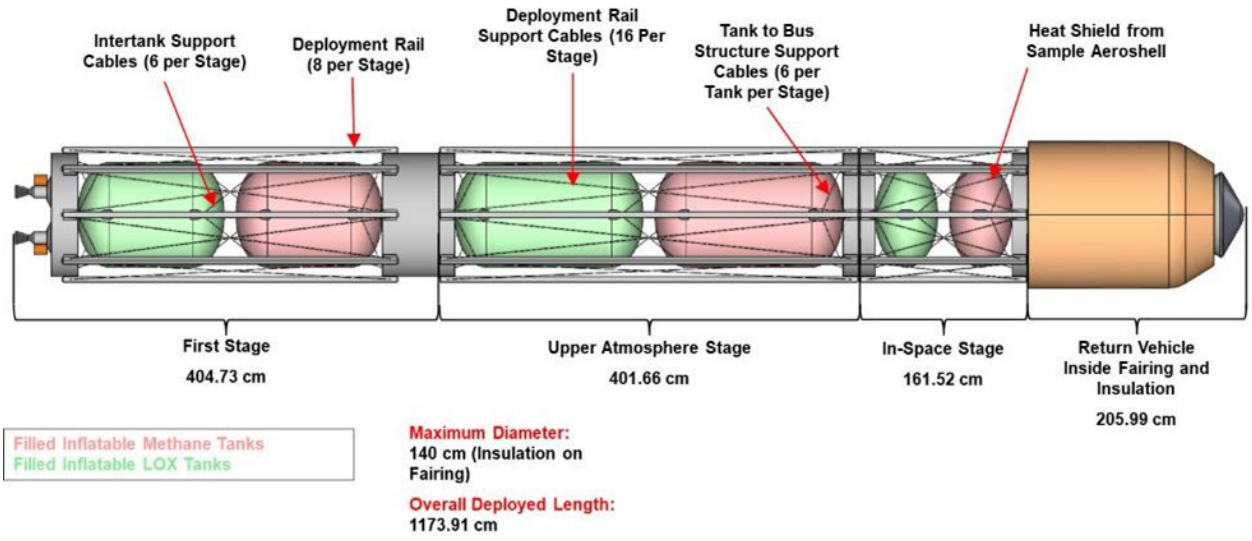

Figure 3.13.—The TISR launch vehicle in its fully deployed configuration.

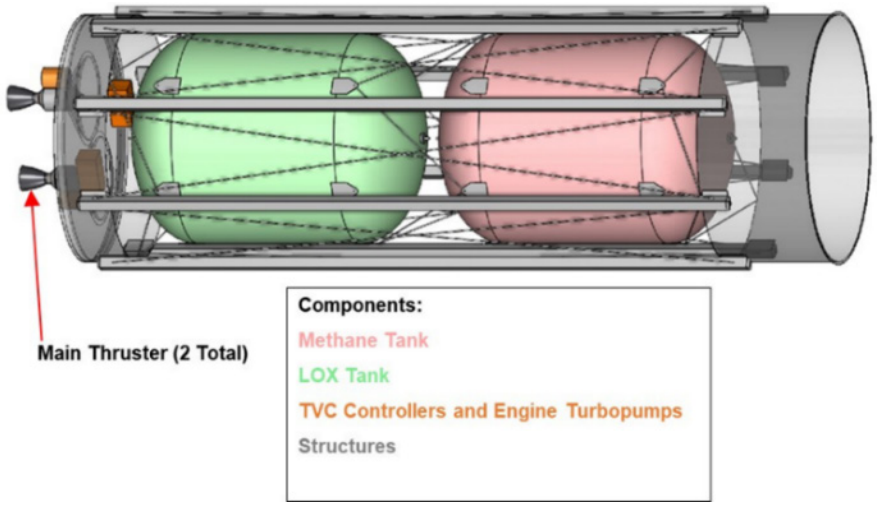

Figure 3.14.—First stage of the TISR launch vehicle.

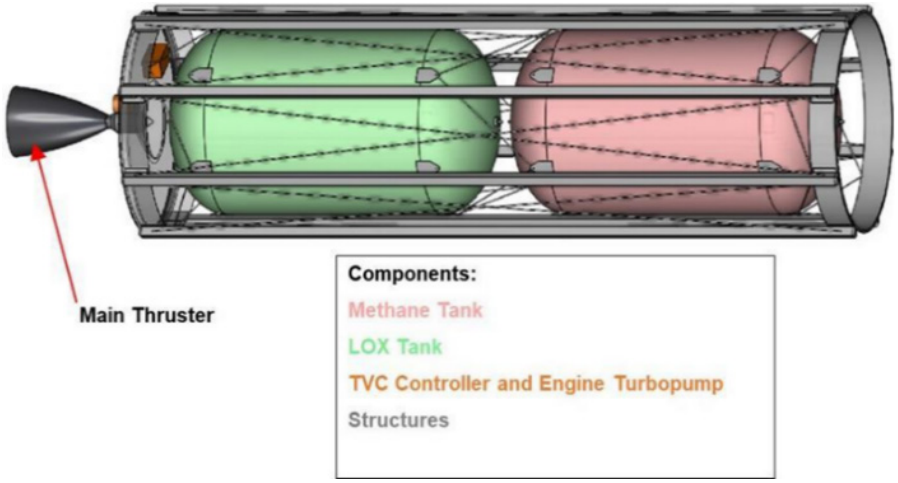

Figure 3.15.—Upper atmosphere stage (second stage) of the TISR launch vehicle.

Figure 3.15 shows the upper atmosphere stage (second stage) in its deployed configuration. This stage has one main engine along with a turbopump and TVC controller. An extendable nozzle is utilized on this thruster to help reduce the overall length of the launch vehicle in both its stowed and deployed configurations. The main engine fits within the volume provided by the longer cylindrical bus structure on the forward end of the first stage when the two stages are attached to one another. A circular deck located in the bottom of the aft cylindrical bus structure is again used for the engine interface and support structure as well as the mounting structure for the TVC controller. The forward cylindrical bus structure is identical in size as the aft bus structure as it does not have to provide a large volume for the much smaller in-space stage (third stage) engines when the two stages are attached to one another. As with the first stage, both tanks are identical with the LOx tank at the aft end of the stage, though these tanks are longer than those located on the first stage. A similar rail and cable system as the first stage is used for deployment for structural stiffening and tank support.

Figure 3.16 shows the in-space stage (third stage) in its deployed configuration. This stage has four main engines equally distributed around the inside perimeter of the aft cylindrical bus structure. Similar to the other two stages, a circular deck acts as the interface and support structure for the main engines. There are no turbopumps for these four thrusters and TVC is not used, therefore there are no TVC controllers

associated with them. Again, the CH_4 and LOx tanks are identical to one another with the LOx tank located aft of the CH_4 tank, however due to the lower propellant loading requirement, these tanks contain no cylindrical section and have only one set of tabs around the diameter for the support cables. As with the upper atmosphere stage, the forward cylindrical bus structure is the same size as the aft one. The eight deployment rails run between the two bus cylinders and a cable system is used for structural stiffness and supporting the tanks. With this being the last stage of the launch vehicle, a conical payload adaptor is bolted to the top of the forward bus cylinder to support the return vehicle. An 18-in. Lightband system is used to separate the return vehicle from the in-space stage. Mounted to the inside of the payload adaptor are two batteries and a N_2 pressurant tank. As the main engines do not have their own turbopumps, the N_2 is used as pressurant for the CH_4 and LOx tanks. There is also a circular deck mounted inside the forward bus cylinder that is used to hold the insulation required to thermally separate the warm batteries and warm return vehicle from the cryogenic CH_4 tank. More details on many of these launch vehicle components can be found in their relative subsystem section later in this document.

The payload fairing that encapsulates the return vehicle is comprised of two halves that extend from the base of the payload adaptor up to where the heatshield and backshell of the return aeroshell meet. A complete encapsulation of the aeroshell with the fairing could not be done as the heat shield must swing open from the backshell while on the Titan surface to allow the sample to be deposited in its canister for return to Earth. This design requires the heat shield of the aeroshell to act as both as the nose cone for the launch vehicle and the thermal protection for the sample during Earth entry. Mounted inside one of the fairing halves is a single GPHS block wrapped in insulation. This block provides the heat needed to keep the return vehicle at the required temperatures both during the transit and while on the Titan surface. In order to keep that heat inside the fairing, there is 10-cm of foam insulation around the outside of the entire fairing. This insulation will be dropped prior to liftoff from the Titan surface to help reduce the drag. Figure 3.17 shows the fully deployed launch vehicle including a view of the GPHS block and return vehicle inside the payload fairing.

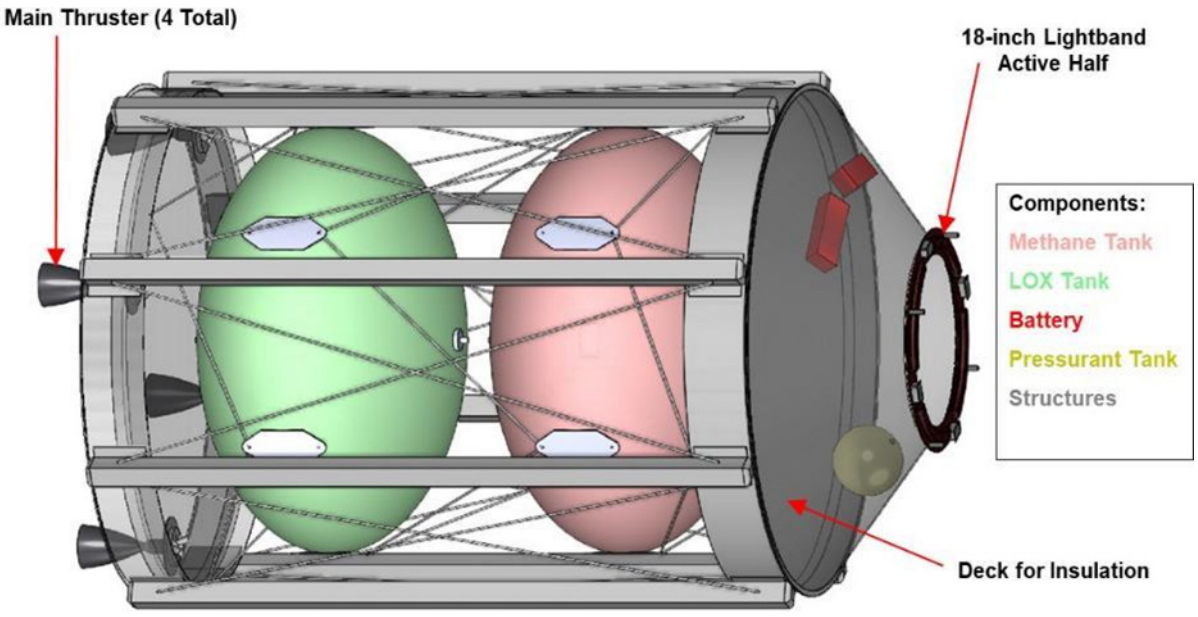

Figure 3.16.—In-space stage (second stage) of the TISR launch vehicle.

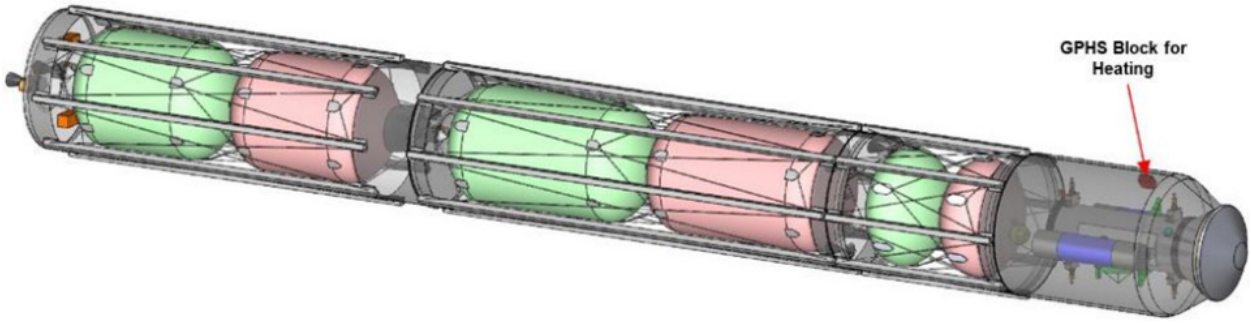

Figure 3.17.—Fully deployed launch vehicle with transparent payload fairing.

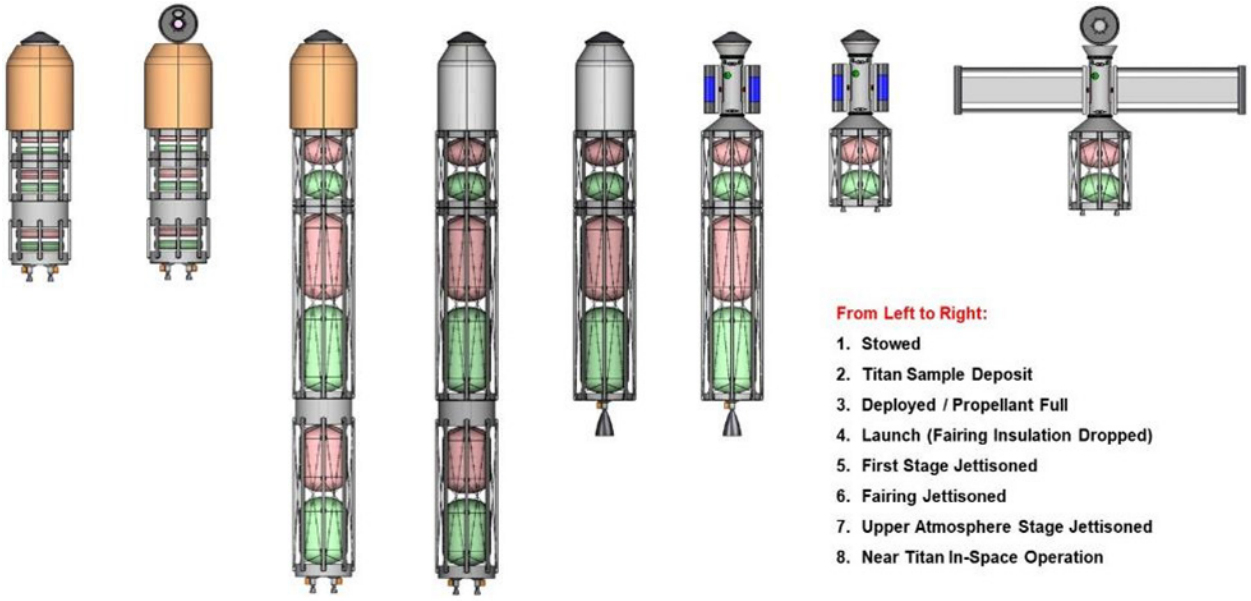

Figure 3.18.—Various launch vehicle configurations during its various mission phases.

Figure 3.18 shows all the various configuration of the TISR launch vehicle from the initial stowed phase to the final in-space operations phase departing Titan. In addition to the fairing insulation being dropped prior to liftoff, it should be noted that the fairing is jettisoned during the upper atmosphere stage (second stage) burn and the return vehicle solar arrays are deployed and aeroshell heatshield opened prior to jettisoning the in-space stage (third stage). Deployment of the return vehicle arrays allows the return vehicle to provide the power to the in-space stage during its operations and the heatshield is opened to allow the sample inside to be exposed to deep space to keep it cooled.

The TISR return vehicle is the element that will return the aeroshell containing the Titan sample back to Earth from Titan orbit. Figure 3.19 shows two isometric views of the return vehicle with the aeroshell attached. To fit within the 2.1-m diameter payload fairing of the launch vehicle, the two large solar arrays must be stowed until the TISR launch vehicle lifts the return vehicle out of the Titan atmosphere at which time they will be deployed. These two solar arrays are the only components on the return vehicle bus that need to be deployed at any time throughout the mission. Figure 3.20 shows the dimensions of the stowed return vehicle with the aeroshell attached.

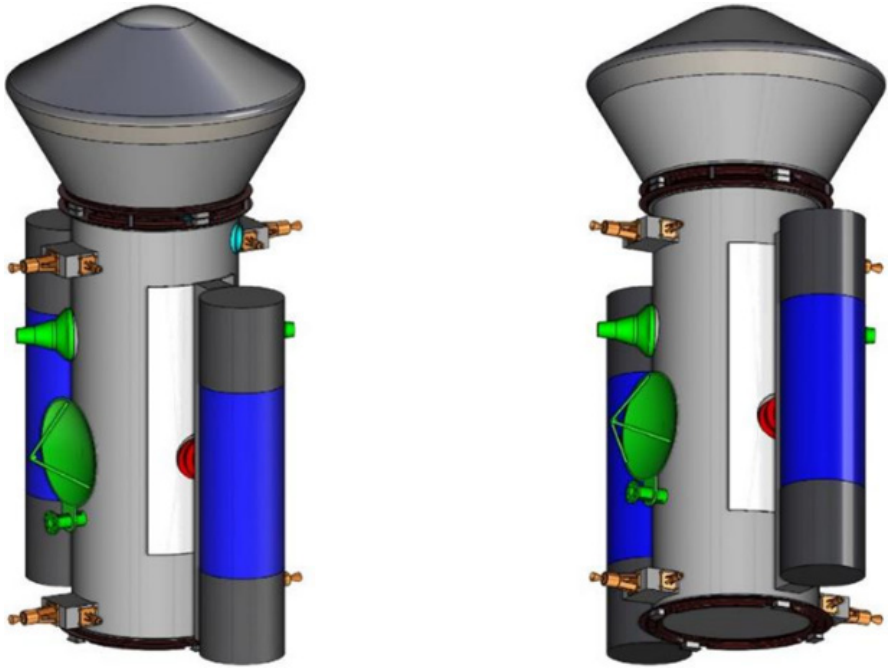

Figure 3.19.—Isometric views of the stowed return vehicle with the sample aeroshell.

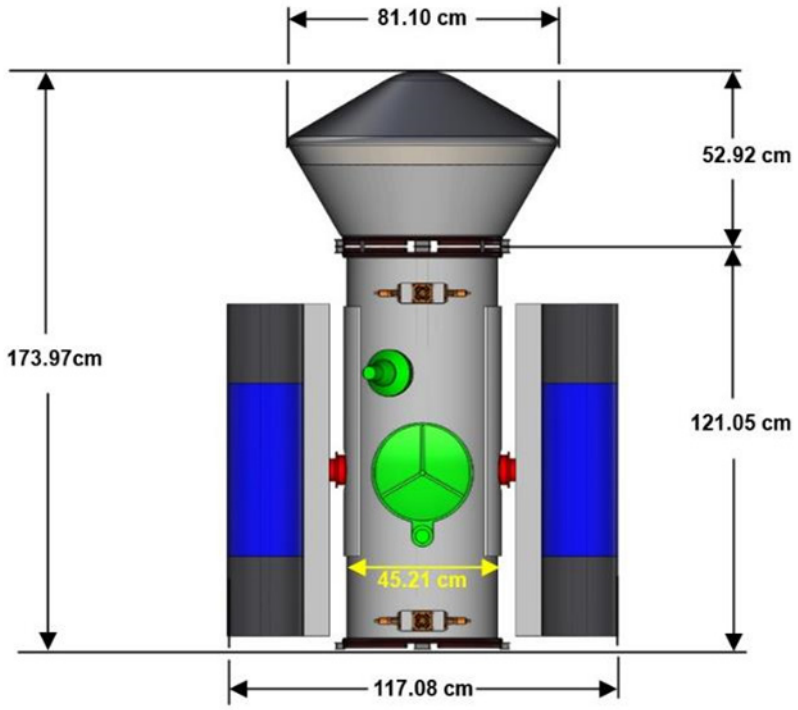

Figure 3.20.—Stowed dimensions of the return vehicle with the sample aeroshell.

Figure 3.21 shows the TISR return vehicle with its arrays deployed, while Figure 3.22 shows the deployed dimensions.

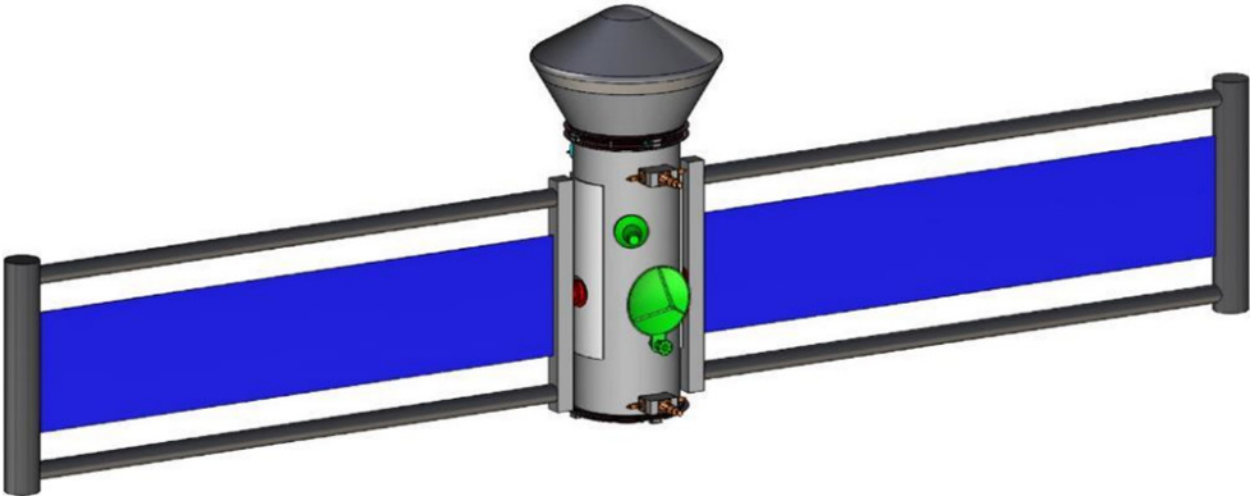

Figure 3.21.—Deployed return vehicle with the sample aeroshell.

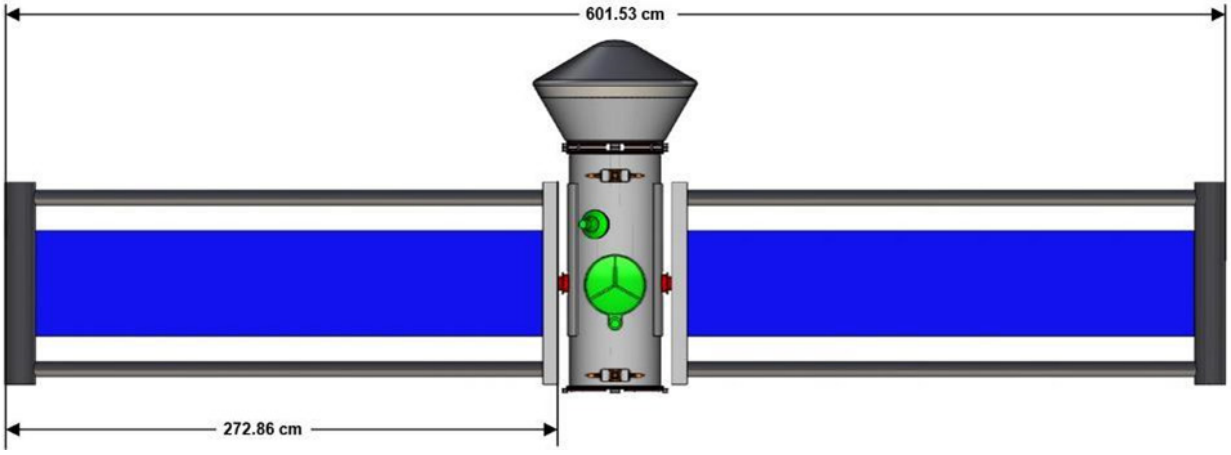

Figure 3.22.—Deployed dimensions of the return vehicle with the sample aeroshell.

Those components located externally to the cylindrical bus structure of the return vehicle include: the two star trackers of the guidance, navigation, and control (GN&C) system, the antennas for the communications system, the two solar arrays and their solar array gimbals, the two electronics radiator panels, the four RCS thruster pods, two Lightband systems for separation events, and the aeroshell containing the Titan sample (Figure 3.23).

The two-star trackers are located near the top of the cylindrical bus just above and on either side of the top RCS thruster pod on that side. They are oriented so that the field-of-view of each are orthogonal from one another and orthogonal from the centerline of the cylindrical bus structure. This location and orientation ensure that neither tracker is blocked by any of the other components on the bus and ensures that one tracker is pointed at either the Sun, Earth, Saturn, or Titan, while the other tracker has a clear view of deep space. More details on the GN&C system can be found in its related section later in this document.

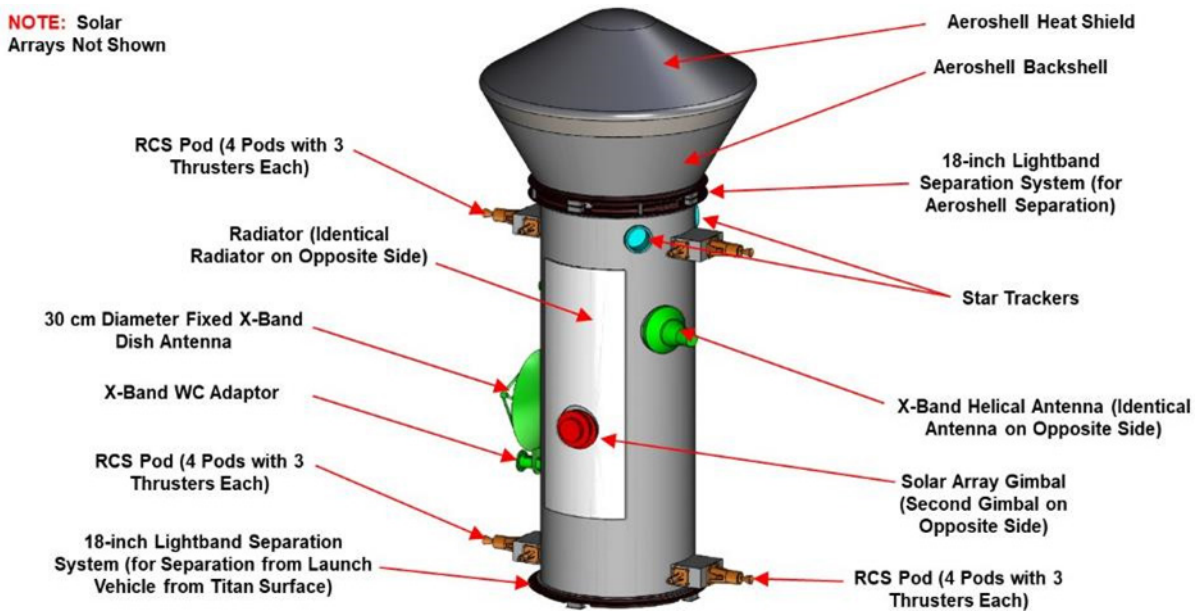

Figure 3.23.—External components on the return vehicle.

Opposite the star trackers and just below the midway point of the cylindrical bus structure is the fixed 30-cm diameter X-band dish antenna. Pointing of the antenna will be done by pointing the entire vehicle in the desired direction. Attached to the outside of and pointing in the same direction as the dish antenna is the X-band Waveguide to Coax (WC) adaptor. Just above the dish antenna and pointed 25° off to the side as the dish antenna is the X-band helical antenna. A second helical antenna is located 180° around the cylindrical bus from the other helical antenna. The locations and use of the two helical antennas ensure there is full 360° of coverage around the spacecraft. Locating the one helical antenna 25° off the pointing of the dish antenna helps to minimize any interference from the dish antenna as well as the RCS thruster pods. More details on the communications system can be found in its related section later in this document.

Located 90° around the cylindrical bus from the dish antenna is a single-axis solar array gimbal, with the second gimbal 180° from the other. This allows the solar arrays to deploy out from opposite sides of the bus to ensure a good mass balance and a good balance in the projected area of the spacecraft for the solar pressure effects on the spacecraft. More details on the solar arrays, gimbals, and the rest of the electrical power system can be found in their relative system section later in this document.

The radiator area required for rejecting the heat from the electronics contained within the bus structure is split into two identical, body mounted radiator panels that are each half of the required area. Each radiator is mounted to the bus on the same sides as the two solar arrays. This location ensures that each radiator will have a minimal view to the Sun as the arrays track the Sun. More details on the radiators can be found in its relative system section later in this document.

The four RCS thruster pods contain three thrusters each. Two 1-N thrusters point out tangentially from the pod in opposite directions from one another while a single 22-N thruster is pointed out radially from the pod. Two of the pods are located near the top of the bus structure opposite one another and 90° from the solar arrays. Directly below each of the upper pods, near the bottom of the bus structure, are the other two RCS pods. These locations and thruster orientations allow full control of the vehicle attitude. More details on the RCS system can be found in its relative section later in this document.

There are two 18-in. diameter Lightband systems attached to either end of the return vehicle bus. The Lightband system on the bottom of the bus is used to separate the return vehicle from the in-space stage of the launch vehicle. The Lightband system at the top of the bus is used to separate the sample aeroshell for Earth entry and descent. More details on the Lightband systems can be found in Section 4.2.2, System Assumptions under Structures and Mechanisms.

Figure 3.24 shows those components on the return vehicle that are located inside the cylindrical bus structure. They include: the RCS propellant tank; the electronics and gimbals for the electrical power subsystem; the avionics enclosure for the C&DH system; all the electronics associated with the communications system; the Inertial Measurements Units (IMUs) and star trackers of the attitude, determination, and control (AD&C) system; and the propellant tank support structures.

Near the top of the bus structure are the AD&C system IMUs and star trackers. All these components are mounted directly to the inside wall of the bus structure. Orientation of the star trackers was discussed earlier as they were listed as external components due to the end of the baffles and their field-of-view protruding outside the bus structure, however a vast majority of the star trackers are contained inside the bus structure. A more detailed discussion on the AD&C components can be found in their relative section later in this document.

Below the AD&C system components are many of the communications electronics and the avionics enclosure of the C&DH system. All these electronics boxes are mounted directly to the inside wall of the cylindrical bus structure. Located just below these components are the battery, the power electronics boxes, and the solar array gimbals of the electrical power system. While the battery and power electronics boxes are mounted directly to the inside wall of the bus structure, the solar array gimbals are attached to the outside wall of the bus structure via the mounting flange located on them. Further below these components are the remainder of the communications electronics, all of which are attached to the inside wall of the bus structure. More details on these components can be found in their relative system sections later in this document.

At the bottom of the bus structure is the RCS propellant tank. The tank is mounted to a flange in the center of the bus cylinder via the flange contained on the pedestal mount structure of the tank. Four structural tubes support the flange to which the tank is mounted. Each tube extends from the flange down to the base of the cylindrical bus structure and are arranged 90° from one another. More details on the return vehicle structures can be found in its relative section later in this document.

Figure 3.25 and Figure 3.26 show a couple more transparent views of the internal components on the return vehicle.

As mentioned earlier, the return vehicle is the spacecraft that will return the Titan Sample, located inside the aeroshell that is located on the top of the return vehicle bus. The sample is contained inside an insulated canister located inside the aeroshell. The aeroshell is designed so that the heatshield separates from the backshell and rotates 90° using a hinge mechanism. This allows the aeroshell to be open during the Earth return phase of the mission so that the canister containing the Titan sample can have a view of deep space to keep the sample cool, preventing the ice contained in the sample from melting. In addition to the aeroshell opening, the sample canister itself can open using a hinge mechanism to allow the sample to be deposited while on the Titan surface. Figure 3.27 shows the three different configurations of the aeroshell and sample canister.

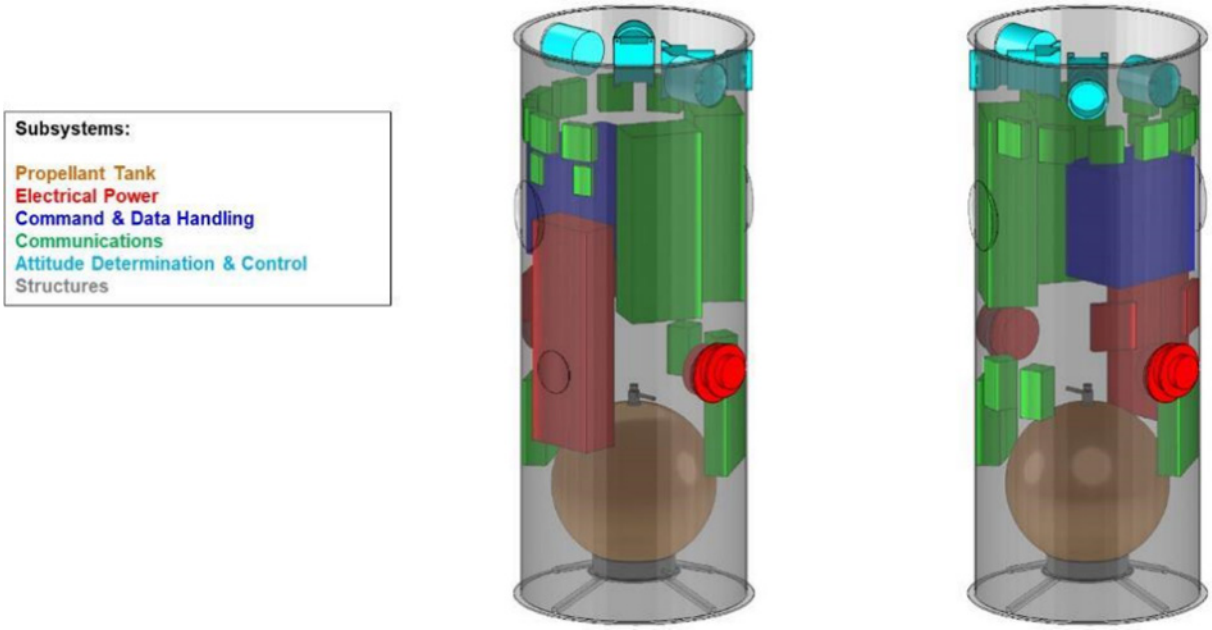

Figure 3.24.—Components on the return vehicle located within the bus structure.

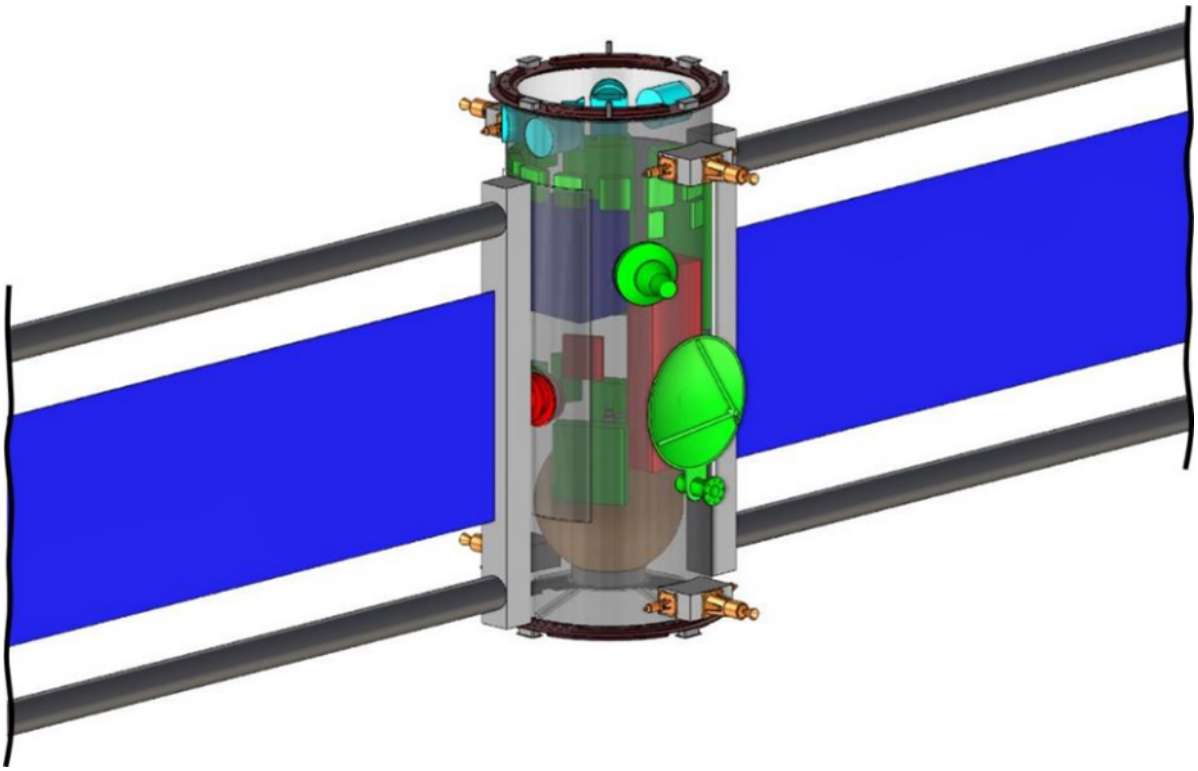

Figure 3.25.—Transparent view of the return vehicle.

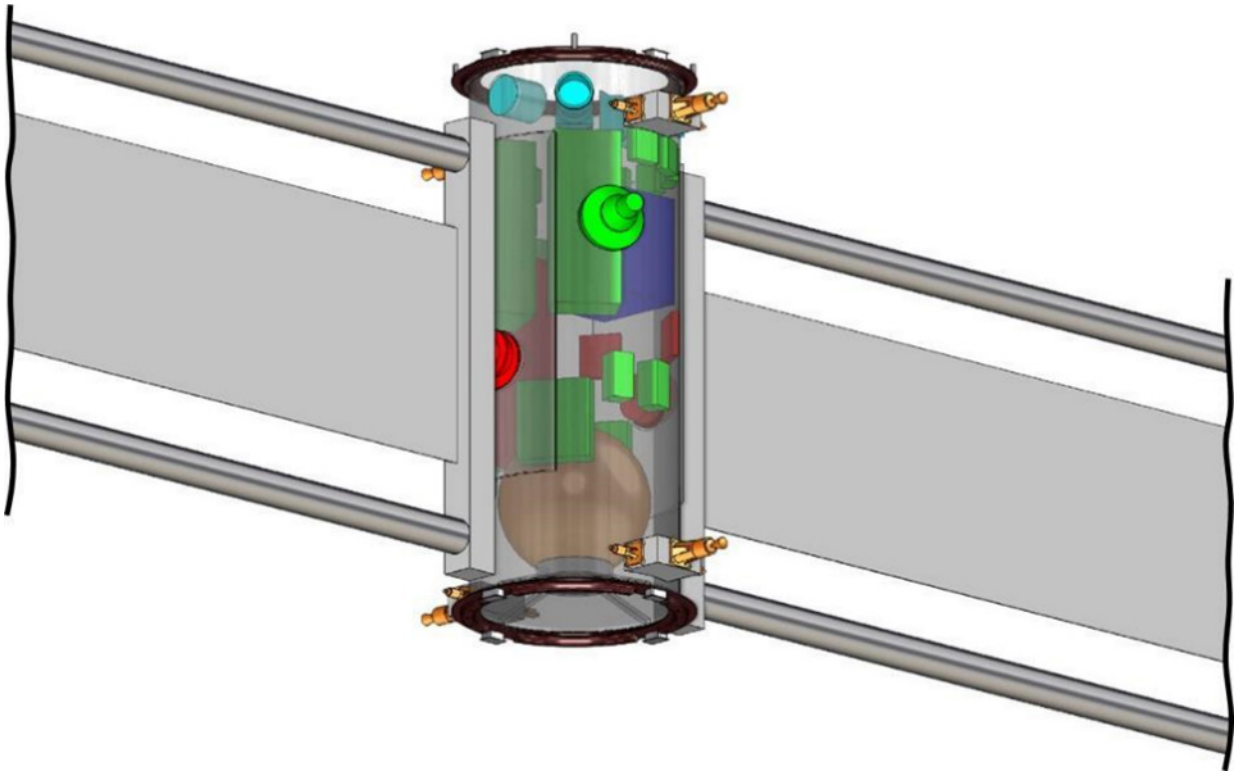

Figure 3.26.—Additional transparent view of the return vehicle.

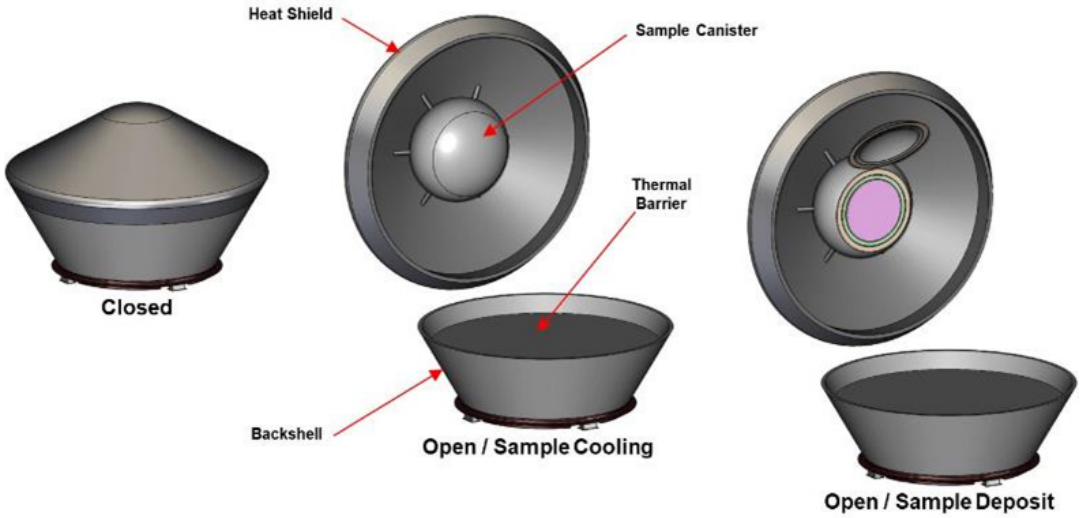

Figure 3.27.—Three configurations of the aeroshell and sample canister for the various mission phases.

Figure 3.28 shows the components contained inside the aeroshell. They include: a parachute canister and parachute; the sample canister and supporting structure; and a thermal barrier (insulated structural plate) between the parachute canister and sample canister.

Mounted directly to the back wall of the backshell is the parachute canister containing the parachute that is used to reduce the velocity of the aeroshell during the descent phase at Earth. Rather than the parachute being deployed by separation of the backshell from the heatshield, as is done for many mission descents, the canister itself will have a door that opens out the back of the backshell to deploy the parachute while the heatshield and backshell still remain attached to one another.

The sample canister is tucked into the nose of the heatshield portion of the aeroshell. A series of six struts is used to attach the canister to the inside surface of the heatshield. These six struts provide the only direct heat flow into the canister and are structurally designed to minimize this heat flow to keep the ice within the sample frozen. More details on the design of these struts and the impact on the heat flow can be found in Section 4.7 of this document.

Between the parachute canister and the sample canister is an insulated plate. This is used to keep any heat that may enter the backshell, either during entry or from the heat of the return vehicle electronics when attached, from subsequently heating the sample return canister. It should be noted that no components that would generate their own heat are located inside the aeroshell and the only heat transfer into the aeroshell will be through the heatshield and backshell walls during the various phases of the mission.

Figure 3.29 shows the sample canister design. It consists of three concentric pressure vessel structures each with a “doorknob” shape and separated from one another by low conductivity separator structures (not shown in the image) to minimize the heat flow from the outside to the inside of the inner canister containing the sample. A layer of insulation is contained between the outer and middle pressure vessels, while the space between the middle and inner pressure vessels will be filled with LOx processed by the ISRU processing plant while on the Titan surface. The innermost pressure vessel contains an approximate 3-kg Titan sample to be returned to Earth. This insulated, concentric pressure vessel design is done to prevent the ice within the Titan sample from melting during all phases of the mission once deposited in the canister. The entire canister will be opened using a hinge mechanism to allow the sample to be deposited while on the Titan surface. More details on the sample canister design can be found in Section 4.7 of this document.

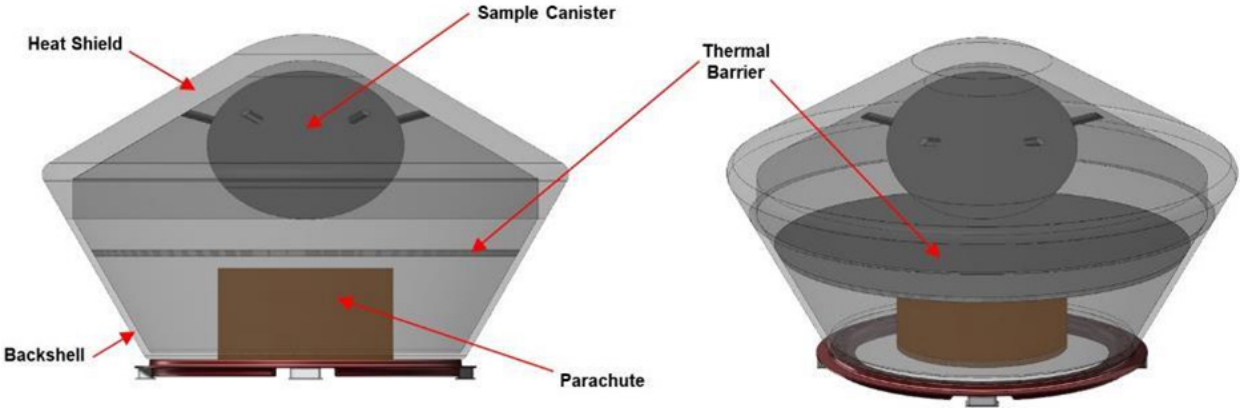

Figure 3.28.—Components located within the sample return aeroshell.

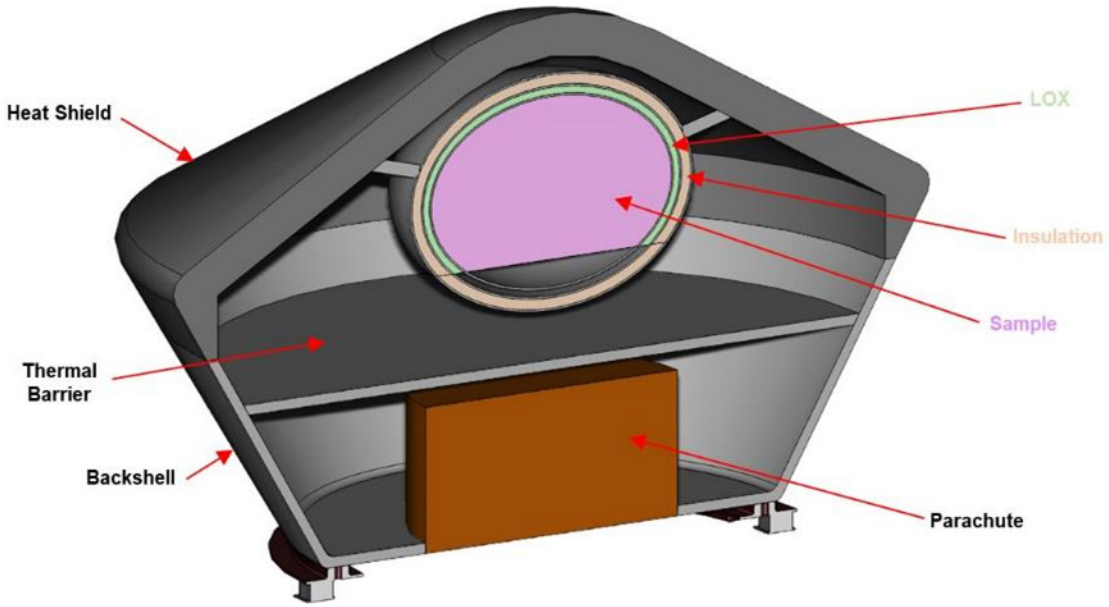

Figure 3.29.—Cross section view of the aeroshell and sample canister.

4.0 Subsystem Breakdown

The following sections outline the details of each subsystem in the designs, including requirements, assumptions, trades, and next steps.

4.1 Science

4.1.1 Scientific Goals

Titan is unique in the outer solar system in that it is the only moon with a thick atmosphere, and the only body in the solar system outside the Earth with liquid seas on its surface. The Titanian oceans, however, are seas of liquid hydrocarbons, and the rocks on the surface are solid water ice.

Titan is scientifically fascinating in many ways (Refs. 3 and 4) , not the least of which is as a representative of the icy Moons of the outer solar system. As a world with an atmosphere and liquid oceans, and the only body other than the Earth with a hydrological cycle (albeit with rains of CH_4 taking the place of water in the phase-change cycle), Titan is a high value study for atmospheric and climate science, both in its own right, and also as an opportunity to learn about Earth by comparison to another, similar body. In addition, beneath a crust of ice, Titan is an ocean world, representative of the many ice-covered liquid oceans found in the solar system including Moons of Jupiter, other Moons of Saturn, Neptune, and even Pluto.

The Compass Team has put particular emphasis here on one science goal: Titan is a high priority target for astrobiology (Refs. 4 to 11).

The surface and atmosphere are rich in the complex organic compounds known as tholins, which are ubiquitous in the outer solar system and Kuiper belt, yet not well understood. These are likely to be the molecules of the early solar system which served as the building blocks from life arose. Samples of Titan's surface and atmospheric tholins, as well as the many other components of Titan's surface, would be invaluable to understanding this relation.

The importance of Titan for astrobiology has been noted by many researchers. Titan is listed as number one in the list of astrobiological targets by Shapiro and Schulze-Makuch (2009) (Ref. 6) due to its

rich organic chemistry and the possibilities of under-standing the early chemical stages that lead to life. Raulin (Ref. 5) emphasized the “many similarities with the prebiotic chemistry which allowed the emergence of life on Earth.” Hörst et al. (Ref. 10) point out that the chemistry of Titan may emulate the prebiotic early Earth, and thus that studies of Titan chemistry could tell us about the conditions for the origin of life on Earth, a point also made in Raulin et al. (Ref. 7).

Many sources show that amino acids and nucleotides, the building blocks of life, can be formed in Titan conditions (including Hörst et al. (Ref. 10), Lorentz et al. (Ref. 4), Neish et al. (Ref. 9), and Cleaves et al. (Ref. 11)).

While some analysis of such compounds may be possible using lightweight instruments on board a probe, a detailed investigation of these complex compounds will require an analysis using a full laboratory on Earth. Because of its value to understanding the organic compounds of the outer solar system which may be the primordial building-blocks of life, return of samples from Titan to laboratories on Earth will be the primary goal of this mission.

Such a mission would be invaluable for its science return, and its contribution to our understanding the origins of organic compounds in the solar system and our place in the universe.

4.1.2 Master Equipment List

Table 4.1 represents the Science Sample Return Vehicle MEL.

4.2 Structures and Mechanisms

The Titan Sample Return spacecraft and lander structures must contain the necessary hardware for avionics, command and data handling, communications and tracking, thermal systems, propulsion, and electrical power. The structural components must be able to withstand applied mechanical and thermal loads. In addition, the structures must provide minimum mass and deflections, sufficient stiffness, and vibration damping. The operational loads include an approximate maximum axial acceleration of –6.0 g along and a non-concurrent maximum lateral acceleration of 2.0 g from the launch vehicle. Environmental temperature is in the range of 91 K.

Mechanisms are used to setup up the various systems into an operational condition. Mechanisms are used to separate from hardware that is no longer necessary for the mission and to deploy other hardware to initiate parts of other systems.

TABLE 4.1.—SCIENCE SAMPLE – RETURN VEHICLE MEL

Description Case 1_Titan_Sample_Return CD-2021-186	QTY	Unit Mass	Basic Mass	Growth	Growth	Total Mass
Science			3.0	0%	0.0	3.0
Science			3.0	0%	0.0	3.0
Samples			3.0	0%	0.0	3.0
Titan Sample	1	3.0	3.0	0%	0.0	3.0

4.2.1 System Requirements

The bus is to support the mounted hardware bearing launch and operational mechanical and thermal loads without failure. The structures shall not degrade for the extent of the mission in the Earth, deep space, and Titan environments.

4.2.2 System Assumptions

The bus provides the backbone for the mounted hardware. The primary materials for the bus are carbon/cyanate ester composite, aluminum, and Monel 400. The carbon/cyanate ester composite, M55J 6k/954-3 as described by Department of Defense MIL-HDBK-17F (Ref. 25), is used as a laminated composite by itself and as laminated composite face sheets with an aluminum honeycomb core in a composite sandwich structure. The aluminum alloy is 7075 T73 as described in the Federal Aviation Administration's Metallic Materials Properties Development and Standardization (MMPDS-14) (Ref. 26). The Monel 400 is used for the bus and tank mount cables. The materials are at a Technology Readiness Level of 6 (TRL 6) as presented by Mankins (Ref. 27). Components are of shells and tubular members. Joining of components is by threaded fasteners, riveting, or bonding.

Secondary structures include decks to support internal hardware and decks to support thrusters. Other secondary structures are the components for installation hardware. Mechanisms include a bus deployment drive system, the passive and active sides of a Marman clamp system, Lightband separation mechanisms, and frangibolts for releasing a fairing.

4.2.3 System Trades

The Compass Team considered a dedicated launch platform, separate from the landing craft. It was determined that the complexity of deploying the unit was excessive and presented reliability concerns. Figure 4.1 illustrates a simple structural analysis model of the launch pad. The unit was modeled with a composite sandwich structure deck with legs utilizing aluminum tubular members.

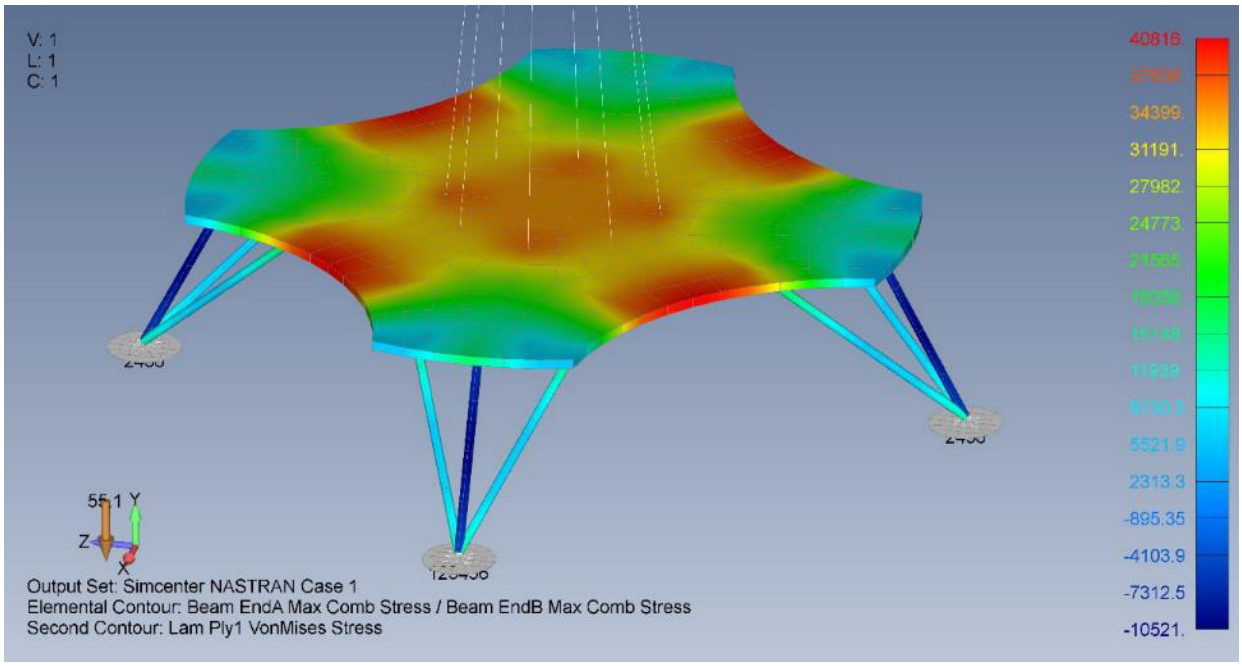

Figure 4.1.—Launch Pad, Separated from the Landing Craft.

A stress contour from a finite element analysis run is provided. The mass of the launch vehicle, represented as a concentrated mass at the approximate height of the center of gravity, under the Titan gravitational field was placed at the center of the platform.

4.2.4 Analytical Methods

Analytical methods were by hand calculations and spreadsheet to conduct preliminary stress analysis. In addition, a quick finite element analysis (FEA) was conducted on a simple model of the main structural components with smaller components being represented by concentrated masses. The FEA model utilized the study's computer aided design (CAD) model.

4.2.5 Risk Inputs

Elevating a launch vehicle on the surface of Titan is a new endeavor. Unexpected environmental conditions may hamper the process. Consequences may range from lower performance from the hardware to loss of mission.

Bus deployment with inflatable tanks is a relatively new technology. Many subsystems have to accommodate the bus segment displacement. Hang-ups or binding of components may occur. As with the launch vehicle elevation process, consequences include range from performance from mounted hardware to a loss of the mission.

In an effort to mitigate the identified risks, the structure and mechanisms are to be designed to NASA standards and fully evaluated for function under the anticipated conditions.

4.2.6 System Design

The main bus cylinder material of the launch vehicle is a carbon fiber reinforced cyanate ester, M55J 6k/954-3, laminated composite. Lamina properties are from the Department of Defense MIL-HDBK-17F (2002) (Ref. 25). Ply thickness is 61 μm (0.0024 in.). The ultimate strength is 2.23 GPa (324 ksi) and the Young's modulus is 329 GPa (47.7×10^6 psi) from the Department of Defense handbook (Ref. 25). The final laminated composite uses a quasi-isotropic layup of $[-45/0/45/90]_{4S}$ with resulting properties of 109 GPa (15.8×10^6 psi) for the Young's modulus in the axial and lateral directions and a failure stress of 330 MPa (47.8 ksi) with the Tsai-Hill failure theory, as described by Agarwal and Broutman (Ref. 28). Collier Research Corporation's HyperSizer® (Ref. 29) was utilized for determining the laminated composite properties. A safety factor of 2.0 is applied to the failure stress, per NASA-STD-5001B (Ref. 30), for a resulting allowable stress of 165 MPa (23.9 ksi). The M55J 6k/954 3 composite density is 1.65 g/cm³ (0.060 lb/in³).

The launch vehicle bus deployment rail material and flange material are aluminum 7075-T73. Per the MMPDS (Ref. 26) the ultimate strength is 455 MPa (66 ksi) and the yield strength is 407 MPa (59 ksi). Applying safety factors of 1.4 on the ultimate strength and 1.25 on the yield strength and selecting the lower value, as per NASA Standard 5001B (2016) (Ref. 30), results in an allowable stress of 325 MPa (47 ksi) at room temperature. The Young's modulus is 71.0 GPa (10.3×10^6 psi) and the density is 2.80 g/cm³ (0.101 lb/in³).

Cables are utilized to stiffen the deployed bus of the launch vehicle and to support the tanks. The cables are 4.8 mm (0.188 in.) diameter with a 7 by 9 cross section. The cable material is Monel 400.

The landing vehicle utilized decks with a composite sandwich structure architecture. The carbon fiber reinforced cyanate ester composite described above is specified for the face sheets over an aluminum honeycomb core.

A preliminary stress calculation was performed on the various elements of the assembly. The components include bus cylinders, bus deployment rails, and launch vehicle support.

The Titan launch vehicle bus cylinder bears the launch vehicle's own weight and the return vehicle on top. It is assumed that the launching of the spacecraft provides the highest acceleration of the bus. The launch vehicle's assumed maximum axial acceleration is 6 g which results in a 49 kN (11,000 lb) load on the bus cylinder. Assuming an equally distributed load on the bus circumference the stress is approximately 6.8 MPa (0.98 ksi). This provides a positive margin of 16.7. Due to the limited duration of the study and the limited information on the bus configuration initially the stress due to the small lateral acceleration was not determined with hand calculations.

The Compass Team also evaluated the structural integrity of the bus deployment rails. The rails bare a load when the bus is in a deployed state launching from the surface of Titan at a 1 g acceleration. The rails are made of aluminum 7075-T73 with an allowable stress of 309 MPa (45 ksi). The supported mass is approximately 3900 kg (8600 lb). The Team assumed that the load is evenly distributed among the rails. The resulting stress is 13 MPa (2.0 ksi) with a margin of 8.2.

The deployed bus of the Titan launch vehicle was evaluated with FEA using NASTRAN. The FEA model was constructed of shell, beam, rod, and concentrated mass elements to approximate its modal responses. Shell elements representing deck had properties of laminated composites with the honeycomb core. Rigid, Radar à Balayage Electronique 2 (RBE2), elements were used to tie components together. Concentrated mass elements were used to represent tanks. The FEA model was evaluated with a modal analysis in a free-free state. Figure 4.2 illustrates the analysis model with its first non-rigid body modal frequency. The cable suspended tanks are responsible for many of the lower modal frequencies. The first modal frequency is at 0.4 Hz.

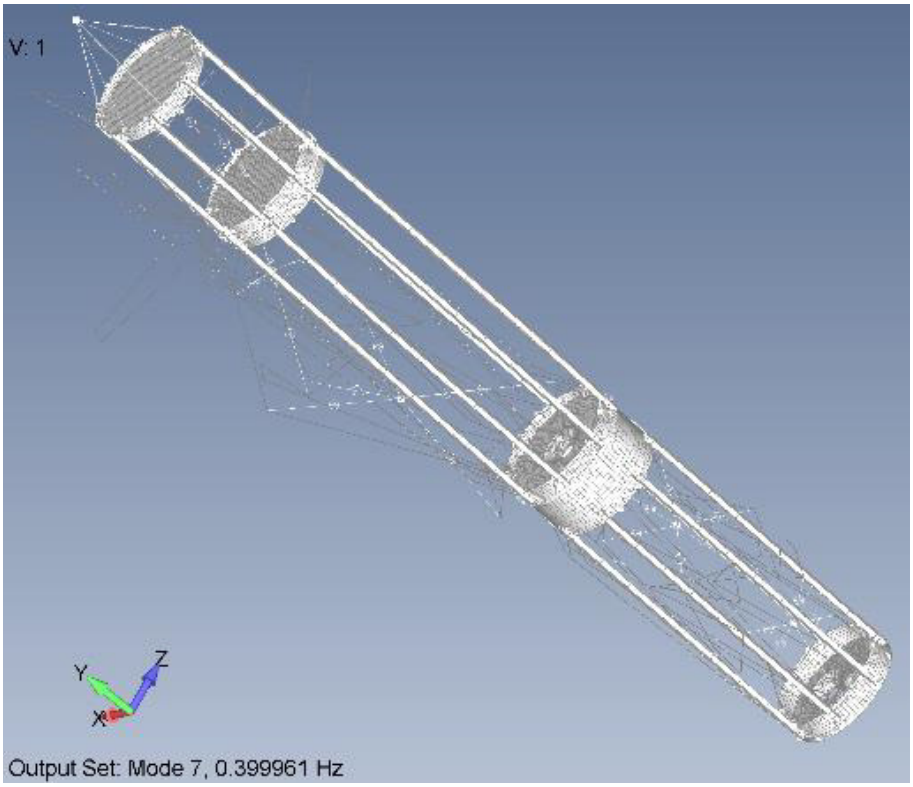

Figure 4.2.—The first non-rigid body motion modal frequency at 0.4 Hz for the Titan launch vehicle with the deployed bus and filled tanks.

A quick evaluation of the A-frame support of the Titan launch vehicle within the X-37 bay was conducted. The frame has square tubular members. The team assumed that the load is equally distributed between two supports. The total supported mass is approximately 800 kg (1800 lb). The maximum axial acceleration is 6 g. The resulting maximum stress is 27 MPa (3.9 ksi) which gives a margin of 11.

A few mechanisms are used with the Titan sample return vehicle assembly. The team assumed Marman clamp systems between the stages. There is a mechanical drive used for the Titan launch vehicle bus deployment system. Two motors with gear boxes are used to raise the Titan launch vehicle into a launch position. The Titan launch vehicle is estimated to have a mass of 800 kg (1800 lb) with a center of gravity being approximately 2.6 m (100 in) above the base. The total torque needed to raise the vehicle is 2900 N-m (25,700 lb-in.). A motor based on the Moog 307 series with an attached gear mounted at each pivot point will meet the necessary requirements.

Part of secondary structures are components for installing main system parts. Installation hardware is calculated as 4 percent of the installed hardware mass. Heineman (Ref. 31) has shown that 4 percent is a good approximation for the mass. The 4 percent installation hardware mass was applied to the command and data handling, communication and tracking, electrical power, thermal control; and propulsion systems.

4.2.7 Recommendation(s)

A high-fidelity structural analysis is needed to help optimize the system. Due to the low modal frequencies the cable supported tanks may utilize additional supports to stiffen the bus and tank support structure. Also, the cables need pre-tensioning.

Orthogrid or isogrid panels may be applied and/or greater use of carbon fiber reinforced polymer composites may be used to improve the structural stiffness of the system.

4.2.8 Master Equipment List

Table 4.2 to Table 4.8 are the Structures and Mechanisms MELs.

TABLE 4.2.—STRUCTURES AND MECHANISMS – RETURN VEHICLE MEL

Description Case 1_Titan_Sample_Return CD-2021-186	QTY	Unit Mass	Basic Mass	Growth	Growth	Total Mass
Structures and Mechanisms			**16.4**	**15%**	**2.4**	**18.8**
Structures			**9.8**	**18%**	**1.8**	**11.5**
Primary Structures			9.5	18%	1.7	11.2
Main Bus	1	9.5	9.5	18%	1.7	11.2
Secondary Structures			0.3	18%	0.1	0.3
Tank Support	1	0.3	0.3	18%	0.1	0.3
Mechanisms			**6.6**	**10%**	**0.7**	**7.3**
Adaptors and Separation			3.3	2%	0.1	3.4
Lightband, passive to LV	1	0.9	0.9	2%	0.0	0.9
Lightband, active to sample capsule	1	2.4	2.4	2%	0.0	2.4
Installations			3.3	18%	0.6	3.9
C&DH Installation	1	0.3	0.3	18%	0.1	0.4
Comm. & Tracking Installation	1	0.5	0.5	18%	0.1	0.6
Electrical Power Installation	1	1.3	1.3	18%	0.2	1.5
Thermal Control Installation	1	0.7	0.7	18%	0.1	0.8
Chemical Propulsion Installation	1	0.5	0.5	18%	0.1	0.6

TABLE 4.3.—STRUCTURES AND MECHANISMS – RETURN VEHICLE SAMPLE CAPSULE MEL

Description Case 1_Titan_Sample_Return CD-2021-186	QTY	Unit Mass	Basic Mass	Growth	Growth	Total Mass
Structures and Mechanisms			**0.9**	**2%**	**0.0**	**0.9**
Mechanisms			**0.9**	**2%**	**0.0**	**0.9**
Adaptors and Separation			0.9	2%	0.0	0.9
Lightband, passive to return vehicle	1	0.9	0.9	2%	0.0	0.9

TABLE 4.4.—STRUCTURES AND MECHANISMS – IN-SPACE STAGE MEL

Description Case 1_TSR_Launch_Vehicle CD-2021-186c	QTY	Unit Mass	Basic Mass	Growth	Growth	Total Mass
Structures and Mechanisms			**41.5**	**14%**	**6.0**	**47.5**
Structures			**30.4**	**16%**	**4.8**	**35.2**
Primary Structures			29.1	17%	4.8	33.9
bus	1	4.7	4.7	18%	0.8	5.5
bus deployment rail	8	1.6	12.7	18%	2.3	14.9
cable, diagonal	16	0.2	2.7	2%	0.1	2.8
frustum	1	4.3	4.3	18%	0.8	5.0
deck	2	2.4	4.8	18%	0.9	5.6
Secondary Structures			1.3	2%	0.0	1.3
cable, tank to cylinder, top & bot	12	0.1	0.8	2%	0.0	0.8
cable, between tanks	6	0.1	0.5	2%	0.0	0.5
Mechanisms			**11.1**	**10%**	**1.2**	**12.3**
Adaptors and Separation			8.9	9%	0.8	9.7
Marman clamp sys, active side	1	2.4	2.4	2%	0.0	2.4
Marman clamp sys, passive side	1	2.4	2.4	2%	0.0	2.5
fairing release, Frangibolt	10	0.0	0.4	2%	0.0	0.4
bus deployment drive system	1	3.7	3.7	18%	0.7	4.3
Installations			2.2	18%	0.4	2.6
Electrical Power Installation	1	0.1	0.1	18%	0.0	0.1
Thermal Control Installation	1	0.2	0.2	18%	0.0	0.2
Chemical Propulsion Installation	1	2.0	2.0	18%	0.4	2.3

TABLE 4.5.—STRUCTURES AND MECHANISMS – UPPER ATMOSPHERE STAGE MEL

Description Case 1_TSR_Launch_Vehicle CD-2021-186c	QTY	Unit Mass	Basic Mass	Growth	Growth	Total Mass
Structures and Mechanisms			**61.0**	**16%**	**9.7**	**70.7**
Structures			**47.2**	**15%**	**7.2**	**54.3**
Primary Structures			45.9	16%	7.1	53.0
bus	1	4.7	4.7	18%	0.8	5.5
bus deployment rail	8	4.0	31.8	18%	5.7	37.6
cable, diagonal	16	0.4	7.0	2%	0.1	7.1
deck	1	2.4	2.4	18%	0.4	2.8
Secondary Structures			1.3	2%	0.0	1.3
cable, tank to cylinder, top & bot	12	0.1	0.8	2%	0.0	0.8
cable, between tanks	6	0.1	0.5	2%	0.0	0.5
Mechanisms			**13.9**	**18%**	**2.5**	**16.3**
Adaptors and Separation			9.3	18%	1.7	10.9
bus deployment drive system	1	4.4	4.4	18%	0.8	5.1
marmn clamp, active side	1	4.9	4.9	18%	0.9	5.8
Installations			4.6	18%	0.8	5.4
Thermal Control installation	1	0.6	0.6	18%	0.1	0.7
Propulsion (Chem) installation	1	4.0	4.0	18%	0.7	4.8

TABLE 4.6.—STRUCTURES AND MECHANISMS – 1ST STAGE MEL

Description Case 1_TSR_Launch_Vehicle CD-2021-186c	QTY	Unit Mass	Basic Mass	Growth	Growth	Total Mass
Structures and Mechanisms			**60.9**	**16%**	**9.6**	**70.5**
Structures			**46.9**	**15%**	**7.1**	**54.1**
Primary Structures			45.6	16%	**7.1**	**52.7**
bus	1	10.8	10.8	18%	2.0	12.8
bus deployment rail	8	3.2	25.4	18%	4.6	30.0
cable, diagonal	16	0.4	7.0	2%	0.1	7.1
deck	1	2.4	2.4	18%	0.4	2.8
Secondary Structures			1.3	2%	**0.0**	**1.3**
cable, tank to cylinder, top & bot	12	0.1	0.8	2%	0.0	0.8
cable, between tanks	6	0.1	0.5	2%	0.0	0.5
Mechanisms			**13.9**	**18%**	**2.5**	**16.4**
Adaptors and Separation			9.0	18%	**1.6**	**10.7**
bus deployment drive system	1	4.1	4.1	18%	0.7	4.9
marmn clamp, active side	1	4.9	4.9	18%	0.9	5.8
Installations			4.9	18%	**0.9**	**5.8**
Therrmal Control Installation	1	0.5	0.5	18%	0.1	0.6
Chemical Propulsion Installation	1	4.4	4.4	18%	0.8	5.2

TABLE 4.7.—STRUCTURES AND MECHANISMS – PROPELLANT PROCESSING LANDER MEL

Description Case 1_TSR_Propellant_Processing CD-2021-186b	QTY	Unit Mass	Basic Mass	Growth	Growth	Total Mass
Structures and Mechanisms			**191.1**	**18%**	**34.4**	**225.5**
Structures			**129.1**	**18%**	**23.2**	**152.4**
Primary Structures			116.5	18%	21.0	137.4
LV elevator mount flange	1	16.5	16.5	18%	3.0	19.5
LV elevator support stand	2	2.8	5.5	18%	1.0	6.5
Main Deck	1	73.8	73.8	18%	13.3	87.1
Small Deck	1	20.6	20.6	18%	3.7	24.3
Secondary Structures			12.7	18%	2.3	14.9
Main deck box	1	1.6	1.6	18%	0.3	1.9
Small deck box	1	10.6	10.6	18%	1.9	12.5
Antenna boom	1	0.5	0.5	18%	0.1	0.6
Mechanisms			**62.0**	**18%**	**11.2**	**73.1**
Communications Mechanisms			0.3	18%	0.0	0.3
Antenna spring/lock hinge	1	0.3	0.3	18%	0.0	0.3
Adaptors and Separation			45.0	18%	8.1	53.1
Elevator motor	2	20.0	40.0	18%	7.2	47.2
Marman clamp mech.	1	5.0	5.0	18%	0.9	5.9
Installations			16.7	18%	3.0	19.7
C&DH installation	1	0.7	0.7	18%	0.1	0.8
Comm. & Tracking installation	1	1.0	1.0	18%	0.2	1.2
Science installation	1	15.1	15.1	18%	2.7	17.8

TABLE 4.8.—STRUCTURES AND MECHANISMS – ISRU SYSTEM MEL

Description Case 1_TSR_Propellant_Processing CD-2021-186b	QTY	Unit Mass	Basic Mass	Growth	Growth	Total Mass
Structures and Mechanisms			**3.0**	**18%**	**0.5**	**3.5**
Mechanisms			**3.0**	**18%**	**0.5**	**3.5**
Installations			3.0	18%	0.5	3.5
Thermal Control Installation	1	1.5	1.5	18%	0.3	1.8
EP Propulsion Installation	1	1.5	1.5	18%	0.3	1.8

4.3 Electrical Power System (EPS)

The electrical power system (EPS) fully supports all electrical loads during the launch and return stages of the mission. Concentrator solar arrays provide sufficient power only for nominal cruise operations, so all additional power demands near Titan must be supplemented with batteries.

Most of the EPS components – solar arrays, power management and distribution (PMAD), and multi-use Li-ion battery—are located on the return vehicle. The launch vehicle has an additional, single-use Li-ion battery to provide power during initial phases of the return mission but uses the return vehicle's PMAD to do so; the PMAD must thus be active during the entire return mission, from Titan launch through near-Earth operations. Once the launch vehicle has completed its purpose, the stage and its battery are jettisoned. Lander power is discussed in more detail in Section 4.4, Radioisotope Power System (RPS).

4.3.1 System Requirements

The vehicles' operational modes, durations, and associated electrical load demands in each phase of the return mission are given in Table 4.9. At the top of the table, dark blue indicates power modes associated with the return vehicle, and purple indicates power modes associated with the launch vehicle. Pre-launch (Power Mode 1 for the return vehicle) is assumed to be taken care of by ground systems and not included in the following EPS design.

The downstream electrical load demands ("Load Power/Energy Needed") shown are all the non-EPS PEL requirements and include a 30 percent growth margin. The upstream source-level demands ("Array/Battery Power/Energy Needed") were back-calculated from these load demand numbers to include all EPS efficiency losses and internal parasitic power needed for component operation. The source-level demands thus reflect the raw power output required from the arrays and batteries.

The shaded boxes in the source-level demands section illustrates the active spacecraft power source(s) during the various phases of the mission. The launch vehicle battery (light blue) is located on the launch vehicle but supports all launch and burn needs for *both* the launch and return vehicles. Once the system has ascended from the Titan surface, the return vehicle's solar array wings (yellow) deploy and begin to generate enough power for the long cruise home. The return vehicle battery (green), located on the return vehicle, supplements the array by supporting all non-burn power needs throughout the rest of the mission (mid-course corrections and distance communications) and is slowly recharged by the array during the three months in between each use.

The source demands section also gives the limiting-case constraints for array and battery sizing in bolded red numbers. For example, 15.0 W of beginning of life (BOL) array power at Titan calls for a larger array than 206.6 W at end of mission (EOM) near Earth, so 15.0 W at Titan is the array sizing requirement. The launch vehicle battery requires a peak nominal power of 279.1 W (power mode 10) and a total energy of all of the modes for which it is responsible (power modes 8, 2, 9, 10): 262.8 Wh + 548.9 Wh = 811.7 Wh. Table 4.10 summarizes the limiting-case array and battery sizing requirements from the source-level demands of all power modes.

TABLE 4.9.—EPS REQUIREMENTS PER POWER MODE

Vehicle	Return	Launch	Return	Launch	Launch	Return	Return	Return	Return	Return
Power Mode	1 Pre-Launch	8 Launch	2 Launch	9 In-Space Stage Coast	10 In-Space Stage Burns	3 Cruise/ Sleep	4 Mid-Course Corrections	5 Distance Comm	6 Prepare EDL Ops	7 Near-Earth Comm
Duration	5 min	90 min	90 min	12 mo	1.97h total	7 yrs	10 min, 3 times	8h every 3 mo	30 min	8h every 3 mo
Location	Titan	Titan	Titan	Titan	Titan	Titan	Titan / Interplanetary	Titan / Interplanetary	Earth	Earth
Load Power Needed (W)[1]	N/A	7.80	154.1	0	262.6	9.10	84.8	161.9	191.4	174.9
Load Energy Needed (Wh)[1]	N/A	11.7	231.1	0	516.5	---	14.1	1294.8	---	---
Array Power Needed (W)[1, 2]	N/A	0		0	0	**15.0**	15.0	15.0	206.6	189.0
Battery Power Needed (W)[1, 2]	N/A	175.2		0	**279.1**	0	79.1	**161.1**	0	0
Battery Energy Needed (Wh)[1, 2]	N/A	**262.8**		0	**548.9**	0	**13.2**	**1288.5**	0	0

[1] Includes 30% growth [2] Includes EPS losses **Limiting case**

Array operation | LV battery operation | RV battery operation

TABLE 4.10.—SUMMARY OF SOURCE-LEVEL SIZING REQUIREMENTS

Component	Power (W)	Energy (Wh)
Array	15.04 (at Titan)	----------
LV Battery	279.1	811.7
RV Battery	161.1	1301.7

4.3.2 System Assumptions

EPS sizing assumptions regarding the mission and the design/operation of individual components are as follows.

- Mission:
  - All Titan surface and pre-launch activities are fully handled by the nuclear subsystem, with no additional EPS support needed.
  - No power is needed to support the launch vehicle during its in-space stage coast (Power Mode 9).
  - There are seven in-space stage burns (Power Mode 10) that occur across 12 months for a total of 1.97 h (118 min).
  - The total return mission duration from launch to Earth entry is 7 years.
- Solar Arrays:
  - The solar array wings have continuous, near-perfect Sun pointing near Titan. (Near Earth, they may be offpointed to adjust for the excess power levels.)
  - There is no shadowing of the solar array wings once deployed.
  - The arrays can concentrate solar flux by at least 7x, and its radiator area is 7x its cell receiver area (Refs. 32 and 33).
  - The efficiency loss from LILT (low intensity, low temperature) solar cell mismatch is no more than 6 percent.
  - The deployed solar arrays are subjected to a maximum of 0.1g in structural loads, which the Compass Team assumes the array booms can adequately support.
  - The array structure uses 0.35 in. pitch when stowed (rolled).
  - Solar array gimbals can adequately withstand the environmental conditions near Titan.
- Li-Ion Batteries:
  - The batteries are already fully charged prior to launch.
  - Nominal battery operations allow a maximum depth of discharge (DoD) of ~80 percent due to the relatively few charge/discharge cycles.
  - Each battery includes one spare string for redundancy (single-fault tolerance).
  - Battery mass estimates include a mass factor of 1.5 to account for any additional battery components (circuit protection devices, battery enclosure, wiring, etc.).
  - Battery volume estimates include a packing factor of 1.2.
- Power Management and Distribution (PMAD):
  - The power conditioning and distribution unit (PCDU) has 12 fundamentally identical converter blocks that can be configured to suit a variety of inputs and outputs (Ref. 34).
    - Each block can support 3-55 V and up to 8 A.
    - Each block is a buck/boost converter with a minimum efficiency of 97 percent.

        - Input blocks used for solar array regulation have maximum power point tracking (MPPT) capability to optimize array power generation at Titan. This point can be adjusted to restrict excess power input.
        - Internal bus regulation is maintained at ~60 V.
    - A second, identical PCDU is available as a cold spare (single-fault tolerance).
    - The wire harnessing mass is approximated as 25 percent of the base EPS mass.
- Electrical Loads:
    - The electrical loads require 28 Vdc.
    - A 30 percent growth factor is applied to all electrical load demands from other vehicle subsystems.

4.3.3 System Trades

The final EPS components selected as well as other options considered are given as follows.

4.3.3.1 Solar Arrays

The solar arrays use a Stretched Optical Lens Architecture with Roll-Out Solar Array (SOLAROSA) design (Refs. 32 and 33) from Redwire Space, formerly Deployable Space Systems (DSS). These are flexible ROSA blankets that incorporate Stretched Lens Array (SLA) technology consisting of *refractive* arched Fresnel lens concentrators.

The SOLAROSAs in this Titan design do not incorporate the patent-pending high-beta-angle-tolerant lens technology (Ref. 32), but this option can be considered for future design iterations.

The Compass Team had initially considered using FACT (Flexible Array Concentrator Technology) ROSAs (Ref. 35), which consist of lightweight reflective concentrator assemblies. However, the team ultimately selected the SOLAROSAs partly for their ability to provide higher flux concentration. Flux concentration reduces the number of solar cells needed, the associated solar cell testing costs, and the negative effects of LILT solar conditions near Titan.

The SOLAROSA wings use state-of-the-art SolAero Inverted Metamorphic (IMM)-α (Ref. 36) solar cells, which have a 32 percent efficiency (BOL, 28 °C, 1 AU).

The commercial off the shelf (COTS) Ruag Septa 31 Solar Array Drive Assembly (SADA) (Ref. 37) allows for a maximum power transfer of 2.2 kW and was used to size the single-axis gimbal for each wing.

4.3.3.2 Batteries

The launch vehicle and return vehicle batteries are both composed of COTS LG 18650 MJ1 (Ref. 38) cylindrical Li-ion battery cells, which are secondary (rechargeable) cells.

Because the launch vehicle only requires a single battery discharge cycle for launch and burns, various primary (non-rechargeable) Saft and EaglePicher Technologies cells of higher specific energies (Wh/kg) than the LG MJ1 were initially considered for the launch vehicle battery. However, the Compass Team determined that the system's peak power and current needs required too many of these primary cells, so LG MJ1 cells were ultimately selected for mass and volume efficiency. The launch vehicle battery is thus labeled as a "single-use" battery because even though it is technically rechargeable, the battery is only discharged once before being discarded.

Future design iterations may also choose to consider combining the two LG MJ1 batteries, which would provide extra energy reserves for the return vehicle and mitigate the slow recharging risk detailed in the Risk Inputs section. This option was not ultimately selected here in order to discard as much mass with the launch vehicle as possible.

4.3.3.3 PMAD

The all-in-one PCDU selected for the system was Pumpkin Space Systems' Electrical Power System Module 1 (EPSM 1) (Ref. 34). This compact COTS module provides integrated PMAD functionality (array regulation, battery charge/discharge regulation, power distribution) and was chosen for its low idle power consumption (~3 W), which is critical in the power-limited conditions near Titan, and for its capability to handle higher power levels near Earth. Modular PMAD components such as Terma electronics consumed too much power even with their spare modules designated as cold spares.

While the user manual dedicates six EPSM blocks for solar array input (8-55 V, 2A/4A), three blocks for regulated output (3-55 V, 5-8 A), two blocks for battery I/O (3-55 V, 5-8 A), and one block for programmable output (3-55 V, 5-8 A), the launch and return vehicle batteries will actually need three I/O blocks in order to stay under the PMAD EPSM current and voltage limits per block. However, because the manual states that the twelve blocks are "fundamentally identical," the Compass Team assumes that configuring another block for battery purposes is not unreasonable, and our final PCDU operating assumptions are given in the preceding assumptions section.

4.3.3.4 Technology Readiness Levels (TRLs)

Table 4.11 provides the TRL estimates for the EPS components.

4.3.4 Analytical Methods

The different EPS components were sized as follows:

- The solar arrays and batteries were sized using Compass EPS array and battery spreadsheets. Stowed array volume estimates were based on ISS ROSA (IROSA) information.
- The array gimbals were based on the COTS Ruag gimbals.
- The PMAD is the COTS Pumpkin EPSM 1 PCDU.

TABLE 4.11.—EPS TRL ESTIMATES

Component	TRL	Comments
Solar arrays	5	Prototypes, small demonstrations, and some mission sizing estimates exist for the SOLAROSA.
Gimbals	6	The COTS gimbal is rated for Earth orbit conditions, so more environmental testing is needed for Titan missions.
Batteries	7	The battery cells are off-the-shelf, and cell qualification testing was recently completed by ABSL/Quallion (EnerSys) (Ref. 39). Space-rated versions of the batteries are unavailable off-the-shelf and need to be custom-designed using the specified cells.
PCDU	6	The EPSM 1 has been used for low Earth orbit (LEO) CubeSats. Minor customizations will be needed for the TISR mission.
Harnessing	8	Harnessing will be based on heritage missions.

4.3.5 Risk Inputs

4.3.5.1 Risk Statement

Given that the return vehicle battery recharges very slowly near Titan, there is a possibility that the spacecraft will not have adequate energy reserves for off-nominal scenarios.

Due to the limited array power output at Titan, the return vehicle's battery takes a minimum of ~1.5 months after distance communications to recover its original 100 percent state of charge (SOC). This may be a problem if there are any off-nominal situations that render the spacecraft unable to provide full array power near Titan for significant periods of time.

4.3.5.2 Mitigation Strategy

Future design iterations may consider

1. Increasing the number of spare battery strings for lower battery depth of discharge (DoD),
2. Allowing for larger stowed array volume (and thus larger deployed arrays) for faster battery recharging, and/or
3. Investigating arrays with higher-concentration lenses or improved packing (W/m^2) for increased array power.

4.3.6 System Design

The combined EPS for the launch and return vehicles is shown in Figure 4.3. The return vehicle contains most of the EPS components (blue), and the remaining components (purple) reside on the launch vehicle.

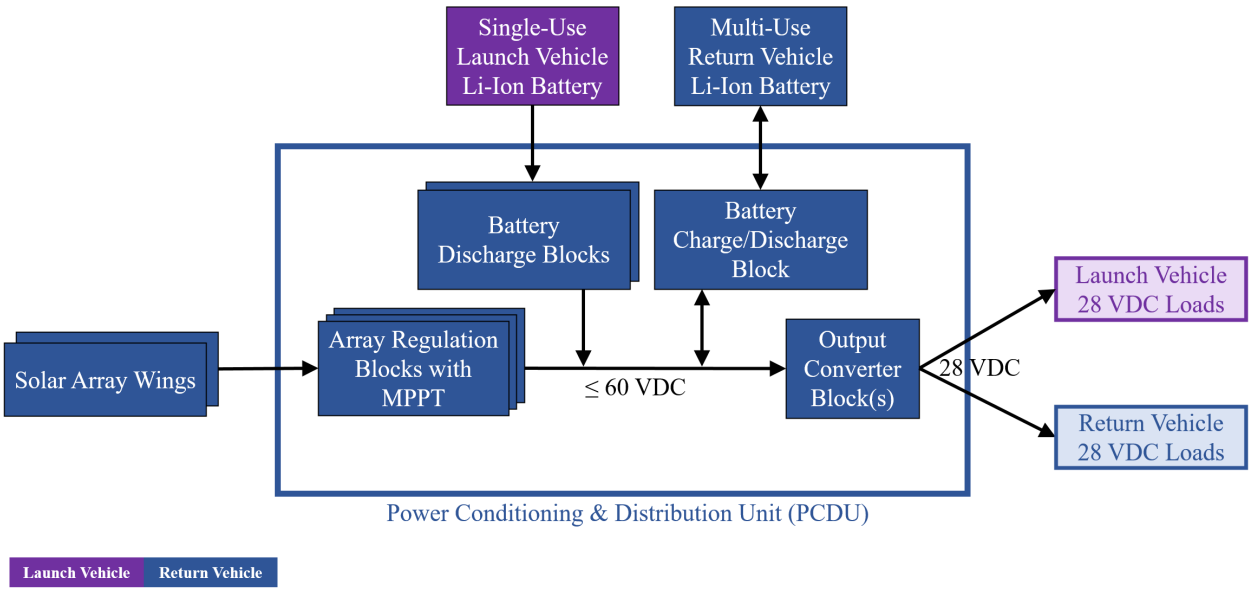

Figure 4.3.—EPS Block Diagram of Combined Launch + Return System.

4.3.6.1 Launch Vehicle

As stated in Section 4.2, the single-use battery is considered part of the launch vehicle but supports *all* launch requirements, including those of the return vehicle (see Table 4.9). To do so, the launch vehicle uses the return vehicle's PMAD system to manage the distribution of electrical power to the launch vehicle loads. The single-use battery consists of LG MJ1 cells arranged in a 7S-12P configuration to provide 1068.7 Wh of energy at 100 percent DoD. The battery is about 15.1 cm by 25.9 cm by 7.8 cm (3056.9 cm^3) and has a specific energy of 173.1 Wh/kg. Not including the spare string, it nominally depletes to 82.9 percent DoD. The battery voltage range is 17.5 to 29.4 V, and the nominal voltage is 25.4 V; however, because all PCDU inputs and outputs are converted to/from the internal PCDU voltage, the battery input voltage is not too important as long as it does not fall outside the permissible block voltage range listed in the assumptions.

Due to the higher power requirements of the in-space stage burns, the launch vehicle battery will need two PCDU blocks for discharge, hence our assumptions on minor PCDU customizability as stated in the assumptions and trades sections.

Harness mass for the launch vehicle EPS was estimated at 25 percent of the launch vehicle battery mass. When the launch vehicle has completed its portion of the mission, the battery and harnessing are jettisoned along with other parts of the launch vehicle.

4.3.6.2 Return Vehicle

The return vehicle EPS must be active from Titan launch through EDL at Earth.

The return vehicle has two flexible solar array wings on either side of the return vehicle that will generate electrical power. During launch from Titan, the solar array wings and booms are rolled about a 1.0 m, 6-in.-diameter mandrel and stowed inside the shroud of the launch vehicle. Once the shroud is jettisoned, the wings unfurl under the strain energy of the elastic slit-tube booms (3-in.-diameter each after deployment) located on each side of the blanket. The arrays do not have the ability to retract. Each deployed solar array blanket is 1.30 m^2, which includes the radiator area. The arrays produce 15.2 W total at Titan (BOL, 10.0 AU, –150 °C) and 586 W at Earth (EOM, 1.0 AU, 70 °C).

The solar array wings each have single-axis tracking ability with the Ruag Septa 31 single-axis SADA. This gimbal will allow the solar array wings to achieve the fine pointing that is necessary for the optical concentrator array.

The return vehicle has a secondary battery to support an occasional increased load demand on the return vehicle for mid-course corrections and/or communication links. The secondary battery consists of LG MJ1 cells arranged in a 9S-15P configuration to provide 1717.5 Wh at 100 percent DoD. The battery is about 19.4 cm by 32.4 cm by 7.8 cm (4912.9 cm^3) and has a specific energy of 173.1 Wh/kg. Not including the spare string, it nominally depletes to 81.2 percent DoD if the mid-course corrections and communications modes occur consecutively without recharging time in between. The solar array wings have only a small amount of surplus power generation, so the return vehicle battery is expected to take a minimum of 1.5 months (up to 3 months if necessary) to recharge for additional communications links. The battery voltage range is 22.5 to 37.8 V, and the nominal voltage is 32.7 V; however, because all PCDU inputs and outputs are converted to/from the internal PCDU voltage, the battery input voltage is not too important as long as it does not fall outside the permissible block voltage range listed in the assumptions.

The PMAD uses the commercially available Pumpkin Space Systems EPSM 1 Power Conditioning and Distribution Unit. The EPSM 1 has dedicated blocks to cover solar array inputs with max power point tracking, battery control for the batteries on the return vehicle and launch vehicle, and output blocks with fixed DC voltage control. An additional EPSM 1 is included as a cold spare.

The return vehicle harnessing mass was approximated as 25 percent of the return vehicle's base EPS mass. A detailed EPS wire harnessing layout was not completed for this study.

4.3.7 Master Equipment List

Table 4.12, Table 4.13, and Table 4.17 are the EPS MELs.

4.4 Radioisotope Power System (RPS)

The Titan Propellant Processing Plant power system consists of 3 Dynamic Radioisotope Power Systems (DRPS) modified for the Titan surface and an energy storage subsystem for power peaking. This DRPS uses 6 heritage GPHS which provide heat to 8 Stirling convertors embedded in a cylindrical housing (Figure 4.4). Each generator provides over 300 W DC at BOL. Waste heat from the DRPS is used for process heat and warming of electronics during the production of ISRU propellants.

TABLE 4.12.—ELECTRICAL POWER SYSTEMS - RETURN VEHICLE MEL

Description Case 1_Titan_Sample_Return CD-2021-186	QTY	Unit Mass	Basic Mass	Growth	Growth	Total Mass
Electrical Power Subsystem			**30.3**	**43%**	**13.2**	**43.5**
Power Generation			**13.9**	**33%**	**4.5**	**18.4**
Solar Array	2	5.2	10.5	35%	3.7	14.1
Array Single-Axis Gimbal	2	1.7	3.4	25%	0.9	4.3
Power Management & Distribution			**6.5**	**94%**	**6.2**	**12.7**
Power Electronics Box	2	0.2	0.5	20%	0.1	0.6
Harness	1	6.1	6.1	100%	6.1	12.1
Energy Storage			**9.9**	**25%**	**2.5**	**12.4**
Rechargeable Li-ion Battery	1	9.9	9.9	25%	2.5	12.4

TABLE 4.13.—ELECTRICAL POWER SYSTEMS - IN-SPACE STAGE MEL

Description Case 1_TSR_Launch_Vehicle CD-2021-186c	QTY	Unit Mass	Basic Mass	Growth	Growth	Total Mass
Electrical Power Subsystem			**7.7**	**40%**	**3.1**	**10.8**
Power Management & Distribution			**1.5**	**100%**	**1.5**	**3.1**
Harness	1	1.5	1.5	100%	1.5	3.1
Energy Storage			**6.2**	**25%**	**1.5**	**7.7**
Single-Use Lithium-Ion Battery	1	6.2	6.2	25%	1.5	7.7

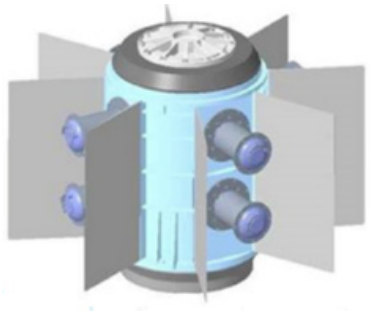

Figure 4.4.—GPHS, 8 Convertor Generator.

TABLE 4.14.—POWER MODE REQUIREMENTS

	Power Mode 1	Power Mode 2	Power Mode 3
	Propellant Processing	Communications Only	Propellant Processing and Rover Recharge
	1.5 years	8 h/day every 8 days	12 h/day
Total System power with growth	1023	1126	1166
Power Produced (W)	1131	1131	1131
Power Excess/Deficit (W)	108	5	35
Excess/Deficit Energy Per Day (Wh)	2592 1728-16 h	120	–396

4.4.1 System Requirements

The DRPS(s) is required to provide on average over 1.1 kWe to the system bus when operating on the Titan surface and this sets the power requirements of the system. Table 4.14 shows the total system power requirement (including growth). This power system is required to provide at most 1126 W (including margin) during Power Modes 1 and 2 while on the Titan surface (Table 4.14). During rover recharging and propellant processing (Power Mode 3) it is required to provide 1166 W. The mission duration is estimated at 12 years total including 3 years of storage and launch preparation, 7 years of transit to Titan and 2 years of operation on the surface. The DRPS are required to work on the Titan surface which is outside of their projected temperature qualification limits. The very dense (1.5 atm) and cold (80 K) N_2 atmosphere on Titan require modification to the DRPS which will result in both mass and power output changes from their nominal radiative deep space thermal environment.

4.4.2 System Assumptions

It is assumed that a DRPS based upon Sunpower Stirling convertors and GPHS modules will be the building block power system which will provide power to the spacecraft during Titan surface operation. Additionally, it is assumed that modifications to the DRPS will be allowed such that operation on the Titan surface is possible. Degradation rates of 1.3 percent per year, consistent with the values projected for the DRPS development will be achieved and that operation during ground operations and transit will be possible even with the modifications necessary for Titan operation. 3 DRPS generators are required for this mission with nominal power outputs in a deep space environment with each generator providing 335 W DC at BOL.

4.4.3 System Trades

Trades were performed on Stirling cold end temperature operation for operation during Titan surface operation. These trades consisted of varying fin lengths on the DRPS generator and insulation thickness around the generator. Trades were also made for various locations within the landing craft which considered both wind generated convective heat removal and isolated convection on a wind-shielded generator.

4.4.4 Analytical Methods

Both Microsoft Excel and MATLAB®/Simscape™ models were used for this analysis to model the DRPS. These provided both mass estimates and power output estimates from the generators by estimating temperatures in various locations of the landing craft and in turn the generator and at different times of operation. These models enabled estimates of power output from each DRPS.

4.4.5 Risk Inputs

As with any system that is still in the design phase, it is possible that the generator development will not be completed or that the final design layout and/or performance may be different. Additionally, changes in operational envelope were assumed beyond the current DRPS requirements for operation on the Titan surface. These changes may not be possible in a final DRPS generator if development is completed.

4.4.6 System Design

The GPHS has been the core element of modern RPS used for many deep space missions when there is a lack of adequate solar illumination to power solar cells. It is a Department of Energy (DOE) standardized thermal source that produces nominally 250 W of thermal power at BOL. Table 4.15 shows the dimensions of a GPHS module.

PuO_2 is the ceramic form of ^{238}Pu that is used as the fuel for the GPHS. PuO_2 is placed in four iridium capsules and surrounded by a graphite shell to form each GPHS module. ^{238}Pu is attractive because most of its radioactive decay energy comes from an alpha emission, and it has a long half-life (87.7 years). Relatively low amounts of neutron emission come from both spontaneous fission and (α, n) reactions, which result from the interactions of the high-energy alpha particles with materials of low atomic mass. Specifically, the iridium capsule prevents the alpha particles from leaving the fuel pellet (and interact with the surrounding graphite), but interactions with both O_{16} and O_{17} in the PuO_2 mixture does produce some neutron flux as well as spontaneous fissions of the ^{238}Pu. Production of ^{238}Pu is commonly done by neutron irradiation of ^{237}Np in a high-flux reactor. The product of this irradiation is ^{238}Np that decays (2.117 day half-life) via beta emission into ^{238}Pu. Because the plutonium fuel is decaying, and other fixed losses occur in the system it is necessary to match the DRPS power output with the number of years from fueling. Total estimated degradation rate is 1.3 percent/yr including 0.8 percent/yr fuel degradation and 0.5 percent/yr degradation from fixed losses within the generators.

Stirling convertors have an impressive record of very long-life operation. At NASA Glenn Research Center (GRC) gas bearing convertors like those under development by SunPower for this DRPS contract have over 10 years of operation without a failure. Both convertors continue to operate on their respective test stands today. This design utilizes a DRPS consisting of 6 GPHS modules and 8 Sunpower Stirling convertors that convert thermal power into electrical power. The 8 Stirling converters are operated as a balanced pair to create four strings in the generator. Each pair of Stirling convertors has a controller which monitors the health of it connected pair of convertors, provides an AC source to control both stroke and frequency of the pair and then converts the AC power output from the Stirlings to 28 Vdc. Figure 4.5 is the block diagram of a typical DRPS operating in a deep space sink of 4 K.

For this design we are using 3 DRPS generators in the configuration discussed above. Because these generators are capable of operation in an atmospheric environment no changes were required for the internal insulation used in the generator. However, because of the very high heat convention rates and cold N_2 atmosphere surrounding the generators a layer of insulation around the heat rejection surfaces is required to prevent the generators from dropping below their minimum qualification temperatures. One of these generators will use its waste heat for high temperature (100 °C) waste heat to facilitate propellant generation. Because the heat rejection temperature of the Stirling cycle can be reduced the remaining two DRPS will use the very cold 100 K ambient environment to generate higher power output. These 3 generators and their associated temperatures and power outputs are shown in Table 4.16.

4.4.7 Master Equipment List

Table 4.17 is the MEL for the RPS.

TABLE 4.15.—STEP 2 GPHS DIMENSIONS

Height (cm)	Width (cm)	Length (cm)
5.82	9.32	9.96

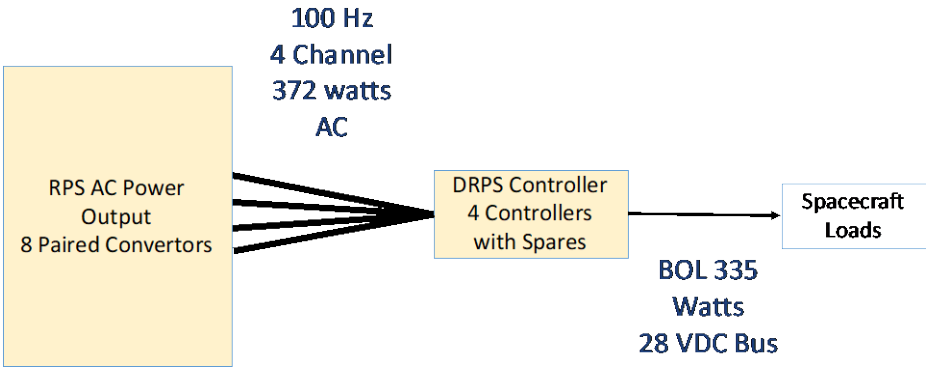

Figure 4.5.—Block diagram of a typical DRPS operating in a deep space sink of 4 K.

TABLE 4.16.—DRPS GENERATORS WITH ASSOCIATED TEMPERATURES AND POWER OUTPUTS

No. of GPHS Modules	Power Output (Electrical) AC at BOL (W_e)	Power Output Degradation Rate-AC EOL Power[a]	Thermal Power at BOL (W_{th})	Heat Rejected at BOL (W_{th})	Tcold Temperature, °C	Generator Mass (kg)[b]
6	392 W- Deep Space or High Temperature Heat Used for ISRU	1.3%/yr – 336 W	1500	1107	100	95
6 (X2 Generators)	443 W with Low Temperature Heat Used for ISRU	1.3%/yr -379 W	1500	1127	20	95
Total Power (W AC)	1279 W	1131 W				

[a]Percent per year-EOM Power-4.5 years
[b]Specific power 3.8 W/kg; Includes controller.

TABLE 4.17.—RPS MEL

Description Case 1_TSR_Propellant_Processing CD-2021-186b	QTY	Unit Mass	Basic Mass	Growth	Growth	Total Mass
Radioisotope Power System			**395.1**	**19%**	**75.6**	**470.7**
RPS System			**395.1**	**19%**	**75.6**	**470.7**
DRPS	3	81.0	243.0	20%	48.6	291.6
Controller	3	14.0	42.0	20%	8.4	50.4
Switchgear	2	30.3	60.6	18%	10.9	71.5
DC Remote Power Control Module	2	4.7	9.5	18%	1.7	11.2
Wire Harness	1	18.8	18.8	20%	3.8	22.6
battery	1	2.3	2.3	20%	0.5	2.8
BCDU	1	1.0	1.0	20%	0.2	1.2
DRPS Insulation	1	7.9	7.9	20%	1.6	9.5
In Transit Heat Rejection Radiator	1	10.0	10.0	0%	0.0	10.0

4.5 Propulsion

The propulsion system for this design consists of a two-stage launch vehicle with a cryogenic upper stage and a sample return vehicle. The first and second stages have inflatable tanks and 6 kN (1,350 lb_f) class thrusters, while the cryogenic upper stage also has inflatable tanks, but much smaller 90 N class thrusters. The sample return vehicle has a single COTS membrane tank and RCS thrusters utilizing AF-M315E monopropellant.

4.5.1 System Requirements

The propulsion system is required to provide adequate ΔV performance for a Titan surface launch and sample return to Earth. This system is required to utilize ISRU propellant from Titan's surface, since taking propellants from Earth is prohibitive mass wise. This requires the vehicle to be fueled prior to launch via an ISRU plant. The system is also required to be single fault tolerant.

4.5.2 System Assumptions

For the launch vehicle to fit inside a landing craft, the Compass Team assumed that the propellant tanks are inflatable or expandable, so that they can be collapsed for transit and deployed once on Titan's surface. In an additional effort to save mass and volume on the lander, the Team assumed that the launcher's propellant tanks will also serve as the ISRU propellant plant storage tanks as the propellants are produced. Although other propellants were initially evaluated as part of this study, the combination of LOx and LCH_4 became the clear choice due to its high I_{sp} and ease of storage at Titan ambient surface conditions. The same is therefore assumed for the launcher portion this design. The return vehicle, however, is assumed to utilize AF-M315E as propellant, due to its inherent cold tolerance, high I_{sp} density, and to the fact that cryogenic propellants will have long term storage and boil-off issues during the long trip back to Earth.

The high ambient surface pressure on Titan imposes the assumption of high chamber pressure and a low area ratio nozzle for the first stage engine to obtain adequate performance. The Team assumed that the second stage will have a deployable nozzle for increased I_{sp} at higher altitudes, and that the engines will have thrust vector control TVC systems. It is assumed that COTS or near COTS components will be used as applicable to reduce both cost and risk, and that valves will be a dual coil design for redundancy and to simplify the feed and pressurization systems.

4.5.3 Propulsion System Trades

As a part of this study, various propulsion system trades are conducted. These include propellants, overall tank design, and main engine cycle and performance trades.

4.5.3.1 Propellants

To satisfy the ISRU requirement, several potential propellant combinations that are possible using available Titan surface materials are evaluated. First, hydrazine is evaluated since it can be made using ammonia, which can be made from water and N_2 present on Titan. Hydrazine can be made using a hydrogen peroxide-based process but requires a ketone that must be brought from Earth. It can also be made via the Olin-Raschig process, but that also requires a consumable brought from Earth, mainly sodium hypochlorite. For higher performance, hydrazine could be used with NTO, which can be made via catalytic oxidation of ammonia. Even though hydrazine and NTO is a high TRL bipropellant combination, the production draw backs and low freezing points of only 0 °C for hydrazine and –11.2 °C for NTO led to it being removed from consideration. Other hydrazine derivatives are also entertained, such as monomethyl hydrazine (MMH) and unsymmetrical dimethylhydrazine (UDMH), which do have lower freezing points (–52 and

–57 °C, respectively) (Ref. 40). However, both propellants require even more complex chemical processing to manufacture and also require NTO for use as propellants, thus they are also removed from consideration.

Another potential ISRU combination is LOx and LH_2, which could be produced from the anticipated solid water ice on the Titan surface. The LOx is relatively easy to store at Titan surface ambient temperature, but the H_2 would require large tanks and active cryo-cooling, which requires additional power and cooling hardware. Therefore, LH_2 was removed from the trade tree as a potential ISRU fuel. Other concepts, such as LN_2 and Ti power were also briefly considered, but the mass of Ti required and its low I_{sp} doomed this concept.

Finally, LCH_4 is evaluated as an ISRU fuel for the launch vehicle. Being relatively easy to obtain from the atmosphere without complex chemical processing, having high I_{sp} in combination with LOx, easily storable at Titan surface temperatures, and chemically compatible with almost all the typical materials used in aerospace propulsion systems, LCH_4 is the preferred choice for this design. In addition, existing programs are developing flight hardware with this propellant combination, thus making high TRL materials, components, and processes available to a potential engine development program, thus potentially reducing both cost and risk.

4.5.3.2 Tank Design

Initial calculations showed that the volume of propellant required by the Titan surface launch vehicle required tanks that would be extremely difficult to land in a useable configuration. To find a lower volume solution, various tank concepts are traded, including collapsible, 3D printed, and inflatable tanks. First, the collapsing tank concepts are evaluated. Most of these concepts work by replacing the cylindrical section of a tank with a series of nested cylindrical sections (Ref. 41). The tanks then typically deploy by using internal pressure and the segments lock into position. This design allows for traditional Ti alloys to be used and does allow for a reduction in total length of ~50 percent, as shown in Figure 4.6. However, this design does require seals at all the at all the sliding joints that must work during deployment and hold for extended periods of time at cryogenic temperatures.

Next, the Compass Team evaluated using 3D printing to print the tanks on Titan's surface. This concept removed any tank volume issues, since they were printed on site. In addition, the 3D printer scaffold could be used as a launch gantry once printing was complete. A printing system could conceivably print not just the tanks, but the structure, adapters, and other components. However, issues arose regarding how to integrate sensors, wiring harnesses, electronics boxes, thrusters, plumbing, and attaching separation mechanisms. These operations could conceivably be completed with the addition of a robotic arm and a tool package to perform key surface facing operations, drilling, fastener insertion, etc. Unfortunately, these additional components would greatly increase the mass, complexity, and power requirements of the landed system. Thus, it was not selected for this design.

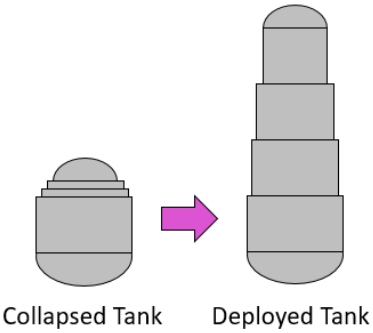

Figure 4.6.—Collapsible Tank.

Finally, inflatable tanks based on Thin Red Line's ultra-high-pressure vessel (UHPV) technology are evaluated. These tanks consist of a flexible bladder sounded by high strength tendons that are attached to bosses located at the tank's poles. Since they are flexible, they can be folded down almost completely flat for packaging. Materials and fabrication techniques that are compatible with cryogenics are currently being tested. Short door-knob style tanks have been built and pressure tested, concepts for equatorial ring mounting systems are being evaluated, and concepts for integral tank internals also exist. The tank mass is anticipated to be less than that of Ti alloy tanks for the same mean operating pressure (MOP) and volume. Due to this systems light weight and very low packaged volume, it was selected for this design.

4.5.3.3 Engine Type

The high ambient atmospheric pressure on Titan's surface presents an interesting challenge for the first stage engine design. To get reasonable I_{sp}, a high chamber pressure is required. Ascent trajectory analysis, however, shows that a low thrust level is preferred. This combination of high chamber pressure and low thrust level is a unique combination of engine requirements. The Team traded various engine cycles and nozzle types to find a good solution for this design (Ref. 42). Table 4.18 shows a summary table of the options being considered.

Of the various engine cycles available, the expander cycle is the initial baseline. This cycle is well understood, and RL-10 variants based on it have been shown to be very throttleable (Ref. 43). Expander cycles are, however, limited at the high and low end of the thrust scale. Once the thrust level required by the trajectory analysis became available, and the 300 W TVC power requirement was applied, it was very questionable whether an expander cycle could develop adequate turbine power to provide the high pump discharge pressures required with a very small thrust chamber and low area ratio nozzle from which to draw thermal energy. Thus, the expander is dropped from consideration.

TABLE 4.18.—ENGINE CYCLE AND NOZZLE TRADE OPTIONS

	Type	Pros	Cons
Engine Cycle	Gas Generator	High Power Density, Not Turbine Power Limited, Scalable	Can Experience Turbine Runaway, Higher Complexity, Consumes Some Propellant to Drive Turbine
	Expander	Utilizes Regen Cooing, No Additional Propellant Consumption to Drive Turbo-Pump Assembly (TPA)	Heat Transfer and Turbine Power Availability Issues at Both Small and Large Scale, Lower Power Density than Gas Generator
	Tap-Off	No Additional Burner Required, High Power Density	Can be Difficult to Mechanically Implement; Lower Turbine Pressure Ratio Relative to Gas Generator
	Electrical Pump	Relatively Easy Design	Very Large Battery Required; Typically has Larger Engine Mass than Other Cycles
Nozzle Type	Bell	Well-Understood, Light Weight, Deployable Uncooled Composite Extensions Available (such as RL-10)	Designed to Single Back Pressure; High Overall Length, Reduced Performance with High Back Pressure
	Aerospike	Altitude Compensating Performance; Short Overall Length	Higher Weight, Cooling Issues; Less Accurate Thrust Vectoring via Differential Burner Performance or Fluidic Injection
	Expansion/ Deflection	Altitude Compensation; Short Overall Length	Complex Integration; Cooling Issues

Due to the low thrust levels required, the electrically driven pump seems like a good candidate at first glance. It requires a battery, thus removing the TVC power requirement from the engine. The engine does require a high-power pump to produce adequate chamber pressure. A preliminary analysis shows that for a 103-bar chamber pressure, a 137-bar pump discharge pressure would be required once the estimated injector pressure drop is accounted for. Assuming a nominal 65 percent adiabatic pump efficiency, approximately 57 kW is required at full thrust per engine. For the first stage, a nominal 4.5 min is required to consume all the propellant, if at full power, thus requiring a total ~8.7 kW-h, or ~50 kg battery, just to run the engine pumps. Although the electrically driven pump is a relatively simple design, the battery and electric motor mass remove it from consideration for this design.

The requirement for a high chamber pressure makes the higher power density engine cycles a better option for this design. The tap-off cycle has heritage and a high-power density. It can, however, create cooling issues around the tap-off port on the thrust chamber creating mechanical integration issues at a very small scale, and it has a lower turbine pressure ratio than a gas generator. Although a good option for this particular design, the gas generator is a slightly better choice, and is thus selected. They have very high-power density and scale well with thrust level (Ref. 42). For this design, a basic gas generator with the turbine exhaust gas dumped through a smaller secondary nozzle is considered. Its high-power density can provide the high pump power required and be scaled up to meet any additional power loads with a minimal impact on additional propellant consumption. This concept, however, can be more difficult to design properly.

With the engine cycle selected, various nozzle systems are traded. Because of Titan's high ambient surface pressure, a pressure compensating nozzle would be a good solution. Expansion-deflection nozzles are very compact and are altitude compensating but are difficult to cool (especially the center body) and tend to be difficult to integrate mechanically relative to other options. Therefore, it is removed from consideration.

An aerospike nozzle is another altitude compensating nozzle system, and has been tested at full scale on earth, such as the J-2T and XRS-2200 (Ref. 44). This design has been tested extensively, even at large thrust levels, and has continuous altitude adaptive capabilities. It has significant performance gains over bell nozzles, especially at higher backpressures. For this design, however, the size of the engine components and the implementation of TVC became issues. To sustain a high area ratio plume expansion, a high chamber pressure is needed, but that also results in a very thin throat slot. Even for an area ratio of 40 the throat slot is 2 mm around a nozzle plug diameter of 16 cm. For a 25 percent length plug, the total length of just the center body is 20 cm, which is within a few centimeters of the bell nozzle design.

There are several methods to implement TVC on an aerospike nozzle. These include differential throttling, center body flaps, and fluidic injection (Ref. 44). Due to the small size of the engine, it is unclear if individual controllable thrust chambers can realistically be implemented. It is also unclear if there is adequate volume for flap actuators within the center body. Fluidic injection is the most likely TVC option for an aerospike engine at this scale. Although concepts have been tested via cold flow tests, to date it hasn't been implemented on an actual design. Regardless, if flaps or fluid injection are selected, TVC hardware will occupy the majority of the center body volume, meaning that the turbo-pump assembly (TPA) has to be mounted outside the engine envelope. This effectively makes the overall engine design longer and yet more complex. Although the Titan surface would be an ideal place to utilize the back pressure compensating capabilities of the aerospike design, the complex engine design and TVC integration issues led to this design being passed over for this mission.

The remaining option is the traditional bell nozzle. Although longer than the other options, at Titan surface ambient pressure only low area ratios are possible while obtaining reasonable I_{sp}, even with a high chamber pressure. With a low thrust requirement, high chamber pressure, and a low area ratio nozzle,

there is no discernable length penalty on the first stage for a bell nozzle relative to the aerospike. This design is lower risk, is compatible with traditional TVC methods, and leverages developing LOx/LCH_4 engine technology. Since the vehicle is staged, the performance penalty for a fixed first stage nozzle can be somewhat offset with a high area ratio second stage engine that has a deployable nozzle skirt to better fit inside the inter-stage adapter. Therefore, for this particular mission, the gas generator with a bell nozzle appeared to be the best combination for the launchers first and second stage engines when considering overall performance, system integration, development risk, mass, and complexity.

4.5.3.4 Thrust Vector Control System Power

The TVC requires power to both actuate and to hold position during engine operation. As the surface launch profile matured, it became clear that the first and second stages would experience long burn times. This would require a large battery to provide the power and total energy needed by the TVC systems during the ascent. In order to save mass, a large, dedicated battery is traded against a small electrical generator mounted on each engine's TPA to provide unconditioned power to a power conditioner, which then supplies the TVC systems. This would require additional propellant, as the gas generator would be taxed to provide additional shaft power. Analysis shows that adding an additional 300 W continuous load onto the TPA output shaft would require ~2 kg of additional propellants to be consumed via the gas generators of each engine during their respective burns. This additional propellant mass, the generator mass, estimated wiring, and power conditioner had a lower overall mass than the battery required. This system also did not have the thermal conditioning requirements of the battery system, which saved some additional mass. Although a unique type of system, it is selected to provide TVC power on the first and second stages of this design.

4.5.3.5 Titan Sample Return Vehicle Propellant

The Titan sample return vehicle propellant is required to fit within the body of the spacecraft, as well as provide adequate thrust and ΔV performance to complete the mission. Several propellant options are traded early in the design, including LOx/LCH_4, hydrazine, and AF-M315E. Initially, hydrazine is the preferred option, due to its high TRL. However, thermal analysis showed that it would be extremely difficult to keep it from freezing on Titan's surface.

LOx/LCH_4 is the next obvious choice, since the other three stages of the launch vehicle used the same propellant combination. For the return vehicle, however, this combination suffered from two major drawbacks. First, the volume of propellant required didn't fit inside vehicle. Second, as the vehicle came back toward Earth, the estimated boil-off would become an issue, thus it was removed from consideration.

Finally, AF-M315E has sufficient cold tolerance as to be storable on Titan with radioisotope heater units (RHUs) on the tank, undergoing a glass transition at –80 °C. It also has a 50 percent higher I_{sp} density than hydrazine, which allowed a sufficient quantity to be stored comfortably inside the vehicle in an existing COTS membrane tank. It is an ionic liquid monopropellant based on hydroxyl ammonium nitrate (HAN) that was developed by Air Force Research Lab and is green (less toxic) compared to hydrazine. It has an extremely low vapor pressure and is not able to activate non-preheated thrusters. A catalyst bed temperature of 285 °C is required for general operation, but pulse start from lower temperature is possible (Ref. 45). AF-M315E flew on the Green Propellant Infusion Mission (GPIM) but does currently lack the flight heritage of hydrazine. It is selected for this design primarily due to its high I_{sp} density and cold tolerance.

4.5.4 Analytical Methods

The methods used to design the propulsion system involved using a mix of published values, empirical data, and analytical tools. Published values for COTS components and empirical data are used

wherever possible, with analytical tools being employed as necessary. Empirical data is used to aid in the mass and size estimation of similar components when published values are not available. Numerous analytical tools are used in this analysis, including National Institute of Standards and Technology (NIST) (Ref. 46) tables, fluid and gas property codes, as well as custom tools developed from basic physical relationships and conservation equations with empirical based inclusions for real life hardware requirements (mounting bosses, flanges, etc.). Tank masses are estimated by interpolating among existing designs and adjusting them based on MOP.

4.5.5 Risk Inputs

There are several propulsion system related risks for this design. The first major risk is the inflatable tank system, which uses a new type of tank that has no flight heritage, nor has it yet been used for cryogenic applications. Tanks are, however, currently under development with candidate material coupon testing for cryogenic applications having shown very encouraging results. Therefore, there are numerous potential developmental risks, as well as currently unknown system level behaviors and interactions that could adversely affect mission performance, as well as posing both a cost and schedule risk.

Second, the in-space stage N_2 pressurization system is a unique system with limited heritage. This design utilizes warm vaporized N_2 gas for propellant tank pressurization by passing small quantities of pumped LN_2 across heat exchangers mounted on the thrusters. This novel system has no known flight heritage but is very similar to the LHe system used to pressurize the Ariane 5 LOx tank (Ref. 47) and the He heating system on the J-2 engine (Ref. 48). Due to its uniqueness and lack of heritage, there are unknown system level behaviors and interactions that could adversely affect development.

Thirdly, there is a risk of the launch vehicle exhaust plume potentially damaging the lander during launch. During launch, the first stage thruster plumes will shower the lander with hot exhaust gas for a brief moment during lift-off. Although the lander will be exposed to hot exhaust plume for a brief period, it may cause thermal or other damage to portions of the lander, IRSU plant, or rover, potentially rendering them inoperable. A few lightweight concepts, such as simple sheet metal plume deflectors, are discussed as part of this study, but their design and performance evaluation are beyond the scope of the work presented here.

4.5.6 System Design

The Titan sample return launch vehicle is comprised of a four-stage system. The first two stages are used for Titan surface launch and orbital circularization. The third, or in-space, stage is used primarily for maneuvers in the Saturn system to place the fourth stage, the sample return vehicle, on a trajectory toward Earth. All four stages have dedicated propulsion systems, and a summary of each stage is shown in Figure 4.7.

4.5.6.1 First Stage

The Titan sample return launch vehicle's first stage is comprised of a LOx/LCH_4 based system with dual engines. These engines are sized to provide 6 kN (1,350 lb_f) of thrust and 270 s I_{sp} at Titan sea level. They utilize a gas generator cycle with an oxidizer to fuel ratio (O/F) of 3.0, operate with a 103 bar (1500 psi) chamber pressure, and are regen cooled to the nozzle exit, which is a nozzle area ratio of 20:1. Each engine has a 300 W class electrical generator attached to its TPA to provide power for its electromechanical TVC system, which allows each engine to be independently gimballed a nominal ± 10° in two axes. These TVC systems are based on existing Moog designs (Ref. 49), have redundant closed loop controllers per actuator pair, are MIL-STD-1553B and RS-422 compatible (Ref. 50), and provide redundant drive motors on each actuator.

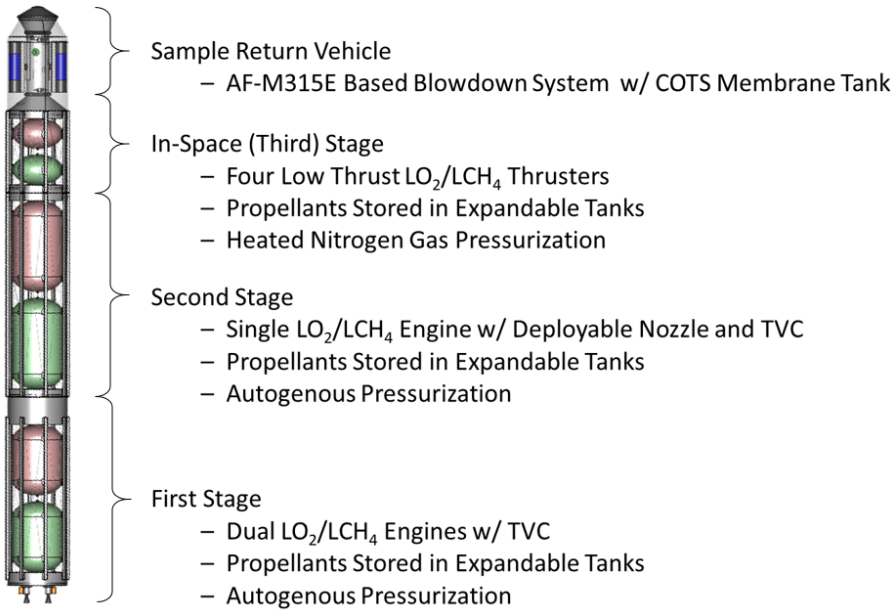

Figure 4.7.—Titan Sample Return Launch Vehicle Stage Description.

The tanks are designed to be identical in size in order to reduce cost and simplify design development. This leads to the CH_4 tank being oversized by 10 percent for an engine O/F of 3.0, but does allow for the engine O/F to decrease slightly if future detailed engine design work shows a need for slightly more fuel film cooling. The tanks are stored collapsed and folded for transport, and then slowly inflated as the launch vehicle structure is deployed. The tanks have a MOP of 3.4 bar (50 psi) and are attached to the cable structure via a tabbed ring located at both ends of the tank's barrel section. Figure 4.8 shows the overall layout for the first stage.

The tank MOP is sufficient to store the propellants subcooled at ambient Titan surface conditions, while also providing sufficient net positive suction pressure (NPSP) to the engine's pumps during the engine start sequence until the autogenous pressurization system becomes available. To save additional tank mass and volume, the first stage propellant tanks are autogenously pressurized during engine operation with both vaporized fuel and oxidizer which is tapped from each engine and used to pressurize the appropriate propellant tank. Due to the deployable nature of the first stage design, propellant, pressurant, and feed lines to the second stage have flexible line segments. The O_2 feed line, however, may not need a flexible segment due to the proximity of the O_2 tanks aft dome to the stage's aft bulkhead assembly, which may allow for a direct fixed connection to the engine's O_2 manifold. This particular detail may allow for a small mass saving but is beyond the scope of this study. Therefore, the Team assumed a flexible line segment.

Although the propellants are cryogenic, the first stage feed system is simple. Due to the cold ambient Titan surface temperature, both the LOx and LCH_4 propellants can be loaded without the thermal and pressurization issues typically associated with cryogenic propellants. This allows for a greatly simplified pressurization and feed system design compared to typical Earth based stages. Both tanks have redundant pressure relief systems mounted in parallel to the active solenoid valve used to control tank pressure during fueling. Both tanks are filled from the bottom via the engine manifolds. Once loaded, the isolation valves are closed, and the propellants are routed up to the second stage. Figure 4.9 shows a preliminary plumbing and instrumentation diagram (PID) of the first stage.

Each engine has a 300 W class electrical generator that extracts power from the TPA to provide power for TVC system. This unconditioned electrical power is sent to a power conditioner, which then passes power to the TVC controller for distribution to actuators. The power conditioner has redundant circuitry and sends data to both the TVC controllers and the spacecraft computer. Figure 4.10 shows a schematic of the TVC power system.

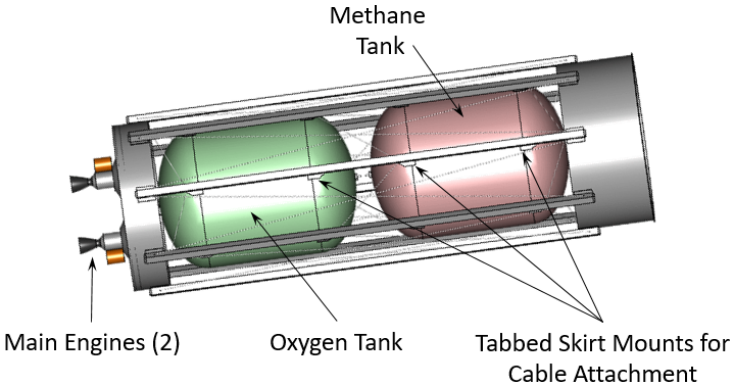

Figure 4.8.—First Stage Propulsion System Configuration.

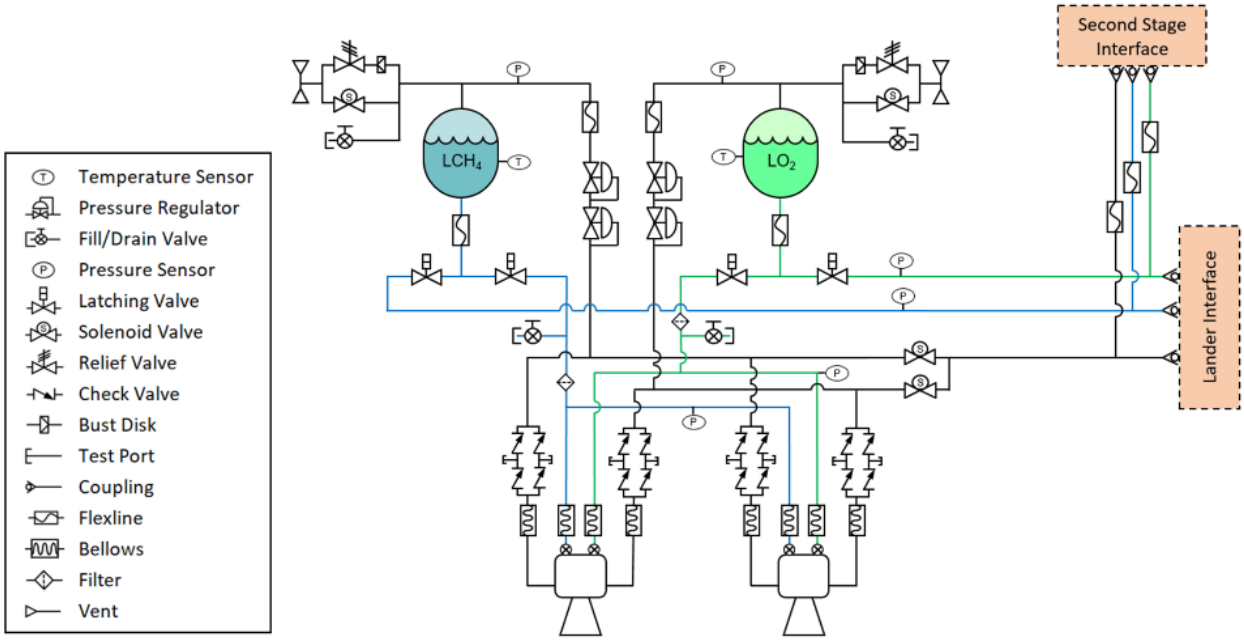

Figure 4.9.—First Stage Preliminary PID.

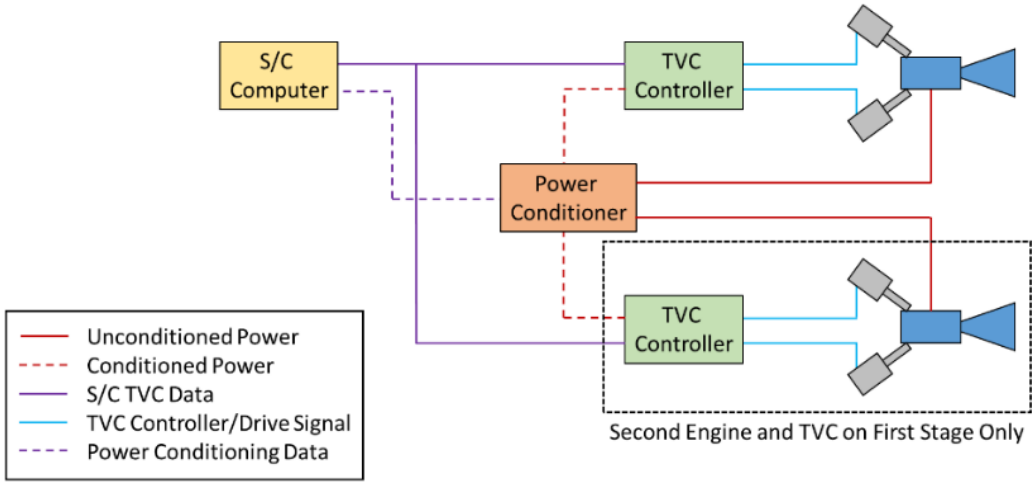

Figure 4.10.—TVC Power System Schematic.

4.5.6.2 Second Stage

Like the first stage, the second stage is also a LOx/LCH_4 based system, but with a single engine. This engine is a derivative of the first stage's engine with the same thrust chamber and TPA, but with a deployable radiatively cooled nozzle extension yielding a total nozzle area ratio of 120:1 for better high-altitude performance. The engine develops 7.6 kN (1,700 lb_f) of thrust and 342 s I_{sp} in vacuum, utilizes a gas generator cycle with an O/F of 3.0 and a 103 bar (1,500 psi) chamber pressure. Like the first stage engine, it also has a 300 W class electrical generator attached to its TPA to provide power for the TVC system, which is identical to the first stage's system and allow the engine to be gimballed a nominal ±10° in two axes.

Similar to the first stage, the tanks are designed to be identical in size in order to reduce cost and simplify design development. This leads to the CH_4 tank being oversized by 10 percent for an engine O/F of 3.0 but does allow for the total engine O/F to decrease slightly if future detailed engine design work shows a need for slightly more fuel film cooling. The tanks are stored collapsed and folded for transport, and then slowly inflated as the launch vehicle structure is deployed. The tanks have a MOP of 3.4 bar (50 psi) and are attached to the cable structure via a tabbed rings located at both ends of the tank where the barrel section and domes interface. Figure 4.11 shows the overall layout for the first stage.

The tank MOP is sufficient to store the propellants subcooled at ambient Titan surface conditions, while also providing sufficient NPSP to the engines during the engine start sequence until the autogenous pressurization system becomes available. As with the first stage, the propellant tanks are autogenously pressurized during engine operation with both vaporized fuel and oxidizer being tapped from the engine and used to pressurize the appropriate propellant tank. Due to the deployable nature of the second stage design, propellant, pressurant, and feed lines to the in-space stage have flexible line segments. The O_2 feed line, however, may not need a flexible segment due to the proximity of the O_2 tanks aft dome to the stage's aft bulkhead assembly, which may allow for a direct fixed connection to the O_2 manifold. This particular detail may allow for a small mass saving but is beyond the scope of this study. Therefore, a flexible line segment is assumed.

Similar to the first stage feed system, the second stage feed system is fairly simple, due to the low ambient Titan surface temperature. Both propellants can be loaded without the typical thermal and pressurization issues associated with cryogenic propellants, which allows for a greatly simplified pressurization and feed system design compared to typical Earth based stages. Both tanks have a redundant pressure relief system located in parallel to the active solenoid valve used to control tank pressure during fueling, and both tanks are filled from the bottom via the engine manifolds. Once loaded,

the isolation valves are closed, and the propellants are routed up to the in-space stage. Figure 4.12 shows a PID of the second stage propulsion system.

4.5.6.3 In-Space Stage

The third, or in-space, stage is also a LOx/LCH_4 based system with a single LOx and LCH_4 tank. This stage, however, has four pressure fed thrusters and an additional N_2 storage tank. The propellant tanks are ellipsoidal in shape and are much smaller than those on the first and second stage. They are attached to the cabling system by tabbed mounts located on an equatorial ring. The N_2 for pressurization is stored as a liquid in a Ti alloy tank based on ATK/NG model 80454-1 (Ref. 51). Figure 4.13 shows the in-space stage configuration.

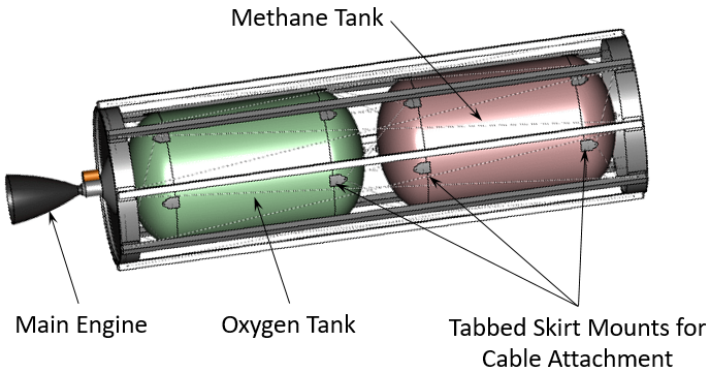

Figure 4.11.—Second Stage Propulsion System Configuration.

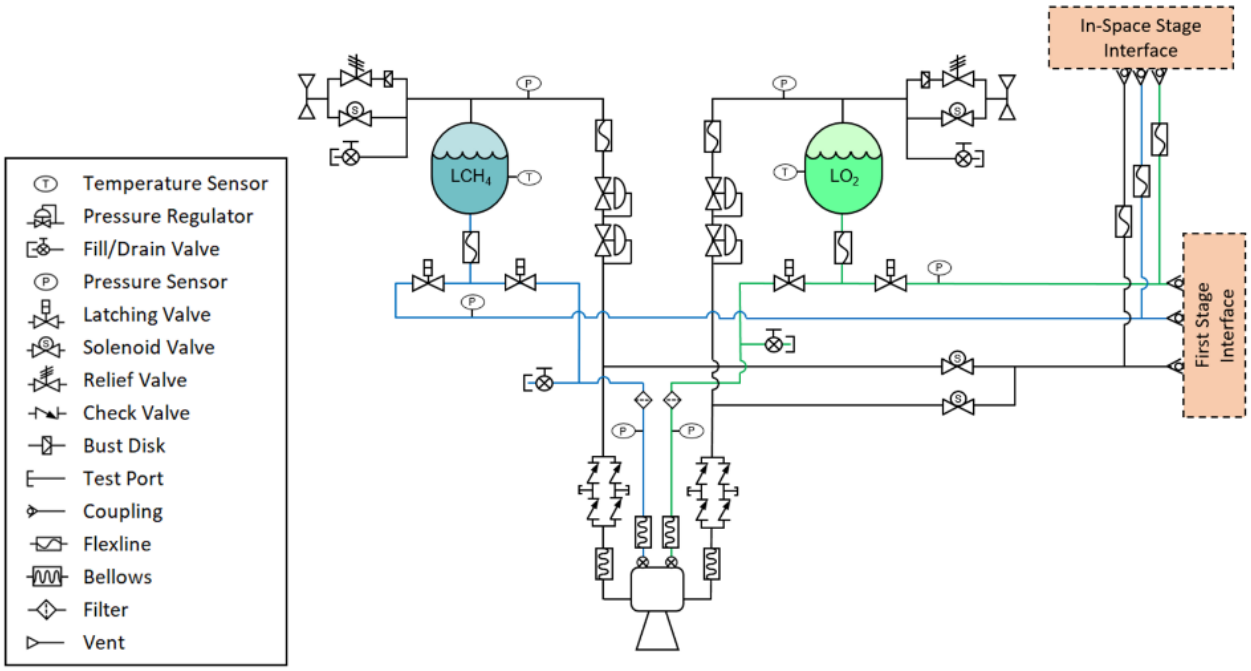

Figure 4.12.—Second Stage Preliminary PID.

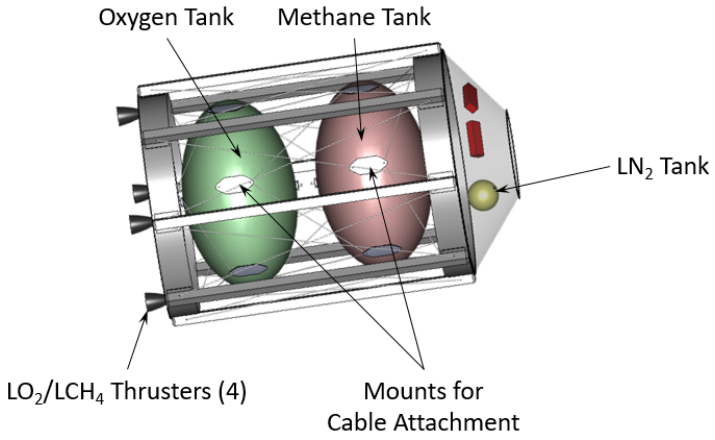

Figure 4.13.—First Stage Propulsion System Configuration.

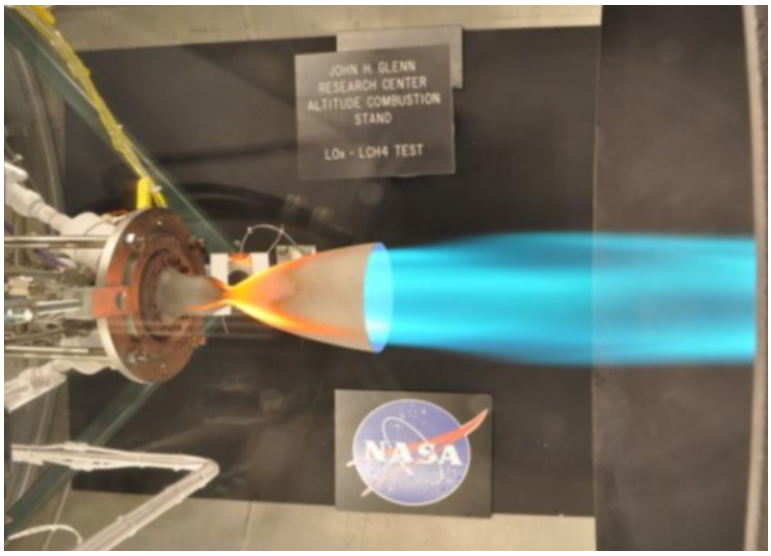

Figure 4.14.—LOx/LCH_4 Thruster Testing.

The thrusters are a pressure fed design, deliver 89 N (20 lb_f) thrust each, and 350 s vacuum I_{sp}. They have an 8.6 bar (125 psi) chamber pressure, a 150:1 area ratio nozzle, radiatively cooled chamber and nozzle, and an overall O/F of 3.0. The thrusters do not have a TVC system, and are based on a thruster tested at GRC, which is shown in Figure 4.14. One major difference, however, is the addition of a small heat exchanger to outside of the thrust chamber. This heat exchanger is used to vaporize pressurized LN_2 so it can be used as a pressurant gas.

Similar to the first and second stages, the tanks are designed to be identical in size in order to reduce cost and simplify design development. This leads to the CH_4 tank being oversized by 10 percent for an engine O/F of 3.0.

Due to the thrusters being pressure fed, the MOP for the in-space stage tanks is 12.4 bar (180 psi), which is much higher at than for the first two stages. Due to the deployable nature of the in-space stage design, propellant, pressurant, and feed lines have flexible line segments. The O_2 feed line, however, may not need a flexible segment due to the proximity of the O_2 tanks aft dome to the stage's aft bulkhead assembly, which may allow for a direct fixed connection to the O_2 manifold. This particular detail may allow for a small mass saving but is beyond the scope of this study. Therefore, the Team assumes a flexible line segment.

The pressurization system is based on the Ariane 5 LOx tank pressurization system design, but with a pump to provide system pressurization. In this design, LN_2 is pumped up to 17.2 bar (250 psi) and then passed across small heat exchangers located on the thrusters, resulting in warm (0 to 25 °C) N_2 gas that is then regulated down to propellant tank MOP at an estimated total flow rate of 1.8 g/s. Two thrusters are used to vaporize the O_2 side pressurant, and the other two are used to vaporize the CH_4 side pressurant. It is envisioned that the thrusters will be mounted so that opposing thrusters vaporize N_2 for the opposite propellant. This ensures warm N_2 pressurant gas to both propellants in the event of an engine out scenario, where a failed thruster and the opposing one are shut down. Once a burn is complete, most of the N_2 trapped in the propellant tanks needs to be vented until the tank pressure reaches approximately 3.4 bar (50 psi). This ensures the N_2 pressurant gas remains in the gas phase. Otherwise, the gaseous N_2 will slowly cool and condense into a liquid and mix with the propellant in the tank. Figure 4.15 shows a preliminary PID of the in-space stage propulsion system.

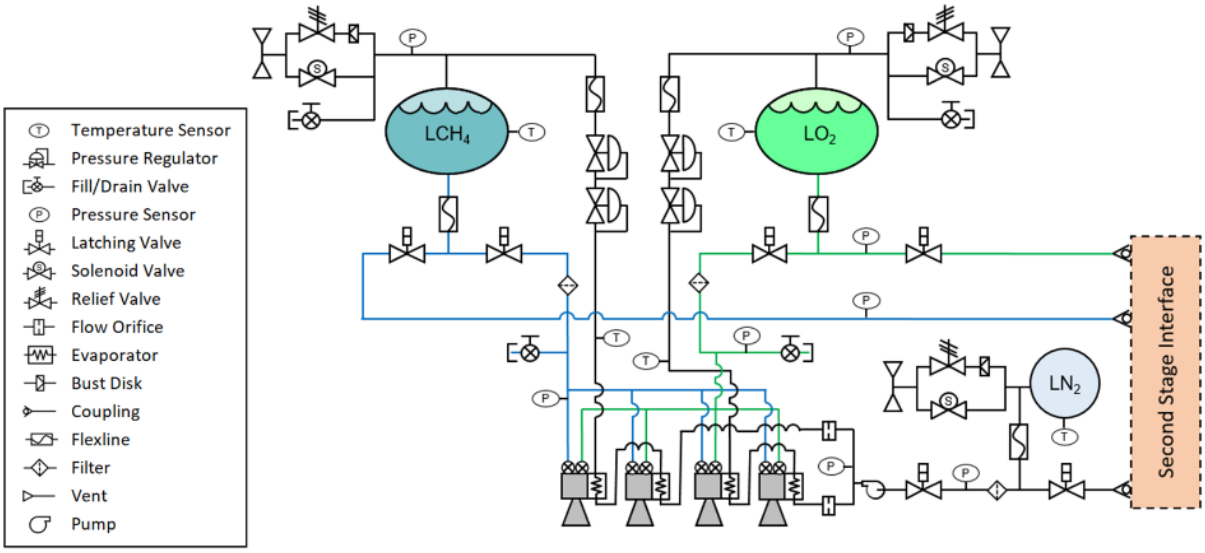

Figure 4.15.—In-Space Stage Preliminary PID.

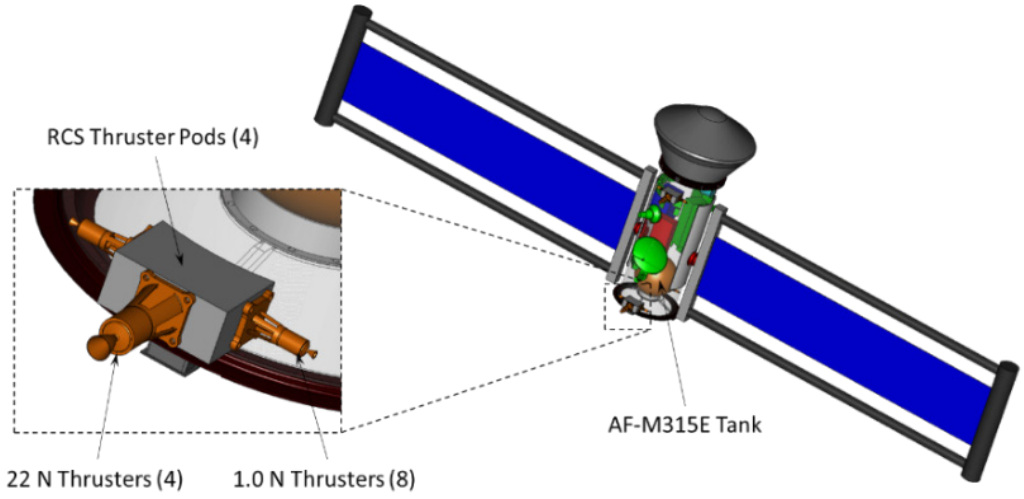

Figure 4.16.—Return Vehicle Propulsion System Configuration.

4.5.6.4 Return Vehicle

The Titan sample return vehicle propulsion system is an AF-M315E based blow-down system with eight 1.0 N (0.25 lb_f) RCS thrusters and four 22 N (5.0 lb_f) main thrusters. The thrusters are mounted in four pods, with each pod containing one 22 N thruster and two 1.0 N thrusters each. The propellant is stored in a single spherical COTS tank (ATK/NG model 80216-1). This tank is a pedestal mounted spherical Ti alloy tank with an AF-E-322 elastomeric membrane, has a MOP of 27.6 bar (400 psi), and is 32.7 cm (12.9 in.) in diameter (Ref. 52). Due to the cold ambient temperatures during the mission, RHUs are used to maintain the propellant above –50 °C. Figure 4.16 shows this configuration.

The feed system is comprised of normally closed pyrotechnic valves for isolation, a filter, nominal instrumentation suite, and redundant latch valves for isolation once the system is activated. Unlike on the in-space stage, the N_2 gas used to pressurize the AF-M315 tank is loaded on Earth prior to mission launch. GN_2 is selected instead of He, due to the length of the mission and He's propensity to slowly leak over time. Figure 4.17 shows a preliminary PID of the Titan sample return vehicle.

The thrusters are based on the GR-1 and GR-22 thrusters developed for the GPIM mission that develop 1.0 N (0.25 lb_f) and 22 N (5.0 lb_f) of thrust, respectively (Ref. 45). Like hydrazine thrusters, the thrust varies very linearly with feed pressure, while I_{sp} tends to slowly reduce as the feed pressure is dropped. This trend is seen in the performance curves for both thrusters shown in Figure 4.18.

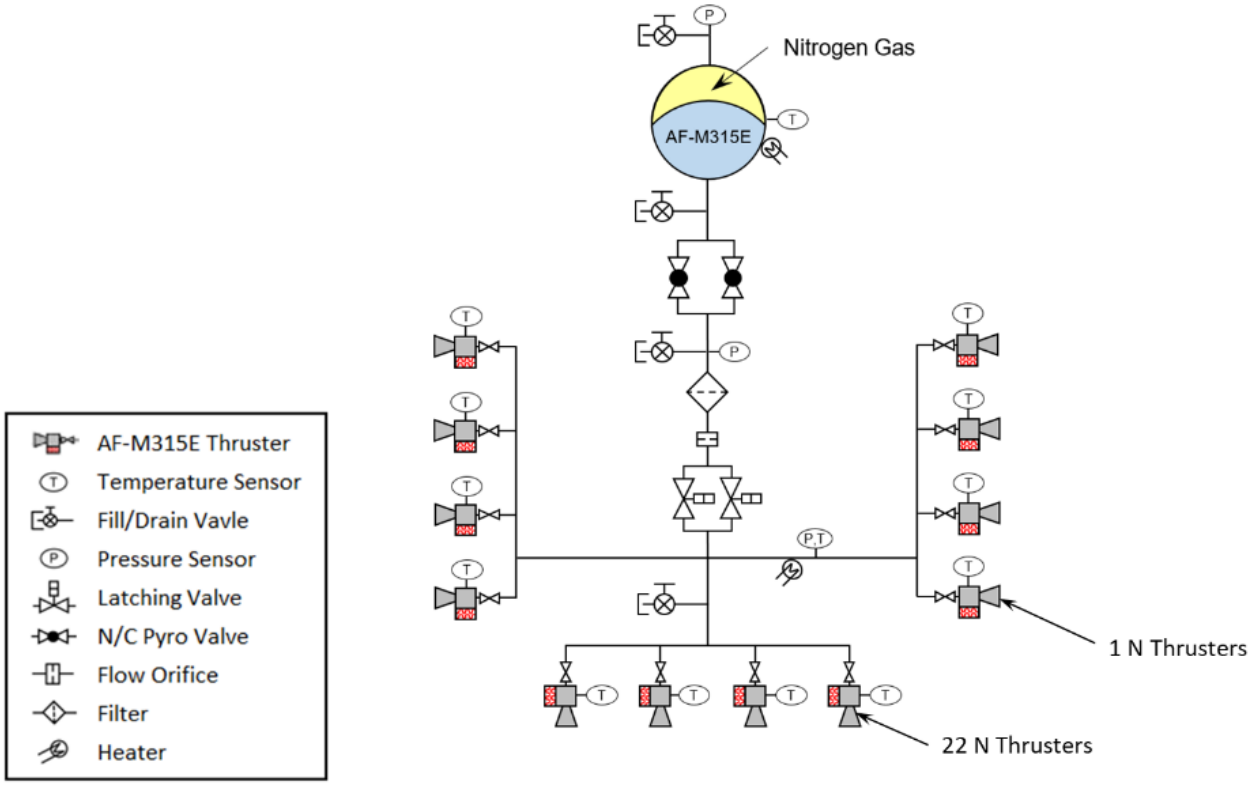

Figure 4.17.—Return Vehicle Preliminary PID.

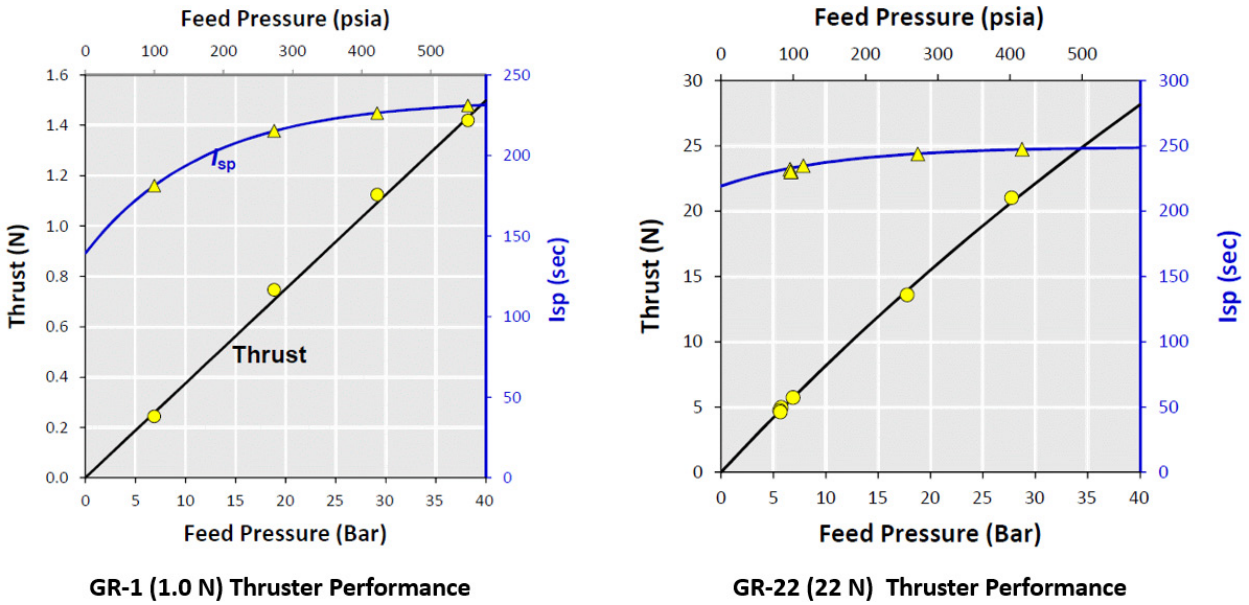

Figure 4.18.—AF-M315E Thruster Performance.

TABLE 4.19.—TITAN SAMPLE RETURN LAUNCHER STAGE PROPELLANT LOADS

Propellant	Type	First Stage (kg)	Second Stage (kg)	In-Space Stage (kg)	Return Vehicle (kg)	Mission Total (kg)
LCH_4	Useable	301	375	76.7	-----	765
	Residuals	4.5	5.6	2.3	-----	
LOx	Useable	903	1,126	230	-----	2,296
	Residuals	13.5	16.9	6.9	-----	
AF-M315E	Useable	----------	----------	----------	13	14
	Margin	----------	----------	----------	0.9	
	Residuals	----------	----------	----------	0.3	
N_2 Pressurant		1.0	1.0	10.3	0.1	13
Total Propellant and Pressurant		1,224	1,526	326	15	3,089

4.5.6.5 Propellant Loads

The Titan surface launch vehicle has a LOx/LCH_4 based propulsion system on the first, second, and in-space stage, while the sample return vehicle is AF-M315E based. For the LOx/LCH_4 stages, the margin propellant is consumed during the various engine burns and is handled in the mission analysis as a decrement in delivered I_{sp}. It is therefore included indirectly in the useable propellant. The first two stages are autogenously pressurized, and thus have no dedicated pressurant tank, but do have trapped ullage gas that pressurizes the tanks until their respective engines start. The in-space stage has a dedicated pressurant tank, while the sample return vehicle has a membrane tank with the pressurant gas stored inside the propellant tank. Table 4.19 shows a summary of propellants and pressurants stored in all the stages.

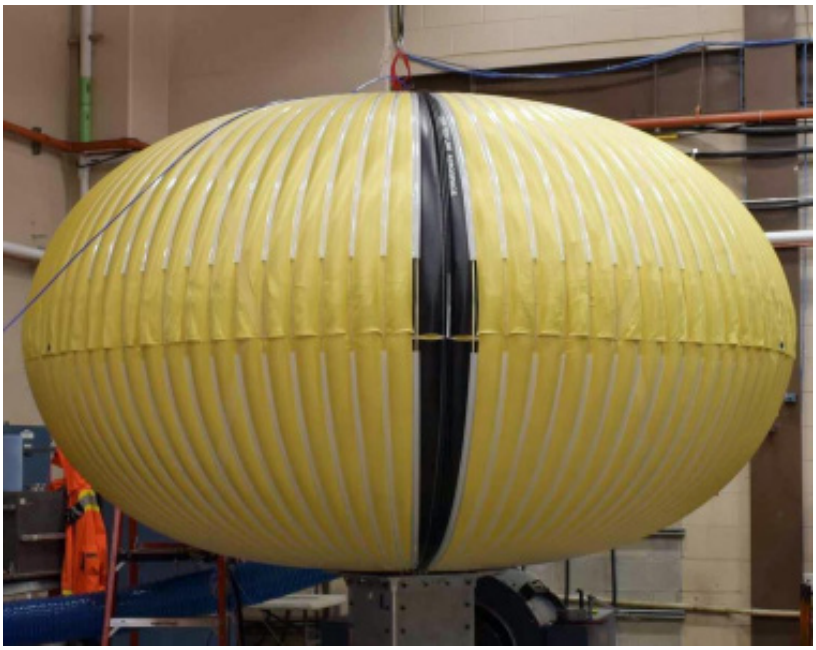

Figure 4.19.—Inflatable Structure Testing.

4.5.6.6 Inflatable Tanks

4.5.6.6.1 Design and Construction

Various inflatable tank concepts are currently being investigated by NASA. The basic tank design consists of thin polymer-based bladder that is reinforced by longitudinal load carrying tendons which are connected to polar bulkhead assemblies (Figure 4.19). Initial designs based on Thin Red Line Aerospace's ultra-high-pressure vessel technology show overall tank mass to be very competitive with Ti alloy tanks for the same volume and MOP, showing a possible 30 to 50 percent mass savings. There are even designs for an integrated micrometeoroids and orbital debris (MMOD) and multi-layer insulation (MLI) system (Ref. 53).

Currently, materials are being evaluated for cryogenic applications, including polyimide films, annealed metal films, and fluorinated ethylene propylene (FEP) which is LOx compatible. Various joint configurations are also under evaluation, with adhesive lap joints of barrier materials exhibiting high strength even at cryogenic temperatures, which was also shown in testing at NASA Lewis in the 1960s (Ref. 54). Additional design features are also being developed, including equatorial skirt mounting systems, integral slosh baffles and propellant management devices (PMDs), and tanks with cylindrical form factors.

4.5.6.6.2 Inflation Sequence

Once on Titan's surface, the launch vehicle is rotated to a vertical position and its structure deployed. While the stages are slowly deployed, N_2 gas is transferred to the inflating tanks from the ISRU plant via the pressurization system interface on the appropriate stage. A low nominal pressure is maintained in both the fuel and oxidizer tank to aid in tank unfurling and stage deployment. Once the stage is fully deployed, the pressure is raised in the tanks to a slightly higher pressure and propellant transfer to the launcher from the ISRU plant begins. As the tanks are slowly filled, N_2 gas is periodically vented to maintain nominal tank pressure and keep the propellants subcooled. Once the tanks are completely fueled, the remaining N_2 gas in the tank's ullage volume provides adequate NPSP for engine start until the autogenous pressurization system engages.

4.5.6.7 First and Second Stage Engine Design

The Titan sample return launch vehicle's first and second stage engines utilize LOx/LCH_4 propellants and are powered via an open gas generator cycle. In an effort to reduce cost and risk, the two first stage engines and the one second stage engine utilize a common single shaft TPA and powerhead assembly. The second stage engine; however, has a deployable nozzle skirt to increase its nozzle area ratio for high altitude performance. The engines have an overall O/F of 3.0 and have a 300 W electrical generator integrated into its TPA to provide electrical power for the TVC system. To minimize size, mass, and complexity, a single shaft TPA is assumed for this design. The engines also have gaseous O_2 and CH_4 taps to provide autogenous pressurization.

To obtain adequate performance at Titan surface conditions, a chamber pressure of 103 bar (1500 psi) is selected with a 20:1 area ratio regeneratively cooled nozzle and thrust chamber assembly. This short nozzle provides ideal expansion at an altitude of ~9.5 km on Titan and an I_{sp} of 270 s at Titan's surface. The second stage engine includes a short length of uncooled nozzle extension followed by a deployable radiatively cooled carbon composite nozzle skirt to help minimize the engines packaged length while adding additional area ratio. This larger nozzle gives this engine a total area ratio of 120:1, which allows it to develop 342 s of vacuum I_{sp}. The uncooled extension could also be used to house a toroidal manifold to inject the gas generator exhaust into the nozzle for further expansion and a little additional thrust, whereas on the first stage engine, the turbine exhaust is simply ducted to a small nozzle at the base of the engine. Figure 4.20 shows a comparison of these two configurations. Figure 4.21 plots the performance curves of these two configurations, and shows that their I_{sp} curves cross at a Titan altitude of ~35 km and an I_{sp} value of 311 s. This crossover of the I_{sp} curves is used to trigger staging in the trajectory analysis.

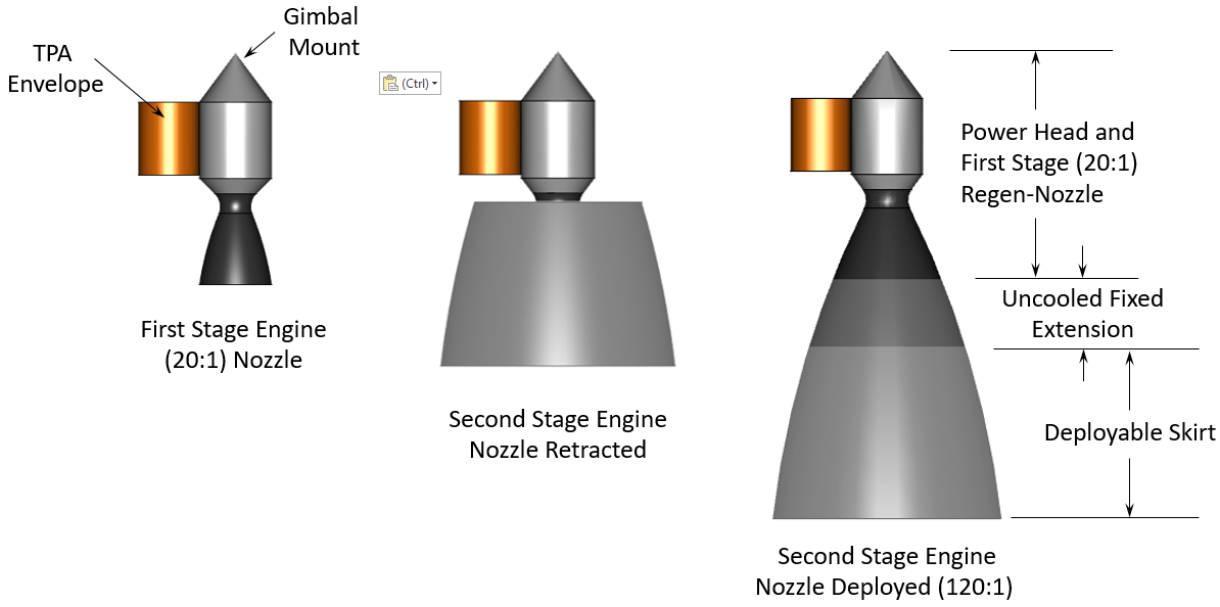

Figure 4.20.—First and Second Stage Comparison.

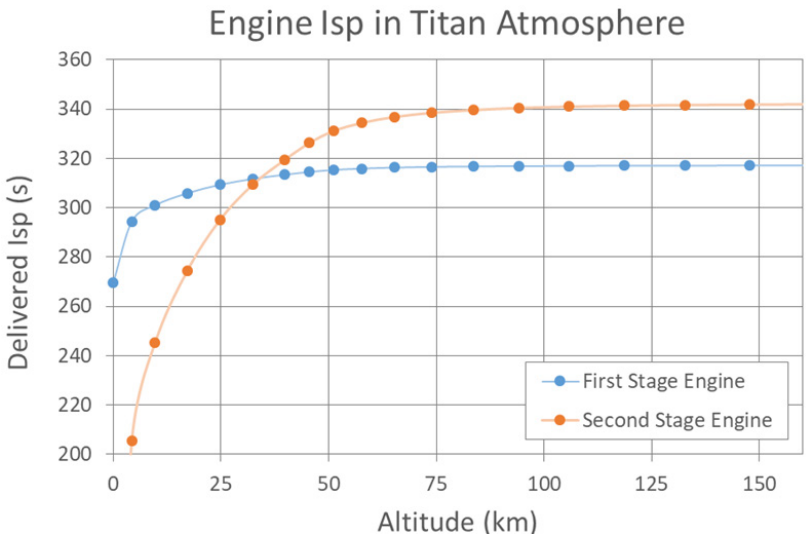

Figure 4.21.—First and Second Stage Engine Performance Comparison.

4.5.7 Recommendation(s)

There are several propulsion system recommendations. First there is the recommendation to perform a detailed engine cycle analysis and engine system layout. Engine performance dictates propellant load and vehicle GLOM, so an accurate assessment of delivered I_{sp} and the actual TPA performance with electrical power take-off should be conducted. Second, it is recommended to evaluate the effect of launch vibrations on the propellant tanks and their frequency response. Materials tend to become brittle, and the tanks or flexlines may have either brittleness, resonance, or fatigue issues during the relatively long launch segments. Next it is recommended to develop requirements for, and perform design work on, the inflatable flexlines used in this design. They need to be lightweight, provide adequate flow rate to the engines and be flexible enough to deploy with the launcher structure at cryogenic temperatures. It is also recommended to perform an evaluation of both the various valves used in the feed systems and the TVC components for use in a long-term cryogenic environment. Finally, it is recommended to perform a detailed analysis on the in-space stage pressurization system. This is a unique system, and further analysis is needed to ensure that it will perform as anticipated.

4.5.8 Master Equipment List

The MELs containing the propulsion system hardware components for the first, second and in-space stages of the Titan sample return launch vehicle and the Titan sample return are shown in Table 4.20 to Table 4.29.

TABLE 4.20.—PROPULSION (CHEMICAL HARDWARE) – RETURN VEHICLE MEL

Description Case 1_Titan_Sample_Return CD-2021-186	QTY	Unit Mass	Basic Mass	Growth	Growth	Total Mass
Propulsion (Chemical Hardware)			**18.4**	**11%**	**2.0**	**20.4**
Primary Chemical System Hardware			**18.4**	**11%**	**2.0**	**20.4**
Main Engine Hardware			18.4	11%	2.0	20.4
1 N AF-M315E Thrusters	12	0.3	3.8	5%	0.2	4.0
22 N AF-M315E Thrusters	1	2.3	2.3	15%	0.3	2.6
Fuel Tanks	1	2.7	2.7	3%	0.1	2.8
Thruster Pods	4	1.3	5.2	15%	0.8	6.0
Feed System	1	4.3	4.3	15%	0.6	4.9

TABLE 4.21.—PROPULSION (CHEMICAL HARDWARE) – IN-SPACE STAGE MEL

Description Case 1_TSR_Launch_Vehicle CD-2021-186c	QTY	Unit Mass	Basic Mass	Growth	Growth	Total Mass
Propulsion (Chemical Hardware)			**49.9**	**14%**	**6.9**	**56.8**
Primary Chemical System Hardware			**49.9**	**14%**	**6.9**	**56.8**
Main Engine Hardware			49.9	14%	6.9	56.8
Lox/LCH4 Engine	4	2.0	8.0	10%	0.8	8.8
Feed System	1	5.9	5.9	12%	0.7	6.6
Methane Tank	1	14.0	14.0	15%	2.1	16.1
Oxygen Tank	1	14.0	14.0	15%	2.1	16.1
Nitrogen Tank	1	0.8	0.8	8%	0.1	0.9
Press. System	1	7.2	7.2	15%	1.1	8.3

TABLE 4.22.—PROPULSION (CHEMICAL HARDWARE) – UPPER ATMOSPHERE STAGE MEL

Description Case 1_TSR_Launch_Vehicle CD-2021-186c	QTY	Unit Mass	Basic Mass	Growth	Growth	Total Mass
Propulsion (Chemical Hardware)			**102.2**	**15%**	**15.1**	**117.3**
Primary Chemical System Hardware			**102.2**	**15%**	**15.1**	**117.3**
Main Engine Hardware			102.2	15%	15.1	117.3
Main Engine	1	16.0	16.0	15%	2.4	18.4
Feed System	1	6.1	6.1	15%	0.9	7.0
TVC	1	4.5	4.5	10%	0.5	5.0
TVC Controller	1	2.0	2.0	15%	0.3	2.3
Oxygen Tank	1	35.0	35.0	15%	5.3	40.3
Methane Tank	1	35.0	35.0	15%	5.3	40.3
Press System	1	3.6	3.6	15%	0.5	4.1

TABLE 4.23.—PROPULSION (CHEMICAL HARDWARE) - 1ST STAGE MEL

Description Case 1_TSR_Launch_Vehicle CD-2021-186c	QTY	Unit Mass	Basic Mass	Growth	Growth	Total Mass
Propulsion (Chemical Hardware)			**110.4**	**15%**	**16.1**	**126.5**
Primary Chemical System Hardware			**110.4**	**15%**	**16.1**	**126.5**
Main Engine Hardware			110.4	15%	16.1	126.5
Main Engine	2	13.5	27.0	15%	4.1	31.1
Feed System	1	6.4	6.4	15%	1.0	7.4
TVC	2	4.5	9.0	10%	0.9	9.9
TVC Controller	2	2.0	4.0	15%	0.6	4.6
Oxygen Tank	1	30.0	30.0	15%	4.5	34.5
Methane Tank	1	30.0	30.0	15%	4.5	34.5
Press System	1	4.0	4.0	15%	0.6	4.6

TABLE 4.24.—CHEMICAL PROPELLANT – RETURN VEHICLE MEL

Description Case 1_Titan_Sample_Return CD-2021-186	QTY	Unit Mass	Basic Mass	Growth	Growth	Total Mass
Propellant (Chemical)			**14.4**	**0%**	**0.0**	**14.4**
Propellant			**11.2**	**0%**	**0.0**	**11.2**
Fuel			11.1	0%	0.0	11.1
Fuel Usable	1	10.2	10.2	0%	0.0	10.2
Fuel Margin	1	0.6	0.6	0%	0.0	0.6
Fuel Residulals (Unused)	1	0.2	0.2	0%	0.0	0.2
Pressurant			0.1	0%	0.0	0.1
Nitrogen Pressurant	1	0.1	0.1	0%	0.0	0.1
RCS Propellant			**3.2**	**0%**	**0.0**	**3.2**
Fuel			3.2	0%	0.0	3.2
Fuel Usable	1	2.8	2.8	0%	0.0	2.8
Fuel Margin	1	0.3	0.3	0%	0.0	0.3
Fuel Residulals (Unused)	1	0.1	0.1	0%	0.0	0.1

TABLE 4.25.—CHEMICAL PROPELLANT – IN-SPACE STAGE MEL

Description Case 1_TSR_Launch_Vehicle CD-2021-186c	QTY	Unit Mass	Basic Mass	Growth	Growth	Total Mass
Propellant (Chemical)			**326.4**	**0%**	**0.0**	**326.4**
Propellant			**326.2**	**0%**	**0.0**	**326.2**
Fuel			79.0	0%	0.0	79.0
Fuel Usable	1	76.7	76.7	0%	0.0	76.7
Fuel Residulals (Unused)	1	2.3	2.3	0%	0.0	2.3
Oxidizer			236.9	0%	0.0	236.9
Oxidizer Usable	1	230.0	230.0	0%	0.0	230.0
Oxidizer Residuals (Unused)	1	6.9	6.9	0%	0.0	6.9
Pressurant			10.3	0%	0.0	10.3
Nitrogen	1	9.5	9.5	0%	0.0	9.5
Delta RCS	1	0.8	0.8	0%	0.0	0.8
Delta RCS Margin	1	0.1	0.1	0%	0.0	0.1
RCS Propellant			**0.2**	**0%**	**0.0**	**0.2**
Fuel			0.1	0%	0.0	0.1
Fuel Usable	1	0.1	0.1	0%	0.0	0.1
Fuel Residulals (Unused)	1	0.0	0.0	0%	0.0	0.0
Oxidizer			0.1	0%	0.0	0.1
Oxidizer Usable	1	0.1	0.1	0%	0.0	0.1
Oxidizer Margin	1	0.1	0.1	0%	0.0	0.1
Oxidizer Residuals (Unused)	1	0.0	0.0	0%	0.0	0.0

TABLE 4.26.—CHEMICAL PROPELLANT – UPPER ATMOSPHERE STAGE

Description Case 1_TSR_Launch_Vehicle CD-2021-186c	QTY	Unit Mass	Basic Mass	Growth	Growth	Total Mass
Propellant (Chemical)			**1525.7**	**0%**	**0.0**	**1525.7**
Main Engine Propellant			**1525.7**	**0%**	**0.0**	**1525.7**
Fuel			381.0	0%	0.0	381.0
Fuel Usable	1	375.3	375.3	0%	0.0	375.3
Fuel Residulals (Unused)	1	5.6	5.6	0%	0.0	5.6
Oxidizer			1142.9	0%	0.0	1142.9
Oxidizer Usable	1	1126.0	1126.0	0%	0.0	1126.0
Oxidizer Residuals (Unused)	1	16.9	16.9	0%	0.0	16.9
Main Engine Pressurant	2		1.8	0%	0.0	1.8
Extra RCS for Return Vehicle	1	0.8	0.8	0%	0.0	0.8
Nitrogen Presurant	1	1.0	1.0	0%	0.0	1.0

TABLE 4.27.—CHEMICAL PROPELLANT - 1ST STAGE MEL

Description Case 1_TSR_Launch_Vehicle CD-2021-186c	QTY	Unit Mass	Basic Mass	Growth	Growth	Total Mass
Propellant (Chemical)			**1223.1**	**0%**	**0.0**	**1223.1**
Main Engine Propellant			**1223.1**	**0%**	**0.0**	**1223.1**
Fuel			305.5	0%	**0.0**	**305.5**
Fuel Usable	1	301.0	301.0	0%	0.0	301.0
Fuel Residuals (Unused)	1	4.5	4.5	0%	0.0	4.5
Oxidizer			916.5	0%	**0.0**	**916.5**
Oxidizer Usable	1	903.0	903.0	0%	0.0	903.0
Oxidizer Residuals (Unused)	1	13.5	13.5	0%	0.0	13.5
Main Engine Pressurant			1.0	0%	**0.0**	**1.0**
Nitrogen Pressurant	1	1.0	1.0	0%	0.0	1.0

TABLE 4.28.—PROPELLANT POWER – UPPER ATMOSPHERE STAGE MEL

Description Case 1_TSR_Launch_Vehicle CD-2021-186c	QTY	Unit Mass	Basic Mass	Growth	Growth	Total Mass
Propulsion Power			**2.0**	**50%**	**1.0**	**3.0**
Propulsion Power			**2.0**	**50%**	**1.0**	**3.0**
Propulsion Power			2.0	50%	1.0	3.0
PMAD Box	1	1.5	1.5	50%	0.8	2.3
Cabeling	1	0.5	0.5	50%	0.3	0.8

TABLE 4.29.—PROPELLANT POWER - 1ST STAGE MEL

Description Case 1_TSR_Launch_Vehicle CD-2021-186c	QTY	Unit Mass	Basic Mass	Growth	Growth	Total Mass
Propulsion Power			**2.0**	**50%**	**1.0**	**3.0**
Propulsion Power			**2.0**	**50%**	**1.0**	**3.0**
Propulsion Power			2.0	50%	**1.0**	**3.0**
PMAD Box	1	1.5	1.5	50%	0.8	2.3
Cabeling	1	0.5	0.5	50%	0.3	0.8

4.6 Propellant Production

The Titan sample return spacecraft carries the sample taken from the surface of Titan back to earth. To return the sample, the launch vehicle takes off from Titan's surface utilizing O_2 and CH_4 produced from the surface material. A radioisotope power system is used to provide both thermal and electrical power for propellant production process. The thermal system must maintain the designated operating ranges of the temperatures associated with the power generation, electronics utilized on the surface, and the propellant production throughout the surface operation. This is accomplished by sizing the thermal system to reject the waste heat being generated while on the surface as well as by providing heat for the propellant production process. To control temperature within the cold surface environment (94 K), insulated enclosures and heaters as well as waste heat are utilized to ensure the components do not fall below their minimum operating temperature during the mission. The main components that generate

waste heat include the electrical power, data, control, and communications equipment for the surface operations. Significant heat is also utilized by the O_2 production process to heat, melt, and boil surface water ice.

The propellant production process will take place on the surface of Titan. The thermal system and corresponding production process will be sized to operate within this environment. Both radiation and convection (both natural and forced) were used to determine the heat losses to the surroundings. The aspects of the thermal control and environment as well as the system components that were addressed or sized in the design and analysis are listed below.

- Radiator panels
- Enclosure and tank insulation
- Heat pipes and cold plates for moving heat from the electronics to the entry vehicle coolant system as well as utilizing waste heat from the DRPS
- Heaters for controlling the spacecraft components' temperature
- Temperature sensors, controllers, switches, data acquisition
- Heat leak through the insulation and insulation pass-through
- O_2 production method: including tanks, heat exchanger, electrolyzer and associated equipment
- CH_4 gathering method: including tanks, pumps, and associated equipment

4.6.1 System Requirements

The requirements for the thermal system are based on the Titan surface operational environment, given in Section 4.7.2.1 of the Return Spacecraft and Launch Vehicle Thermal Control subsection, and the requirements and specifications for the propellant production system and components. These specifications and the subsequent thermal system requirements are based on the physical characteristics of the systems requiring thermal control, the operational environment and the heat load and temperature requirements for the systems. Table 4.30 identifies the payload specification, assumptions and requirements for the thermal system design and operation.

4.6.2 Propellant Production System Components and Layout

The propellant production system is used to produce the LOx and LCH_4 that is used as propellant for the rocket that will bring the samples from the Titan surface back to Earth. The rocket propellant system utilizes O_2 as the oxidizer and CH_4 as the fuel. A total of 2238 kg of O_2 and 746 kg of CH_4 are needed for the return spacecraft and other ancillary components utilized by the mission. Figure 4.22 shows the components of the propellant production system.

4.6.3 Oxygen Production System

The cryogenic O_2 oxidizer is produced from water ice collected from the surface. Figure 4.23 shows the O_2 production process.

TABLE 4.30.—PROPELLANT PRODUCTION THERMAL CONTROL SYSTEM SPECIFICATIONS AND REQUIREMENTS

Variable/Component	Value/Description
Power System Electronics Enclosure Surface Operations Electronics Enclosure	0.27 m Height, 1.506 m Length, 0.9 m Width 0.178 m Height, 1.055 m Length, 0.455 m Width
Waste Heat Load to be Rejected:	Power System Electronics: 175 W Surface Operations Electronics: 40 W to 335 W
Operating Temperature	Power System Electronics: 287 K Surface Operations Electronics: 300 K Ice Melting Tank: 283 K Water Boiling Tank: 373 K Water Storage Tank: 283 K O_2 Liquification Tank 94 K CH_4 Liquification and Storage Tanks: 94 K
Insulation for Electronics Enclosure and Water Liquification, Boiling and Storage Tanks	Foam Aerogel: Thermal Conductivity (k_i) 0.017 W/mK Density: 20 kg/m^3
Environment	Titan Surface Atmosphere Temperature (T_a): 94 K Atmospheric Pressure1.5 bar Atmosphere Density (r_a): 5.44 kg/m^3 Atmosphere Viscosity (η_a): 6.44E-6 Pa-s Wind Speed (V_w): 5 m/s Atmosphere Thermal Conductivity (k_a): 0.00881 W/mK Atmosphere Specific Heat (c_p): 1039 J/kg K Titan Gravitational Acceleration (g_t): 1.35 m/s^2
Coolant System	Power Electronics: Variable Conductance Heat Pipe based coolant system Operations Electronics: Variable Conductance Heat Pipe based system for distributing waste heat within the enclosure. Pumped atmosphere coolant system during high power operation.

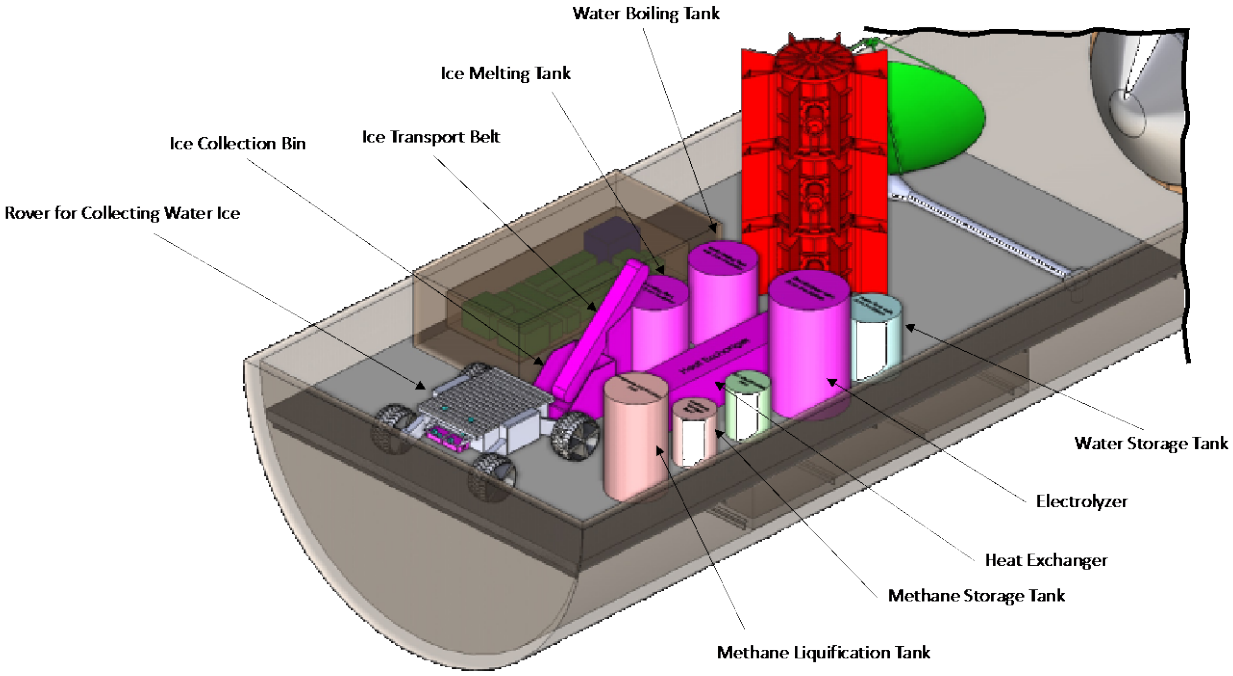

Figure 4.22.—Main Propellant Production System Components.

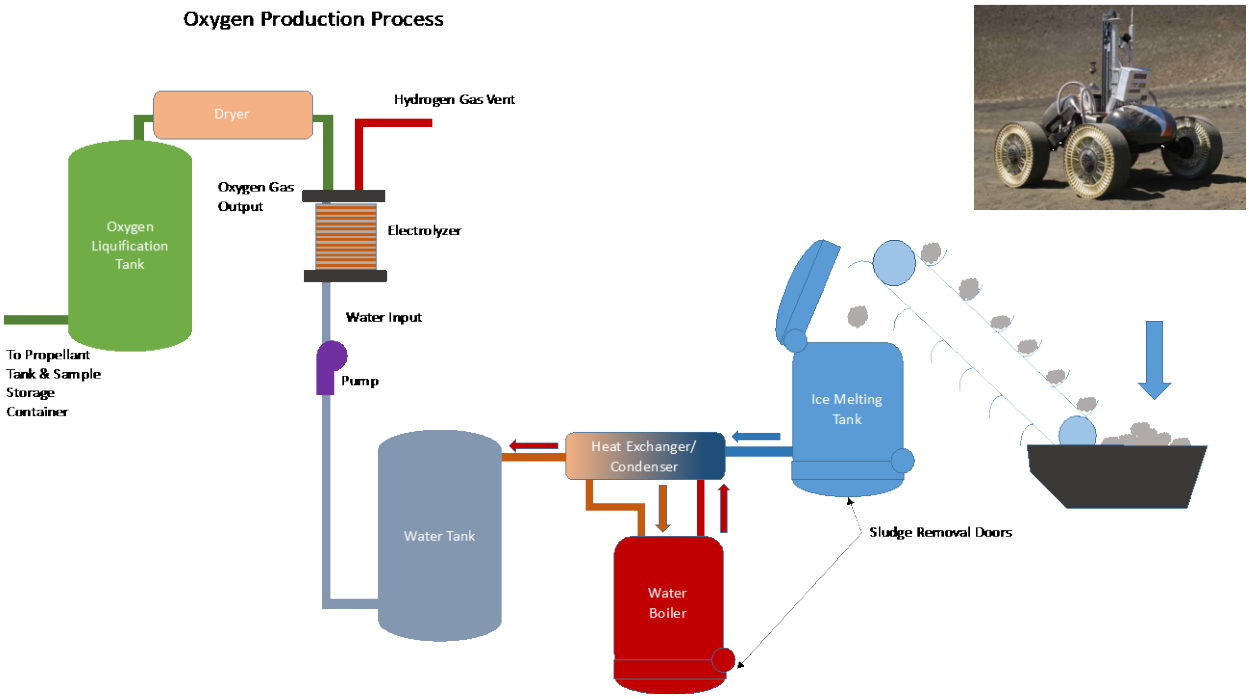

Figure 4.23.—Oxygen Production System Diagram.

The steps in the O_2 production processes are outlined below and Table 4.31 summarizes the critical values for each step. The propellant production process was assumed to be a continuous process over a 2.7 Earth year period.

1. Surface Ice is gathered by the rover and brought to the collection bin.
2. Ice from the collection bin is deposited into the ice melting tank with a conveyor belt system.
3. The ice is melted in the tank. The ice melting tank is periodically emptied to remove any material that builds up in the chamber.
4. The melted ice water then flows through a heat exchanger where it is preheated before entering the water boiler.
5. The water is then boiled to purify it and passes through the heat exchanger/condenser. The water boiling tank is periodically emptied to remove any condensable material that was carried in with the water.
6. The purified water is stored in a water tank.
7. It is then pumped to the electrolyzer where it is separated into O_2 and H_2.
8. The O_2 gas is dried to remove any water vapor and then sent to a liquification tank. The electrolyzer can pressurize the exit stream of O_2 above atmospheric pressure to enable it to liquify when it cools
9. The H_2 gas is vented to the atmosphere.

TABLE 4.31.—SPECIFICATIONS FOR OXYGEN PRODUCTION PROCESS

Step	Total Mass (kg)	Percent Usable Material (%)	Initial Temperature (K)	Final Temperature (K)	Sensible Heat (GJ)	Phase Change Heat (GJ)	Continuous Power (W)
1	5035 Ice	100	94	94	NA	NA	NA
2	5035 Ice	100	94	94	NA	NA	50.9
3	5035 Ice	62.5	94	273	1.44	1.7	34
4	3147 Water	100	273	323	NA	NA	NA
5	3147 Water	80	323	373	0.9 GJ	5.7 GJ	76.6
6	2518 Water	100	350	340	NA	NA	NA
7	2518 Water	100	340	323	NA	NA	484.5
8	2238 O_2	100	323	94	NA	NA	NA
9	280 H_2	100	323	94	NA	NA	NA

The electrolyzer's power requirement will depend on the amount of water that needs to be electrolyzed. The rate of water production ($\dot{M}_w$) is based on the ratio of the molecular weights of the reactant and product of interest, water. The rate of water production in kg/hr is given by Equation (1). Subsequently the rate of O_2 production ($\dot{M}_o$) can then be determined, which is given by Equation (2).

$$\dot{M}_w = \eta_s \dot{M}_i \frac{18}{308} \tag{1}$$

$$\dot{M}_o = \dot{M}_w \frac{16}{18} \tag{2}$$

A proton exchange membrane (PEM) electrolyzer was selected to separate the water into O_2 and H_2. The power required by the electrolyzer (P_e) can be calculated based on the theoretical power needed to break apart water given by the relationship for Gibbs free energy (ΔG) in Equation (3) (Ref. 55). For liquid water at 340 K (T_{H_2O}), the enthalpy change (ΔH) is 285.9 kJ/mol and the entropy change (ΔS) is the change given by Equation (4) where ΔS_{H2O} = 69.94 (J/K)mol, ΔS_{O2} = 205.29 (J/K)mol and ΔS_{H2} = 130.59 (J/K)mol. This results in an entropy change of –0.163 (kJ/K)mol. Therefore, using the previously calculated ΔH and ΔS, the available ΔG is 230.4 kJ/mol or 3,520 Wh/kg. Using this value, the mass flow rate of water, and the efficiency of the electrolyzer (η_e), the electrolyzer power can be determined as given by Equation (5).

$$\Delta G = \Delta H - T_{H_2O} \Delta S \tag{3}$$

$$\Delta S = -\Delta S_{H_2O} + (0.5\Delta S_{O_2} + \Delta S_{H_2}) \tag{4}$$

$$P_e = \Delta G \frac{\dot{M}_w}{\eta_e} \tag{5}$$

The required power decreases exponentially as the time available to make the O_2 increases. Figure 4.24 illustrates this trend to produce 2000 kg of O_2. From this figure it can be seen that the required power is driven mainly by the electrolyzer power requirement.

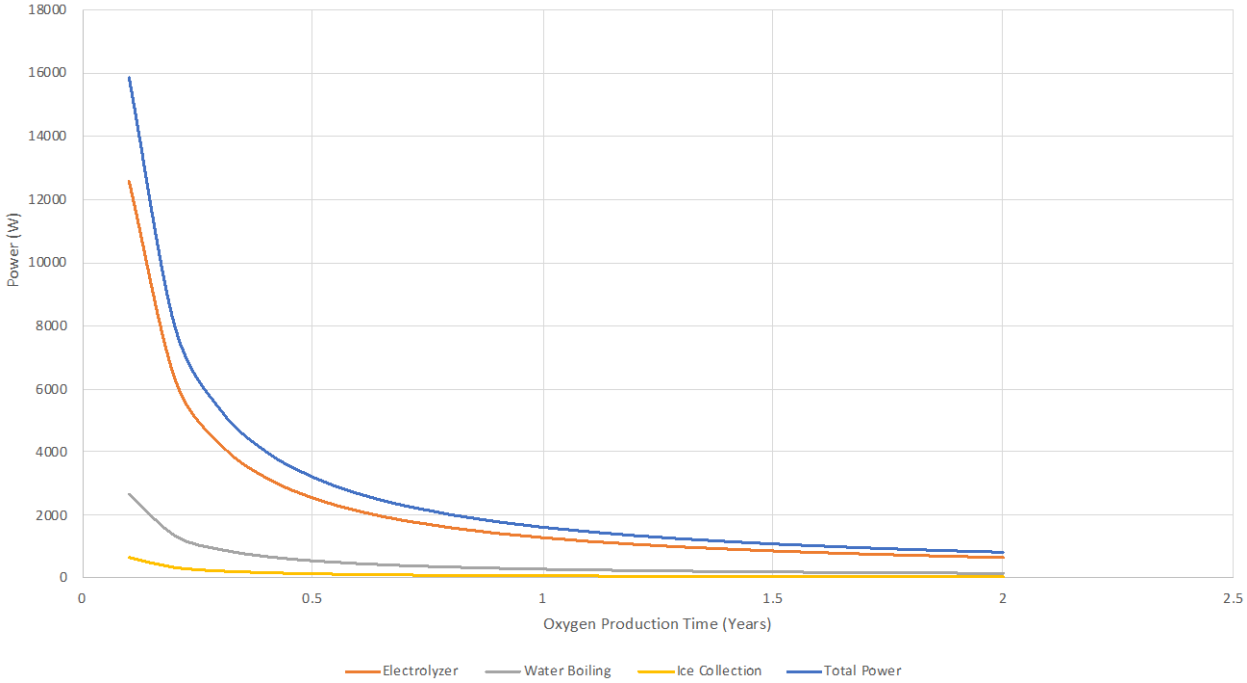

Figure 4.24.—Required Power as a Function of Production Time for 2000 kg of O_2.

TABLE 4.32.—ELECTROLYZER COMPONENT AND SCALING FACTOR BREAKDOWN

Component	Variable	Scaling factor, kg/kW
Electrolyzer stack	S_{es}	2.00
Water tank and heater	S_{wt}	0.10
Filters	S_f	0.12
Propellant lines and fittings	S_{pl}	0.52
Controller unit	S_{cu}	0.16
Wiring	S_w	0.30
Heat exchanger	S_{he}	1.00
Water pump	S_{wp}	0.27
Check valves	S_{chv}	0.08
Flow regulators	S_{fr}	0.62
Control valves	S_{cv}	0.16
Pressure and temperature sensors	S_s	0.07
Flow sensors	S_{fs}	0.06

To determine the mass of the electrolyzer (M_e), it was broken down into a number of components and scaled linearly based on its operational power level. The mass of the electrolyzer is given by Equation (6) and Table 4.32 lists the components along with their scaling factors. The scaling values were based on representative commercially available components over a range of operating parameters as well as projected performance values for certain items. Linear curve fits for this data were used to generate the scaling factors.

$$M_e = P_e(S_{es}+S_{wt}+S_f + S_{pl} + S_{cu} + S_w + S_{he} + S_{wp} + S_{chv} + S_{fr} + S_{cv} + S_s + S_{fs}) \quad (6)$$

The mass for the ice collection, water boiling, and water collection tanks is based on their size and construction material. These were not pressure tanks, they operated at atmospheric pressure. The material mass used for the tanks is given by Equation (7). Table 4.33 provides the values used for each of the tanks.

$$M_t = (\pi d_t l_t + n_l \pi \left(\frac{d_t}{2}\right)^2) t_t \rho_t \quad (7)$$

The heat exchanger is used to condense the steam from the boiling tank and correspondingly preheat the water from the ice melting tank before it enters the boiling tank. Figure 4.25 illustrates this arrangement.

The method for sizing the heat exchanger and determining its mass is given in Colozza and Burke (2011) (Ref. 56). The dryer operates in a similar manner to the heat exchanger. The dryer is a heat exchanger that slowly cools the O_2 gas as it leaves the electrolyzer. This cooling condenses any moisture in the O_2 stream allowing it to be removed from the system.

TABLE 4.33.—PRODUCTION SYSTEM TANKS SIZING PARAMETERS

Tank	Length (l_t, m)	Diameter (d_t, m)	Wall Thickness (t_t, mm)	Number of lids (n_l)	Hours of Stored Material	Tank Material	Material Density (kg/m^3)
Ice Melting	0.33	0.25	0.5	2	48	Ti	4430
Water Boiling	0.33	0.25	0.5	2	48	Ti	4430
Water Storage	0.17	0.25	0.5	2	24	Ti	4430
Ice Collection	0.25	0.35	1.0	1	48	Ti	4430
O_2 Liquification	0.17	0.25	0.5	2	24	Ti	4430

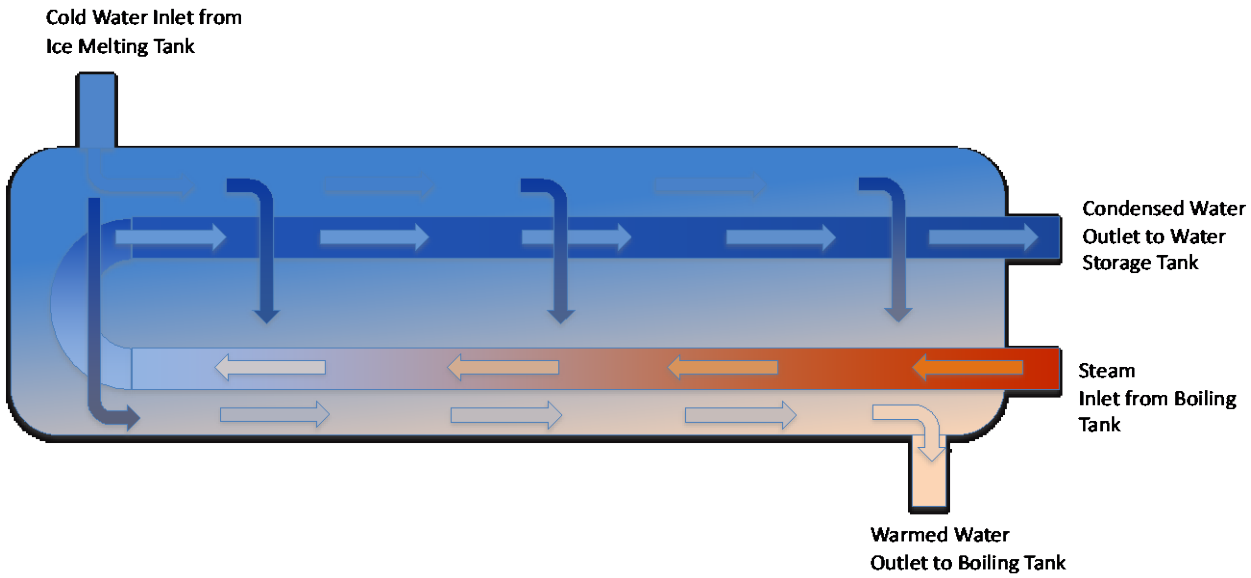

Figure 4.25.—Cross-Flow Heat Exchanger Example for Condensing the Steam and Preheating the Boiling Water.

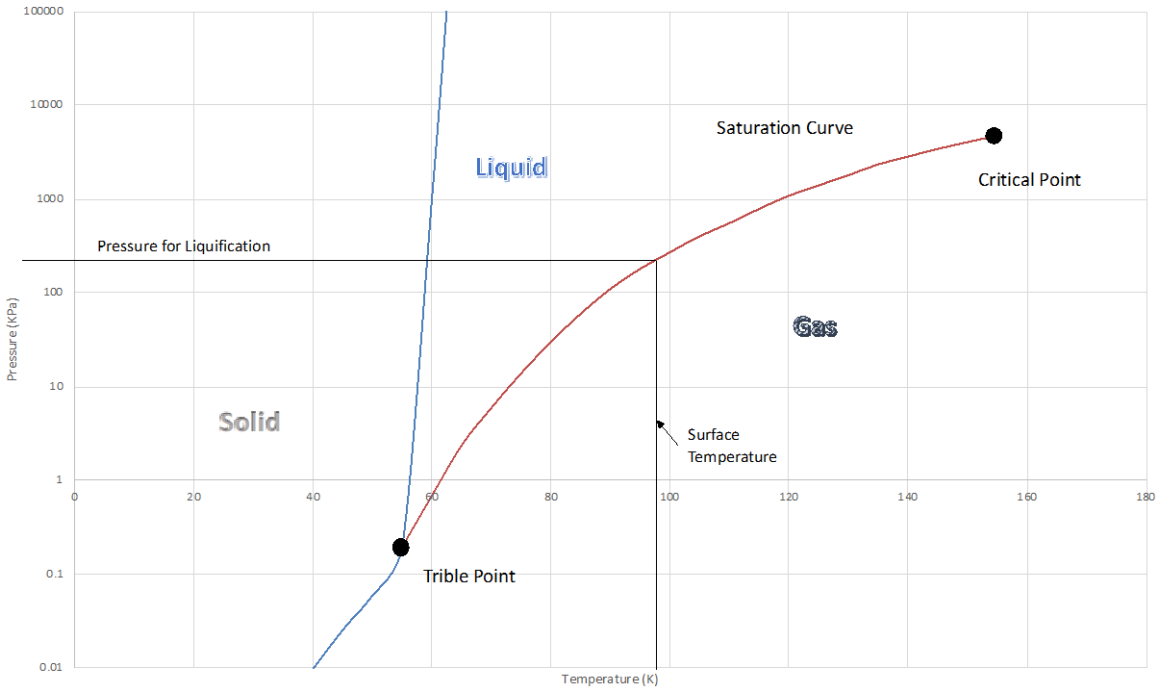

Figure 4.26.—Oxygen Phase Diagram and Liquification Pressure and Temperature.

The last step in the O_2 production process is the liquification of the O_2 gas from the electrolyzer. Because of the surface conditions on Titan, this liquification will take place passively at a pressure slightly higher than atmospheric pressure without the need for a cryocooler. To liquify O_2 at the ambient temperature of 94 K will require a pressure of approximately 2 bar (200 kPa). The output gas pressure of the electrolyzer (~350 kPa) is well above the required pressure to liquify the O_2 as it cools. The phase diagram for O_2 (Figure 4.26) shows this.

4.6.4 CH_4 Production System

CH_4 is collected from the atmosphere and stored as a liquid for fuel for the return rocket. The atmosphere of Titan contains approximately 5.7 percent CH_4 gas. The collection, liquification and storage of the CH_4 is achieved through a process of pumping and compressing the atmosphere to liquify the CH_4 and then storing the LCH_4 at ambient conditions. This system requires a pump, liquification tank, storage tank, and control valves (Figure 4.27).

To produce the CH_4 the atmosphere has to be compressed to 8.8 bar. At that pressure and the ambient temperature, the CH_4 will condense into the collection chamber from the atmosphere. As it condenses and cools to ambient temperature it will fill the collection tank. Once the tank is partially filled with CH_4 the process is stopped, and the LCH_4 is transferred to a storage tank and the liquification tank is vented. This occurs by opening the vent valve in the CH_4 tank to reduce the pressure back to atmospheric conditions, 1.5 bar. During this process the pump is used to flow atmospheric gas into the chamber. The atmospheric gas is continually circulated through the chamber to keep the gas within the chamber at saturation so the liquified CH_4 does not revaporize as the pressure in the tank is reduced for transfer. Once the liquification tank is at atmospheric pressure, the storage valve is opened and the liquid within the tank flows to the storage tank. This cycle of collection, pressurization and cooling is repeated until the desired amount of LCH_4 is collected. The CH_4 phase diagram (Figure 4.28) identifies this process.

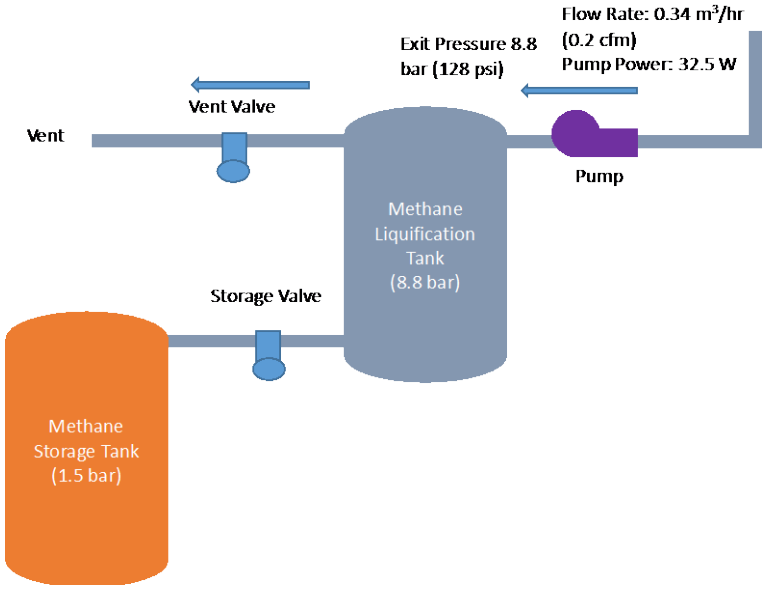

Figure 4.27.—CH_4 Production System Components.

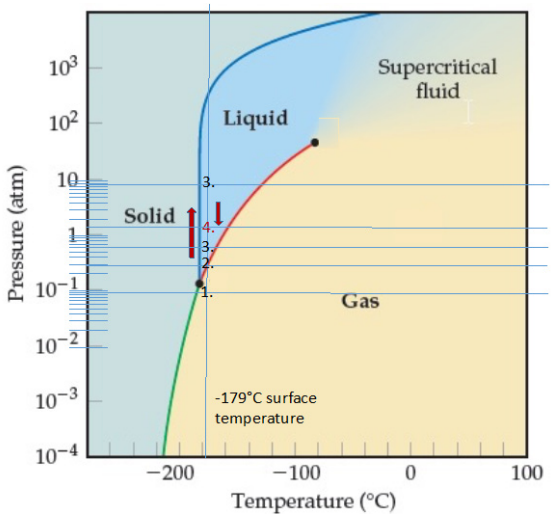

Figure 4.28.—CH_4 Phase Diagram and Liquification Process Points.

The CH_4 liquification process is outlined below. The steps correspond to the numbers on the phase diagram in Figure 4.28.

1. The gaseous CH_4 is at the initial atmospheric conditions, 94 K, 1.5 bar (partial pressure of CH_4 is 0.0848 bar)
2. As the pressure in the tank is increased. The partial pressure of the CH_4 rises above 0.3 bar (5.28 bar total pressure) where it begins to condense.
3. The total pressure is raised to 8.8 bar (128 psi) this corresponds to a partial pressure of CH_4 of ~0.5 bar to condense the CH_4. This total pressure will cause approximately 50 percent of the CH_4 to condense out of the atmosphere. Once the CH_4 condenses to the liquid state it experiences the full atmospheric pressure of 8.8 bar
4. As the liquid is moved from the liquification tank to the storage tank the pressure drops to the atmospheric level of 1.5 bar for storage. Once liquid is generated the liquid can be stored at ambient pressure of 1.5 bar.

TABLE 4.34.—LCH_4 PRODUCTION SPECIFICATIONS

Parameter	Value
Atmospheric Pressure	1.5 bar
Atmospheric Temperature	94 K
Atmospheric Collection Rate	0.06 kg/h, 0.34 m^3/h
Pump	Single Stage Scroll
Pump Power	32.5 W
CH_4 Partial Pressure in the Atmosphere	0.085 bar
CH_4 Atmospheric Composition Fraction	0.0565
Total CH_4 Collected	746 kg
Total Collection Time	2.9 Earth years

Table 4.34 summarizes the CH_4 production details for the system.

4.6.5 Propellant Production Thermal Control

A thermal analysis was performed to size the insulation and determine the heat loss and required power needed to maintain the various processing tanks and electronics enclosures at their desired operating temperature. The heat losses from the interior were through the insulation. It was assumed that all wiring and other physical connections such as fluid tubes and structural components were also insulated and not directly exposed to the ambient environment.

The heat loss from the interior of the tanks or electronics enclosures to the exterior is through conduction from the interior material or components and the exterior in contact with the atmosphere. It was assumed that the interior is at a uniform temperature. The heat loss (Q_i) through the insulation, where k_i is the thermal conductivity of the insulation, A_i is the interior surface area of the insulation, t_i is the insulation thickness, T_i is the interior surface temperature and T_s is the exterior surface temperature is given by Equation (8).

$$Q_i = \frac{k_i A_i (T_i - T_s)}{t_i} \tag{8}$$

Equation (8) sets the heat flow from the interior to the outer surface of the enclosure or tank. The outer surface temperature of these items will depend on the heat flow from the interior and the convective heat transfer (Q_c) from the surface to the atmosphere as given by Equation (9), where A_s is the exterior surface area and T_a is the temperature of the atmosphere which was assumed to be a constant at 94 K.

$$Q_c = A_s h (T_s - T_a) \tag{9}$$

To determine the convective heat transfer from the surface, the convective heat transfer coefficient (h) between the exterior surface and atmosphere, given by Equation (10), must be calculated. The coefficient is based on the characteristic length (L) of the enclosures and tanks along the direction of the flow. Table 4.30 gives the thermal conductivity of the N_2 atmosphere (k_a).

$$h = \frac{Nuk_a}{L} \tag{10}$$

Assuming a worst-case wind speed of 5 m/s the forced convection Nusselt (Nu) number is given by Equation (11) (Ref. 57).

$$\mathrm{Nu} = 0.3 + \frac{0.62\mathrm{Re}^{1/2}Pr^{1/3}}{\left[1+\left(\frac{0.4}{Pr}\right)^{2/3}\right]^{1/4}}\left[1+\left(\frac{\mathrm{Re}}{282000}\right)^{5/8}\right]^{4/5} \tag{11}$$

The Reynolds number, given by Equation (12), is based on the tank diameter or enclosure width (d_t), density of the atmosphere (ρ_a), wind velocity (V_w) and dynamic viscosity of the atmosphere (η_a). These environmental values are given in Table 4.30.

$$\mathrm{Re} = \frac{\rho_a V_w d_t}{\eta_a} \tag{12}$$

The Prandlt Number (Pr), given by Equation (13), is based on the specific heat (c_p), dynamic viscosity and thermal conductivity of the atmosphere, given in Table 4.30.

$$\mathrm{Pr} = \frac{c_p \eta_a}{k_a} \tag{13}$$

The Raleigh number (Ra) is given by Equation (14), is based on the gravitational force on Titan (g_t) and the boundary layer film temperature (T_f) is assumed to be an average between the exterior wall temperature and the atmosphere temperature, as given by Equation (15).

$$\mathrm{Ra} = \frac{g_t\left(\frac{1}{T_f}\right)(T_s - T_a)d_s^3}{\frac{\mu_a k_a}{\rho_a^2 c_p}} \tag{14}$$

$$T_f = \frac{(T_s - T_a)}{2} \tag{15}$$

Equation (8) through Equation (15) are solved iteratively for the exterior wall surface temperature. This is done for a desired interior temperature and insulation thickness which is then used to determine the heat loss through the insulation. Using this analysis, the heat loss from the tanks and insulation thickness was determined (Table 4.35).

There were two electronics enclosures as part of the propellant production system. One enclosed the power system electronics and the other enclosed the electronics for the propellant production system operation. Figure 4.29 shows these enclosures.

TABLE 4.35.—TANK HEAT LOSS SPECIFICATIONS

Tank	Interior Temperature (T_i, K)	Tank Surface Temperature (T_s, K)	Heat Loss (Q_i, W)	Insulation Thickness (t_i, m)	Convective Coefficient (h, W/m^{2}K)
Ice Melting	273	94.6	17.0	0.1	46.7
Water Boiling	373	95.0	26.4	0.1	46.7
Water Storage	340	94.9	23.3	0.1	46.7
Ice Collection	94	94	NA	NA	NA
O_2 Liquification	94	94	NA	NA	NA

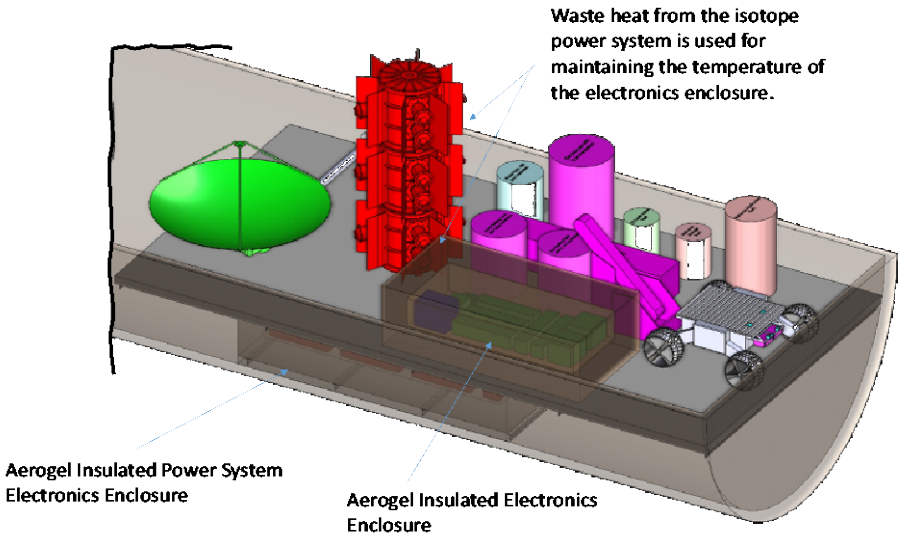

Figure 4.29.—Illustration of the Propellant Production System Electronics Enclosures.

The waste heat from the electronics was used as the primary heat source to maintain the internal temperature of the enclosures within their desired range during operation. For the propellant production system electronics enclosure, the power level varied from a low level of approximately 40 W to up to 335 W during the high-power operation. To maintain the enclosure interior at the desired 300 K operating temperature, waste heat from the isotope heat source was used during low power operation. During high power operation, atmospheric gas is used to control the interior temperature. The atmosphere gas is circulated through the interior of the enclosure as a means of removing the excess heat during this portion of the operation. Servo valves and a pump control the atmosphere flow through the chamber to maintain the internal temperature at the desired 300 K. The flow rate of the atmosphere through the chamber is 1.2×10^{-3} kg/s to maintain the chamber at 300 K and remove the remaining 252 W of heat above that lost through the insulation.

For the power system electronics enclosure, during operation on the surface there is sufficient heat generated by the electronics (175 W) to maintain the interior of the chamber at 287 K. The power system electronics will operate continuously while on the surface and therefore no additional thermal management system is required.

To control the electronics enclosure temperature for both the power system and propellant production electronics during transit to Titan, the EDL thermal control system was utilized. The EDL cooling system utilizes the same interface to the electronic enclosures as the isotope power system. A control valve is used to control heating/cooling flow from either the EDL coolant loop while in transit to Titan or from the waste heat fluid loop from the isotope power system while on the surface of Titan. For the propellant production electronics, a hot plate interface is used to distribute heat within the enclosure on the surface during times when insufficient internal heat is being generated. This same plate acts as a cold plate interface to remove waste heat during transit to Titan through the EDL cooling system. A servo valve is used to shut off this connection during operation on the surface of Titan. A similar cold plate is used with the power system electronics enclosure for removing the waste heat while in transit to Titan. Figure 4.30 illustrates the electronics thermal control system.

Aerogel insulation was also used for the electronics enclosures. Table 4.36 gives the details on the heat loss from the enclosures.

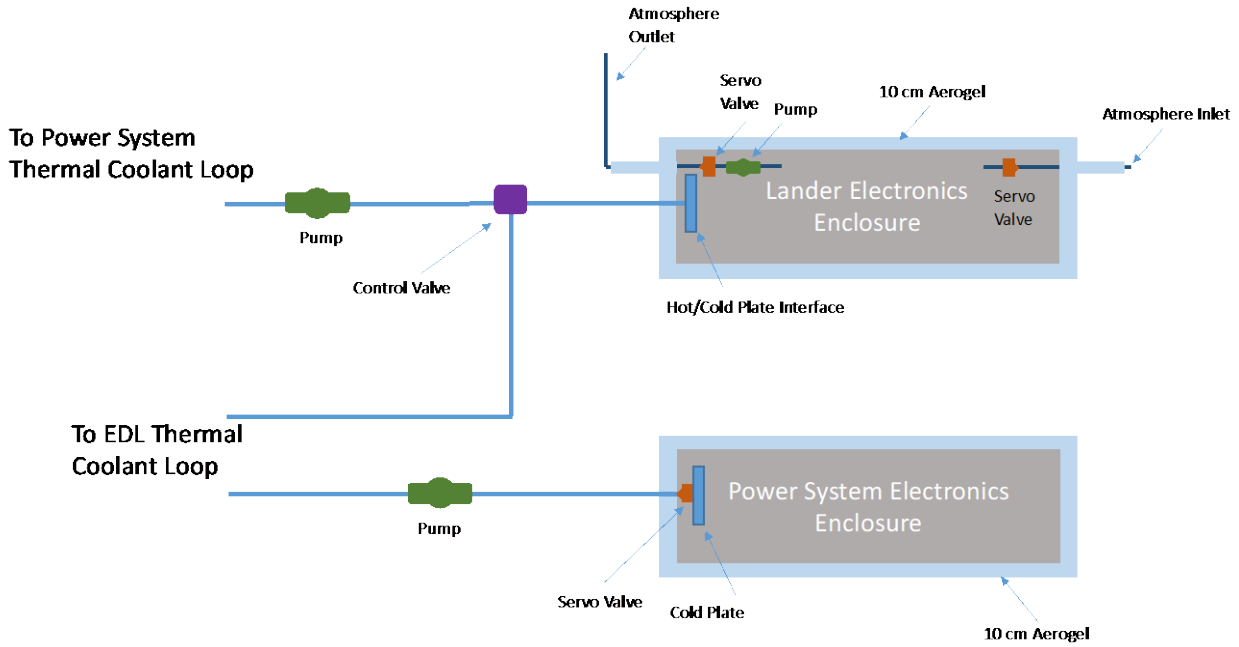

Figure 4.30.—Electronic Enclosure Thermal Control System.

TABLE 4.36.—ELECTRONICS ENCLOSURE LOSS SPECIFICATIONS

Enclosure	Interior Temperature (T_i, K)	Tank Surface Temperature (T_s, K)	Heat Loss (Q_i, W)	Insulation Thickness (t_i, m)	Convective Coefficient (h, W/m^{2}K)
Power Electronics	287	95.3	175	0.1	40.0
Propellant Production Electronics	300	95.4	83	0.1	40.0

TABLE 4.37.—THERMAL CONTROL SYSTEM – PROPELLANT PROCESSING LANDER MEL

Description Case 1_TSR_Propellant_Processing CD-2021-186b	QTY	Unit Mass	Basic Mass	Growth	Growth	Total Mass
Thermal Control (Non-Propellant)			**55.0**	**18%**	**9.9**	**64.9**
Active Thermal Control			**2.4**	**18%**	**0.4**	**2.9**
Therrmal Switches	12	0.1	1.2	18%	0.2	1.4
Thermal Control/Heaters Circuit	12	0.1	0.6	18%	0.1	0.7
Data Acquisition	2	0.3	0.5	18%	0.1	0.6
Thermocouples	12	0.0	0.1	18%	0.0	0.1
Passive Thermal Control			**52.5**	**18%**	**9.5**	**62.0**
Heat Pipes	24	0.1	2.2	18%	0.4	2.7
Fairing Insulation	1	26.4	26.4	18%	4.8	31.2
Cold Plates	12	0.1	1.7	18%	0.3	2.0
Power System Insulation	1	16.1	16.1	18%	2.9	19.0
Electronics Insulation	1	6.1	6.1	18%	1.1	7.2

Master Equipment List

Table 4.37 provides the MEL for the propellant production.

TABLE 4.38.—THERMAL CONTROL SYSTEM – ISRU SYSTEM MEL

Description Case 1_TSR_Propellant_Processing CD-2021-186b	QTY	Unit Mass	Basic Mass	Growth	Growth	Total Mass
ISRU System			**47.3**	**18%**	**8.3**	**55.6**
Active ISRU System			**13.2**	**18%**	**2.4**	**15.6**
Ice Transport Belt	1	10.6	10.6	18%	1.9	12.5
Electrolyzer	1	2.6	2.6	18%	0.5	3.1
Passive ISRU System			**25.1**	**17%**	**4.3**	**29.5**
Ice Collection Container	1	1.0	1.0	18%	0.2	1.1
Ice Melting Tank	1	2.5	2.5	18%	0.5	3.0
Water Boiling Tank	1	2.1	2.1	18%	0.4	2.5
Heat Exchanger Condenser	1	5.5	5.5	18%	1.0	6.5
Water Tank	1	1.7	1.7	18%	0.3	2.0
O2 Liquification Tank	1	1.7	1.7	18%	0.3	2.0
Water & Gas Lines	1	1.2	1.2	18%	0.2	1.4
Methane Liquification Tank	1	4.2	4.2	18%	0.7	4.9
Compressor	1	2.5	2.5	18%	0.5	3.0
Methane Storage Tank	1	1.7	1.7	18%	0.3	2.0
Power Electronics Cold Plate Interface	1	0.6	0.6	0%	0.0	0.6
Electronics Cold Plate Interface	1	0.6	0.6	0%	0.0	0.6
Semi-Passive Thermal Control			**8.9**	**18%**	**1.6**	**10.5**
Electronics Atm Coolant Lines	1	1.1	1.1	18%	0.2	1.3
Electronics Atm Pump	1	1.5	1.5	18%	0.3	1.8
Electronics Atm Valves	1	0.5	0.5	18%	0.1	0.6
Electronics Ext Coolant Lines	1	2.2	2.2	18%	0.4	2.6
Electronics Power System Ext Coolant Pump	1	1.5	1.5	18%	0.3	1.8
Electronics Ext Control Valve	1	0.5	0.5	18%	0.1	0.6
Power Electronics Coolant Lines	1	1.1	1.1	18%	0.2	1.3
Power Electronics Control Valve	1	0.5	0.5	18%	0.1	0.6

4.7 Return Spacecraft and Launch Vehicle Thermal Control

The Titan sample return spacecraft carries the sample taken from the surface of Titan back to Earth. The return spacecraft must keep the sample cold for its return and entry in Earth's atmosphere. The thermal system must maintain the temperature of the electronics and components of the spacecraft within their designated operating ranges throughout the mission. This is accomplished by sizing the thermal system to reject the waste heat being generated during the transit to ensure that the components do not exceed their maximum operating temperature. This also provides insulated enclosures and heaters as well as waste heat to ensure the components don't fall below their minimum operating temperature during the mission. The main components that generate waste heat include the electrical power, data, control and communications equipment for the spacecraft and propulsion system. It also must maintain the return sample at or below the 94 K storage temperature during transit and until it is recovered after entry. This is accomplished by shielding the sample from any heat source during transit and providing a volume of LOx as a phase change material to maintain the sample temperature below 94 K during entry and until recovery.

The spacecraft operation begins on the Titan surface where it is in storage during the surface portion of the mission. During this time, it needs to be maintained within the desired storage temperature of the electronics and components. The next phase will take place from near Titan (9.5 AU) to Earth (1 AU).

The thermal system will be sized to operate within this environment. Solar Intensity and view angle as well as the view to warm bodies such as the spacecraft solar arrays and radiators, and operation during shadow are used to determine the worst case hot and cold conditions. The worst-case warm conditions will occur in sunlight near Earth with all equipment operating. Whereas the worst-case cold will be at Titan in shadow. The aspects of the thermal control and environment as well as the system components that were addressed or sized in the design and analysis are listed below.

- Systems Modeled
  - Radiator Panels
  - Spacecraft Insulation
  - Heat pipes and cold plates for moving heat from the electronics to the radiator
  - Heaters for controlling the spacecraft components temperature
  - Isotope heat source for providing heat while on the Titan surface
  - Thermal paint for maintaining temperature while in orbit
  - Temperature Sensors, Controllers, Switches, Data Acquisition
  - Heat leak through the insulation and insulation pass-throughs
  - Insulated sample return capsule with LOx phase change material

4.7.1 System Requirements

The requirements for the thermal system are based on the operational environment and the requirements and specifications for the spacecraft and launch vehicle components. These specifications and the subsequent thermal system requirements are based on the physical characteristics of the systems requiring thermal control, the operational environment and the heat load and temperature requirements for the systems. Table 4.39 identifies the payload specification, assumptions and requirements for the thermal system design and operation.

TABLE 4.39.—RETURN SPACECRAFT AND LAUNCH VEHICLE
THERMAL CONTROL SYSTEM SPECIFICATIONS AND REQUIREMENTS

Variable/Component	Value/Description
Spacecraft Electronics Enclosure Dimensions Sample Return Capsule Dimensions	0.9 m diameter, 1.15 m length 0.8 m diameter, 0.5 m height
Spacecraft Electronics Waste Heat Load to be Rejected	100 W
Operating Temperature	Spacecraft Electronics: 300 K Rejection Temperature Return Capsule: 94 K Storage Temperature
Insulation (MLI) was used for the electronics	Spacecraft main body: 25 layers of MLI, Bulkhead isolating return capsule: 25 layers of MLI
Environment	Operational Environment: near Earth 1.0 AU (worst case hot), Titan/Saturn 9.54 AU (worst case cold)
Radiator and View Factors	Max 70° Angle to the Sun View Factor to the Spacecraft Solar Arrays 0.20 View Factor to Earth: 0.0
Coolant System	Spacecraft Electronics: Variable Conductance Heat Pipe based coolant system

4.7.2 Operational Environment

The operating environment of the sample return mission consists of two distinct environments. Operation on the surface of Titan and in transit between Saturn and Earth. These environments are very different and pose different requirements on the systems and components operating within them, particularly the thermal control system for the various aspects of the mission.

4.7.2.1 Titan Surface Environment

The harsh environment of Titan provides a number of challenges in the operation of equipment and materials. From entry to descent to the surface, operating within this environment requires a thermal balance between the isotope heat sources and the losses to the environment. This balance is accomplished through thermal insulation and distribution of the heat generated. To accurately size the thermal system, the operational environment throughout each phase of the mission must be defined.

The environmental conditions on Titan are unique and unlike those on any other known planet or moon. In ways, it is very Earth-like. It has a mostly N_2 atmosphere, clouds, lakes, rivers, and rain. However, with a surface temperature of under 100 K the free liquid is not water but CH_4. The low atmospheric temperature also lowers the speed of sound through the atmosphere. Near the surface, the speed of sound is approximately half that on Earth. Due to the distance from the Sun, cloud cover and haze, little sunlight reaches the surface. The atmospheric density at the surface is five times that of Earth and the pressure is 1.5 times greater than that at Earth's surface. Figure 4.31 shows a diagram of the atmosphere and Table 4.40 gives select properties of Titan.

The gravitational acceleration on Titan (1.35 m/s^2) is less than that of Earth's moon. Liquid is present on the surface in the form of CH_4 and ethane. These form the CH_4 seas.

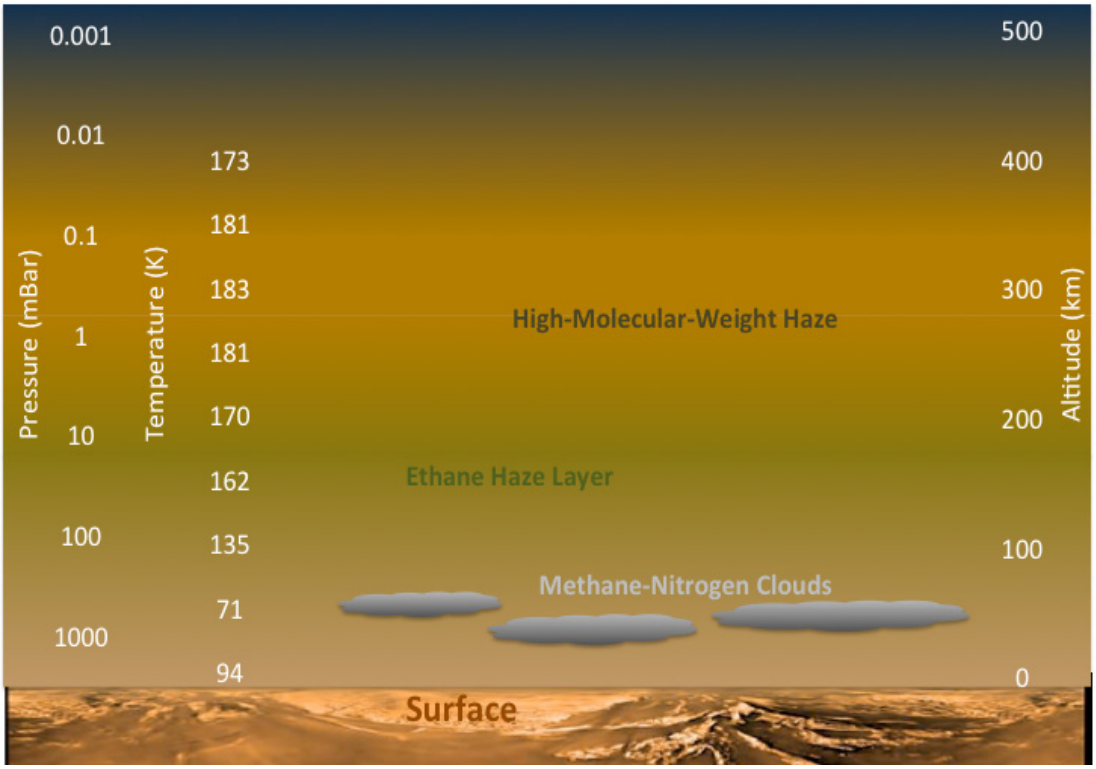

Figure 4.31.—Illustration of Titan Atmosphere (Refs. 58 and 59).

TABLE 4.40.—PHYSICAL AND ORBITAL PROPERTIES OF TITAN (REFS. 59 TO 61)

Property	Value
Maximum Inclination of Equator to Orbit to Saturn (δ_{max})	0.35°
Orbital Eccentricity (ε)	0.0288
Mean Radius of Orbit (r_m) around Saturn	1.22×10^6 km
Day Period (synchronous to the orbital period around Saturn)	15.95 (Earth Days)
Surface Pressure	146.7 kPa
Albedo	0.22
Gravitational Constant (g_v)	1.35 m/s^2
Orbital Period around Saturn	15.95 (Earth Days)
Surface Temperature	93.7 K
Diameter	5152 km
Solar Flux outside Titan's Atmosphere	14.87 W/m^2
Speed of Sound at the Surface	196.5 m/s
Atmosphere Gas Constant (R_a)	296.8 J/kg-K
Atmosphere Ratio of Specific Heats (γ_a)	1.4
Atmosphere Specific Heat (c_{pa})	1039 J/kg-K

4.7.2.2 Saturn to Earth Transfer Environment

The return mission takes the spacecraft from Saturn (9.5 AU) to Earth (1 AU), the thermal environment at each of these locations is evaluated to size the thermal control components (i.e., insulation and radiators) to operate within the worst case hot and cold operating conditions. The first step in sizing the thermal components is to determine an effective sink temperature at each location. This is accomplished by performing an energy balance on an object with no internal heat generation at each of the locations to determine its equilibrium temperature. This equilibrium temperature is the sink temperature at each location. For this analysis a six-sided cube was used for the object shape. Each side of the object has a different view to the heat sources and sinks in the environment around the object. The net power into or emitted from side "i" (P_i) of the object is given by Equation (16) and the total energy balance power (P_{eb}) is given by Equation (17).

$$P_i = \left(\varepsilon_i \sigma T_c^4 - \alpha_{si} I_s \cos(\beta_i + f_{pi} A_p\right) - \alpha_{IRi} I_p f_{pi} - \alpha_{IRi} I_{sa} f_{sa}) A_{si} \tag{16}$$

Where the Stefan-Boltzman Constant: $\sigma = 5.67\times10^{-8}\left(\frac{W}{m^2K^4}\right)$.

$$P_{eb} = \sum_{i=1}^{i=6} P_i \tag{17}$$

The variables used and their corresponding values for each side and planet are given in Table 4.41.

The sink temperature at the Earth and Saturn locations is determined by iterating on the cube temperature (Tc) in Equation (16) so that Equation (17) is equal to 0. The cube temperature at which Equation (17) equals 0 is the sink temperature (Ts) for that location and input conditions. The calculated sink temperature for each location is given in Table 4.41 and shown in the mission illustration in Figure 4.32. Because of the large difference in the environmental conditions between operation at Saturn and Earth the electronic radiator is not needed while near Saturn. To accommodate this change in sink temperature louvers are used to effectively turn off the radiator while at Saturn. During the transition from Saturn to Earth the louvers slowly open increasing the radiative capability as the spacecraft moves to Earth.

TABLE 4.41.—SINK TEMPERATURE PROPERTIES

	Side 1 (i=1)	Side 2 (i=2)	Side 3 (i=3)	Side 4 (i=4)	Side 5 (i=5)	Side 6 (i=6)
Length	1 m	1 m	1 m	1m	1 m	1 m
Width	1 m	1 m	1 m	1m	1 m	1 m
Area (A_{si})	1 m^2	1 m^2	1 m^2	1 m^2	1 m^2	1 m^2
Emissivity (ε_i)	0.85	0.85	0.85	0.85	0.85	0.85
Solar Absorptivity (α_{si})	0.14	0.14	0.14	0.14	0.14	0.14
Solar Angle (β_t)	45	45	45	0	0	0
View to Planet (f_{pi})	0	0	0	0.06	0.06	0.06
View to Solar Array (f_{sa})	0.2	0.2	0.2	0.2	0.2	0.2
IR Absorptivity (α_{IRi})	0.3	0.3	0.3	0.3	0.3	0.3
Location	Earth			Saturn		
Solar Intensity (I_s)	1370 W/m^2			15 W/m^2		
Solar Array IR (I_{sa})	672 W/m^2			7.5 W/m^2		
Albedo (A_p)	0.3			0.34		
IR Emission (I_p)	240 W/m^2			3.76 W/m^2		
Sink Temperature	250 K			44 K		

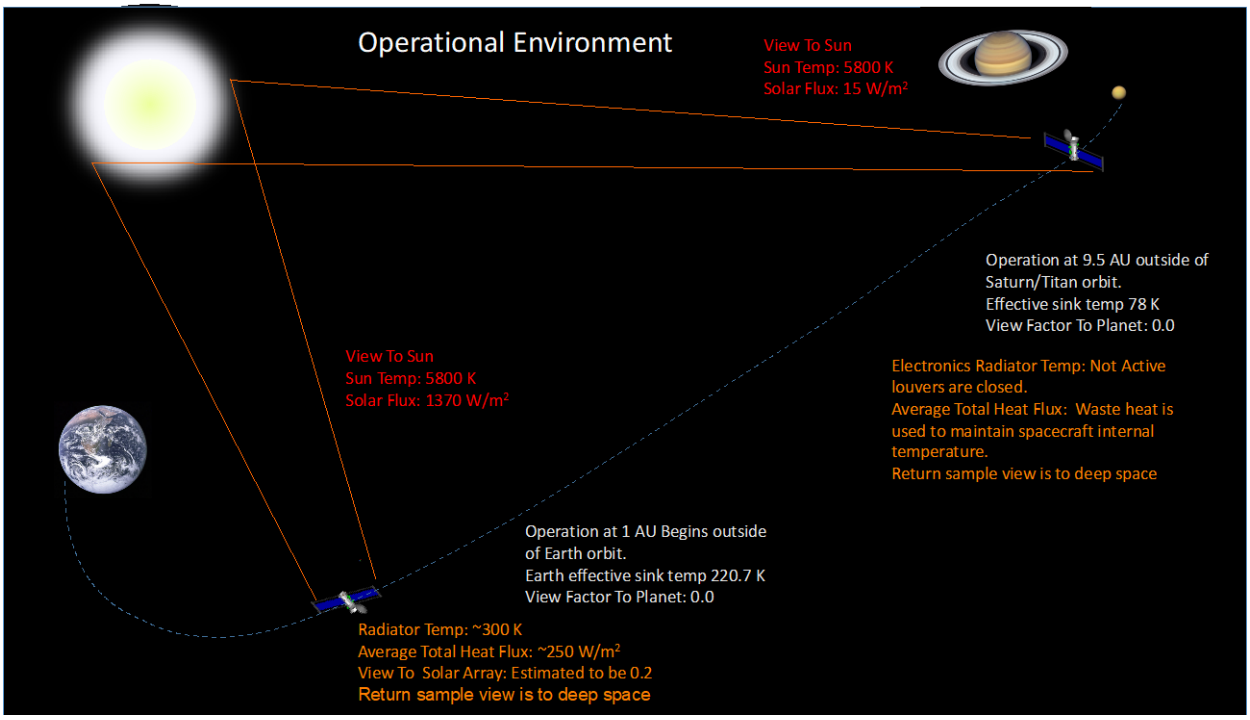

Figure 4.32.—Environmental Thermal Properties Throughout the Mission.

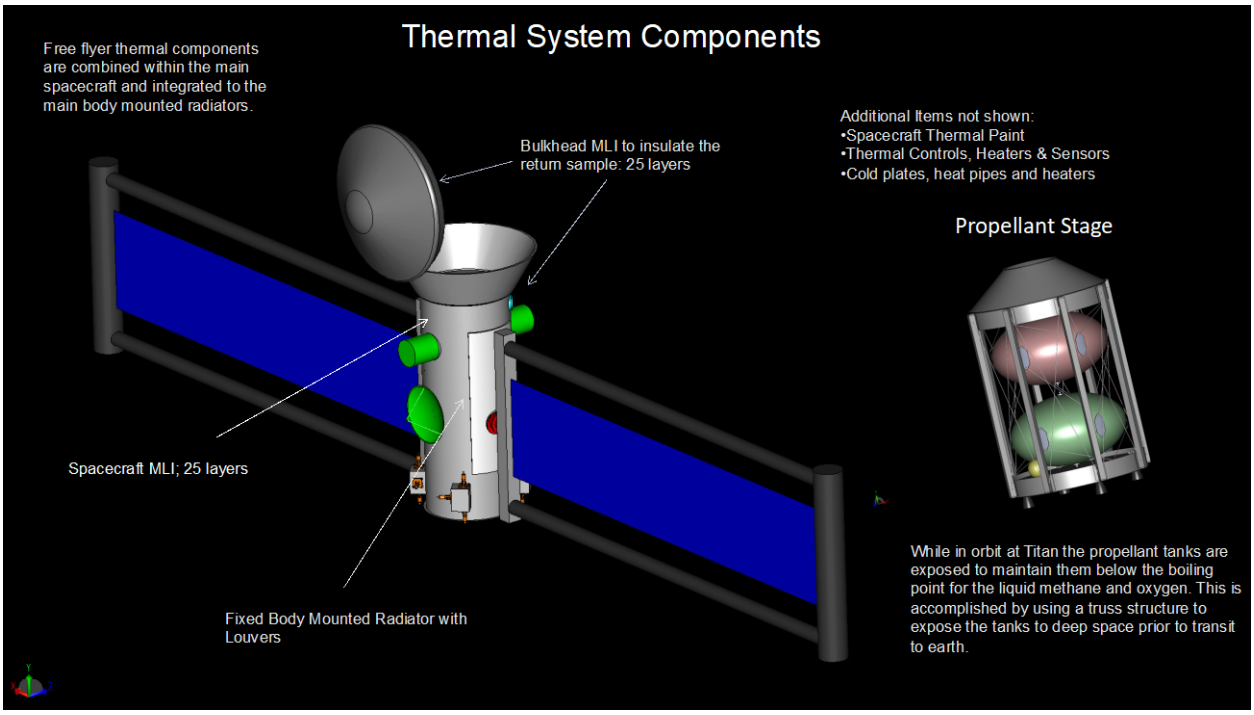

Figure 4.33.—Main Thermal Control Areas.

4.7.3 Thermal System Components and Layout

The thermal system for the launch vehicle and return spacecraft involved a number of aspects of the spacecraft and its operation. These items are shown in Figure 4.33 and include the following main areas:

- Maintaining the In-Space Stage fuel and oxidizer below their boiling point while in orbit prior to use to inject the spacecraft into the Earth transfer orbit.
- Maintaining the return sample at cryogenic temperatures during transfer to Earth.
- Maintaining the spacecraft electronics and interior component of the spacecraft within their required operating temperature while on the surface of Titan and during transit to Earth.

4.7.3.1 In-Space Stage Thermal Control

The cryogenic propellant is stored within tanks in the in-space stage while in orbit prior to Earth transfer orbit injection. This propellant consists of LCH_4 and LOx. The propellant tanks are designed to operate within the Titan environment at or near ambient conditions. The temperature of the LCH_4 is approximately 94 K at 1.5 bar whereas the LOx is at 94 K and 2 bar. The effective sink temperature near Saturn is 78 K. Therefore, the propellant can be maintained within its liquid state by having uninsulated tanks with a high emissivity coating of approximately 0.85 and a view to deep space. To achieve this the tanks were housed in a truss structure enclosure that provided a good view to deep space and were painted with a high emissivity coating such as AZ-93 paint.

4.7.3.2 Return Spacecraft Thermal Control

The return spacecraft has two distinct environments in which it operates, on the surface of Titan and in transit from Saturn to Earth. These environmental conditions provide unique requirements for the thermal control system.

4.7.3.2.1 Return Spacecraft Thermal Control on Titan Surface

For storage operation on the surface the return spacecraft was housed in an insulated faring. The fairing utilized 10 cm of aerogel insulation. Within the fairing was a single insulated GPHS block, illustrated in Figure 4.34, which provides an estimated beginning of life thermal output off approximately 254 W of heat to the fairing interior. This thermal power degrades to approximately 238 W after 8 years. The block provides sufficient heat to maintain the interior of the faring at approximately 265 K while on the surface of Titan near the end of the mission. This arrangement is illustrated in Figure 4.35 and the heat transfer specifications are provided in Table 4.42.

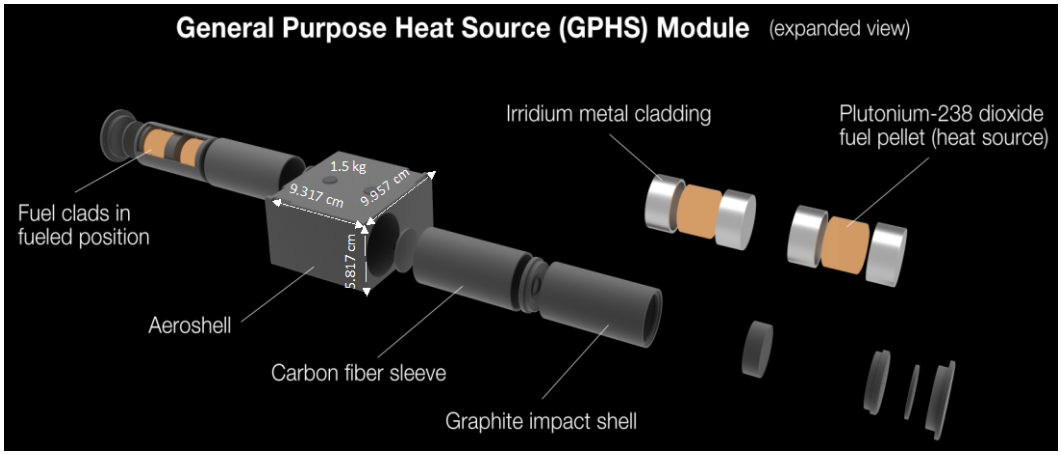

Figure 4.34.—Illustration of GPHS Block.

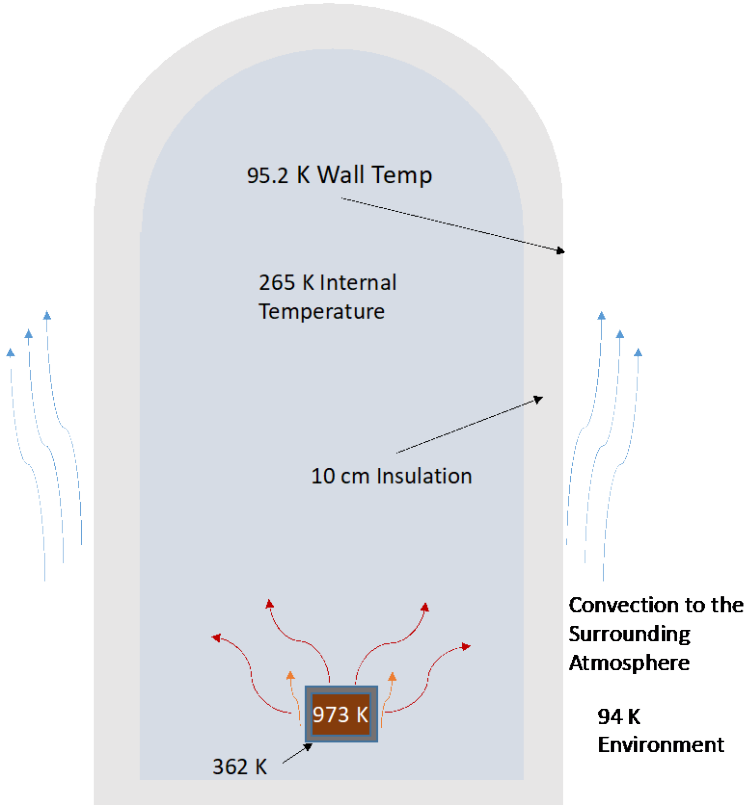

Figure 4.35.—Return Spacecraft Fairing Thermal Control While On the Titan Surface.

TABLE 4.42.—SPACECRAFT FAIRING THERMAL PROPERTIES

Variable	Value
GPHS Block Dimensions	Length: 10 cm, width 10 cm, height 6 cm
GPHS Block Thermal Power	240 W
Fairing Insulation Thickness	10 cm Aerogel
Aerogel Thermal Conductivity	0.017 W/mK
Exterior Surface Area	8.12 m^2
GPHS Block Insulation	1.74 cm Microtherm
Microtherm Thermal Conductivity	0.021 W/mK
Internal GPHS Block Convective Coefficient	3.95 W/m^2K (natural convection)
External Faring Wall Convective Coefficient	25.02 W/m^2K (forced convection 5 m/s wind speed)

4.7.3.2.2 Return Spacecraft Thermal Control During Transit from Saturn to Earth

During transit from Saturn to Earth the thermal environment changes considerably with the sink temperatures ranging from 78 K near Saturn to approximately 221 K near Earth. The thermal system must adjust from keeping the return spacecraft warm enough near Saturn to keeping it cool enough near Earth. To accomplish this the spacecraft is fully insulated and waste heat is used to maintain the temperature near Saturn whereas near Earth radiators are used to reject the excess waste heat to space.

4.7.3.2.3 Multi-Layer Insulation

In the vacuum of space radiation heat transfer is the main mechanism for heat leak into or out of the insulated spacecraft. The desired operating temperature for the electronics enclosure and propellant tanks was 300 K. Therefore, for long term use in space these components must be resistant to heat loss to the surrounding to minimize the amount of heater power needed to maintain their desired operating temperature. To reduce the heat loss, MLI is used as the main barrier to heat leak. MLI is constructed of several layers of metalized material with a nonconductive spacer between the layers. The metalized material has a low absorptivity which resists radiative heat transfer between the layers. MLI can be conformed to fit over various shapes. It can be held in place with Velcro or glue. Examples of MLI and an illustration of its construction is shown in Figure 4.36. For the long duration flight back to Earth the spacecraft will need to be wrapped in MLI to minimize their heat loss to the surroundings.

The heat transfer through the MLI was analyzed to determine the required number of layers and their corresponding mass and the heat leak into the tanks. The insulation model was based on radiation heat transfer analysis of the heat transfer from the spacecraft through the insulation to space. Table 4.43 gives the heat loss for the insulation and the MLI specifications.

4.7.3.2.4 Radiator

The radiator was sized to remove the waste heat from the electronics during the worst case hot operational conditions that occur near Earth at 1 AU. This sizing is based on energy balance approach for rejecting excess heat to the surroundings. Heat inputs and view factors to surrounding components and environmental bodies such as the Sun and planets are taken into account in this energy balance approach. The radiator is coated to reflect the majority of the incoming visible solar radiation from the Sun providing a low solar absorptivity of the radiator surface. This reduces the heat load on the radiator.

The required radiator area (A_r) is determined by the thermal power that needs to be rejected (P_r) as given by Equation (18). The radiator is sized based on the worst-case operating conditions as given by the variables used in its sizing and described in Table 4.44.

$$A_r = \frac{P_r}{\sigma(\varepsilon_r T_r^4) - \alpha_{IR} f_p I_p - \alpha_r I_s (Cos(\theta_{rs}) + f_p A_p) - f_{sc} \alpha_{IR} I_{sc}} \tag{18}$$

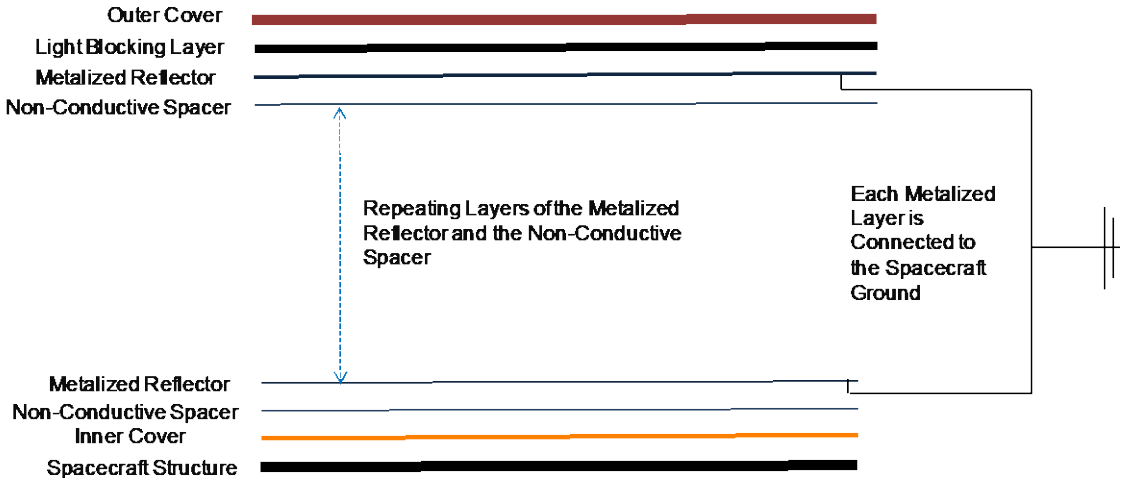

Figure 4.36.—Illustration of MLI Construction Layout and Component Layers.

TABLE 4.43.—MLI SPECIFICATIONS AND ESTIMATED HEAT LOSS

Variable	Value
Spacecraft MLI Material	Aluminized Kapton
Spacecraft MLI Material Aerial Density	
Outer Covering	0.11 kg/m^2
Inner Covering	0.05 kg/m^2
Spacer	0.0063 kg/m^2
Reflective Layer	0.055 kg/m^2
Attachment and Seals Percentage	10 percent
MLI Thickness	1 cm (Thruster Bulkhead and Spacecraft)
Number of Insulation Layers	25
MLI Layer Spacing	0.2 mm
Insulation Heat Loss Min Temperature Operation (9.54 AU)	33.5 W (1.4 W Insulation, 32.2 W Passthroughs)
Insulation Heat Loss Min Temperature Operation (1 AU)	15.3 W (0.85 W Insulation, 14.5 W Passthroughs)

An estimate of the mass of the radiator panel (M_r) can be made based on its required area. The radiator structure can be separated into components with a scaling coefficient for each component to linearly scale the mass based on the required radiator area. These coefficients were derived from satellite and spacecraft radiator mass data and are listed in Table 4.45. Equation (19) gives the total radiator mass.

$$M_r = C_p A_r + C_c A_r + C_t A_r + C_h A_r + C_a A_r + C_s A_r + C_{at} A_r + C_d A_r \quad (19)$$

Due to the relatively small radiator size, the radiator was body mounted rejecting heat from only one side while the other side facing the spacecraft is insulated.

Because of the large sink temperature range, the spacecraft will operate over louvers that are used on the radiator to effectively turn the radiator off during the portion of the mission when the sink temperatures are low. Louvers are active or passive devices that regulate the amount of heat rejected by the radiator by opening and closing to change the view to the surroundings of the radiator radiating surface. Utilizing louvers on the radiator however will increase the required radiator area needed by approximately 30 percent. This is due to the louvers reducing the view factor of the radiator to deep space or other cold surfaces to reject heat.

Active controlled louvers use temperature sensors and actuators to control the louver position whereas passive controlled louvers commonly use a bimetallic spring that opens and closes the louver based on temperature. The louver specific mass is 4.5 kg/m^2.

TABLE 4.44.—RADIATOR SIZING VARIABLES AND RESULTS

Variable	Value
Radiator Solar Absorptivity (α_r)	0.14
Radiator IR Absorptivity (α_{IR})	0.30
Radiator Emissivity (ε_r)	0.84
Max Radiator Sun Angle	30°
View Factor Planetary Body (f_p)	0.06
View Factor to Solar Array and Spacecraft (f_{sc})	0.2
Radiator Operating Temperature (T_r)	Nominal 300 K
Electronics Waste Heat (P_r)	100 W
Radiator Area	0.4 m^2

TABLE 4.45.—RADIATOR MASS SCALING COEFFICIENTS

Radiator Component Coefficient	Value (kg/m^2)
Panels (C_p)	3.3
Coating (C_c)	0.42
Tubing (C_t)	1.31
Header (C_h)	0.23
Adhesives (C_a)	0.29
Stingers (C_s)	1.50
Attachment (C_{at})	0.75
Deployment Mechanism (C_d)	3.4

4.7.3.2.5 Heat Pipes and Cold Plates

To collect the waste heat and move it to the radiators the electronics are mounted to the cold plates and heat pipes are used to transfer heat to the radiator.

Variable conductance heat pipes move the heat from the cold plates to the radiator. The number of heat pipe runs are dependent on the amount of heat to be moved, their capacity and the amount of redundancy needed in the system. The heat pipe condenser sections are distributed throughout the back side of the radiator. Because of the relatively low heat load and the dispersed nature of the heat load, the electronics radiator utilized variable conductance heat pipes to move the heat from the loads to the radiators where it is dissipated to the surroundings.

Heat pipes in general operate by boiling a liquid fluid when the heat pipe is subjected to heat at its design operating temperature. The fluid vapor then moves to the opposite end of the heat pipe (radiator) where heat is rejected, and the fluid condenses back to a liquid. A wick structure in the zero-gravity space environment is used to move the fluid back to the heating section through capillary forces. Once back to the heat input section the fluid will boil again repeating the process. Variable conductance heat pipes operate in a similar fashion but use a varying volume, non-condensable gas to adjust the amount of heat that the heat pipe is capable of moving while maintaining a fixed operating temperature.

At high heat loads the temperature dependent saturation pressure of the working fluid increases. This increase in pressure compresses the non-condensable gas into a reservoir at the end of the heat pipe provide a larger active condenser area. Thereby enabling more heat to be moved to the radiator by the heat pipe. As the heat load decreases the pressure decreases and the non-condensable gas fills up a greater volume of the heat pipe reducing the condenser area and thereby reducing the heat flow. A variable conductance heat pipe is a passive device that adjusts automatically to varying heat load inputs maintaining a constant operating temperature.

The working fluid for the heat pipe is chosen based on the desired operating temperature of the heat pipe and the heat removal requirement. To size the heat pipe and select the best working fluid, a factor

termed the Merit Number is utilized. The Merit number (N) is based on the properties of the working fluid as given by Equation (20). These properties include the latent heat of vaporization (H_v), the density (ρ_{wf}), surface tension (σ_{wf}) and the dynamic viscosity (μ_{wf}).

$$N = \frac{H_v \rho_{wf} \sigma_{wf}}{\mu_{wf}} \tag{20}$$

This number is plotted for various fluids in Figure 4.37. The higher the Merit number the greater the performance of the heat pipe. From this figure it can be seen for the desired operating temperature of 300 K water provides the best choice.

Using the Merit number, the heat pipe thermal power (P_{hp}) transfer capacity can be calculated as given by Equation (21) which is based on the heat pipe wick cross sectional area (A_w), the wick material permeability (K_w), the wick pore radius (r_{wp}) and the heat pipe length (L_{hp}).

$$P_{hp} = \frac{2NA_wK_w}{r_{wp}L_{hp}} \tag{21}$$

The heat pipes were sized for the heat produced by each of the loads. Table 4.46 gives the required heat pipe size and specific mass.

Cold plates are used to interface the heat pipes to the loads. These plates come in several shapes and sizes depending on the heat source configuration. They are used to provide a good thermal connection between the heat source and the heat pipe evaporator section. The heat source is mounted to the cold plate, which in turn has the heat pipe either mounted to it or incorporated into it. This provides a good thermal contact between the cold plate and the heat pipe.

The number of cold plates and heat pipe runs is dependent on the distribution of the loads and the desired redundancy for the thermal system. Each cold plate utilized two heat pipe runs to the radiator. Each heat pipe is sized to accommodate the full heat load. The second heat pipe is a redundant path in case of a failure. During normal operation both heat pipes are operational and operate at one half or less of their total heat carrying capacity. Table 4.47 gives the cold plate specifications and Figure 4.38 illustrates the distribution.

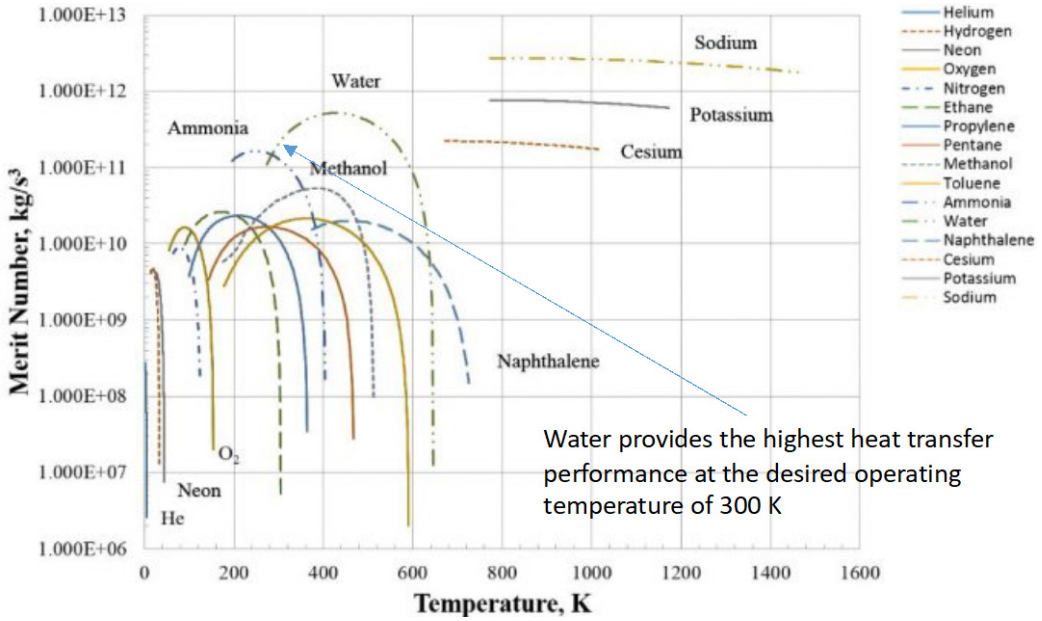

Figure 4.37.—Heat Pipe Merit Number Comparison for Various Working Fluids.

TABLE 4.46.—HEAT PIPE SIZING SPECIFICATIONS FOR EACH LOAD TYPE IN THE PROPULSION SECTION

Heat Pipe	Radius	Effective Length	Heat Transfer Capability	Heat Pipe Specific Mass
Spacecraft Electronics	0.3 cm	2 m	26.9 W/Heat Pipe	0.094 kg/m

TABLE 4.47.—COLD PLATE SPECIFICATIONS

Variable	Value
Cooling Plate and Line Material	Al
Cooling Plate and Line Material Density	2,770 kg/m^3
Number and size of the Cold Plates	Spacecraft Electronics: 6 at 0.1 m by 0.1 m
Cooling Plate Thickness	5 mm

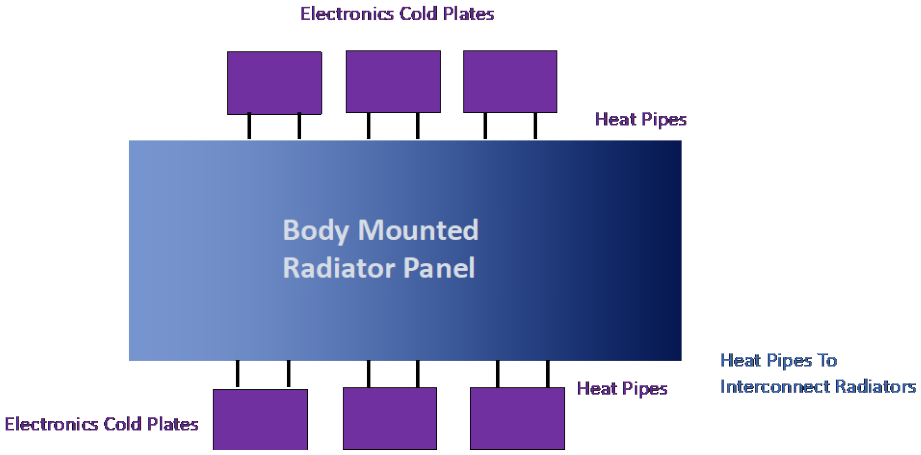

Figure 4.38.—Illustration of the Cryocooler and Electronics Heat Transfer Layout.

4.7.3.2.6 Heaters

Electric heaters are incorporated onto the cold plates as well as on critical components as needed. These heaters are used to maintain the temperature of these components above their minimum operating temperature throughout the mission. Waste heat from the internal components as well as electric heaters are used to provide heat to the spacecraft electronic components if needed. The flexible strip and plate heaters are used to provide heat to the electronic and mechanical components within the spacecraft. Flat plate heaters are used on each of the cold plates to provide heat to the mounted electronics and or packaging if necessary.

Thermal control within the spacecraft is accomplished with a network of thermocouples whose output is used to control the power to the various heaters, and a data acquisition and control computer is used to operate the thermal system. During normal operation it is estimated that the waste heat from the electronics components will be sufficient to maintain the temperature of the components within the spacecraft within their desired operating temperature range. Therefore, the heater power will be minimal during normal operations. Heater power will vary with the mission operation from 0.0 W to 100 W during low power operation.

4.7.3.3 Return Sample Thermal Control

To maintain the integrity of the return sample from Titan it must be kept at or below 94 K during the transit from Titan to Earth and prior to being retrieved for analysis. Due to the length of the transit time and the available power, active cooling is not possible. Therefore, a passive cooling method was utilized. The sample was isolated from the spacecraft to minimize any heat flow from the spacecraft to the sample. After collection, the sample is stored in the aeroshell for launch from Titan.

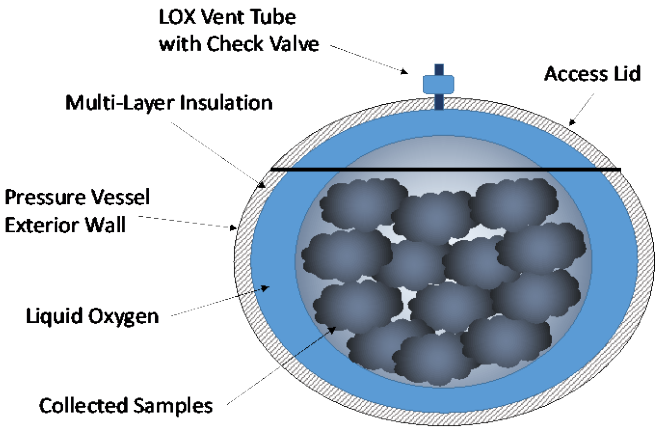

Figure 4.39.—Return Sample Container Thermal Control.

TABLE 4.48.—SAMPLE CONTAINER HEAT LEAK AND EQUALIZATION TEMPERATURE

	At Titan (9.5 AU)	At Earth (1 AU)
Heat Leak Aeroshell Shield	0.002 W/m^2	0.21 W/m^2
Heat Leak Back Shell Shield	0.42 W/m^2	0.42 W/m^2
Sample Equalization Temperature	34 K	36 K

The sample is placed and sealed within a return container. The container is a three-chamber walled ellipsoid structure that contains the sample at the center in the first chamber. The second chamber surrounding the sample is filled with LOx. This is used to maintain the sample at 94 K until it is retrieved once back on earth. The third chamber surrounding the LOx is a pressure vessel containing multi-layer insulation. This insulation is held at vacuum during transit and while on Earth to limit the heat loss from the inner two chambers to the surroundings. Figure 4.39 shows the sample container configuration.

During transit to Earth the sample is maintained at its cryogenic temperature by isolating it from any heat sources and exposing the container to deep space. After launch from Titan, the aeroshell in which the sample container is housed opens to expose the container to deep space. The opening of the aeroshell is similar to how the Stardust mission was configured so that the aeroshell could open and retrieve the solar particle samples and then close for reentry to earth. Figure 4.40 shows the Stardust aeroshell opened for sample collection.

The opened aeroshell acts as a Sun shield to shield both the heat leak from the spacecraft and isolate the return container from any view to the Sun. The orientation of the spacecraft from Titan to Earth is controlled so that the return container is always shielded from the Sun by either the open insulated aeroshell or the insulated back shell. Figure 4.41 illustrates this configuration. This type of shielding and the exposure of the container to deep space will drop the temperature of the container to levels below the boiling point of the LOx. This will maintain the LOx for use in maintaining the sample temperature while in Earth prior to retrieval. Table 4.48 gives the heat leak and equalization temperature for the container.

Once the spacecraft is near Earth, the aeroshell is closed and released from the spacecraft for reentry. This occurs approximately 45 min prior to entry. Once the aeroshell is closed, the sample container no longer has a view to deep space and will begin to warm. Through entry, descent and while on the surface, the LOx boil-off will be used to maintain the temperature of the sample at 94 K.

The Earth entry of the aeroshell was based on an entry speed of 14 km/s and a worst-case entry angle of 25°. Figure 4.42 shows the descent profile.

Figure 4.40.—Stardust Aeroshell Opened for Sample Collection.

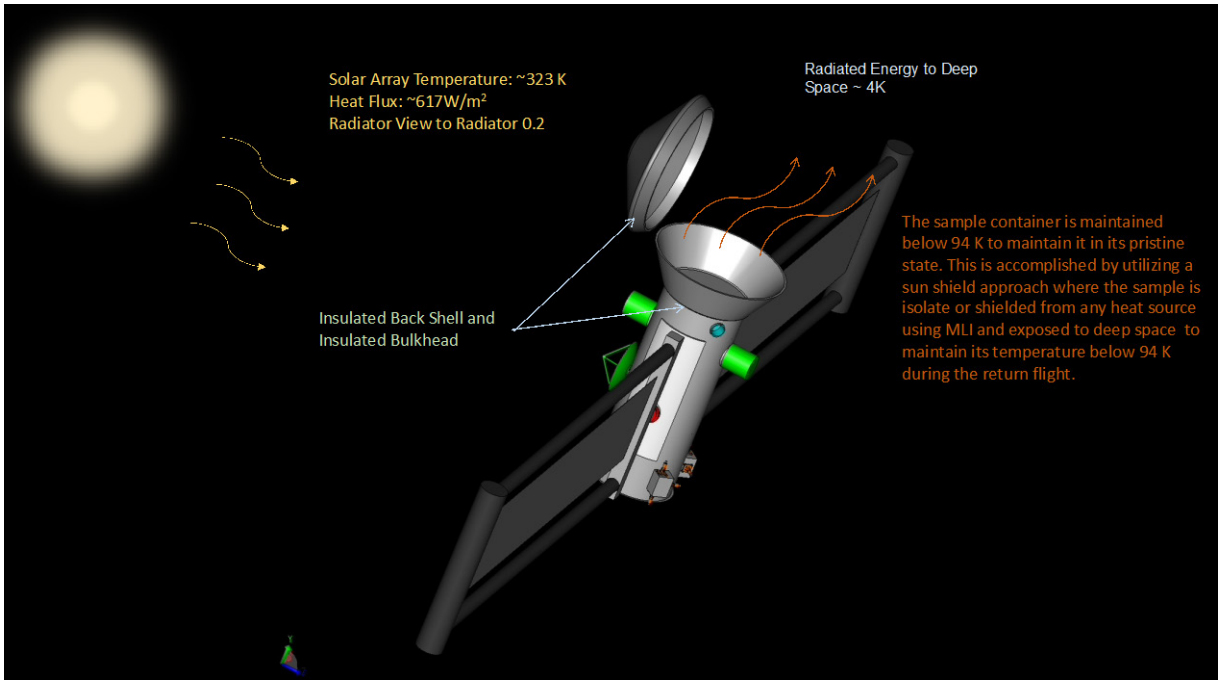

Figure 4.41.—Illustration of the Return Container Sun Shield by the Aeroshell for Return to Earth.

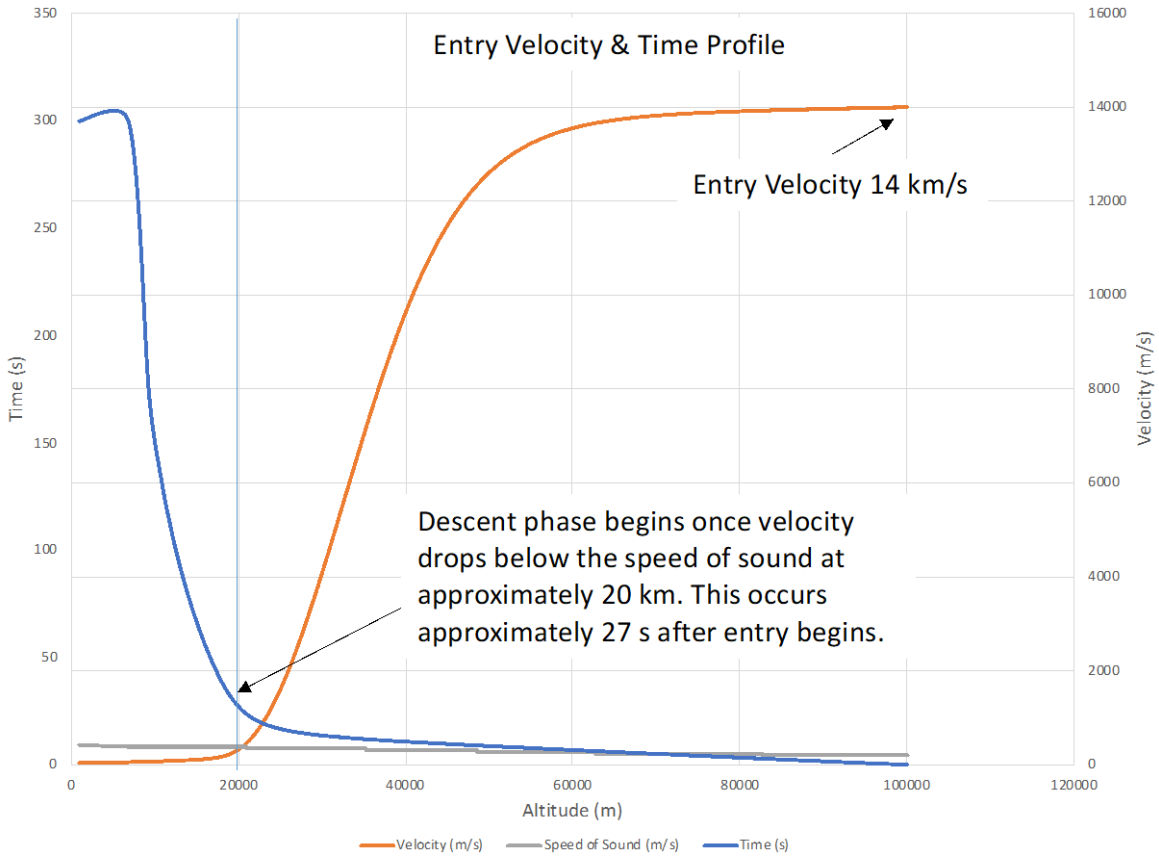

Figure 4.42.—Return Capsule Earth Entry Velocity and Time Profile.

Figure 4.43.—Stardust Aeroshell and Heat Shield After Earth Entry.

The heat shield for the entry capsule was also scaled from the Stardust and similar Genesis heat shield. Figure 4.43 shows the Stardust aeroshell and heat shield after Earth entry.

The heat shield is constructed of 1.5 cm of Phenolic Impregnated Carbon Ablator (PICA) ablative insulation material with a 2.5 cm thick Ti honeycomb backing.

Because of the high entry velocity and potentially steep entry angle the loading on the aeroshell and sample container can be significant. Figure 4.44 shows the G-load on entry. This load profile shows that a peak loading of 225 g occurs at an altitude of 36.9 km 11.5 s after entry into the atmosphere.

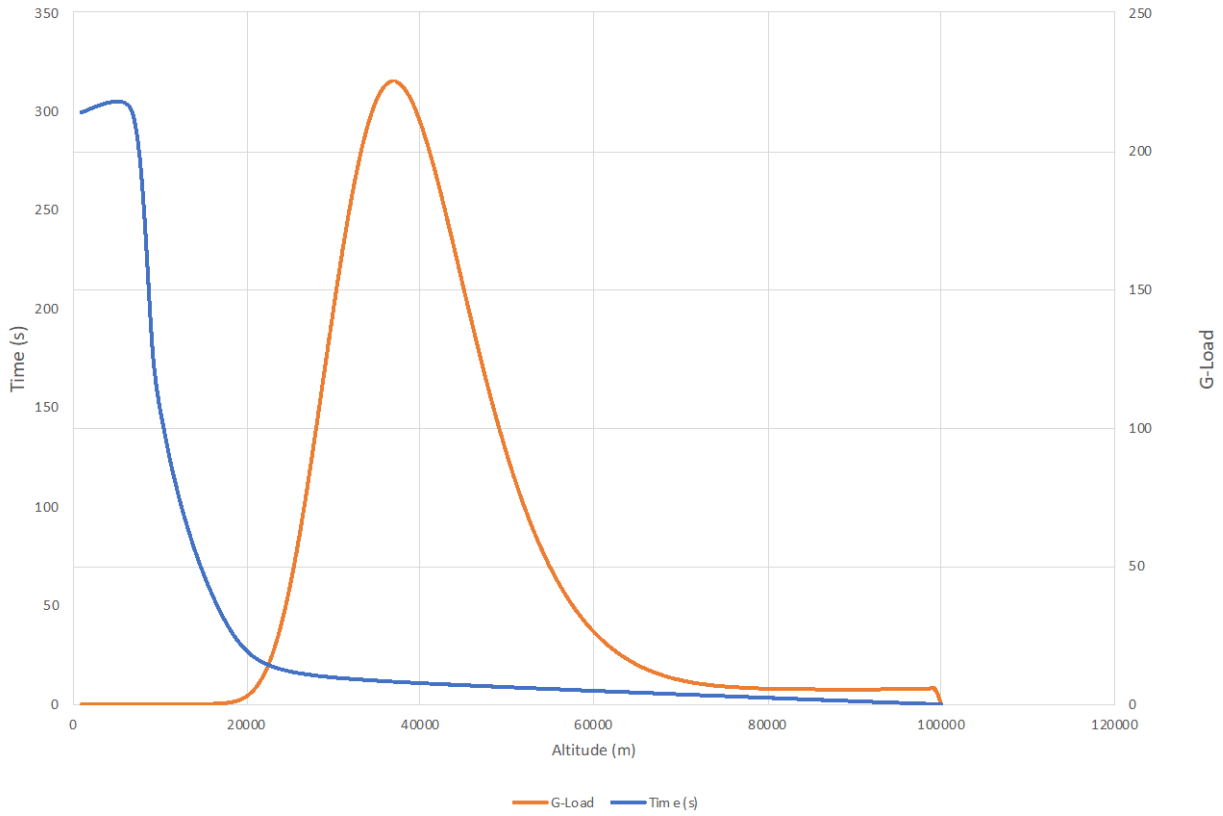

Figure 4.44.—Entry G-Load as a Function of Altitude.

Figure 4.45 shows the corresponding drag load and heat generation. The maximum heat produced occurs before the maximum drag load. This is due to a combination of the entry velocity profile and atmospheric density. It should be noted that the heat generated represents the total heat load produced due to the slowing of the aeroshell during entry. This heat load is not all absorbed by the heat shield. A majority of the heat produced goes into heating the air surrounding the aeroshell.

It is assumed that the entry begins at an angle of 25°. From Figure 4.46, subsonic velocity is achieved at 20 km altitude with a descent angle of 49°. The descent angle reaches 90° at an altitude of approximately 9 km. This is the point where all the entry horizontal velocity from entry is dissipated. Figure 4.46 shows the entry angle during descent.

Once subsonic descent is achieved at approximately 20 km the free fall portion of the descent begins. At an altitude of 2 km the parachute is opened for the final descent to the surface. Opening the parachute at a low altitude is beneficial since it will speed the descent to the surface and minimize the time for sample recovery. The total descent time for this portion of the entry is 18 min 24 s. The impact velocity when the entry capsule strikes the surface is 2.3 m/s. Figure 4.47 shows the final descent profile.

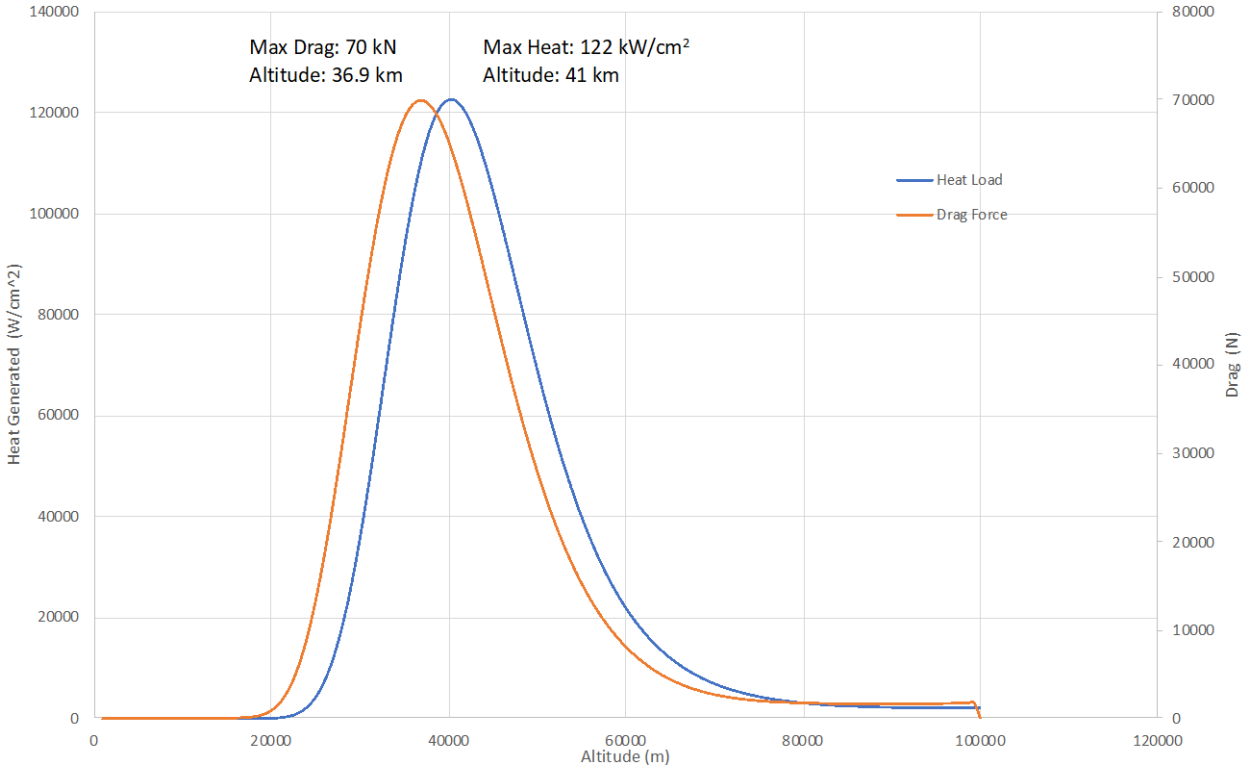

Figure 4.45.—Drag and Heat Load During Entry.

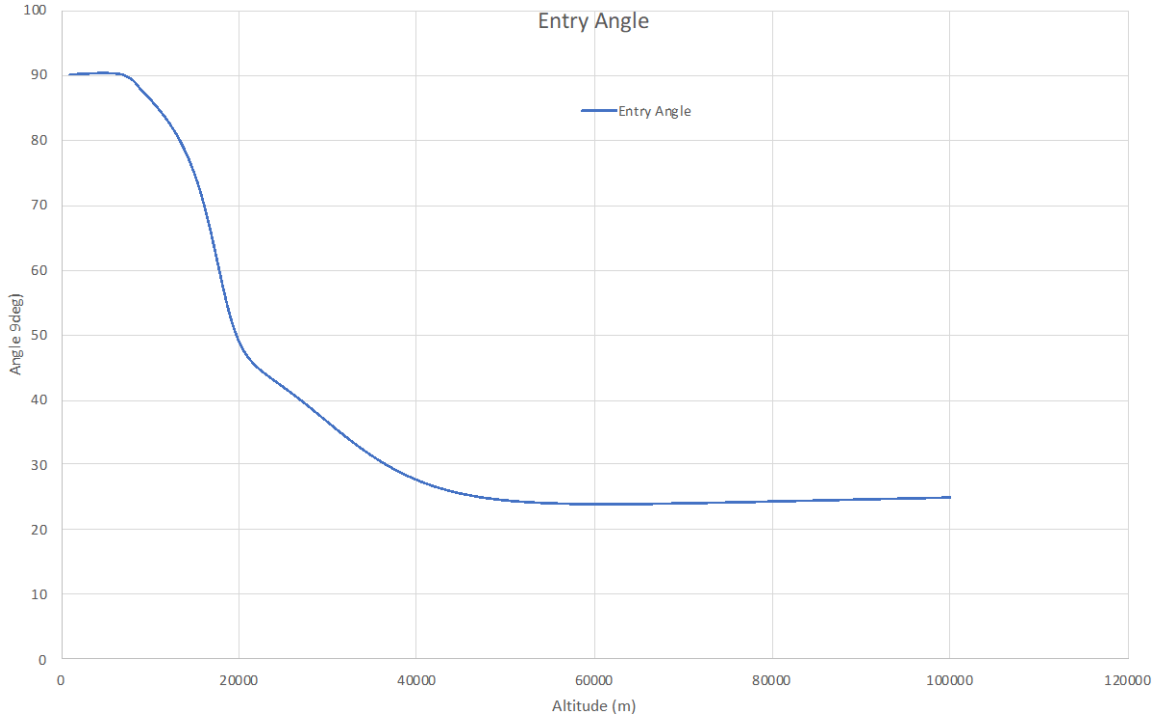

Figure 4.46.—Entry Descent Angle.

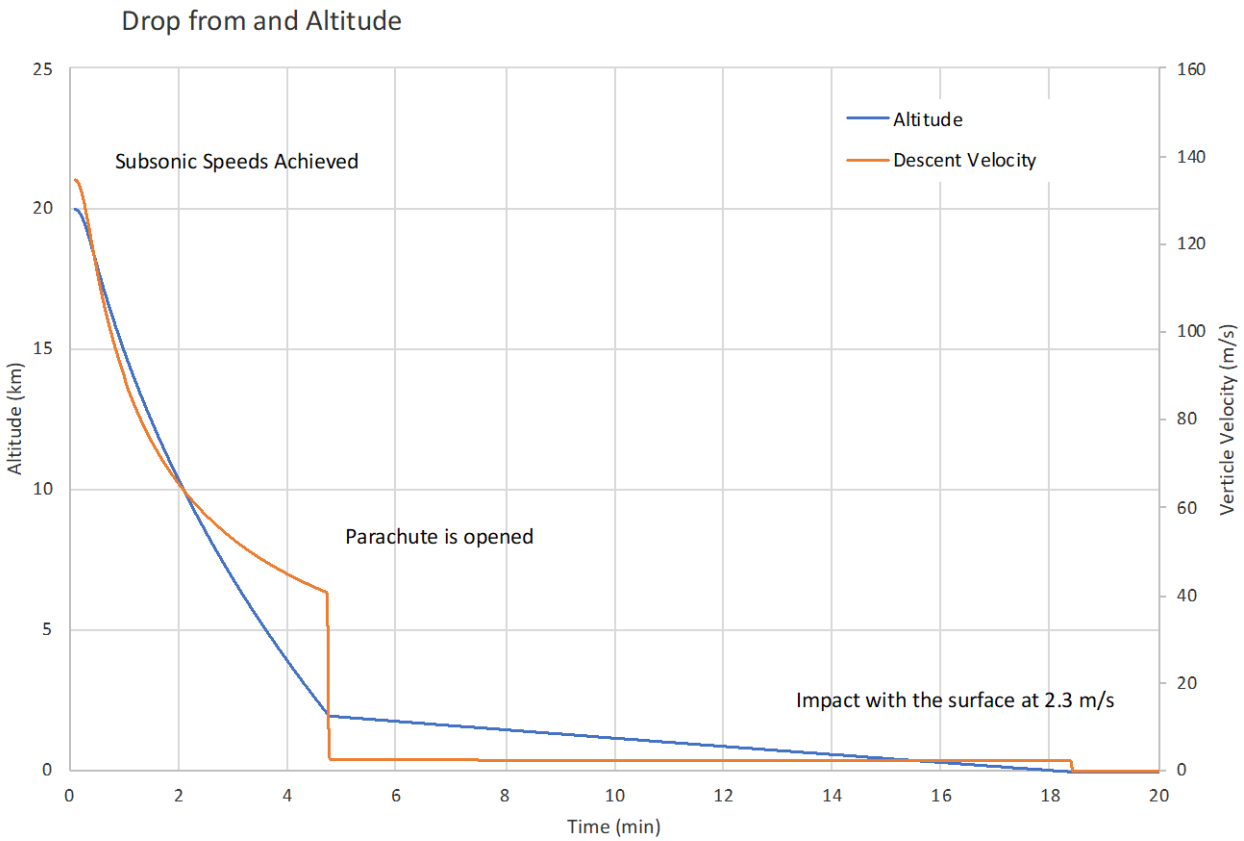

Figure 4.47.—Final Descent Velocity and Time Profile.

The total entry timeline from closing the aeroshell to impact on the surface is 64 min 18 s. Figure 4.48 illustrates this timeline.

The amount of LOx stored within the sample container must be sufficient to sustain the internal temperature of the sample at 94 K during this time plus additional time for recovery and stowage of the sample container in a cryogenic chamber. The sample container was sized to hold 1 kg of LOx, which has a heat of vaporization of 213 kJ/kg. Table 4.49 gives the heat leak and subsequent mass of LOx boiloff during the entry and descent process. The LOx consumption shows that 1 kg of LOx would provide sufficient cooling during entry and descent and provide up to 9 h for recovery and storage within a cryogenic chamber. This provides considerable amount of margin to the entry process and should ensure that the sample is maintained at the desired 94 K temperature until recovered for analysis.

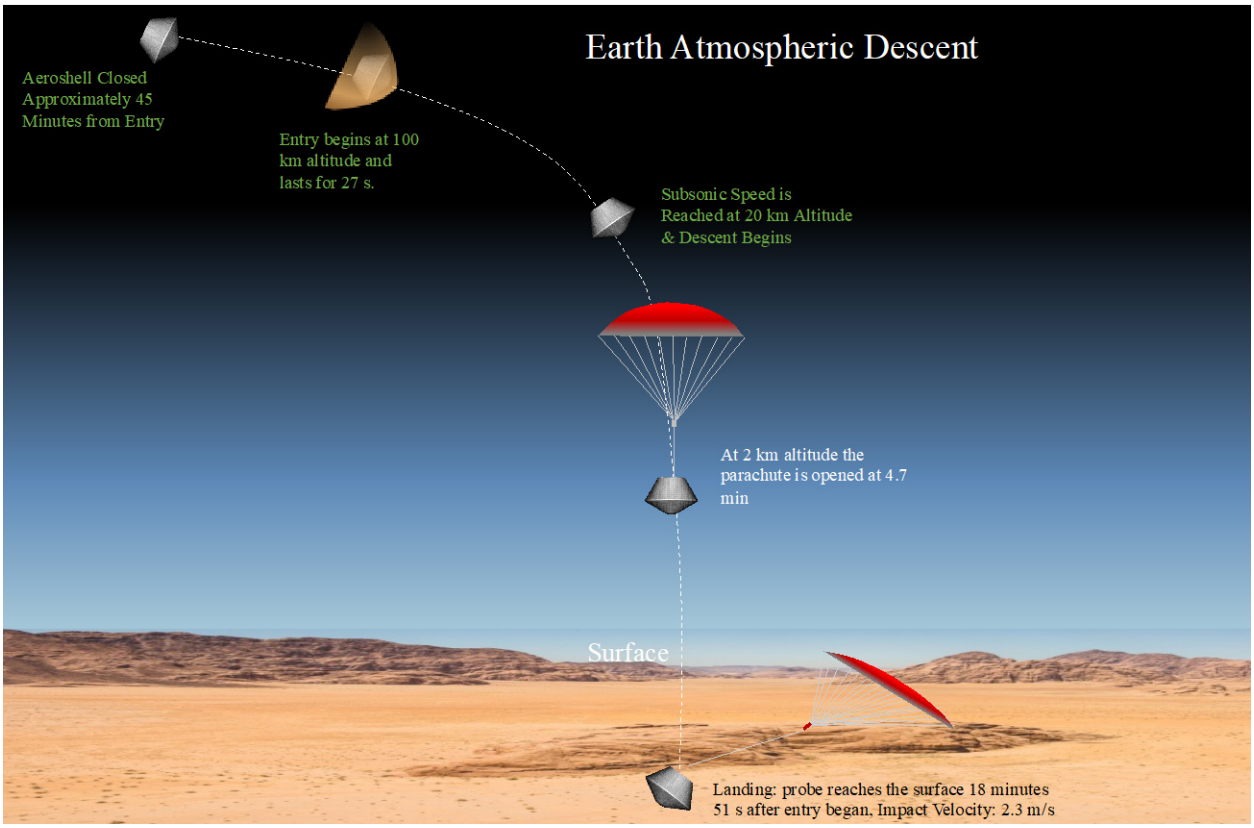

Figure 4.48.—Entry and Descent Timeline.

TABLE 4.49.—LOx CONSUMPTION DURING ENTRY AND PRIOR TO RECOVERY

Entry Event	Heat Leak into Sample Container (W)	Duration	Energy Required (J)	LOx Consumed (kg)
Closing of Aeroshell To Beginning Entry	3.27	45 m	8829	0.04
Entry	34	27 s	918	0.004
Descent	5.3	18 m 51 s	5994	0.03
On Surface	6.1	Up to 9 h	197,640	0.93

4.7.4 Master Equipment List

Table 4.50 to Table 4.55 are the Return Spacecraft and Launch Vehicle Thermal Control MELs.

TABLE 4.50.—THERMAL CONTROL SYSTEM – RETURN VEHICLE MEL

Description Case 1_Titan_Sample_Return CD-2021-186	QTY	Unit Mass	Basic Mass	Growth	Growth	Total Mass
Thermal Control (Non-Propellant)			**17.1**	**18%**	**3.1**	**20.2**
Active Thermal Control			**1.2**	**18%**	**0.2**	**1.4**
Heaters	6	0.1	0.3	18%	0.1	0.4
Thermocouples	6	0.0	0.1	18%	0.0	0.1
Data Acquisition	1	0.3	0.3	18%	0.0	0.3
Switches	6	0.1	0.6	18%	0.1	0.7
Passive Thermal Control			**10.9**	**18%**	**2.0**	**12.9**
MLI Insulation	1	6.1	6.1	18%	1.1	7.1
Electronics Cold Plates	6	0.1	0.8	18%	0.1	1.0
Electronics Heat pipes	12	0.1	1.1	18%	0.2	1.3
thermal paint	1	0.6	0.6	18%	0.1	0.7
Mass Spacecraft Bukhead MLI	2	1.2	2.4	18%	0.4	2.8
Semi-Passive Thermal Control			**4.9**	**18%**	**0.9**	**5.8**
Electronics Radiator	1	3.1	3.1	18%	0.6	3.7
Radiator Louvers	1	1.8	1.8	18%	0.3	2.1

TABLE 4.51.—THERMAL CONTROL SYSTEM – RETURN VEHICLE SAMPLE CAPSULE MEL

Description Case 1_Titan_Sample_Return CD-2021-186	QTY	Unit Mass	Basic Mass	Growth	Growth	Total Mass
Thermal Control (Non-Propellant)			**45.5**	**18%**	**8.2**	**53.7**
Active Thermal Control			**20.2**	**18%**	**3.6**	**23.9**
Parachute	1	4.3	4.3	18%	0.8	5.0
Avionics	1	4.5	4.5	18%	0.8	5.3
Mechanisms	1	11.4	11.4	18%	2.1	13.5
Passive Thermal Control			**25.3**	**18%**	**4.6**	**29.8**
Container Insulation	1	0.4	0.4	18%	0.1	0.4
Aerroshell Support Structure	1	0.3	0.3	18%	0.1	0.4
Aeroshell Thermal Paint	1	0.2	0.2	18%	0.0	0.3
Entry Heat Shield	1	14.7	14.7	18%	2.7	17.4
Backshell	1	4.3	4.3	18%	0.8	5.0
Aeroshell MLI	1	2.8	2.8	18%	0.5	3.3
LOX	1	1.0	1.0	18%	0.2	1.2
Sample Container	1	1.6	1.6	18%	0.3	1.8

TABLE 4.52.—THERMAL CONTROL SYSTEM – IN-SPACE STAGE MEL

Description Case 1_TSR_Launch_Vehicle CD-2021-186c	QTY	Unit Mass	Basic Mass	Growth	Growth	Total Mass
Thermal Control (Non-Propellant)			**4.7**	**18%**	**0.8**	**5.5**
Passive Thermal Control			**4.7**	**18%**	**0.8**	**5.5**
MLI Insulation	1	2.3	2.3	18%	0.4	2.7
Engine MLI	1	2.3	2.3	18%	0.4	2.7
RHU	4	0.0	0.2	18%	0.0	0.2

TABLE 4.53.—THERMAL CONTROL SYSTEM – UPPER ATMOSPHERE STAGE MEL

Description Case 1_TSR_Launch_Vehicle CD-2021-186c	QTY	Unit Mass	Basic Mass	Growth	Growth	Total Mass
Thermal Control (Non-Propellant)			**2.5**	**18%**	**0.5**	**3.0**
Passive Thermal Control			**2.5**	**18%**	**0.5**	**3.0**
Cable	1	2.5	2.5	18%	0.5	3.0

TABLE 4.54.—THERMAL CONTROL SYSTEM - 1ST STAGE MEL

Description Case 1_TSR_Launch_Vehicle CD-2021-186c	QTY	Unit Mass	Basic Mass	Growth	Growth	Total Mass
Thermal Control (Non-Propellant)			**2.5**	**18%**	**0.5**	**3.0**
Passive Thermal Control			**2.5**	**18%**	**0.5**	**3.0**
Cabling	1	2.5	2.5	18%	0.5	3.0

TABLE 4.55.—THERMAL CONTROL SYSTEM – EDL MEL

Description Case 1_TSR_Propellant_Processing CD-2021-186b	QTY	Unit Mass	Basic Mass	Growth	Growth	Total Mass
Thermal Control (Non-Propellant)			**18.0**	**18%**	**3.2**	**21.2**
Active Thermal Control			**18.0**	**18%**	**3.2**	**21.2**
Parachute	1	18.0	18.0	18%	3.2	21.2

4.8 Command and Data Handling

The TISR C&DH subsystem is responsible for the general avionics, command and control, and health management of the spacecraft. All components used within this analysis are based on military/space rated commercially available products from verified aerospace vendors. These components are all TRL 6-7 to account for the long duration and low-power requirements of the mission. Included in this assessment are the preliminary study requirements, system assumptions, analytical methods used, design and recommendations in the MEL.

4.8.1 System Requirements

The TISR C&DH baseline study requirements are as follows:

1. All avionics equipment, including flight computers, memory units, IO interface boards, motor drivers and actuators, other control units and harnessing shall be rated for 100 kRad total ionizing dose (TID) and have single event upset (SEU)/Single Event Functional Interrupt (SEFI) detection and reset for the duration of the mission.
    a. *Rationale:* The Avionics equipment will be exposed to external space and internal RPS radiation sources. The enclosures will dampen but not eliminate the radiation exposure to the devices.
2. All Avionics equipment in this study shall be single fault tolerant with cold backups.
    a. *Rationale:* In the event an SEU/SEFI or an unrecoverable anomaly occurs in the Avionics system, backups are necessary to safely maintain nominal operations during the mission.
3. Avionics shall provide command, control, and health management to the TISR return vehicle.

4.8.2 System Assumptions

The TISR C&DH baseline study assumptions are as follows:

1. TISR C&DH system for Propellant Processing system not designed for this run. A representative processing model from the Titan Fission Lander study was selected.
2. All non-COTS hardware is rated for 100k TID.
3. Flight computer and interface cards are customized for low-power modes.
4. Command and control of the GN&C system is handled by the GN&C subsystems with interfaces to the C&DH system.
5. Power requirements for motor drivers and actuators.
6. Data budgets and software requirements.
7. 100 percent wire mass growth and 30 percent equipment growth used based on the AIAA guidelines.
8. Waste heat from driving the motors and actuators was considered negligible to average power consumption. This is justified by the long timeframes of the power modes and the infrequent use of the motors.
9. 3U form-factor compact Peripheral Component Interconnect (cPCI) compatible system assumed for consistent avionics.

4.8.3 System Trades

There were no specific C&DH system trades for this design.

4.8.4 Analytical Methods

A suite of avionics software was used to estimate the mass and power usage of the C&DH system. This suite contains a motor driver mass/power estimator, an avionics enclosure dimension/mass estimator and a wire harnessing mass estimator. Each of these tools are described and results are given in the following sections.

The TISR C&DH study analytical methods are detailed in the following two sections.

4.8.4.1 Motor Driver Estimation

The motor drivers were estimated by separately calculating the waste heat and area of each form-factor printed circuit board (PCB), using Moog's servo motor controller (Ref. 62). The waste heat is calculated from Equation (22):

$$\text{Waste Heat} = \frac{\text{Motor Power}}{\text{Driver Power Supplied}} * \text{driver dissipation} * \text{motor count} \tag{22}$$

The area required by the PCB is similar to the waste heat calculation:

$$\text{Area} = \frac{\text{Motor Power}}{\text{Driver Power Supplied}} * \text{area per channel} * \frac{\text{motor count}}{100} \tag{23}$$

The area required is then used to calculate the 3U cPCI card count. Table 4.56 shows an example result.

4.8.4.2 Wire Harnessing Estimation

A Monte Carlo method-based software estimation tool was used to estimate the mass of the wiring required to interface between the peripherals of the TISR return vehicle and the avionics box. The Monte Carlo method is used for drawing a sample at random from an empirical distribution. The method then performs an unbiased risk analysis by creating a model of possible solutions around a probability distribution. As applied to a wire mass simulation, the Monte Carlo method is used for drawing a random length of wire from a distribution between estimated minimum and maximum wire lengths. The mean-value Monte Carlo method is used in this analysis to determine wire mass and is represented in Equation (24).

$$\hat{\theta} = \frac{1}{B} * \sum_{b=1}^{B} f(u_b) \tag{24}$$

In this equation, $\hat{\theta}$ represents the solution for the mass of the wire harness, B is the number of samples, and the function $\sum_{b=1}^{B} f(u_b)$ represents the summation of the samples in the distribution. Table 4.57 shows an example run.

TABLE 4.56.—RETURN VEHICLE MOTOR DRIVER ESTIMATION EXAMPLE

Actuator Name	Peak Power/Actuator	Num Actuators	Waste Heat	PCB Area Required (cm^2)	Mass Required (kg)	Num 3U cPCI Required	Total 3U cPCI
RCS Valves	28	15	16.5	240.0	0.8	1.5	3
Solar Array Gimbals	4.5	2	0.4	5.1	0.0	0.032142857	
ROSA Frangibolts	30	4	4.7	68.6	0.2	0.428571429	

TABLE 4.57.—RETURN VEHICLE WIRE HARNESSING 1 RUN MONTE CARLO EXAMPLE

Unit	Wire Protocol	kg/m	No. cables	Min Length (m)	Max Length (m)	Run1
RCS Valves	22 AWG	0.0035	36	1	5	0.53
Solar Array Gimbals	24 AWG	0.0022	6	1	5	0.06
ROSA Frangibolts	22 AWG	0.0035	12	1	5	0.07
Sensors	26 AWG	0.0015	50	1	5	0.16
MIL-STD-1553	Twinax 28 AWG	0.058	2	1	5	0.57

4.8.5 Risk Inputs

Risk Statement: The radiation environment external to the TISR vehicle may cause single event effects (SEEs) on electronics as well as long-term damage from ionizing doses of radiation. Due to single-fault tolerant electronics, there is a low risk of an SEU interrupting critical operations.

Mitigation Strategy: For long-term damage from ionizing doses, select parts with a TID tolerance > 100 kRad. For SEUs, combine multiple mitigation techniques such as triple mode redundancy (TMR) with voting in code, error detection and correction (EDAC), hardened memory cells and data scrubbing.

4.8.6 System Design

The C&DH avionics packages are designed around the AiTech SP0 single board computer (SBC) (Ref. 63) and adhere to single-fault tolerant requirements. Each computer is responsible for the C&DH of all subsystems including most actuator controllers, and the avionics package contains a standard IO interface card and motor drivers. Each unit attached to the cPCI backplane adheres to the 3U avionics card size standard, and the cPCI handles all DC-to-DC power conversion required by the avionics package. Each SP0 SBC operates with 8 GB of storage, which will contain the real time operating system (RTOS), C&DH specific flight software and any emergency backup storage required. All components are radiation tolerant up to 100k TID.

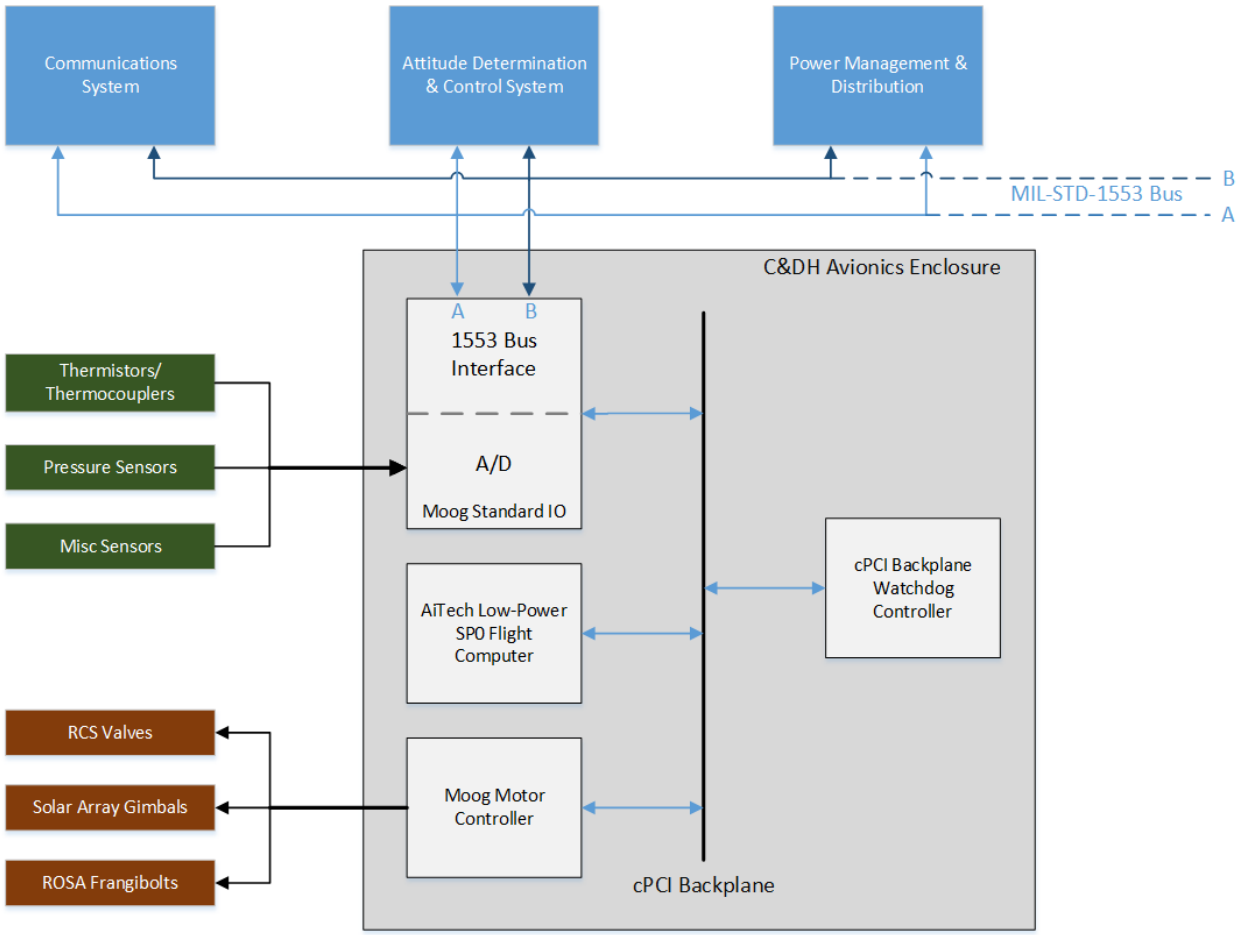

Figure 4.49.—Return Vehicle Avionics Enclosure block diagram.

The spacecraft will utilize the MIL-STD-1553 redundant communication standard (Ref. 64) for all digital interfaces. The cPCI backplane will provide the cold back switch control in the event of primary equipment failure. This will also be responsible for powering down unnecessary equipment during low-power modes.

The following list is comprised of the main avionics components as input to the MEL shown in Table 4.58.

- AiTech SP0 main computers (Ref. 63)
- Moog standard (SMOAB) IO cards (Ref. 49)
- Moog actuator controller cards (Ref. 49)
- Avionics enclosure
  - Includes watchdog controller for cold backup switching.
- Wire harnessing
- 200k software lines of code (SLoC)

4.8.7 Recommendation(s)

The TISR C&DH Compass Team recommends the following improvements to the study:

- Estimation of software lines of code is based on legacy flight missions and previous studies. Software requirements will have changed, and a newer analysis will likely provide a different estimate.

4.8.8 Master Equipment List

The C&DH MELs are in Table 4.58 and Table 4.59 (note that the second MEL was taken from a previous study and was not designed specifically for this mission).

TABLE 4.58.—COMMAND AND DATA HANDLING – RETURN VEHICLE MEL

Description Case 1_Titan_Sample_Return CD-2021-186	QTY	Unit Mass	Basic Mass	Growth	Growth	Total Mass
Command & Data Handling			**9.4**	**47%**	**4.5**	**13.9**
C&DH Hardware			**8.3**	**40%**	**3.4**	**11.7**
Custom AiTech SP0 SBC	2	0.4	0.8	30%	0.2	1.0
Moog SMOAB Standard IO	2	0.4	0.8	30%	0.2	1.0
Moog Motor Controller	6	0.4	2.4	30%	0.7	3.1
Avionics Enclosure	1	4.3	4.3	50%	2.2	6.5
Instrumentation & Wiring			**1.1**	**100%**	**1.1**	**2.2**
Harnessing	1	1.1	1.1	100%	1.1	2.2

TABLE 4.59.—COMMAND AND DATA HANDLING – PROPELLANT PROCESSING LANDER MEL

Description Case 1_TSR_Propellant_Processing CD-2021-186b	QTY	Unit Mass	Basic Mass	Growth	Growth	Total Mass
Command & Data Handling			16.8	32%	5.3	22.1
C&DH Hardware			14.8	32%	4.7	19.5
Processor Board	2	1.0	2.0	30%	0.6	2.6
Time Generation Unit	1	0.5	0.5	30%	0.2	0.7
Command and Control Harness (data)	1	3.0	3.0	50%	1.5	4.5
cPCI enclosure with power supply	1	3.0	3.0	20%	0.6	3.6
Valve Drivers	2	1.4	2.8	30%	0.8	3.6
Separation Drivers	1	1.5	1.5	30%	0.5	2.0
Additional shielding	1	2.0	2.0	30%	0.6	2.6
Instrumentation & Wiring			2.0	30%	0.6	2.6
AD/DA/SDI card	2	0.5	1.0	30%	0.3	1.3
Pressure and Temperature sensors	20	0.1	1.0	30%	0.3	1.3

4.9 Attitude Determination and Control System (AD&CS)

This section will focus on launch from Titan, the return flight from Titan to Earth, and Earth EDL. The gathering of material necessary to process the propellant used to depart Titan and return to Earth is conducted by a rover notionally based on conceptual lunar rovers with semi-autonomous capabilities.

4.9.1 System Requirements

The AD&CS system must be capable of providing an estimate of the vehicle's state (translation and attitude), determining the vehicle attitude based on multiple attitude constraints, and actuating the control necessary to achieve both the commanded attitude and perform Delta Vs (ΔV) computed by Mission Design. Throughout, it is important that the AD&CS system be at least single fault tolerant. The driving requirements for the AD&CS system are:

- Mitigating environmental torques on the various spacecraft involved with the sample return effort
- Pointing accuracy for the return vehicle (RV), when attached to the in-space stage or independently, of ±1° for power gathering purposes
- Maintain spin-stabilization of the RV post separation from the in-space stage until sample deploy.

4.9.2 System Assumptions

The analysis and design of the AD&CS system is valid given the following assumptions:

- The launch procedure occurs at a time when wind in the atmosphere, especially near altitudes where first stage separation takes place, are near their expected values
- Thruster off-pointing errors are negligible
- The TVC systems in the first and second stages can articulate quickly enough to mitigate wind gust torques
- Tracking, state updates, and burn plans are provided to the RV prior to burns
- The distribution of components within the RV can be altered from the notional layout shown to better accommodate spin-stabilization about the geometrically selected body frame.

4.9.2.1 Sensors

Some of the common AD&CS sensors used during flight (including EDL) are IMUs, star trackers, Sun sensors, acceleration switches, and proximity sensors (e.g., radar, lidar, imaging, etc.). Due to power constraints and the assumed availability of the deep space network (DSN) prior to critical events, IMUs, star trackers, Sun sensors, and acceleration switches are the only AD&CS sensors proposed for this design.

The launch phase up to the jettison of the payload fairing is a canned sequence which relies of the active RV IMU for attitude rate measurements. Once the fairing is jettisoned and the atmosphere is tenuous, the RV star trackers become available for precise inertial attitude measurements.

The current sensor suite on board the RV provides the capability for closed-loop attitude (including rate and acceleration) AD&CS through the utilization two IMU 3-axis gyros and two-star trackers. Additionally, burn performance can be estimated via the IMU accelerometers. Beyond the fault tolerance afforded by redundant sensors, contingency situations can be managed using the six Sun sensors and coarse Sun direction measurements inferred from the solar panel output.

Translational state estimates of the in-space stage and the RV, once separated, are conducted on the ground via DSN tracking measurements. Burn plans are prepared on the ground and uplinked to the RV prior to planned burn events. The burn is executed via open-loop control based on parameters contained within the burn plan.

4.9.2.2 Active Attitude Control

The current design has resulted in a vehicle that is very sensitive to mass on the return from Titan. Additionally, Titan's distance from the Sun results in power constraints. Independently, the mass or power constraints would be enough to rule out reaction wheels or control moment gyros (CMG); therefore, the two constraints together make a strong argument for an attitude control system (ACS) that is integrated with the primary ΔV system. Reaction wheels and CMGs are also not ideal for the long coast phases in the mission design when the spacecraft is in a sleep state since the spinning components of the actuators will eventually come to a stop due to internal friction if their spin-rates are not actively being maintained.

The TVC systems on-board the first stage acts as the sole means of active attitude control prior to first stage separation. The two dual-axis gimbals can provide attitude control about all three body axes. The second stage contains a single dual axis gimballed TVC system which can provide control about two body axes. Rotation about the length of the second stage is uncontrolled prior to fairing jettison but assumed to be small based on symmetry of the vehicle and aerodynamic drag resisting such motion.

The RCS system on-board the RV can be utilized as soon as the fairing is jettisoned. Nominally, it is only used for attitude control about the length of the stage prior to second stage separation. Once the in-space stage phase begins, a combination of RV RCS and in-space stage main engine pulsing is used for attitude control. Primarily, pulsing of the in-space stage engines will be done to maintain a desired burn attitude during the Titan flyby sequence and powered Saturn flyby. Table 4.60 provides information on the expected torque available from Titan launch through RV deployment.

TABLE 4.60.—EXPECTED TORQUE RANGES FOR VARIOUS CONFIGURATIONS AND PROPELLANT FILL LEVELS

Config	Fill Level	Mass	CG Of Stack			Approx Max TVC Torque			RCS Torque Ranges		
			x	y	z	x	y	z	x	y	z
	%	kg	m	m	m	Nm	Nm	Nm	Nm	Nm	Nm
1S-2S-3S	100%	3745.00	0.00	4.89	0.000	6793.00	305.00	6793.00	---	---	---
1S-2S-3S	0%	2565.00	0.00	6.36	0.000	8835.00	305.00	8835.00	---	---	---
2S-3S	100%	2360.00	0.00	6.76	0.000	7043.00	---	7043.00	---	---	---
2S-3S	0%	890.00	0.00	8.51	0.000	8869.00	---	8868.00	---	[-1 1]	---
3S	100%	698.00	-0.01	9.29	0.000	---	---	---	[-100 100]	[-1 1]	[-65 65]
3S	0%	382.00	-0.01	9.91	0.010	---	---	---	[-85 85]	[-1 1]	[-62 62]

In terms of configurations, 1-S is short for first stage, 2-S is short for second stage, and 3-S is short for in-space stage. All configurations include the RV. The location of the center of gravity (CG) is relative to a body frame fixed to the center of the flat plate at the bottom of the first stage as seen in Figure 4.50.

TVC torques assume the first and second stage engines can be gimballed in either direction by 10°. Furthermore, the amount of thrust available is assumed to be 4000 N per engine for the first stage and 6000 N for the second stage. It is not expected the engines will be immediately throttled up to attain a higher torque as they are more so calibrated to perform the ascent as detailed in the mission design.

The RCS torque ranges are determined by examining the torque generated by firing all unique combinations of four separate thrusters at the same time. Figure 4.51 and Figure 4.52 show a graphical representation of torque envelopes for the in-space stage as well as the RV for full fill levels.

The component values shown in Figure 4.51 and Figure 4.52 are with respect to the coordinate frame shown in Figure 4.50 after it has been translated to the CG of the aforementioned configurations. The black circles represent discrete torque outcomes from firing a four-engine combination. The in-space stage torque estimates assume the engines on the aft of the in-space stage can be pulsed to provide torques about the x and z axes as shown in Figure 4.50. The available torque for the in-space stage is higher in the x-axis due to the 22 N TCM thrusters on-board the RV providing torque.

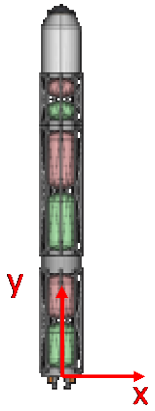

Figure 4.50.—Body-fixed analysis coordinate frame.

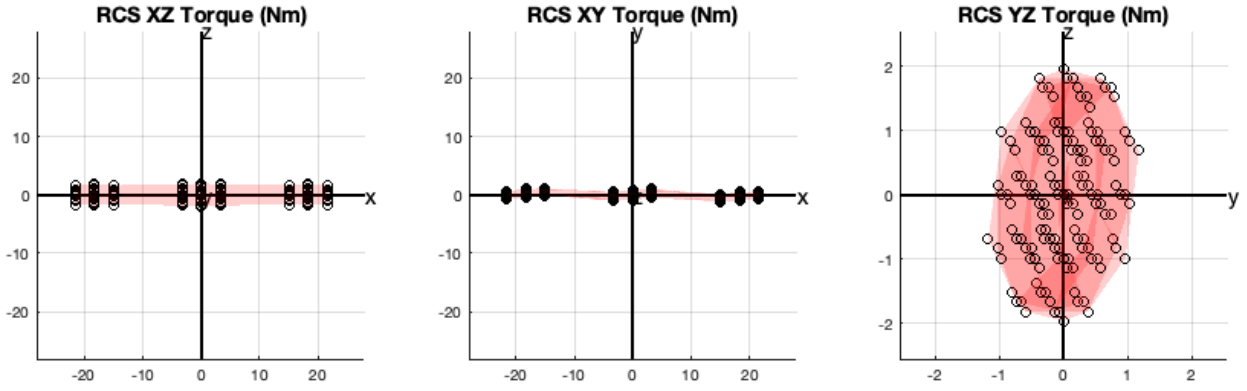

Figure 4.51.—RCS torque envelope for RV.

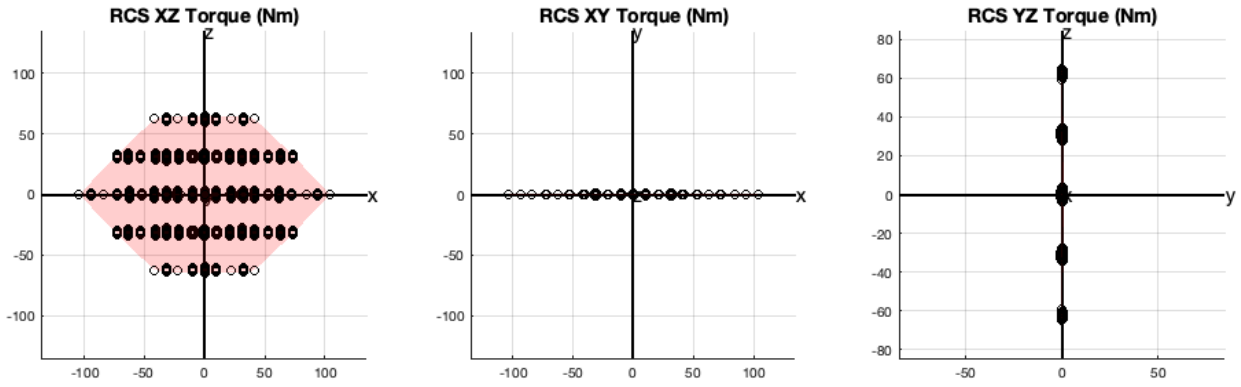

Figure 4.52.—RCS torque envelope for In-Space stage.

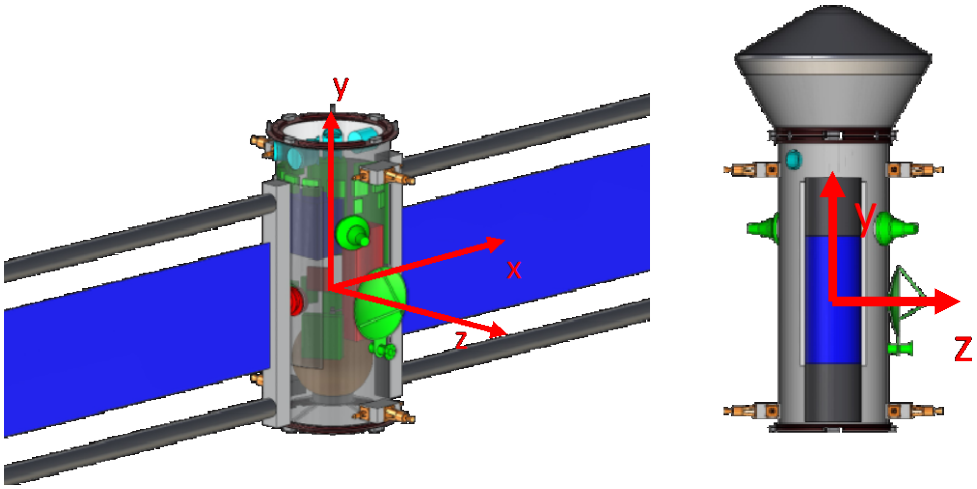

Figure 4.53.—Return Vehicle with Sensors (cyan), Antennas (green), and Thrusters (orange).

The compact size of the in-space stage and the RV, along with the typically large distance they are away from massive bodies, results in negligible gravity gradient torques. Additionally, the spin-stabilization and small projected area of the RV when in transit to Earth results in negligible solar radiation pressure disturbance torques. Conservative estimates of maintaining the attitude of each configuration are assumed when sizing the RCS propellant tank for the RV.

4.9.2.3 Passive Attitude Control

For the majority of the flight from Titan and Earth EDL, control of the vehicle will be maintained through spin stabilization. Spin stabilization of the descent capsule responsible for protecting the return sample during EDL removes the necessity for additional control mechanisms within the return capsule while maximizing the size of the sample that can be returned.

The solar panels require ±1° pointing about the axis orthogonal to the gimbal and array face axes, e.g., the y-axis for the configuration shown in Figure 4.53. Because of this tight pointing requirement and the return vehicle's estimated moment of inertia (MOI), spin stabilization for the return flight is about the z-axis as shown in Figure 4.53.

A form of passive monitoring of the RV spin axis when it is in the spin-stabilized mode is conducted using acceleration switches. Once the expected centrifugal acceleration perpendicular to the spin axis is below a certain threshold, a signal is sent to the on-board C&DH system to start up systems necessary to

assess the off-nominal condition and correct it via RCS pulsing to re-align the z-axis with the intended inertial spin axis.

4.9.3 Analytical Methods

4.9.3.1 Wind Forces During Launch

In addition to the normal challenges associated with launch, Titan winds are likely strong enough to pose a significant impact to launch vehicle dynamics both as a force pushing the launch vehicle downrange or as a torque imparted about the center of pressure. The familiar drag equation is given as

$$F_D = \frac{1}{2} r u^2 c_D A \tag{25}$$

where F_D is the force due to drag, ρ is the atmospheric density using data from Reference 65 and a tool from Reference 66, u is the wind velocity (given in Table 4.61), c_D, is the drag coefficient, and A is the vehicle surface area in the wind direction approximated from the CAD model in Section 3.3. The least straight-forward of all the values is the drag coefficient; in practice, this would likely be estimated by measuring the drag imparted on a model in a wind tunnel. While it is simple enough to approximate the launch vehicle as a rough cylinder based on the tank and return vehicle diameters, most approximations are for travel through Earth's atmosphere. It is therefore necessary to approximate the drag coefficient for the anticipated atmospheric conditions, beginning with the Reynolds number associated with the wind.

4.9.3.1.1 Estimation of Reynold's Number and Drag Coefficient

Reynold's number can be found using wind velocity (u), whetted surface area (A), and the kinematic viscosity (ν) of the atmosphere according to

$$\mathrm{Re} = \frac{uA}{\nu} \tag{26}$$

In this case, u comes from Table 4.61, A is the approximate diameter of the vehicle tanks (1.2 m), and ν is assumed to be 1/12 the kinematic viscosity of Earth's (Ref. 68) or approximately 1.2×10^{-6} m^2/s. Based on these values, the lowest value of Reynold's number associated with the slowest estimated wind speed at 20 km is 2.27×10^7 with this value only increasing with higher wind speeds. This value is sufficient since there is minimal variation in the drag coefficient with respect to flow velocity when the Reynolds number is this large.

According to Reference 69, for Reynold's numbers above 3.5×10^6, the drag coefficient of a large circular cylinder becomes constant with respect to Reynold's number. While it is well beyond the scope of this study as well as unlikely to happen due to the geometry of the launch vehicle, it should be noted that the article indicates that the flow around cylinders in Reynold's numbers this high can result in vortex shedding, which could potentially cause catastrophic loads during launch.

TABLE 4.61.—POSSIBLE ATMOSPHERIC WIND VELOCITIES (REF. 67)

	Altitude (km)								
Case	20	40	60	80	100	120	140	160	180
Low	23	26	30	31	32	32	33	34	34
Med	40	63	66	80	83	86	88	89	90
High	57	86	90	102	107	110	112	113	114

TABLE 4.62.—ESTIMATED MAXIMUM
FORCES DUE TO WIND IN NEWTONS

Wind Case	Geometry	20 km Alt	40 km Alt
Low	Before drop	3.80×10^{3}	----------
	After drop	----------	1.14×10^{3}
Med	Before drop	1.15×10^{4}	----------
	After drop	----------	6.67×10^{3}
High	Before drop	2.33×10^{4}	----------
	After drop	----------	1.24×10^{4}

4.9.3.1.2 Estimation of Force Due to Wind During Launch

It again must be noted that this analysis is very high level with a significant number of assumptions and approximations. That being said, using the above values to estimate force, the highest anticipated wind forces are expected to be experienced between 20 and 40 km. Assuming the first stage is dropped around 33 km, Table 4.62 collects the forces expected at either 20 or 40 km altitude based on the approximate surface area of the launch vehicle with and without the first stage attached for the three wind profile cases from Table 4.61.

The data provided in Table 4.62 assumes the launch vehicle is subjected to atmospheric wind gusts of magnitudes provided in Table 4.61. If these are instead sustained winds at the heights indicated, then the launch vehicle will naturally be pushed in the direction of the winds during the ascent, ultimately reducing the values shown in Table 4.62. Wind was not modelled during the ascent trajectory design; thus, the extent to which sustained wind pushes the launch vehicle and its subsequent effect on the ascent profile is unknown.

Preliminary mass properties and center of pressure (CP) estimates for the launch vehicle prior to first stage separation were calculated. This event was thought to result in the largest offset between the CG and CP during the ascent. Additionally, the vertical profile of the launch vehicle during this event and relatively high atmospheric density at 33 km was thought to result in high aerodynamic loading on the side of the launch vehicle. These factors all contribute to a high aerodynamic torque on the launch vehicle which seeks to rotate the vehicle about the x and/or z body axes.

Multiplying the forces shown in Table 4.62 by the estimated CP-CG offset of 0.78 m results in the aerodynamic torques for a vertical orientation. By comparing the aerodynamic torques to the estimated TVC torques in Table 4.60 it is clear the low fill first stage configuration would need to devote a significant fraction of the thrust vectors to mitigating a medium-case wind load. A high-case wind load is beyond the control capability of the TVC system to correct for based on the assumptions of the analysis. Additionally, there is a period lasting several seconds between first stage separation and second stage ignition. During this time, aerodynamic torques on the second stage cannot be mitigated.

With that said, an ascent profile which models sustained winds would lessen their impact.

4.9.4 Risk Inputs

Table 4.63 to Table 4.66 detail prominent risks to the AD&CS system for the various phases of the mission as well as possible mitigation strategies for those risks.

4.9.5 System Design

The attitude AD&CS is primarily driven by the pointing constraints imposed on the vehicle by different components. These components along with their proposed orientation in the body frame, their relative sensitivity to attitude, and the priority with which to point each component. It should be noted that the pointing sensitivities and the priorities in Table 4.67 are very rudimentary.

TABLE 4.63.—AD&CS RISK: TITAN LAUNCH WIND SPEEDS

Risk Title:	Titan Launch Wind Speeds						Risk Owner:	AD&C
Risk Statement:	High atmospheric density and high winds could perturb the launch vehicle							
Context:	Launch winds and wind gusts are potentially severe based on estimates and high atmospheric density. Strong gusts and high winds have the potential to affect flight path and attitude of launch vehicle while in atmosphere during launch.							
Likelihood:	2/5	Consequence Scores:						
		Safety:	3/5	Performance:	3/5	Schedule:	0/5	Cost:	0/5
Mitigation Strategy:	The lengthy propellant collection process provides ample time for multiple launches of weather balloons with the purpose of estimating upper atmospheric wind patterns near the launch site in addition to data collected by NASA's Dragonfly mission (Ref. 70). While unpredictable wind gusts pose a threat during launch, predictable sustained winds can be utilized as a tailwind and to impart torques necessary to achieve ideal launch attitudes. Ideally, the launch vehicle will have a center of pressure that is (marginally) higher on the stack than the center of gravity and the launch will occur in the direction of the prevailing winds.							

TABLE 4.64.—AD&CS RISK: TITAN ORBIT INSERTION

Risk Title:	Titan Orbit Insertion						Risk Owner:	AD&C
Risk Statement:	Errors built up during launch as well as errors in the insertion burn can result in a suboptimal orbit about Titan.							
Context:	Open-loop control of the launch vehicle through the entire ascent of an ill-defined atmosphere, canned stage separation, and an imperfect circularization burn can result in large errors to accumulate in the estimated state of the vehicle. The error accumulation could lead to a scenario in which the periapsis of the initial Titan orbit is too low; thus, it is affected by the atmosphere of Titan.							
Likelihood:	1/5	Consequence Scores:						
		Safety:	2/5	Performance:	3/5	Schedule:	0/5	Cost:	0/5
Mitigation Strategy:	Use of acceleration switches and/or the IMU to detect excessive drag half an orbit after insertion (i.e. at periapsis) can be used to trigger a safety burn at apoapsis which raises periapsis a prescribed amount. This is the only translational burn that will be done autonomously if needed.							

TABLE 4.65.—AD&CS RISK: SPIN AXIS OFFSET WOBBLE

Risk Title:	Spin Axis Offset Wobble						Risk Owner:	AD&C
Risk Statement:	The offset between the nominal spin axis (defined in the body frame) and the principal axis of inertia increases the risk of developing a wobble during spin stabilization.							
Context:	As currently modelled, the axis the Return Vehicle is spin stabilized about is roughly 15° offset from largest principal axis of inertia. Spin about the ideal body axis given the estimated mass properties would result in a coning effect about that body axis.							
Likelihood:	2/5	Consequence Scores:						
		Safety:	2/5	Performance:	3/5	Schedule:	0/5	Cost:	2/5
Mitigation Strategy:	Finer balancing of the internal components of the RV should bring the spin axis closer to the intended body axis to be spun about. Adjusting the position of the EDL Heat Shield also mitigates the offset (e.g. partially open during transit versus open 90°).							

TABLE 4.66.—AD&CS RISK: MINIMAL ATTITUDE SENSOR ON TIME

Risk Title:	Minimal Attitude Sensor On-Time						Risk Owner:	AD&C
Risk Statement:	Knowledge of the Return Vehicle attitude is only sensed prior to burns after second stage separation to reduce power consumption.							
Context:	Due to power constraints, the attitude sensors onboard the Return Vehicle cannot operate outside of the burn windows. Accumulating attitude errors may go unnoticed, which impacts sample safety, communication capability, propellant efficient, etc.							
Likelihood:	3/5	Consequence Scores:						
		Safety:	3/5	Performance:	3/5	Schedule:	0/5	Cost:	0/5
Mitigation Strategy:	Simulation and analysis should be capable of providing an upper limit to accelerations in any direction. Acceleration switches can be incorporated into the design such that they are tripped when accelerations exceed nominal levels. When tripped, the control system would assess the current attitude state using the IMUs and star trackers and correct the error trend during the in-space and spin hibernation operations.							

TABLE 4.67.—VEHICLE COMPONENTS WITH PONTING REQUIREMENTS

	Sample	Solar Arrays	X-band Helical Antenna	X-band 0.3 m MGA	Star Trackers
Constraint	Face deep space	Toward Sun	One toward Earth	Toward Earth	Not toward Sun
Orientation wrt Body Frame	Faces z-axis when open	Free rotation about x-axis	–30° rotation about x-axis from ±z-axis	–z-axis	±45° from z-axis about y-axis
Pointing Sensitivity	10s of degrees	degrees	hemispheric	degrees	10s of degrees

The thrusters are collected into four pods with each pod containing one 22 N thruster and two 1 N thrusters. Figure 4.53 shows the thruster pods locations with the 22 N thrusters pointed in the ±z-axis and the 1 N thrusters pointed into/out of the page. This configuration provides 3-axis attitude control as well as translational control in the ±z,x directions. Because the cruise spin stabilization is about the z-axis, the return vehicle does not need to be spun down for TCM burns, only precessed such that the z-axis is aligned with the inertial burn direction.

4.9.6 Recommendation(s)

The launch ascent occurs within a particularly dense atmosphere by a launch vehicle with exposed tankage and structure. It is thought this will cause substantial drag loads during attitude slews and from wind. A computational fluid dynamics (CFD) simulation of the launch using the ascent profile vehicle states and environmental conditions should be conducted to further assess this. Such a simulation would also provide valuable insight into the effect of wind-driven translation.

It was found that adjusting the angle of the Sample EDL heat shield could be used to balance the mass distribution of the RV such that the nominal spin axis coincided with the z-body axis as shown in Figure 4.53. If balancing the internal components of the RV does not provide sufficient alignment, then adjusting the angle of the EDL lid could assist.

The Star Tracker selected will need to operate while the RV is spinning at $\geq$ 5 rpm based on this design. Most COTS Star Trackers can achieve an attitude solution for slew rates on the order of degrees per second. The software of the Star Tracker may need to be adapted to handle the larger nominal rotation of the RV that is used for spin stabilization and sample capsule spin up.

TABLE 4.68.—GUIDANCE, NAVIGATION, AND CONTROL MEL

Description Case 1_Titan_Sample_Return CD-2021-186	QTY	Unit Mass	Basic Mass	Growth	Growth	Total Mass
Attitude Determination and Control			3.9	16%	0.6	4.5
Guidance, Navigation, & Control			3.9	16%	0.6	4.5
IMU	2	0.8	1.5	18%	0.3	1.8
Star Tracker	2	0.9	1.8	18%	0.3	2.1
Sun Sensors	6	0.1	0.6	3%	0.0	0.6

4.9.7 Master Equipment List

Table 4.68 is the AD&CS MEL.

4.10 Communications Subsystem

Titan in-situ sample return vehicle (RV) comm requires communications links (a) full-duplex from around Titan's space direct to Earth (DTE); (b) full-duplex from TISR return vehicle near-Earth; and (c) simplex from TISR launch vehicle comm to the Titan lander.

4.10.1 Communications Subsystem Requirements

TISR Return Vehicle Communications (Comm) Subsystem requirements are providing (a) Single Fault Tolerant full-duplex X-band comm links between Titan's space and 34/70 m DSN Earth stations; (b) single fault tolerant full-duplex X-band comm links between near-Earth and 34/70 m DSN Earth stations; and (c) zero fault tolerant simplex ultra-high frequency (UHF)-436 MHz comm link from the launch vehicle to the Titan lander.

4.10.2 Communications Subsystem Assumptions

The communications subsystem design for TISR consists of the following components:

(a) One single-fault-tolerant X-band Comm subsystem with 0.30-m outer diameter (OD) Fixed 8.3° half-power-beamwidth (HPBW) primary antenna and one circular waveguide WC-33 mm ID (inner diameter) secondary antenna (±32° HPBW) for DTE communications with DSN, as well as direct from Earth (DFE) links, simultaneously;

(b) The same Single-Fault-Tolerant *X-band Comm* Subsystem connected with two circularly polarized (CP) helical antennas (±90°EL, 360°AZ) for Near-Earth full-duplex DSN communications; and

(c) One zero-fault-tolerant UHF-436 MHz Comm Subsystem with CP (±90°EL, 0dBi) antenna capable of hemispherical coverage.

Further assumptions for TISR are a minimum DTE at 8.4 GHz data rate of 100 bps with an effective isotropic radiated power (EIRP) of 36.14 dBW via the Primary 0.3-m OD antenna at a maximum separation distance of 11.3 AU and a –3 dB atmospheric loss when choosing 99.99 percent annual link availability (ALA) at a 10°-elevation angle for the 70-m DSN facility at Goldstone, California. The assumptions for the 33 mm ID circular waveguide secondary antenna use an EIRP value of 19.4 dBW for a data rate of 2 bps.

The Compass Team is using single fault tolerant (i.e., redundant) components for communications subsystem electronics and a 3 dB link margin, which is included in the communications link for the link

budget analysis. A 3 dB link margin is typical for space design applications due to the uncertainty of the components' performance and available end-of-life (EOL) EIRP. DVB-S2 QPSK (1/4) at 10^{-7}-bit error rate (BER) modulation/coding scheme has been chosen with an implementation/coding loss of –3.5 dB.

4.10.3 Communications Subsystem Trades

(a) The parabolic dish used at 8.4 GHz is designed for three times that frequency. Because of that, if 70 percent antenna efficiency is assumed instead of 55 percent then an extra 1 dB of primary antenna gain would be realized;

(b) The impact of using 34-m vs. 70-m DSN Earth station is that (i) a 0.7-m OD reflector is needed on the launch vehicle to talk to the 34-m DSN Facility and (ii) for the near-Earth comm links, only a maximum distance of 0.66 AU could be reached instead of the required minimum of 1 AU (Figure 4.54); and

(c) If a higher data rate than 2 bps is desired through the WC-33 mm ID secondary antenna, this waveguide to coax transition piece could be replaced with a cone-feed of a 6 dB higher gain value.

4.10.4 Analytical Methods (Link Budgets)

The communications subsystem design for higher information rates is a function of the transmitted power, the atmospheric absorption (gas/cloud/rain fade) at both ends, the modulation/coding scheme, antenna pointing at both ends, depolarization, cable/waveguide loss, the distance between the two nodes, and the characteristic G/T (antenna gain/system noise temperature) and EIRP of the Earth Station.

Link budget analysis at 8.4 GHz was performed, with an available radio frequency (RF) output power level of 17 W from a solid-state power amplifier. Table 4.69 shows the best DTE information rates with variation in EIRP via the 34/70-m DSN Goldstone Facility (35.35° N latitude, –116.8833° W longitude).

Direct from Earth (DFE) data rates, since the 70-m DSN Facility is clearly the desirable ground station, should not be a problem. In fact, they are higher than the DTE rates.

TABLE 4.69.—X-BAND TITAN LINK BUDGETS (DTE AND NEAR-EARTH)

TITAN LINK BUDGET	DTE from Titan's Vicinity			NEAR EARTH	
	Xb-HGA	Xb-MGA	Xb-LGA	HELIX DTE	HELIX DTE
Carrier Frequency [GHz]	8.4	8.4	8.4	8.4	8.4
Carrier Wavelength [λ= c/f] [cm]	3.57	3.57	3.57	3.57	3.57
Available RF Power [W]	17	17	17	17	17
Available RF Power [dBW]	12.30	12.30	12.30	12.30	12.30
Tx Antenna O.D. [m]	0.7	0.3	WC-33mm ID	HELIX	HELIX
Tx-3dB Beamwidth [70λ/d] [°]	3.57	8.33	64	180	180
Tx Antenna Efficiency [%]	55	55	—	—	—
Tx Antenna Gain [dBi]	33.2	25.8	9.1	-2	-2
Transmission/Pointing Loss [dB]	-2	-2	-2	-3	-3
EIRP [dBW]	43.5	36.14	19.4	7.3	7.3
Distance [AU]	11.3			1.53	0.66
Space Path Loss [dB]	-295.5			-278.1	-270.8
Earth's Atmospheric Loss [dB]	-3.0 [99.99% Annual Link Availability, *EL* /10°]				
Depolarization [dB]	-1.00			0	
Rx Antenna Diameter [m]	34	70	70	70	34
Rx-3dB Beamwidth [70λ/d] [°]	0.07	0.04	0.04	0.04	0.07
Rx Antenna Gain [dBi]	68.24	74.09	74.09	74.09	68.24
G/T [dB/K]	54.2	61.5	61.5	61.5	54.2
DVB-S2 QPSK (1/4) @ 10^{-7} BER	102 bps	100 bps	2 bps	8 bps	8 bps
Implementation/Coding Loss [dB]	-3.5				
Link Margin [dB]	3				
	1 AU = 149,597,870 km				

4.10.5 Risk Inputs

Risk Statement: The main risk factor identified for the communications subsystem is based upon available RF power subject to atmospheric attenuation, antenna pointing, component aging, and the requirement for higher information rates; moreover, any generated plasma cloud from ionization of the gases around the vehicle may temporarily disable communications (blackout period).

Strategy: The current mitigation strategy is to increase X-band transmit power and/or primary antenna size. A longer-term solution could be to design flight hardware to overcome the bottleneck effect on downlink data rates by using a dual feed antenna such that X-band is only used to receive data for navigation and command of the spacecraft from Earth and Ka-band is only used to transmit data to Earth and/or increasing the Ka-band dish diameter with or without deployable means. (Ka-Band is only available on 34-m DSN Platforms.) Plasma-induced communications blackouts are generally of short duration.

4.10.6 Communications Subsystem Design

The subsystem design shown in Figure 4.54 consists of X-band Communications at a maximum space separation of 11.3 AU via a 0.3-m OD parabolic antenna (primary) that radiates 36.14 dBW (EIRP) towards Earth, capable of 100 bps data rate, and an open circular waveguide-to-coax adapter (secondary antenna) that radiates 19.4 dBW (EIRP) towards Earth, capable of 2 bps data rate.

For near-Earth communications with DSN two semispherical-coverage CP antennas are used at diametrically opposite sides on the spacecraft to provide omni coverage at a 1 AU distance from Earth with a minimum data rate of 8 bps.

The comm subsystem electronics are fully redundant as are the 8 A/B Single-Pole Double-Throw (SPDT) switches in the array (Table 4.69, Figure 4.54, and Figure 4.55).

For the communication link between the spacecraft and the lander the Compass Team chose 436 MHz UHF-band between CP omni antennas (0 dBic) with hemispherical coverage (Figure 4.56). With a transmit power of 1W and an EIRP of –1 dBW, at a distance of 3000 km away, a G/T of –28.4 dB/K (600 K galactic noise), the data rate is 1.02 kbps using Uncoded binary phase shift keying (BPSK) with a bit error rate (BER) of 10^{-7}, and a link margin of 3 dB.

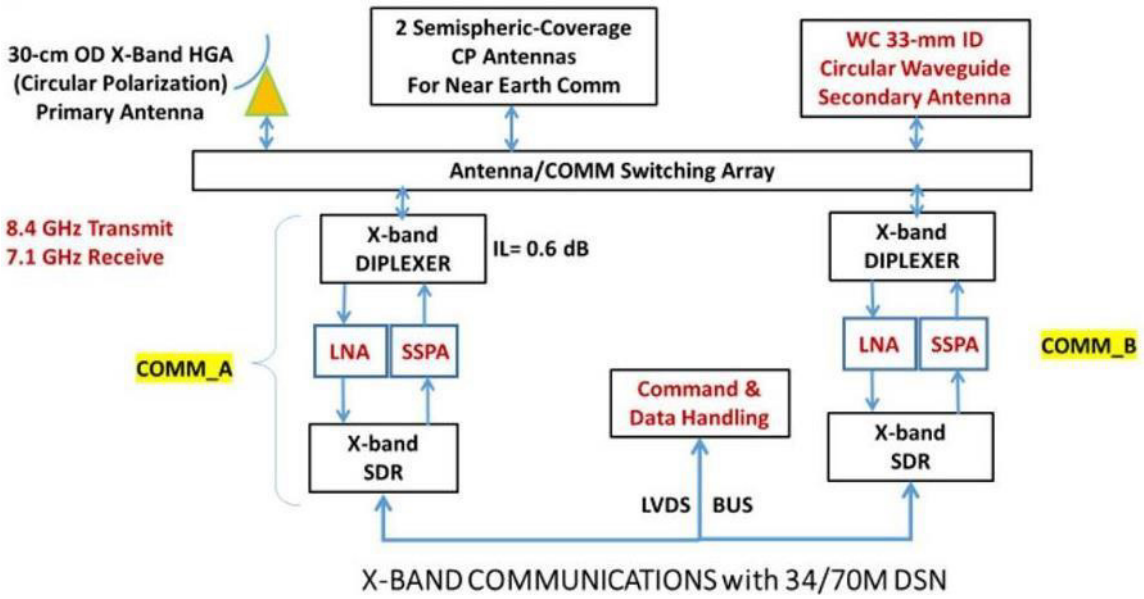

Figure 4.54.—X-band Titan Communications with DSN, including Near-Earth Comm.

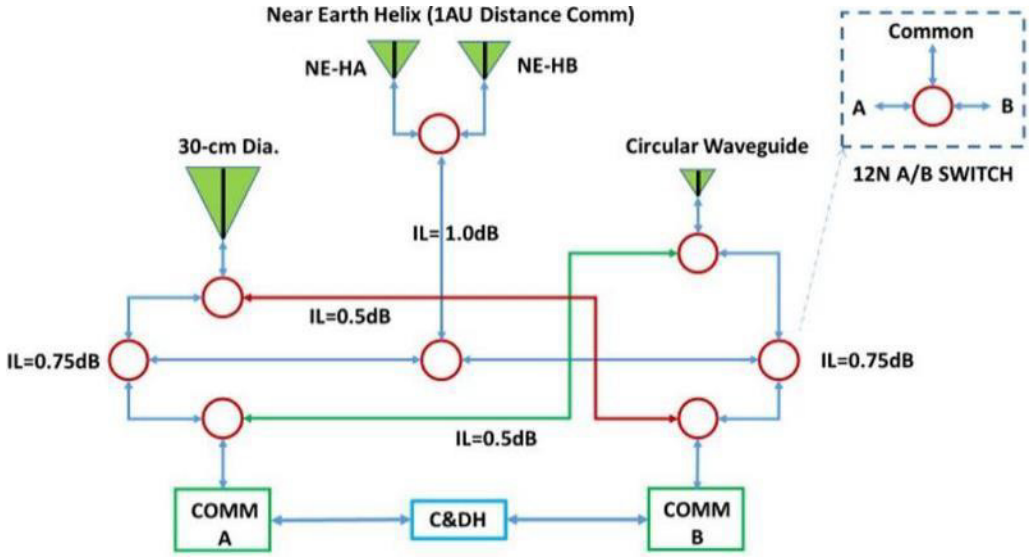

Figure 4.55.—Connecting the Antennas via A/B Switches to Redundant COMM Boxes.

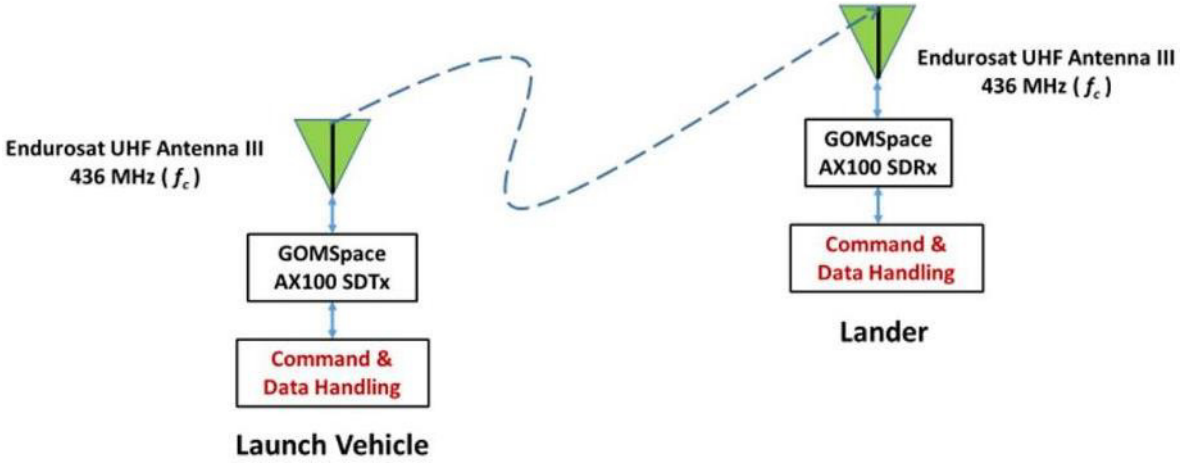

Figure 4.56.—UHF-band Spacecraft to Lander, Hemispherical Coverage.

4.10.7 Recommendations

If higher data rates of return to Earth are desired and/or the 70-m DSN X-Band Facility somehow is not available, using a dual-feed Ka-band antenna system for X-band DFE, Ka-band DTE, and/or increasing the Ka-band dish diameter and size of Traveling Wave Tube Amplifier (TWTA) can accomplish that via the 34-m DSN X/Ka-band Earth stations.

4.10.8 Master Equipment List (MEL)

Table 4.70 and Table 4.71 list the Communications Subsystem MELs for TISR Return Vehicle Communications.

TABLE 4.70.—COMMUNICATIONS AND TRACKING – RETURN VEHICLE MEL

Description Case 1_Titan_Sample_Return CD-2021-186	QTY	Unit Mass	Basic Mass	Growth	Growth	Total Mass
Communications and Tracking			**12.7**	**10%**	**1.3**	**14.0**
X Band System			**12.7**	**10%**	**1.3**	**14.0**
Xb.Reflector/Feed	1	3.0	3.0	10%	0.3	3.3
Xb.Coax.Switch	8	0.1	1.0	10%	0.1	1.1
Xb.Diplexer	2	2.2	4.4	10%	0.4	4.9
Xb.LNA	2	0.1	0.2	10%	0.0	0.2
Xb.SSPA	2	1.4	2.7	10%	0.3	3.0
Xb.SDR	2	0.2	0.4	10%	0.0	0.4
Xb.WC.Adapter	1	0.4	0.4	10%	0.0	0.4
Xb.Helix.Antenna	2	0.3	0.6	10%	0.1	0.7

TABLE 4.71.—COMMUNICATIONS AND TRACKING – PROPELLANT PROCESSING LANDER MEL

Description Case 1_TSR_Propellant_Processing CD-2021-186b	QTY	Unit Mass	Basic Mass	Growth	Growth	Total Mass
Communications and Tracking			**24.4**	**8%**	**2.0**	**26.4**
X band Communications System			**24.4**	**8%**	**2.0**	**26.4**
X band TWTA, 625 W	3	1.0	3.0	10%	0.3	3.3
X band EPC for dual TWTAs	2	1.2	2.4	10%	0.2	2.6
UHF System	1	0.8	0.8	5%	0.0	0.8
T-Coupler/Phase Balanced TWTA Power Combi	1	0.2	0.2	5%	0.0	0.2
Deep Space Transceiver	2	2.0	4.0	5%	0.2	4.2
Cabling	1	2.0	2.0	5%	0.1	2.1
X-Y antenna cryogenic gimbal	1	5.0	5.0	10%	0.5	5.5
Switches	2	0.5	1.0	5%	0.1	1.1
X-band 1.0m Antenna, Solid, External	1	6.0	6.0	10%	0.6	6.6

4.11 System Name: ISRU Support Systems-Rover, Command and Data Handling, Communications and Tracking, and Lifting Body

Due to the vast number of systems being designed for this mission, a number of subsystems were taken from previous unpublished Compass designs. The propellant processing lander's command and data handling system and communications system were taken from an unpublished Titan lander study. A rover will be used to excavate the required regolith for propellant processing. The rover mass and power requirements are also based on a previous unpublished Compass Team design modified to account for changes necessary to excavate. Further refinement of the rover concept is warranted, as this estimate serves only as a placeholder. Finally, an allocation was carried for a representative lifting body to carry the TISR systems to Titan. A modified X-37C was used for configuration purposes.

4.11.1 Master Equipment List

Table 4.72 and Table 4.73 list the ISRU Support Hardware Rover MELs.

TABLE 4.72.—ISRU SUPPORT HARDWARE – ROVER MEL

Description Case 1_TSR_Propellant_Processing CD-2021-186b	QTY	Unit Mass	Basic Mass	Growth	Growth	Total Mass
Rover			37.5	25%	9.4	46.9
ISRU Support			37.5	25%	9.4	46.9
Excavation Hardware			37.5	25%	9.4	46.9
LEPRECAN Rover	1	37.5	37.5	25%	9.4	46.9

TABLE 4.73.—PROPULSION (CHEMICAL HARDWARE) – EDL MEL

Description Case 1_TSR_Propellant_Processing CD-2021-186b	QTY	Unit Mass	Basic Mass	Growth	Growth	Total Mass
		(kg)	(kg)	(%)	(kg)	(kg)
Lifting Body			1500.0	0%	0.0	1500.0
Lifting Body			1500.0	0%	0.0	1500.0
Lifting Body			1500.0	0%	0.0	1500.0
Lifting Body	1	1500.0	1500.0	0%	0.0	1500.0

5.0 Publications

The mission elements have been documented in nine of publications at technical conferences:

G.A. Landis and S.R. Oleson, "Proposal for a Sample Return from Titan," *18th International Planetary Probe Workshop*, June 17, 2021.

S.R. Oleson, *et al*., "Titan Sample Return Mission using In-Situ Propellant Production," *Titan Through Time V*, Boulder, CO, August 10-12, 2021.

S.R. Oleson and G.A. Landis, "Titan Sample Return Mission using In-Situ Propellants," *NASA Innovative Advanced Concepts Symposium*, Sept. 22-24 2020.

G.A. Landis and S.R. Oleson, "Sample Return from Titan," Planetary Science and Astrobiology Decadal Survey 2023-2032*; Bulletin of the American Astronomical Society, Vol. 53,* Issue 4, e-id. 309 (2021).

G.A. Landis, S.R. Oleson and R.D. Lorenz, "Mission Incredible: A Titan Sample Return Using In-Situ Propellants," paper AIAA 2022-1570, *AIAA Science and Technology Forum*, Jan 3-9 2022.

G.A. Landis, S.R. Oleson and R.D. Lorenz, "Titan Sample Return Mission," *53rd Lunar and Planetary Science Conference*, March 7-11 2022.

S.R. Oleson, G.A. Landis, and the COMPASS team, "NASA Innovative Advanced Concepts: Mission Studies by the NASA Glenn COMPASS Team," *Nuclear & Emerging Technology for Space Conference*, Cleveland OH, May 8-12, 2022.

D. Smith and J. Pekosh, "An Optimized Trajectory for a Two-Stage, Surface-to-Orbit Titan Launch Vehicle," *2022 AAS/AIAA Astrodynamics Specialist Conference*, Charlotte, NC, August 7–11, 2022.

J. Pekosh, "Titan Sample Return Mission using V-Infinity Leveraging," *2022 AAS/AIAA Astrodynamics Specialist Conference*, Charlotte, NC, August 7–11, 2022.

6.0 Lessons Learned

Return of a sample from the surface of Titan would have great science value but is a very difficult mission to accomplish with conventional technology. This conceptual design study showed that using in-situ propellants provides a mass and volume feasible solution for returning a cryogenic sample from Titan. Various propellants were considered but the use of CH_4 distilled from the atmosphere along with O_2 generated from water ice from the surface allowed for all the needed propellants to be produced in under 3 years with a relatively low power (1 kWe) radioisotope power system. The use of these cryogenic propellants was greatly simplified by the Titan environment; the CH_4 was easily collected, and both were stored as liquid propellants in the launcher tanks without insulation due to the 94 K environment. A three-stage launcher incorporating inflatable propellant tanks was developed that both saved mass and volume and could deliver the sample back to Earth without the need for a rendezvous with a return stage in Titan orbit. This mission would be invaluable for its science return, and its contribution to our understanding the origins of organic compounds in the solar system and of our place in the universe.

Appendix A.—Acronyms and Abbreviations

ΔV	Delta-V, Change in Velocity
ACS	Attitude Control System
AD&C	Attitude, Determination and Control
AD&CS	Attitude Determination and Control System
AIAA	American Institute for Aeronautics and Astronautics
ALA	Annual Link Availability
ANSI	American National Standards Institute
BOL	Beginning of Life
BPSK	Binary Phase Shift Keying
C&DH	Command and Data Handling
CAD	Computer Aided Design
CBE	Current Best Estimate
Cc	Cross Forces
Cd	Drag Coefficient
CFD	Computational Fluid Dynamics
CG	Center of Gravity
CMG	Control Moment Gyroscope
CONOPS	Concept of Operations
COTS	Commercial off-the-Shelf
CP	Center of Pressure
CP	Circularly Polarized
cPCI	compact Peripheral Component Interconnect
dBic	Antenna gain, decibels referenced to a circularly polarized, theoretical isotropic radiator
DFE	Direct from Earth
DOD	Depth of discharge
DOF	Degrees of Freedom
DRPS	Dynamic Radioisotope Power System
DSN	Deep Space Network
DSS	Deployable Space Systems
DTE	Direct to Earth
ECLSS	Environmental Control and Life Support System
EDAC	Error Detection and Correction
EDL	Entry, Descent, and Landing
EIRP	Effective Isotropic Radiated Power
EOL	End of Life
EOM	End of Mission
EPS	Electrical Power System
EPSM	Electrical Power System Module
EVEE	Earth-Venus-Earth-Earth
FACT	Flexible Array Concentrator Technology
FEA	Finite Element Analysis
FEP	Fluorinated Ethylene Propylene
FPA	Flight Path Angle
G/T	Antenna Gain/System Noise Temperature
GLOM	Gross Lift-Off Mass
GN&C	Guidance, Navigation and Control
GPHS	General Purpose Heat Source
GPIM	Green Propellant Infusion Mission
GRC	Glenn Research Center
HAN	Hydroxyl Ammonium Nitrate
HPBW	Half-Power-Beamwidth
ID	Inner Diameter
IMM	Inverted Metamorphic
IMU	Inertial Measurement Unit
IROSA	ISS ROSA
I_{sp}	Specific Impulse

ISRU	In-situ Resource Utilization
ISS	International Space Station
LEO	low Earth orbit
LILT	Low Intensity, Low Temperature
LTO	Low Titan Orbit
MEL	Master Equipment List
MGA	Mass Growth Allowance
MLI	Multi-Layer Insulation
MMH	Monomethyl Hydrazine
MMOD	Micrometeoroid and Orbital Debris
MMPDS	Metallic Materials Properties Development and Standardization
MOI	Moment of Inertia
MOP	Mean Operating Pressure
MPPT	Maximum Power Point Tracking
MTAS	Mars Transportation Assembly Study
NASTRAN	NASA Structural Analysis
NIAC	NASA Innovative Advanced Concept
NIST	National Institute of Standards and Technology
NPSP	Net Positive Suction Pressure
NTO	Nitrogen Tetroxide
O/F	Oxidizer to Fuel Mass Ratio
OD	Outer Diameter
OTIS	Optimal Trajectories by Implicit Simulation
P	Pressure
PID	Plumbing and Instrumentation Diagram
PCB	Printed Circuit Board
PCDU	Power Conditioning and Distribution Unit
PEL	Power Equipment List
PEM	Proton Exchange Membrane
PICA	Phenolic Impregnated Carbon Ablator
PMAD	Power Management and Distribution
PMD	Propellant Management Device
RAAN	Right Ascension of the Ascending Node
RBE2	Radar à Balayage Electronique 2
RCS	Reaction Control System
RF	Radio Frequency
RHU	Radioisotope Heater Units
ROSA	Roll-Out Solar Array
RPS	Radioisotope Power System
RTOS	Real Time Operating System
RV	Return Vehicle
S/C	spacecraft
SADA	Solar Array Drive Assembly
SEE	Single Event Effects
SEFI	Single Event Functional Interrupt
SEU	Single Event Upset
SLA	Stretched Lens Array
SLoC	Software Lines of Code
SLS	Space Launch System
SOC	State of Charge
SOLAROSA	Stretched Optical Lens Architecture on Roll-Out Solar Array
SPDT	Single-Pole Double-Throw
SSTO	Single Stage to Orbit
ST	Star Tracker
T	Temperature
TCM	Trajectory Correction Maneuver
TID	Total Ionizing Dose
TISR	Titan ISRU Sample Return
TMR	Triple Mode Redundancy
TPA	Turbo-Pump Assembly

TRL	technology readiness level	TWTA	Traveling Wave Tube Amplifier
TSR	Titan Sample Return	UDMH	Unsymmetrical Dimethylhydrazine
TSTO	Two-Stage to Orbit	UHF	Ultra-High Frequency
TVC	Thrust Vector Control	UHPV	Ultra-High Pressure Vessel
T/W	Thrust to Weight Ratio	WC	Waveguide to Coax

Appendix B.—Study Participants

Titan ISRU Sample Return (TISR) Design Session			
Subsystem	Name	Affiliation	Contact email
Design Customer POC/PI	Geoffrey Landis	GRC	Geoffrey.a.landis@nasa.gov
Compass Team			
Compass Team Lead	Steve Oleson	GRC	Steven.r.oleson@nasa.gov
System Integration, MEL, and Final Report Documentation	Betsy Turnbull	GRC	Elizabeth.r.turnbull@nasa.gov
Technical Editing	Lee Jackson	HX5	Lee.a.jackson@nasa.gov
Science	Geoffrey Landis	GRC	Geoffrey.a.landis@nasa.gov
APL Scientist	Ralph Lorenz	JPL	Ralph.lorenz@jhuapl.edu
Mission	Brent Faller Jeffrey Pekosh Zachary Zoloty Laura Burke (mentor) Steven McCarty (mentor)	GRC	Brent.f.faller@nasa.gov Jeffrey.d.pekosh@nasa.gov Zachary.c.zoloty@nasa.gov Laura.m.burke@nasa.gov Steven.McCarty@nasa.gov
Launch Vehicle Mission	David Smith	HX5	David.a.smith@nasa.gov
Thermal	Tony Colozza	HX5	Anthony.j.colozza@nasa.gov
AD&CS	Brent Faller Christine Schmid	GRC	Brent.f.faller@nasa.gov Christine.l.schmid@nasa.gov
Power	Lucia Tian Steven Korn Nicholas Uguccini	GRC	Lucia.tian@nasa.gov Steven.korn@nasa.gov Nicholas.r.uguccini@nasa.gov
Power RPS	Paul Schmitz	PCS	Paul.c.schmitz@nasa.gov
Propulsion	Jim Fittje	SAIC	James.e.fittje@nasa.gov
Structures and Mechanisms	John Gyekenyesi	HX5	John.z.gyekenyesi@nasa.gov
C&DH	Christopher Heldman W. Peter Simon	GRC	Christopher.r.heldman@nasa.gov William.p.simon@nasa.gov
Communications	Onoufrious Theofylaktos	GRC	Onoufrios.theofylaktos-1@nasa.gov
Configuration	Tom Packard	HX5	Thomas.w.packard@nasa.gov

References

1. Rodriguez, S.; Vinatier, S.; Cordier, D.; Tobie, G.; Achterberg, R.K.; Anderson, C.M.; Badman, S.V.; et al., "Science Goals and New Mission Concepts for Future Exploration of Titan's Atmosphere, Geology, and Habitability: Titan Polar Scout/Orbiter and In Situ lake lander and Drone Explorer (POSEIDON)," ArXiv preprint:2110.10466, 2021.
2. Landis, G. and Oleson S., "Sample Return from Titan," *Planetary Science and Astrobiology Decadal Survey 2023-2032,* vol. 53, no. 4, pp. e-id. 309, 2021.
3. MacKenzie, S., et al, "Titan: Earthlink on the Outside, Ocean World on the Inside," *The Planetary Science Journal,* vol. 2, no. 3, p. 112, 15 June 2021.
4. Lorenz, R.D.; Lunine, J.; Zimmerman, W., "Post-Cassini Exploration of Titan," *Adv. Space Research,* vol. 36, no. 2, pp. 281-285, 2005.
5. Raulin, F., "Astrobiology and Habitability of Titan," *Space Science Review,* vol. 135, pp. 37-48, 2008.
6. Shapiro, R. and Schulze-Makuch, D., "The Search for Alien Life in OUr Solar System: Strategies and Priorities," *Astrobiology,* vol. 9, no. 4, 11 June 2009.
7. Raulin, F.; McKay, C.; Lunine, J.; and Owen T., "Titan's Astrobiology," in *Titan from Cassini Huygens*, Springer Verlag, Dordrecht, 2009.
8. Sarker, N.; et al., "Titan Aerosol Analogues: Analysis of the Nonvolatile Tholins," *Atrobiology,* vol. 3, no. 4, pp. 719-726, 5 July 2004.
9. Neish, C.D.; Somogyi A.; and Smith, M.A., "Titan's Primordial Soup: Formation of Amino Acids via Low Temperature Hydrolysis of Tholins," *Astrobiology,* vol. 10, no. 3, pp. 337-347, April 2010.
10. Horst, S.M.; et al., "Formation of Amino Acides and Nucleotide Bases in a Titan Asmopshere Simulation Experiment," *Astrobiology,* vol. 12, no. 9, pp. 809-817, Sept 2012.
11. Cleaves II, H.J.; et al., "Amino Acids Generated from Hydrated Titan Tholins: Comparison with Miller-Urey Electric Discharge Products," *Icarus,* vol. 237, pp. 182-189, 15 July 2014.
12. Landis, G. and Oleson, S., "Proposal for a Sample Return from Titan," in *18th International Planetary Probe Workshop*, Virtual, 2021.
13. Lorenz, R.D., Saturn's Moon Titan, Haynes, 2021.
14. Lacomini, C.S. and Sridhar, K.R., "Electolyzer Power Requirements for Oxidizer Production on Mars," *J. Propulsion and Power,* vol. 21, no. 6, Nov-Dec 2005.
15. Grantz, A.C., "X-37B Orbital Test Vehicle and Derivatives," in *AIAA Space 2011 Conference & Exposition*, Long Beach, CA, 2011.
16. Paris, S.W.; et al., *Optimal Trajectories by Implicit Simulation: OTIS,* Vols. I-IV, 2008.
17. Waite, H.H.; Bell, J.; Lorenz, R.; Achterberg R.; Flasar, R.; and Flasar, F.M., "A Model of Variability in Titan's Atmospheric Structure," *Planetary and Space Science,* vol. 86, p. 45, 2013.
18. Donahue, B., "Titan Sample Return Mission Concept," in *57th JANNAF Propulsion Meeting*, Colorado Springs, CO, 2010.
19. NASA, "NASA Cassini Mission: Grand Finale Overview: Orbit Guide," NASA, https://solarsystem.nasa.gov/missions/cassini/mission/grand-finale/grand-finale-orbit-guide/. Accessed January 11, 2022.
20. Smith, David A., "An Optimized Trajectory For a Two-Stage, Surface to Orbit Titan Launch Vehicle," in *AAS/AIAA Astrodynamics Specialist Conference*, Charlotte, NC, 2022.
21. Pekosh, Jeffrey D. and McCarty, Steven L., "Titan Sample Return Mission Using V-Infinity Leveraging," in *AAS/AIAA Astrodynamics Specialist Conference*, Charlotte, NC, 2022.

22. AIAA, “Standard: Mass Properties Control for Space Systems (ANSI/AIAA S-120A-2015 (2019)),” AIAA, Reston, VA, 2019.
23. Wade, Mark, “Star 63F,” Astronautix, 2019. http://www.astronautix.com/s/star63f.html. Accessed June 13, 2022.
24. NASA Launch Services Program, “Launch Vehicle Performance Website,” NASA, https://elvperf.ksc.nasa.gov/Pages/Default.aspx. Accessed January 12, 2022.
25. Department of Defense, Composit Materials Handbook (MIL HDBK 17 2F), vol. 2, Department of Defense, 2002.
26. Federal Aviation Administration, Metalic Materials Properties Development and Standardization (MMPDS) Handbook - 14, vol. MMPDS 14, Columbus, OH: Battelle Memorial Institute, 2019.
27. Mankins, J. C., “Technology Readiness Levels,” NASA, Washington, 1995.
28. Agarwal, B. D. and Broutman, L. J., Analysis and Performance of Fiber Composites ISBN 0-471-05928-5, New York: John Wiley & Sons, Inc., 1980.
29. Collier Research Corporation, “HyperSizer,” 1995. http://hypersizer.com. Accessed 13 October 2020.
30. National Aeronautics and Space Administration (NASA), “Structural Design and Test Factors of Safety for Spaceflight Hardware (NASA-STD-5001B),” NASA, Washington, 2016.
31. Heinemann, Jr., W., “Design Mass Properties II: Mass Estimating and Forecasting for Aerospace Vehicles Based on Historical Data,” NASA Johnson Space Center, Houston, TX, 1994.
32. O'Neill, Mark; McDanal, A.J.; Brandhorst, Henry; Schmid, Kevin; LaCorte, Peter; Piszczor, Michael; Myers, Matt, “Recent Space PV Concentrator Advances: More Robust, Lighter, and Easier to Track,” in *2015 IEEE 42nd Photovoltaic Specialists Conference (PVSC)*, New Orleans, LA, 2015.
33. Rodiek, Julie A.; O'Neill, Mark, “Stretched Lens Solar Array: The Best Choice for Harsh Orbits,” in *6th International Energy Conversion Engineering Conference (IECEC)*, Cleveland, OH, 2008.
34. Pumpkin, Inc., “CubeSat Kit Electrical Power System Module 1 (EPSM 1) - Hardware Rev. C, Doc Rev. E,” Pumpkin, Inc., San Francisco, CA, 2019.
35. Deployable Space Systems, “DSS's FACT, Mega-ROSA, and SOLAROSA Technologies Highlighted in NASA's Tech Briefs,” Deployable Space Systems (DSS), 1 November 2012. https://www.dss-space.com/post/dss-fact-mega-rosa-and-solarosa-technologies-highlighted-in-nasas-tech-briefs. Accessed July 2021.
36. SolAero Technologies, “IMM-alpha Preliminary Data Sheet,” SolAero Technologies Corp, 2018.
37. RUAG Space, “Septa 31 Solar Array Drive Assembly,” RUAG Space, Zurich, Switzerland.
38. Lee, Kwan Hee, “Product Specification / Rechargeable Lithium Ion Battery / Model: INR18650 MJ1 3500 mAh,” LG Chem, Seoul, Korea, 2016.
39. Lefholz, Tyler; Bienvenu, Lindsey, “LG Chem MJ1 Cell Space Qualification,” in *38th Annual Space Power Workshop*, El Segundo, CA, 2021.
40. Schmidt, Eckart W., Hydrazine and Its Derivatives, Ney York: John Wiley & Sons, Inc., 1984.
41. Fleming, C. David and Hegab, Hisham, E., “Design of a Collapsible Liquid Oxygen Storage Vessel for Mars (AIAA 2002-1457),” in *43rd AIAA/ASME/ASCE/AHS/ASC Structures, Structural Dynamics, and Materials Conference*, Denver, CO, 2002.
42. Huzel, Dieter K. and Huang, David H., Modern Engineering for Design of Liquid-Propellant Rocket Engines, Washington, D.C.: AIAA, 1992.
43. Giuliano, Victor J., et. al., “CECE: A Deep Throttling Demonstrator Cryogenic Engine for NASA's Lunar Lander (2007-5480),” in *43rd AIAA/ASME/SAE/ASEE Joint Propulsion Conference*, Cincinnati, OH, 2007.

44. Bach, C., Propst, Martin, Sieder-Katzmann, Jan, and Tajmar, Martin, "Evaluation of the performance potential of aerodynamically thrust vectored aerospike nozzles," in *67th International Astronautical Congress (IAC)*, Guadalajara, Mexico, 2016.
45. Masse, R.K., et al., "GPIM AF-M315E Propulsion System (AIAA 2015-3753)," in *AIAA Propulsion and Energy Form*, Orlando, FL, 2015.
46. National Institute of Standards and Technology, "NIST Chemical WebBook, SRD 69," National Institute of Standards and Technology, 2018. https://webbook.nist.gov/chemistry/fluid/. Accessed 2020.
47. Teissier, Alain, "Liquid Helium Storage for Ariane 5 Main Stage Oxygen Tank Pressurization," AIAA 95-2956, AIAA, 1995.
48. NASA, "Saturn V News Reference," December 1968. https://www.nasa.gov/centers/marshall/pdf/499245main_J2_Engine_fs.pdf. [Accessed August 2021].
49. MOOG Space and Defence Group, "Modular Linear EM Actuators," 2018. https://www.moog.com/content/dam/moog/literature/Space_Defense/Space_Access_Integrated_Systems/SAIS_Modular_EMA_Rev_0315.pdf. Accessed September 2021.
50. MOOG Space and Defense Group, "Controllers," 2015. https://www.moog.com/content/dam/moog/literature/Space_Defense/spaceliterature/spacecraft_mechanisms/SAIS_Modular_CEU_Rev_0615.pdf. Accessed September 2021.
51. Northrop Grumman, "PMD Tanks Data Sheets," 2020. https://www.northropgrumman.com/space/pmd-tanks-data-sheets-sorted-by-volume/. Accessed July 2020.
52. Northrop Grumman, "Diaphram Tanks Data Sheets," 2020. https://www.northropgrumman.com/space/diaphragm-tanks-data-sheets-sorted-by-part-number/. Accessed July 2020.
53. Thin Red Line Aerospace, "Thin Red Line Aerospace," http://www.thin-red-line.com/projects.html. Accessed September 2021.
54. Lark, Raymond F., "Cryogenic Positive Expulsion Bladders," NASA Lewis, Cleveland, OH, 1968.
55. Guangzai, Nong; Yijing, Li; and Yin, Yongjun, "Energy Analysis on the Water Cycle Consisting of Photo Catalyzing Water Splitting and Hydrogen Reacting with Oxygen in a Hydrogen Fuel Cell," *Chemical Physics Letters X,* vol. 4, 2019.
56. Colozza, A.J. and Burke, K.A., "Evaluation of a Passive Heat Exchanger Based Cooling System for Fuel Cell Applications," NASA/TM—2011-216962, NASA, January 2011.
57. Incropera, D.P.; and Dewitt, F. P., Fundamentals of Heat and Mass Transfer, Third Edition, John Wiley & Sons Publisher, 1990.
58. NASA, *Cassini Huygens Saturn Arrival Press Kit,* NASA, 2004.
59. Flasar, F.M.; et al., "Titan's Atmospheric Temperatures, Winds, and Composition," *Science,* vol. 308, pp. 975-978, 13 May 2005.
60. R. Brown, J. Lebreton and J. and Waite, Eds., *Titan from Cassini Huygens,* Springer Science Business Media, 2009.
61. NASA, "Solar System Exploration: Titan (moon)," March 2013. https://solarsystem.nasa.gov/moons/overview/. Accessed January 12, 2022.
62. Moog, "Moog Servo Motor Controller Electronics," 2016. https://www.moog.com/content/dam/moog/literature/Space_Defense/Space_Access_Integrated_Systems/AVIONICS_Servo_Motor_Controller_Electronics_Datasheet_032416.pdf. Accessed May 20, 2020.
63. AiTech, "AiTech SP0 3U cPCI Radiation Tolerant PowerPC SBC," https://aitechsystems.com/product/sp0-s-rad-tolerant-3u-compactpci-sbc/. Accessed May 20, 2020.

64. U.S. Military, “Digital Time Division Command/Response Multiplex Data Bus (MIL-STD-1553),” United States Air Force Life Cycle Management Center - Aircraft Systems, 2018.
65. Yelle, R. V.; Strobell, D. F.; Lellouch, E.; Gauter, D., “Entineering Models for Titan's Atmosphere,” 1998.
66. NIST, “NIST Standard Reference Data,” NIST, 2021. https://www.nist.gov/srd/refprop. Accessed 2021.
67. Li, Jianping; Liu, Dong; Coustenis, Athena; Liu, Xinhua, “Possible Physical Cause of the Zonal Wind Collapse on Titan,” *Planetary and Space Science,* Vols. 63-64, pp. 150-157, 2012.
68. Yu, Xinting, “The Effect of Adsorbted Liquid and Material Density on Saltation Threshold: Insight from Laboratory and Wind Tunnel Experiments,” *Icarus,* vol. 297, 06 2017.
69. Roshko, Anatol, “Experiments on the flow past a circular cylinder at very high Reynolds number,” *Journal of Fluid Mechanics,* vol. 10, pp. 345-356, 1961.
70. The Johns Hopkins University Applied Physics Laboratory LLC, “Dragonfly,” The Johns Hopkins University Applied Physics Laboratory LLC, 2022. https://dragonfly.jhuapl.edu/. Accessed 13 June 2022.

Bibliography

Deployable Space Systems, “Concentrator Solar Array Systems,” Deployable Space Systems (DSS), https://www.dss-space.com/products-concentrators. Accessed August 2021.